Impact of Bromide Ion Concentration, Time, Dissolved Organic Carbon and Molecular Weight Cutoff on Haloacetonitrile, Haloketone, Chloropicrin and Trihalomethane Formation Potentials

by
Steve H. Via

This research is submitted to the Faculty of the Environmental Division, Department of Civil Engineering, School of Engineering, Virginia Polytechnic Institute and State University in partial fulfillment of the requirements for the degree of

Masters of Science
in
Environmental Science and Engineering

APPROVED

Andrea M. Dietrich, Chair

Daniel L. Gallagher

John C. Little

May, 1995
Blacksburg, Virginia

IMPACT OF BROMIDE ION CONCENTRATION, TIME, DISSOLVED ORGANIC CARBON AND MOLECULAR WEIGHT CUTOFF ON HALOACETONITRILE, HALOKETONE, CHLOROPICRIN AND TRIHALOMETHANE FORMATION POTENTIALS

by
Steve H. Via

Chairman, Andrea M. Dietrich

Environmental Sciences and Engineering

(ABSTRACT)

This research investigated the formation potential (FP) for haloacetonitriles (HANs), haloketones (HKs), chloropicrin (CP) and trihalomethanes (THMs) under conditions of constant DOC, constant Cl:DOC ratio, variable [Br^-] and variable apparent molecular weight (AMW) for coagulated water from a full-scale water treatment plant. Coagulated, high humic water (4.5 mg DOC/L) was fractionated into <1K, <10K, and <30K MWCO fractions. The DOC of the fractions was adjusted to the same value (e.g., ~ 2 mg/L). Fractions were chlorinated at 3:1 Cl_2:TOC ratio under varying [Br^-]. Observed, non-THM species occurred at low concentrations (<0.3-9.0 ug/L). As expected THMFP speciation was strongly affected by Br^-:Cl ratio; this research demonstrated similar effects on specific HANs and HKs. Increasing quantities of brominated HANs and HKs were observed with increasing [Br^-]. DCANFP remained relatively constant while BCANFP and DBANFP increased with increasing [Br^-]. Increases in brominated species resulted in a larger relative change in THANFP than TTHMFP, suggesting that more HAN precursor material reacted when Br^- was present. Elevating Br^-:Cl to 0.03 resulting in HANFPs comparable to $CHBr_3FP$. Change in HAN and HK species with respect to molecular weight cutoff (MWCO) and coagulated-raw water comparisons suggest that HANFP results from reaction with small, reactive, nitrogen containing compounds (<1K AMW) and larger (<30,000 MWCO) proteinaceous matter.

Acknowledgements

Thanks are extended to each of my committee members: Dr. Andrea M. Dietrich, Dr. Daniel L. Gallagher, and Dr. John C. Little for their guidance and assistance in this research. Appreciation is also owed Dr. John T. Novak for his interest and participation in my defense. Special thanks are due Marilyn Grender, Julie Petruska, and Patsy Owens whose council was of great assistance in using the analytical instruments and methods employed in this research.

Table of Contents

Abstract ii

Acknowledgements iii

Table of Contents iv

Table of Tables viii

Table of Figures x

Chapter 1. Introduction 1
Regulatory History 1
Research Objectives 4

Chapter 2. Literature Review 6
Background 6
Impact of Organic Carbon Concentration 9
Characterizing Dissolved Organic Matter 10
Characteristics Associated with Apparent Molecular Size 13
Effects Associated with Coagulation 15
Formation Potential as a Function of Chlorine Dose 17
Effect of Bromide 18
Effect of pH on Formation Potential and Formation Potential Removal 22
Formation Potential 23
Coagulation 23
Formation Potential as a Function of Temperature 24
Pre-oxidation with Potassium Permanganate 25
Nitrogen Sources and Haloacetonitrile Formation 25
Description of Source Water 26
Description of Harwood's Mill Facility 26
Water Quality and Treatability, Owen *et al.*, 1993 30
NOM Characterization, Bokka and Schafran, 1994 32
Coagulation and DBP Formation Potential, Smith *et al.*, 1994 33

Chapter 3. Methods and Experimental Design 34
Sample Preparation 34
Chlorine Residual 34
Trihalomethane Formation Potential (THMFP) 35
Non-Purgable Dissolved Organic Carbon (NPDOC) 37

Table of Contents continued

Bromide 37
Trihalomethanes 38
Haloacetonitriles, Haloketones, and Chloropicrin 40
DOC Equalization 43
Ultrafiltration 43
Experimental Design 46
Determining Experimental Conditions 47
Summary of Experimental Matrices 48

Chapter 4. Results and Discussion 53
Preliminary Findings 53
EPA MDL Method Response to Variation in Procedure 55
EPA Method vs Inverse Regression. 58
Matrix 1 59
Matrix 2 64
Matrix 3 64
General 65
THMs 65
HANs 69
HKs and CP 69
Coagulation's Effect on Specific Formation Potential 70
Investigating Br^-:DOC Ratio Effect 70
Matrix 4 71
General Summary of Response and Comparison to Matrix Three 73
THMs 73
HANs and HKs 74
Effect of DOC Equalization On DOC Normalized Formation Potential . . . 74
Effect of Experimental Parameters on DOC Normalized Specific Formation Potential 77
Matrix 5.1 78
THMs 79
HANs 79
HKs and CP 81
Effect of Initial Br^-:Cl Ratio on DOC Normalized Specific Formation Potential 81
Spearman Correlation Coefficient Analysis 83
Wilcoxon Signed Rank Test 86
Matrix 5.2 86

Table of Contents continued

Comparison with Matrix 3 89
Independent 1,000 MWCO-Br^-:Cl Condition Trials 89
Matrix 6 89
General 90
Comparison to Matrix 3 91
Effect of Br^-:DOC Ratio 91
Relationship to Research Objectives 93
Harwood's Mill Reservoir Water 95
Br^-:Cl Ratio 96
Br^-:DOC Ratio 96
Substrates and DBP Formation 98
Halogen Substitution 98
Hydrolysis of DCAN 99
Molecular Weight Cutoff Fraction 99
1,000 MWCO Nitrogen Sources 99
Coagulation and Formation Potential 100

Chapter 5. Summary and Conclusions 101
Observed Formation Potential 101
Br^-:Cl Ratio Effect 102
Molecular Weight Cutoff and Non-THM Formation 102
Formation Potential for Coagulated vs. Raw Water 104
Conclusions 105
Reaction Time 105
Br^-:DOC Ratio 105
MWCO Fraction 106
Br^-:Cl Ratio 106
Testing $CHCl_3$ and DCAN as DBP Formation Substrates 106
Method Detection Limit Analysis 106

Chapter 6. Future Research Opportunities 107
Nanofiltration 107
Stable Isotope Analysis 108
Distribution System Data 109

Appendix 1. Sample Chromatograms 110

Appendix 2. Inverse Regression Plots for Method Detection Limit Determination . 113

Table of Contents continued

Appendix 3. Matrix 1, Graphs of DOC Normalized DBP Concentration with Time 118

Appendix 4. Matrix 2, Graphs of DOC Normalized DBP Concentration with Time 125

Appendix 5. Matrix 3, Graphs of DOC Normalized DBP Concentration with Time 129

Appendix 6. Matrix 4, Graphs of DOC Normalized DBP Concentration with Time 139

Appendix 7. Matrix 5.1, Graphs of DOC Normalized DBP Concentration with Time 147

Appendix 8. Matrix 5.2, Graphs of DOC Normalized DBP Concentration with Time 164

Appendix 9. Matrix 6, Graphs of DOC Normalized DBP Concentration with Time 169

Bibliography 174

Vita 186

Table of Tables

Table 2.1. Finished Water DBP Type and Concentration Determined from a Seasonal Survey of 35 U.S. Water Utilities 8
Table 2.2. Total Organic Carbon Concentration Distribution in Raw Waters . . . 10
Table 2.3. Characteristics of Fulvic and Humic Substances 12
Table 2.4. Relative Chlorination Byproduct Yields for Ten Humic Substances . . 13
Table 2.5. Bromide Concentration Distribution in Raw Waters 18
Table 2.6. DBP Formation with Respect to pH 24
Table 2.7. Raw Water Characteristics 31
Table 2.8. Post-Bench Scale Coagulation Character 32
Table 2.9. Removal of DBP Formation Potential from Raw Water by Coagulation Observed During Bench Scale Coagulation Study of Harwood's Mill Reservoir Water 33
Table 3.1. Method 501.1 Retention Times and Detection Limits 40
Table 3.2. Method 551 Retention Times and Detection Limits 41
Table 3.3. Summary of DOC Manipulation Required by Experimental Matrix . . 44
Table 3.4. Sampling Event Conditions 47
Table 3.5. Summary of Experimental Matrices 48
Table 4.1. EPA Method 501.1 and 551 MDLs 54
Table 4.2. Application of Method Detection Limit Values to THM Data Generated by Method 501.1 54
Table 4.3. Application of Method Detection Limit Values to THM Data Generated by Method 551 55
Table 4.4. MDL Calculated at Different Low Level Concentrations Using the EPA Method 57
Table 4.5. Variation in Method 551 Detection Due to Non-Sample Sources . . . 58
Table 4.6. Description of Sharaf Method MDL Analysis 59
Table 4.7. THMFP at 96 Hour Time Point as Function of Initial Br^-:Cl Ratio (0.5 mg Br^-/L, 0, 2, and 4 mg Cl_2/L) 62
Table 4.8. Initial DOC Concentration by MWCO Fraction, Matrix Three 65
Table 4.9. Coagulation Effect, Matched Pair Wilcoxon Ranked Sum Test 70
Table 4.10. Raw and Coagulated DOC Normalized DBPFP by MWCO Fraction (168 hour) 72
Table 4.11. DOC Concentrations in Matrix 4 by MWCO Fraction 73
Table 4.12. Matrix 4, 168 Hour DOC Normalized Specific Formation Potentials by MWCO 75
Table 4.13. Effect of Equalization on DBPFP Associated with Each MWCO Fraction, Paired Wilcoxon Ranked Sum Probability 77

Table of Tables continued

Table 4.14. Correlation Between DOC Normalized Molar Response to Matrix 4 Experimental Factors, Spearman Correlation Coefficient. 78
Table 4.15. DOC Normalized 168 Hour Formation Potential by MWCO Fraction 82
Table 4.16. Correlation Between DOC Normalized DBPFP and Initial Br^-:Cl Ratio by MWCO Fraction, Spearman Correlation Coefficients, ... 84
Table 4.17. TTHM Formation Potential as Percentage of TDBP Formation at 168 Hour Time Point (Averaged Across Fractions) 85
Table 4.18. DOC Normalized DBP Formation, Relatedness to MWCO Fraction as Reflected by Wilcoxon Signed Rank Statistic (Varied Initial Br^-:Cl dose, 168 Hour) 88
Table 4.19. DBP Formation Potentials (168 Hour), A Side-by-Side Trial 90
Table 4.20. Spearman Correlation Coefficient Analysis of DBPFP with Respect to Experimental Parameters. 92
Table 4.21. DOC Normalized DBPFP with Respect to Experimental Parameters. . 92

Table of Figures

Figure 2.1. Drinking Water Disinfection Practices Observed in Survey of 280 Water Utilities in United States, 1990 7

Figure 2.2. Comparison of Drinking Water Disinfection Practices Observed in Industry Surveys, 1978 and 1990 7

Figure 2.3. Harwood's Mill Water Treatment Plant Flow Diagram 28

Figure 4.1. Chromatogram of Haloacetonitrile and Haloketone Standard, 0.25 ug/L, Column: 30 m, 0.25 mm i.d., DB-1, helium carrier gas at 23 cm/sec, nitrogen make-up gas at 30 mL/min.; Temperature Program: 15 min at 33°C, 33-40°C 56

Figure 4.2. $CHCl_3$ and DCAN Concentration Over Time in Matrix 1 (MilliQ®, 100 ug $CHCl_3$/L, 2.5 ug DCAN/L, 0 mg Br^-/L) 60

Figure 4.3. $CHCl_3$ Concentration Observed in Matrix 1 Over Time (MilliQ®, 100 ug $CHCl_3$/L, 2.5 ug DCAN/L) 61

Figure 4.4. DCAN Concentration Observed in Matrix 1 Over Time (MilliQ®, 100 ug $CHCl_3$/L, 2.5 ug DCAN/L) 61

Figure 4.5. $CHCl_2BrFP$ Observed in Matrix 1 Over Time (MilliQ®, 100 ug $CHCl_3$/L, 2.5 ug DCAN/L) 63

Figure 4.6. $CHClBr_2FP$ Observed in Matrix 1 Over Time (MilliQ®, 100 ug $CHCl_3$/L, 2.5 ug DCAN/L) 63

Figure 4.7. Comparison of DBP Formation from Raw and Coagulated Waters, <1,000 MWCO, 2 mg DOC/L, 0.07 mg Br^-/L, 3:1 Cl_2:DOC Ratio . 66

Figure 4.8. Comparison of DBP Formation from Raw and Coagulated Waters, <30,000 MWCO, 2 mg DOC/L, 0.07 mg Br^-/L, 3:1 Cl_2:DOC Ratio 67

Figure 4.9. Comparison of DBP Formation from Raw and Coagulated Waters, <4,500,000 MWCO, 2 mg DOC/L, 0.07 mg Br^-/L, 3:1 Cl_2:DOC Ratio 68

Figure 4.10. $CHCl_3$ Formation in Unequalized Coagulated Water by MWCO Fraction, 96 Hour, 3 mg DOC/L, 6 mg Cl_2/L, 0.07 mg Br^-/L 75

Figure 4.11. Equalized Coagulated Water $CHCl_3FP$ by MWCO Fraction, 96 Hour, 2 mg DOC/L, 6 mg Cl_2/L, 0.07 mg Br^-/L 76

Figure 4. 12. THM DOC Normalized Formation Potential Identified in <30,000 MWCO Fraction as a Function of Br^-:Cl Ratio 80

Figure 4. 13. THAN DOC Normalized Specific Formation Potential Identified in <30,000 MWCO Fraction as a Function of Br^-:Cl Ratio 80

Figure 4. 14. HAN DOC Normalized Specific Formation Potential Identified in <30,000 MWCO Fraction as a Function of Br^-:Cl Ratio 82

Figure 4.15. Relative Change in DOC Normalized TTHM and THAN Formation Potential with Respect to Br^- Concentration in 10,000 MWCO Fraction at 96 Hours 85

Table of Figures continued

Figure 4.16. Formation Potential Response to Initial Br:Cl in 10,000 MWCO Fraction 87
Figure 4.17. TTHM and THAN Response to Br^-:DOC ratio (0.4, 1.5, 3 mg DOC/L; 0.07 mg Br^-/L, 0, 24, 48, 96, and 168 time points). 93
Figure 4.18. BCAN Specific Formation Potential with Respect to Time (4,500 K MWCO, 2 mg DOC/L; 0.07 mg Br^-/L). 94
Figure 4.19. BCAN Specific Formation Potential with Respect to Time (4,500 K MWCO, 0.4, 1.5, 3 mg DOC/L; 0.07 mg Br^-/L). 94
Figure 5.1 Raw Water HAN Species Formation with Time (2 mg DOC/L, 0.07 mg Br^-/L, 6 mg Cl_2/L) 103
Figure 5.2 Coagulated Water HAN Species Formation with Time (2 mg DOC/L, 0.07 mg Br^-/L, 6 mg Cl_2/L) 103
Figure 5.3. DOC Normalized THM Species Specific Formation Potentials, Change with Coagulation (2 mg DOC/L, 0.07 Br^-/L, 6 mg Cl_2/L, 96 Hours) 104
Figure 5.4. DOC Normalized HAN Species Specific Formation Potentials, Change with Coagulation (2 mg DOC/L, 0.07 Br^-/L, 6 mg Cl_2/L, 96 Hours) 105

Chapter 1. Introduction

Throughout the world, the production of drinking water frequently entails the use of chlorination to insure adequate disinfection. Chemical disinfection has been practiced in the U.S. since 1908; installations at Bubbly Creek Filter Plant in Chicago, Il. and Jersey City Water Supply Company, Jersey City, NJ, were some of the first locations to use chlorine. Introducing chlorine into water at levels adequate to insure water quality also results in the formation of chemicals known as disinfection byproducts (DBPs). The group "disinfection byproducts" includes a diversity of organic compounds, many of which have not been adequately described. The common attributes defining DBPs are related to chlorination:

1. Halogenation, the presence of one or more atoms of either chlorine, bromine, iodine, or fluorine.
2. A base structure of organic origin, either cyclical or chain structure.
3. Believed to represent a threat to human health due to toxic or carcinogenic properties.

Several categories of halogenated DBPs have been enumerated including: trihalomethanes (THMs), haloacetic acids (HAAs), haloketones (HKs), and haloacetonitriles (HANs). There are potential health effects associated with ingestion of DBPs, and these risks are believed to be different for different classes of DBPs.

Regulatory History

In 1979, health risks associated with halogenated DBPs resulted in the promulgation of a National Primary Drinking Water Standard for total trihalomethanes, under the Safe Drinking Water Act in 1979 (Means and Krasner, 1993). As a result, THMs have been managed in the United States at a level not to exceed a value of 0.10 mg/L. This is a composite standard which includes four compounds: chloroform ($CHCl_3$), dichlorobromomethane ($CHCl_2Br$), dibromochloromethane ($CHClBr_2$), and bromoform ($CHBr_3$).

In July 1994, the U.S. Environmental Protection Agency (EPA) proposed revising its regulations expanding the number of DBPs subject to regulation and increased compound specificity within the standard. The Disinfectant/Disinfection Byproduct (D/DBP) Rule, as proposed (59 *Federal Register* 38668), emphasized enhanced coagulation as a DBP formation prevention strategy. Stage I, to be promulgated in December 1996, reduces the existing THM MCL to 0.080 mg/L and establishes an MCL of 0.060 mg/L for the sum of five specified HAAs. With Stage II, to be implemented in the year 2000, these MCLs will decrease to 0.040 and 0.030 mg/L for THMs and HAAs respectively, and HANs, HKs and other DBPs will be considered for regulation.

A parallel regulation, known as the Information Collection Rule (*59 Federal Register 6332*), will establish monitoring requirements for HANs and HKs, for the specific purpose of assessing the extent of their formation in U.S. drinking water treatment systems. The absence of such information was one of the factors which shaped the current D/DBP proposal.

Since the mid-20th century, conventional water treatment plant design has consisted of coagulation-flocculation-filtration and disinfection. After raw water is screened and in some instances a treated with a preoxidant (e.g., chlorine, potassium permanganate), then alum, iron salts, and/or organic polymers are added as coagulants in a rapid mix, which is followed by gentle mixing in a flocculator. Lime or sodium hydroxide addition may take place during rapid mix to optimize pH. Floc, consisting partially of DBP precursor material is allowed to settle in sedimentation basins where removal of contaminants occurs as a result of particle surface chemistry and sweep floc formation. Clarified water is filtered through rapid sand filters and chlorine added for disinfection prior to treated water entering the distribution system. Final disinfection is typically accomplished with chlorine but other oxidants are also used.

The draft D/DBP Rule establishes "enhanced coagulation" as best available technology (BAT) for water treatment plants that: (1) are of conventional design with sedimentation basins, (2) utilize a water source that is influenced by surface water, and (3) experience

total organic carbon (TOC) greater than 2 mg/L prior to disinfection. Enhanced coagulation is defined as addition of a coagulant at a dose beyond which addition of 10 mg/L more will remove less than 0.3 mg TOC/L. While pursued as an economical DBP precursor removal method, implementation of enhanced coagulation will increase operational costs due to increased coagulant demand and sludge management costs.

Randtke *et al.* (1994) surveyed 350 drinking water utilities and found that 75 percent of the coagulation facilities employed chlorine for residual disinfection. Table 1.1 summarizes selected DBP management parameters characterized by the study.

Table 1.1. Summary of Water Quality Parameters and Treatment Conditions at 350 Drinking Water Utilities

Parameter	Sample Size	Quartile 0	25	50	75	100
Raw water TOC, mg/L	95	1.0	2.6	4.0	6.0	25.0
Percent Removed TOC, %	85	0	28	41	58	94
Coagulation pH	225	4.8	6.6	7.2	8.0	9.1
Finished pH	243	6.3	7.3	7.6	8.0	9.1
Bromide, mg/L	43	0.00	0.04	0.05	0.10	0.75
Free Cl_2 Residual, mg/L	175	0.2	1.0	1.3	1.7	4.0

Source: Randtke *et al.*, 1994.

The ability of coagulation to remove DBP precursors depends primarily upon the characteristics of the natural organic matter (NOM). NOM with larger apparent molecular weight (AMW) (>30,000 AMW) and a hydrophobic nature is more readily removed compared to small molecular weight (<1,000 AMW), hydrophilic NOM.

Because THMs were recognized as a public health risk in the early 1970s, there is substantially more research in the literature for this category of DBPs. Expansion of the regulations to more organic contaminants has created a need for additional research into the formation potential of DBPs, particularly those DBPs that are proposed to be regulated. Three such classes of DBPs are the HANs, HKs and chloropicrin. HANs include trichloroacetonitrile (TCAN), dichloroacetonitrile (DCAN), dibromochloroaceto-

nitrile (BCAN), and dibromoacetonitrile (DBAN); two haloketones of interest are dichloropropanone (DCP) and 1,1,1-trichloro-2-propanone (TCP).

Research Objectives

Flocculation-coagulation-filtration is the dominant treatment method in the water treatment industry for suspended solid, colloidal particle, and DBP precursor removal. Therefore, the research undertaken here investigated the DBP formation potential associated with chlorination of coagulated waters.

Five related objectives investigating DBP formation potential were formulated, specifically exploring:

1. Species specific haloacetonitrile, haloketone, trihalomethane and chloropicrin formation potential for a representative water as a function of time.

2. The effect of organic substrate:bromide ion ratio on haloacetonitrile, haloketone, trihalomethane and chloropicrin formation potential.

3. The relationship between NOM nominal size fraction, and haloacetonitrile, haloketone, trihalomethane, and chloropicrin formation potential for raw and coagulated waters under conditions of variable NOM AMW distribution and constant bromide concentration, dissolved organic carbon (DOC) concentration, and chlorine dose.

4. The impact of bromide ion (Br^-) concentration:chlorine dose ratio on haloacetonitrile, haloketone, trihalomethane and chloropicrin formation potentials.

5. The likelihood that DCAN is an intermediate product in the formation potential of other DBPs.

Experimental design focused on ultrafiltration partitioned natural and coagulated waters (<1,000, <10,000, <30,000, and <4,500,000 AMW) obtained at Harwood's Mill Reservoir, where TOC values of 4.9 mg/L are typical. Coagulated water used in the study was subject to the water treatment plant's full scale treatment scheme, prior to pre-

filtration chlorination. DOC and bromide ion concentrations were controlled in the laboratory through fortification, concentration, and dilution. Unless chlorine concentration was varied purposefully in an experimental matrix, an initial ratio of free available chlorine (measured as Cl_2/L) to DOC of 3:1 was maintained.

Chapter 2. Literature Review

Chlorination is the predominant disinfection method used in the drinking water supply industry. Over 64 percent of current water works, which serve more than 46 percent of the drinking water customers in the United States, rely on chlorine as the primary disinfectant in the water treatment process (59 *Federal Register* 145). Chlorine is readily available, inexpensive, effective at low concentrations, and forms a disinfectant residual (Reynolds, 1982.).

An AWWA survey conducted in 1989-1990 to determine the distribution of disinfectants in use, found that chlorination was the dominant disinfectant practice in the U.S.. The survey reflects data from 280 water utilities in the U.S. Figure 2.1 summarizes this survey, while Figure 2.2 compares the practices observed in the 1989-1990 survey to the results of a similar effort made in 1978 by Hoehn.

Background

Within the pH range present in typical, coagulation-flocculation water treatment plant, chlorine reacts with water to form hypochlorous acid (HOCl).

$$Cl_2 + H_2O \Leftrightarrow HOCl + HCl \qquad \text{(Eq. 2.1)}$$

Dissociation of HOCl yields hypochlorite ion (OCl^-).

$$HOCl \Leftrightarrow H^+ + OCl^- \qquad \text{(Eq.2.2)}$$

The relative abundance of these two aqueous forms is pH and temperature dependent; HOCl and OCl^- being equally abundant at pH 7.58 at 20°C (Fair *et al.*, 1948; Johnson and Jensen, 1986). Both HOCl and OCl^- are reactive with organic matter and reduced substances, including Fe^{2+}, Mn^{2+}, and NO_2 (Reynolds, 1982). The reaction of chlorine species with organic matter during the disinfection process results in the formation of disinfection byproducts, some of which are believed to adversely affect human health.

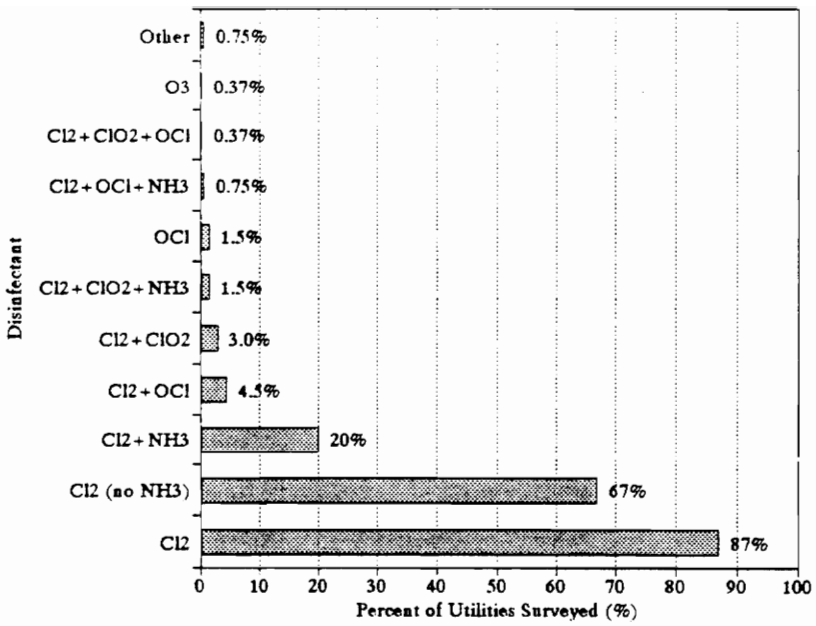

Figure 2.1. Drinking Water Disinfection Practices Observed in Survey of 280 Water Utilities in United States, 1990 (AWWA, 1990)

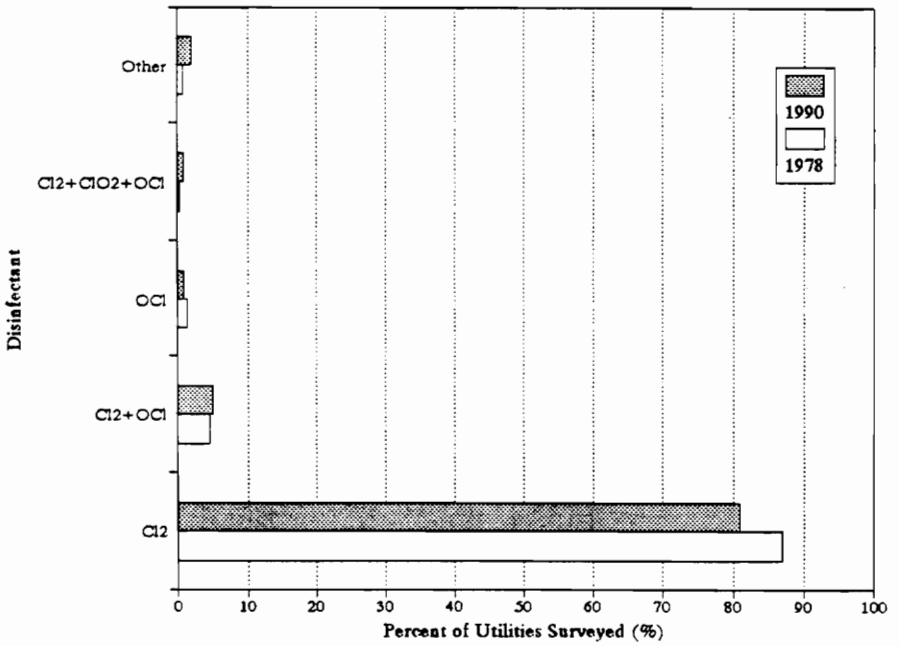

Figure 2.2. Comparison of Drinking Water Disinfection Practices Observed in Industry Surveys, 1978 and 1990 (Hoehn, 1978; AWWA, 1990)

The formation of halogenated disinfection byproducts (DBPs) was reported by Rook in 1974 with the identification of chloroform and other trihalomethanes (THMs) due to chlorination of natural waters. Subsequent research (Rook, 1980; Christman, 1983; Singer and Reckhow, 1990) indicated that THMs represent a small fraction of the halogenated organics created by chlorination. Stevens *et al.* (1989) conducted a survey of 10 water works and identified 196 compounds attributable to chlorination in finished water. Another more comprehensive study of 35 utilities provided a broad based assessment of DBP formation and is summarized in Table 2.1 (Metropolitan Water District of Southern California *et al.*, 1989) .

Table 2.1. Finished Water DBP Type and Concentration Determined from a Seasonal Survey of 35 U.S. Water Utilities

Disinfection Byproduct	Median Concentration (ug/L)
Trihalomethanes	36.50
Haloacetic Acids	17.00
Aldehydes	5.77
Haloacetonitriles	3.28
Chloral Hydrate	2.07
Haloketones	1.18
Cyanogen chloride	0.60
Trichlorophenol	0.40
Chloropicrin	0.12

Source: 59 *Federal Register* 38732
Metropolitan Water District of Southern California *et al.*, 1989

Observed values in Table 2.1 reflect finished water concentrations from four seasonal sampling quarters. Facilities with treatment trains involving ozonation were included in the study; higher levels of some species, like aldehydes, were observed at those facilities. Current regulatory emphasis by the U.S. Environmental Protection Agency (EPA) reflects an increased awareness of DBPs other than THMs.

DBP formation is dependant on a number of parameters including available precursor material, oxidant type, oxidant dose, contact time, pH, and temperature. The following sections summarize previous research particularly relevant to this study and the research objectives outlined in Chapter 1. The last section in Chapter 2 describes the source water utilized in this investigation.

Impact of Organic Carbon Concentration

The abundance of NOM in water subjected to treatment is an important parameter in determining the extent of DBP formation (Singer *et al.*, 1989). Kavanaugh *et al.* (1980, p. 578) noted that a wide variety of reactions occur between chlorine and organic matter including: "double bonds, ionic substitutions, {and} partial oxidation." A review of the American Water Works Association's water industry database indicated that surface water total organic carbon (TOC) levels range from non-detectable to 30 mg/L for surface waters in the continental United States (59 *Federal Register* 38714). This same review found that TOC levels at the 25th, 50th and 75th percentiles were 2.6, 4.0 and 6.0 mg/L respectively. TOC concentrations in natural waters vary with geography; higher TOC values tend to occur in the southeastern United States (Table 2.2).

In a simulated distribution system study Meyer *et al.* (1993) found that a one milligram per liter increase in TOC concentration resulted in a 8.5 ug/L increase in total THM formation potential (TTHMFP) (initial TOC, 6.1 mg/L; initial Cl_2 residual, 1.6 mg/L; 4 day formation potential). Reckhow and Singer (1990) reported a TOC normalized TTHMFP (72 hour, pH 7, 20°, 20 mg Cl_2/L) of 52 ug TTHM/mg carbon. Peterson *et al.* (1993) found average THM yields of 11 ug/mg TOC (168 hour, pH 7, 5 mg Cl_2/L residual) in a survey of water treatment systems in Alberta employing

Table 2.2. Total Organic Carbon Concentration Distribution in Raw Waters

EPA Region		n	Minimum Value (mg/L)	Maximum Value (mg/L)
1.	New England	6	3.00	9.00
2.	Northeast	10	2.10	20.00
3.	Mid-Atlantic	20	nd	25.00
4.	Southeast	11	1.60	30.00
5.	Midwest	14	nd	9.17
6.	Central	10	2.00	10.00
7.	South Central	2	7.00	10.00
8.	West	7	1.00	14.00
9.	Southwest	16	nd	5.90
10.	Northwest	4	1.25	3.30

Source: 59 *Federal Register* 38716, 1994.

conventional treatment (sedimentation-coagulation-filtration and chlorination). Reckhow and Singer (1990) found normalized THM, trichloroacetic acid (TCAA), TCP, and total organic halide (TOX) formation to vary less than 23 percent among eight colored, raw waters. HAN and dichloroacetic acid (DCAA) formation were more variable, particularly DCANFP which had a coefficient of variance of 40 percent. Peters *et al.* (1991) found a positive correlation between available organic carbon and total HAA concentration in finished Dutch waters. While a positive correlation between DBPFP and TOC has been established, only 10-20 percent of dissolved organic matter (DOM) in natural waters has been described with respect to chemical character (Servais *et al.*, 1987) providing limited insight into the precursor material to DBPs.

Characterizing Dissolved Organic Matter

DBP formation is believed to result from the halogenation of NOM particularly "humic substances." Humic substances are precursors of sixty percent of TTHMFP in colored waters (Reckhow, 1994). Both autochthonous sources of organic matter, principally extracellular products released by algae (Davis and Gloor, 1981; Hoehn *et al.*, 1984) and allochtanous humic substances contribute DOC in most natural waters.

Numerous authors (Uden and Miller, 1983, Thurman, 1985; Peterson *et al.*, 1993) identified allochtanous sources of aquatic DOC. Randtke *et al.* (1987) identified impoundments where aquatic weeds were a primary source of THM precursors. Hoehn (1980, *et. al*; 1984) identified specific THM precursor production by algal biomass. There has been significant and unresolved debate as to which component of "humic substances" contribute most to the formation of DBPs.

Humic Substances

Humic substances are a group of physical and biodegradation products within the DOC fraction of natural waters (Thurman, 1985). Humic substances are present at different concentrations as a function of conditions in each individual watershed, but in general humic substances can be anticipated at concentrations of 0.5 - 4 mg C/L in larger rivers (Thurman, 1985). Because humic substances are the product of organic decomposition, they include the major functional groups found in organic structures. carboxyl, hydroxyl, carbonyl, and phenolic hydroxyl (Thurman, 1985; Peshel and Wildt, 1988). Carbohydrates and amino acids are present at trace levels, one to three percent of the humic fraction reflecting humic source material: carbohydrates (50-60 percent), protein (1-3 percent), and lignins/phenolics (10-30 percent) (Choudhry, 1984; Thurman, 1985).

This diverse chemical character is reflected in efforts either to fractionate DOC into its individual components or coagulate natural waters to remove DBP precursors. To facilitate discussion of humic substances, this broad category is typically divided into two components; fulvics and humics. Humic and fulvic substances are functional definitions derived from soil science, and based on acid solubility (Choudhry, 1984). In typical riverine, raw waters the fulvic and humic fractions are 82 and 15 percent of the dissolved NOM present (Thurman, 1985). Fulvic substances tend to be smaller than humic substances and are acid soluble; the fulvic fraction is generally viewed as more reactive than the humic fraction. The fulvic fraction is typically composed of substances less than

2,000 AMW, while humic materials are typically greater than 2,000 AMW (Thurman, 1985; Amy *et al.*, 1992). Others suggest a larger AMW distribution for fulvics and hydrophilic neutral fraction, 1,000-5,000 AMW. There is general consensus that the 1,000-10,000 AMW fraction is a major source of TTHMFP (Reckhow, 1992).

There are differences in the abundance of functional groups between the humic and fulvic substances (Table 2.3).

Table 2.3. Characteristics of Fulvic and Humic Substances

Characteristic	Fulvic	Humic
Acidic Functional Groups	More	Less
Carboxyl Functional Groups	More	Less
Aromatic Structures	More	Less
Polysacchridelike Structures	More	Less

Source: after Blondeau, 1986.

J de Laat (1982) found that aliphatic, acid, aldehyde, and alcohol structures are relatively inert to chlorination. Thurman (1985) estimated the aromatic:aliphatic ratio in the fulvic fraction to be 1:2. He also noted that while total nitrogen content was only one percent by weight, amino acids were the source of 15 to 20 percent of the nitrogen present. Nitrogen and amino acid content in the humic fraction was typically twice that observed in the fulvic fraction (Thurman, 1985).

Color and UV absorption are attributable to the structural composition of the DOC present in the water. Oliver and Thurman (1983) found strong correlations between THMFP and water color. UV absorbance is particularly attributable to the aromatic structures, which are active as precursors for THM formation (J de Laat, 1982; Reckhow *et al.*, 1990; Amy *et al.*, 1992). Observing coagulation effects, Najm *et al.* (1994) noted a stronger correlation between UV absorbance reduction and DBP formation than DOC removal, suggesting a larger role for UV absorbing precursors in DBPFP. Analyzing trends in bench scale and field data tests, Harrington *et al.* (1992) found that an increase in UV 254 nm absorbance was correlated with decreasing THM precursor apparent

molecular weight. A 15 hour reaction study by J de Laat (1982) indicated that the presence of activating groups, -OH and -NR_2, enhanced chlorine reactivity with aromatic precursor molecules.

The relative abundance of functional groups, particularly carboxyl groups, and longer fatty-acid chains, results in a tendency for the humic fraction to be hydrophobic (Thurman, 1985). This hydrophobic character contributes to humics associating with iron and aluminum oxides in solution (Thurman, 1985). Reckhow *et al.* (1990) found this hydrophobic fraction to be rich in precursors to TCAA and DCAN and poor in precursors to TCP. Employing 72 hour formation potential tests on ten humic and fulvic acids at high chlorine doses (e.g., 20 mg Cl_2/L), Reckhow (1992) observed that the humic fraction produced more DCAN than the fulvic fraction, while the hydrophilic base fraction produced more DCAN on a weight basis.

Table 2.4 after Reckhow and Singer (1990) compares the chlorination products of humic and fulvic substances. Chlorination produced chlorinated byproduct yields which were very similar to those obtained in similar tests of humic and fulvic substances.

Table 2.4. Relative Chlorination Byproduct Yields for Ten Humic Substances

	Percent Cl	Percent of TOX			
Fraction	Incorporation	$CHCl_3$	TCAA	DCAA	DCAN
Fulvic Acid	27.7	19.8	15.3	5.3	0.22
Humic Acid	24.6	19.6	21.0	6.1	0.38
10 City Average	23.0	23.0	22.2	6.8	0.34

After: Reckhow and Singer, 1990.
Notes: Formation potential test conditions were pH 7 and 72 hour.

Characteristics Associated with Apparent Molecular Size

Researchers routinely separate NOM into apparent molecular weight (AMW) size fractions using ultrafiltration. Nominal molecular weight cutoffs (MWCOs) range from 500 to 300,000 AMW. Response to treatment can be segregated into specific AMW bins

(e.g., 1,000-10,000, 10,000-30,000 AMW) using serial filtration or arithmetic manipulation of MWCO fraction responses.

In a summary of research from ultrafiltration and gel separation experiments, Thurman (1985) found little consistency among natural waters in the relative distribution of NOM within the fractions observed. The primary area of agreement in prior research was the appearance of most aquatic NOM in the 10,000 MWCO fraction. Distribution of DBP precursors among AMW fractions is also source water specific. Laine *et al.* (1993) found up to 21 percent variation in TOC removal by nanofiltration membranes (e.g., 200 and 500 MWCO) among three waters; variation in removal of UV absorbing substances was even larger at 39 percent, thus illustrating the source water specificity of NOM AMW distribution and chemical characteristics.

A number of researchers evaluated the linkage between THM formation and AMW. While the structural character of the DOC present is most critical to determining which DBPs will be generated upon chlorination, Table 2.4 illustrates that general trends can be attributable to general characteristics like AMW (Oliver and Thurman, 1983; Veenstra and Schnoor, 1980; El-Rehaili and Weber, 1987; Reckhow *et al.*, 1992). Oliver and Visser (1980) fractionated stream and lake fulvic and humic acids, then they investigated $CHCl_3$ formation as a function of substrate and AMW fraction. This work demonstrated discernable fulvic and humic acid THM formation (72 hours, 15 mg Cl_2/L, 20°C, pH 11, 1 mg DOC/L). $CHCl_3$FP from lake and stream fulvic and humic acids in the 1,000-30,000 AMW fraction was greater than formation potential in larger MWCO fractions. In substrate specific trials of size separated soil, natural water, and yeast culture extracts, $CHCl_3$ formation was only observed in <1,000 AMW fraction, when the substrate was a microbial extract. TOC normalized formation potentials were more evenly distributed across AMW fractions than formation on a per liter of sample basis.

Joyce *et al.* (1984) made more limited but similar findings to Oliver and Visser (1980). Using soil extracted fulvic acid samples and natural waters, a greater $CHCl_3$FP, by weight, was attributed to the greater number of active sites in the <10,000 AMW

fraction and particularly the 1,000-5,000 AMW range. Veenstra and Schnoor (1980) found 88 percent of the TOC and 87 percent of TTHMFP to occur in the <3,000 AMW fraction.

In pilot scale filtration tests ultrafiltration (100,000 MWCO) did not change THM simulated distribution system formation (SDS) response, but HANSDS response decreased 25 percent. Nanofiltration (400-600 MWCO) reduced both THMSDS and HANSDS greater than 70-80 percent respectively (Laine *et al.*, 1993). DBPSDS was reduced with nanofiltration treatment when the molecular weight cutoff (MWCO) was 200 to 300 AMW (Laine *et al.*, 1993; 72 hour, 0.1-0.55 Cl_2/L residual, 20°C, ambient pH). Laine *et al.* (1993) also cited Mulford *et al.* (1991) who used gas chromatography-mass spectrometry (GC-MS) to observe 90 percent reduction of 26 disinfection byproducts by removing precursor material using a nanofiltration system with a 500 MWCO. DBPFP reduction was attributed to removal of precursor materials by the MWCO filters. Peak HAN and TTHM formation was observed in higher AMW fractions in ultrafiltration range (i.e., 30,000 AMW) by Reckhow *et al.* (1990). Positive correlation between nitrogen content with increasing humic substance size was suggested as a reason for this observation (Reckhow *et al.*, 1990).

Effects Associated with Coagulation

Removing NOM and thereby organic precursors to DBP formation is increasingly the operational goal for coagulation processes in water treatment plants. Removal of NOM through coagulation has been an active research topic. Previous research identified two NOM removal mechanisms, "precipitation by cationic species and adsorption on organic or inorganic solids" (Dempsey *et al.*, 1984). Reckhow and Singer (1990) found that coagulation removed 50 to 90 percent of DBP formation potential from an impounded water (6.8 mg DOC/L, 40 NTU).

Individual authors have pointed out significant trends in coagulation treatment that are particular to humic and fulvic substances. Amy *et al.* (1992) found low molecular weight

fulvic acids to be hydrophilic and not amenable to coagulation; the higher carboxylic acidity of fulvic acids played a role in this behavior. Reckhow and Singer (1990) noted that coagulation resulted in a species shift in DBP formation specifically citing a change in the three day, pH 7 TCAAFP:THMFP ratio from 1.3 to 0.5 after coagulation.

Davis and Gloor (1981) noted that organic compounds with molecular weights below 1,000 were poorly adsorbed to colloidal alumina and that adsorption peaked with organic compounds for molecular weights between 1,000 and 3,000. Sinsabaugh *et al.* (1985,1986) found preferential precipitation of larger hydrophilic and hydrophobic dissolved organic molecules and persistence of DOC <500 AMW in Harwood's Mill Reservoir water coagulated using iron sulfate. Studying this same water Knocke *et al.* (1986) found alum provided greater removal of <1,000 AMW DOC fraction than ferric sulfate. Sinsabaugh *et al.* (1985, 1986) noted a shift in TTHM precursor dominance from fulvic acids to low-AMW, neutral compounds as a result of coagulation; these researchers also cited lower specific THM yields after treatment, and witnessed slower reaction rates due to the shift in DOC character resulting from treatment.

Knocke *et al.* (1986) observed a 50 percent reduction in THMFP studying waters from southeastern Virginia, including Harwood's Mill Reservoir water; the relative rate of THM formation increased with treatment (30 percent). Coagulation with aluminum and ferric salts successfully removed >10,000 AMW NOM. Several authors have investigated selectivity within DOC removal by coagulation (Weber and Jodellah, 1985; El-Rehaili, 1987; Tipping *et al.*, 1991). Summarizing this research Amy *et al.* (1992, p. 68) suggested that in general "coagulation ... reflects the intact removal of mostly high-molecular size material."

Reviewing research in the field, Reckhow and Singer (1990) found that coagulation preferentially removing the larger, humic acid fraction and hence UV absorbent fraction more effectively that the fulvic acid fraction. Based on raw water from 10 southeastern United States sources, Reckhow and Singer (1990) suggested that following degree of coagulation effect on DBPFP removal: "DCANFP > TCAAFP > DCAAFP > THMFP

(TOXFP) > TOC > TCPFP" and attributed the high degree of DCANFP removal to the hydrophobic humic fraction. More recently researchers (Randtke *et al.*, 1994; Smith *et al.*, 1994) have made similar findings with respect to TTHM, THAA, total organic halogen (TOX), and UV absorbance with respect to one and seven day formation potential tests. Smith *et al.* (1994) found relative CH and THAN formation potential reduction by coagulation to be greater in high TOC (≥ 4 mg/L) waters than in low TOC (≤ 2 mg/L) waters. THK formation appeared to be insensitive to coagulation in this same study.

Formation Potential as a Function of Chlorine Dose

Kavanaugh *et al.* (1980) and Najm *et al.* (1994) found a correlation between chlorine dose and free chlorine contact time with DBP formation. Kavanaugh (1980) conducted a series of batch tests to evaluate the effect of chlorine dose on the rate of THM formation, and found a positive and increasing trend with THM formation. Meyer *et al.* (1993) observed THM formation of 19.6 ug/L for every milligram of chlorine introduced to water with a DOC of 1.56 mg/L. CH formation was also observed to increase with Cl_2 dose. Engerholm and Amy (1983) evaluated the relationship between $CHCl_3$ formation and Cl_2/TOC ratio in 96 hour, pH 7, 20°C formation potential tests; these researchers found that the $CHCl_3$ formation reaction to be limited at Cl_2/TOC ratios between 2 and 6. When observing SDS formation tests Symons *et al.* (1993) observed that lower chlorine dosages (free chlorine concentrations less than 1 mg/L) resulted in little chlorinated HAA species formation.

General agreement on the correlation of free available chlorine and total THM formation potential lead to the inclusion of a standard free available chlorine (FAC) residual, 3 - 5 mg Cl_2/L, in Standard Method 5710B, TTHMFP Test (Standard Methods, 1989). Symons *et al.* (1993) notes that a FAC residual of 3 mg/L insures adequate reaction even in the presence of Br^- and does not artificially inflate THMFP. Work by this same author (Symons *et al.*, 1994) employed four day free chlorine residuals of 3 -

5 mg/L in recent research efforts. Peterson *et al.* (1993) evaluating DOC equalized formation of THMs maintained 5 mg/L final chlorine residuals.

Effect of Bromide

In development of the proposed D/DBP rule EPA developed a DBP Regulatory Assessment Model, to predict DBP formation after different treatment scenarios, including coagulation-flocculation. Calibration of this model found that predictions substantially based on available THM and HAA data underestimated TTHM formation by 20 to 30 percent when source waters contained high bromide ion concentrations (Harrington *et al.*, 1992). This same trend was observed for THM and HAA concentrations in low-bromide, North Carolina waters (Grenier *et al.*, 1992).

Bromide occurrence in natural waters varies with geographic location (Table 2.5). A nationwide survey of 70 water utilities by Amy *et al.* (1992) found bromide ion concentrations to range from <0.005 to >3.0 mg/L. An earlier survey indicated a similar range, and reported a median bromide level of 0.1 mg/L (Krasner *et al.*, 1989).

Table 2.5. Bromide Concentration Distribution in Raw Waters

EPA Region	n	Minimum Value (mg/L)	Maximum Value (mg/L)
1. New England	8	0.005	0.089
2. Northeast	4	0.023	0.093
3. Mid-Atlantic	8	0.005	0.276
4. Southeast	7	0.010	0.190
5. Midwest	6	0.012	0.322
6. Central	7	0.014	>3.000
7. South Central	6	0.042	0.206
8. West	7	0.006	0.368
9. Southwest	11	0.008	0.429
10. Northwest	6	<0.005	0.015

Source: 59 *Federal Register* 38722, 1994.

Particular sources of bromide include salt water intrusion, brines present in groundwater, urban/agricultural runoff. Bromide can also be introduced to drinking water as an impurity in chlorine used to disinfect (Cooper *et al.*, 1985). Once introduced to a natural water bromide is a conservative substance taking part in few chemical reactions (Hutton and Chung, 1994).

When bromide is present in drinking water, it is in equilibrium with two dissociated forms, hypobromous acid (HOBr) and hypobromite ion (OBr^-) (Eq. 2.3).

$$HOBr \Leftrightarrow OBr^- + H^+ \qquad \text{(Eq. 2.3)}$$

$$HOCl + Br^- \rightarrow HOBr + Cl^- \qquad \text{(Eq. 2.4)}$$

Br^- and NH_3 compete for HOCl (Eq. 2.4); "NH_2Cl formation is favored at moderately high pH (≈8)" (Bousher, 1989). HOBr reacts with organic matter to form brominated DBPs (Minear and Bird, 1980; Oliver, 1980; Dore *et al.*, 1988; Glaze *et al.*, 1993; Laine *et al.*, 1993 after Morris, 1975). The generally held view regarding bromine-chlorine kinetics was summarized by Laine:

> "Hypobromous acid competes with chlorine for precursor material to form brominated THMs. Hypobromous acid reacts more rapidly with precursor material than chlorine to form THMs thus as Br^- concentration increases more hypobromous acid is produced, greater concentrations of brominated compounds are observed" (Laine, 1993, p. 97)

Differences in THM speciation are attributed to "chlorine acting preferentially as an oxidant, whereas bromine is a more effective halogen-substituting agent" (Cooper, 1985). Cooper (1985) interprets research by Luong *et al.* (1982) to suggest that the addition of bromide enhances chlorine oxidation reaction rates and results in increased "total halogen consumption". Hutton (1994) suggests that the speciation of brominated DBPs is not simply the product of stoichiometric equations.

Bunn *et al.* (1975) observed increased THM yield and shifts in THM speciation with increasing bromide concentration. Both field tests and laboratory studies by Fayad (1993)

in Saudi Arabia illustrated that chlorination of desalinated water-groundwater blends where Br^- was 0.3-8.0 mg/L and nonvolatile DOC (NVDOC) was <0.1-17.5 mg/L, TTHM formation was dominated by brominated THMs. Siddiqui and Amy (1993) found that bromide ion concentrations between 0.5 and 1.5 mg/L affected the distribution of DBP species formed (0.4-1 residual Cl_2/L, pH 6.4-9.4, reaction time 2-40 hours). Summers *et al.* (1993, p. 89) summarized previous THMFP studies noting that "with increasing bromide, the concentration of $CHCl_3$ decreases, the concentration of $CHBr_3$ increases, and the concentrations of both $CHCl_2Br$ and $CHClBr_2$ pass through a maximum formation" (168 hour, pH 7, 25°C, 11.2 mg/L Cl_2 dose, 2.8 mg NVTOC/L). Oliver (1982) observed increasing TTHM formation (24 hour, 20°C, pH 7, 25 mg Cl_2/L,2.5 mg substrate/L), as well as speciation to more brominated THMs with increasing bromide concentration. Beyond speciation, bromide incorporation as a percentage of TTHMFP at a range of temperatures (10°, 20°, 30°C), chlorine doses (2.5, 5, 10 mg Cl_2/L) and pH ranges (pH 6-9) varied with Br^- concentration; percent incorporation increasing with declining Br^- concentration (Minear and Bird, 1980; Veenstra and Schnoor, 1980)

Recognizing conservative passage of Br^- through ultrafilter membranes, Summers *et al.* (1993) conducted THMFP trials under controlled Br^-:DOC ratios (16 mg Cl_2/L, 23°C, 3 day, pH 7.4-7.8, 0.03 mg Br^-/L; 11 mg Cl_2/L, 20°C, 7 day, pH 7, 0.18 mg Br^-/L, Cl_2:DOC ratio of 2:1). Summers *et al.* (1993) observed a shift to brominated THM species and higher brominated THM formation under low DOC concentrations (e.g., high Br^-:DOC ratio).

Symons *et al.* (1993) found that bromide concentration impacts speciation of DBPs generally, and increased total DBP yield. Harrington *et al.* (1992, p.81) utilizing data from bench scale coagulation studies and field data from geographically diverse locations found that "an increase in bromide concentration leads to an increase in the AMW of the THM species formed."

Pourmoghaddas *et al.* (1993) observed shifts in HAA pattern described earlier as a function of bromide ion concentration . Dibromochloroacetic acid (DBCAA) formation

was observed to decrease while monobromoacetic acid (MBAA) formation increased. Peters *et al.* (1991) in a study of 20 water treatment plants determined that brominated HAAs were present in treated Dutch waters (bromide range 0.1-0.5 mg/L). This study identified eight HAAs, six of which were brominated and constituted 65 percent on a mass basis; moreover, dibromoacetic acid (DBAA) was the dominant HAA identified by the study. While chlorination (0.06-0.4 mg Cl_2/L) resulted in three to seven fold increase in HAA abundance, HAAs were present at detectable quantities in all the surface waters tested even those not chlorinated.

In a parallel study of nine Dutch finished waters, Peters *et al.* (1990) estimated DCAN, BCAN, DBAN, $CHCl_3$, $CHClBr_2$, $CHClBr_2$, and $CHBr_3$ formation. Observed DOC values ranged from 1.7 to 5.6 mg/L. At six plants applying chlorine the DOC:Cl_2 dose weight:weight ratio ranged from 0.34 to 186.7. Brominated HANs were more abundant than chlorinated HANs, totaling 60 percent of the observed HAN concentration. HAN formation was 5 percent THM formation on a weight basis. Brominated HAN species concentrations were greatest when the DOC:Cl_2 dose ratio was between 5.6 and 11.8 but insufficient data was developed to explain HAN speciation.

Laine *et al.* (1993) employed Br:Cl weight ratios to illustrate the effect of bromide ion on THM and HAA speciation. These authors suggested that total DBP production will be constrained by DOC concentration even when bromide ion is present in abundance. Specific DBP observations in this research included a doubling in raw water simulated distribution system HAA formation potential (HAASDS) concentrations with increasing bromide concentration from <0.4 to 1.6 mg Br^-/L. Laine *et al.*'s observations were made under constant Cl_2:TOC wt:wt ratios of 1.5 to 1.7; Br^-:Cl_2 dose wt:wt ratios ranged from 0.06 to 0.64 (raw to nanofiltration) employing 3 day SDS tests (20°C, ambient pH). Laine *et al.* suggested that, while water quality and membrane type affect total THMSDS and HAASDS formation, the Br:Cl ratio is more significant than the type of precursor material present or filtration membrane treatment in determining the distribution of THMSDS and HAASDS species.

Symons *et al.* (1993) suggested that the initial Br^-:average Cl^+ molar ratio controls bromide substitution reactions in THM formation; kinetics drive this substitution reaction to completion even in the presence of HOCl which will only form $CHCl_3$ if it is present in excess when the bromide substitution reaction is complete. Both Symons *et al.* (1993) and Summers *et al.* (1993) found the rate of THM-Br formation to be faster than THM-Cl formation. Symons *et al.* (1993) predicted precursor limited THM formation due to TTHM-Br consumption of available sites prior to TTHM-Cl formation.

Formation Potential as a Function of Time

Several researchers have investigated the role of time in the formation of DBPs. $CHCl_3$ formation is generally accepted as increasing with chlorine contact time (Johnson and Jensen, 1986). Stevens *et al.* (1989) found that DCAA, like $CHCl_3$, increased with reaction time. Symons *et al.* (1994) suggested that this increasing trend was true of HAAs and THMs generally, and that while continuing to increase DBP formation is essentially complete after 4 days (Standard Method 5710B test conditions). Pourmoghaddas *et al.* (1993) observed DBCAA, TCAA and DCAA formation to increase as a function of reaction time. Two DBPs, chloral hydrate (CH) and DCAN, have been observed to achieve peak formation potentials and decline with time. Studying DBP formation in an artificial distribution system Meyer *et al.* (1993) found CH reached a peak concentration at 24 hours. DCAN decreased as a function of reaction time decaying completely over a seven day period at a pH of 7 (Stevens *et al.*, 1989, Reckhow *et al.* 1992).

Effect of pH on Formation Potential and Formation Potential Removal

Both specific DBP formation potentials and degree of precursor removal by coagulation are affected by pH.

Formation Potential

Stevens *et al.* (1989) asserted that pH is the most important chemical variable in chlorination byproduct formation. THM species formation resulting from chlorination increase with increasing pH (observed pH 5, 7, 9.4) at a fixed reaction time (Stevens *et al.*, 1989; Kavanaugh, 1980; Engerholm and Amy, 1983). CH also forms more rapidly when pH is high, but formation rate is unaffected by change in pH when the working range is between 5 and 7 (Stevens *et al.*, 1989).

Other non-THM species were found to decrease with increasing pH at chlorination (Stevens *et al.*, 1989). Pourmoghaddas *et al.* (1993) found DBCAA followed this general trend and DBAA was unresponsive to pH change between 5 and 9.4, but DCAA and TCAA formation increased with increasing pH over this same range. These authors found TCAA formation to be consistent with time at pH 5 and 7 but "significantly lower at pH 9.4". Stevens *et al.* (1989) also found DCAA formation to be independent of pH, but responsive to reaction time.

DCAN was observed to be stable at a pH of 5 and decreased in concentration with increasing pH. Declining non-THM DBP production with increasing pH is also associated with TOX generally (Johnson and Jensen, 1986; Stevens *et al.* 1989). Table 2.6 summarizes this discussion graphically.

Coagulation

Aluminum-fulvic acid complexes are stable at pH 3 to 5 (Schnitzer, 1978). Researchers have found that complexation with aluminum is generally favored at intermediate pHs (Saar and Weber, 1982; Benschoten and Edzwald, 1990). Najm *et al.* (1994) observed maximum THM removal by coagulating at pH 5.5. This same research proposed that alum coagulation preferentially removes HAA precursors over THM precursors.

Table 2.6. DBP Formation with Respect to pH

DBP	pH 5	pH 7	pH 9.4
TTHM	Lower formation		Higher formation
Haloacetic Acids			
TCAA	---------- Similar formation ----------		Lower formation
DCAA	---------- Similar formation ----------		
Haloacetonitriles			
DCAN	Higher formation	Forms in 4 hours and decays over time to <5 ug/L.	Trend not discernable (<2 ug/L)
BCAN	---------- Trends not discernable (<2 ug/L) ----------		
DBAN	---------- Trends not discernable (<5 ug/L) ----------		
TCAN	---------- Not detected. ----------		
Haloketones			
1,1,1-TCP	Higher Formation	Trends not discernable (<2 ug/L)	Not detected
Chloral Hydrate	---------- Similar formation ----------		Forms in 4 hours and decays over time.
Chloropicrin	---------- Trends not discernable (<1 ug/L) ----------		

Source: after Stevens *et al.*, 1989

Formation Potential as a Function of Temperature

Evaluating data published by Stevens, Kavanaugh (1980, p.581) suggested that the $CHCl_3$ "formation rate constant doubles with every 10°C increase in temperature" (range, 0-30°C). Engerholm and Amy (1983) observed increased $CHCl_3FP$ with increasing temperature at pH 7 and temperatures of 10, 25, and 35°C. Siddiqui and Amy (1993) found that bromoform formation increased with increasing temperature. Stevens *et al.* (1989) proposed that increasing temperature will either yield higher concentrations of DBPs or result in the hydrolysis of CH, dihaloacetonitriles (DHAN), CP and HAAs to yield a net decrease in DBP concentrations.

Pre-oxidation with Potassium Permanganate

Reviewing previous research by Blanck, Kreft, Lang and Singer, Gillford *et al.* (1989) suggested that raw water oxidation using potassium permanganate ($KMnO_4$) at concentrations greater than 1 - 1.5 mg/L can effectively decrease organic precursor reactivity with chlorine, to form less THMs. Harrington (1992) noted that pre-oxidation of NOM decreased NOM molecules size and increased NOM particle charge.

Nitrogen Sources and Haloacetonitrile Formation

Oxidation and substitution were two mechanisms of chlorine-organic reaction identified by Johnson and Jensen (1986). Chlorine substitution was identified as the dominant chlorine-organic reaction mechanism, but at higher chlorine doses, oxidation and cleavage reaction processes are believed to yield increased THM formation. These authors suggested that chlorine oxidation of organics and organic nitrogen generally yields stable acids (carboxylic), nitrogen gas and chloride. Substitution of chlorine into the organic reactant is less frequent, but both carbon and nitrogen can act as substitution sites. Johnson and Jensen cite Stanbro (1979) stating that chloramines are formed by chlorination of amino acids.

Bieber and Trehy identified BCAN and DCAN as DBPs in 1979 (Bieber and Trehy, 1983). Chlorination of amino acids (aspartic, tryptophan and tyrosine) at a Cl:amino acid weight ratio of 16 resulted in the formation of DCAN and CH (Trehy *et al.*, 1986). Chlorination of lake waters by these same authors also demonstrated DCAN and CH formation, moreover, DCANFP and CHFP occurred independent of $CHCl_3FP$ suggesting different precursors. Regression analysis of DCANFP and humic substrate nitrogen content by Reckhow *et al.* (1990) found a significant r^2 of 0.87. Berne *et al.* (1994) studied amino acid and nitrogen levels in the drinking water treatment train at Méry sur Oise, finding that amino acid concentrations in raw water and finished water concentrations ranged from 33 to 85 ug/L N and 22 to 50 ug/L N, respectively, over a 13 month period. Organic nitrogen levels were more stable than amino acid concentration; average observed raw and finished water concentrations were 44 ± 5 and 48 ± 3 ug/L N, respectively. Seasonal fluctuations reflected higher values during the growing season.

Young and Uden (1994) demonstrated that chlorination of cytosine will result in the formation of $CHCl_3$ and DCAN. These researchers also observed formation of CH, DCAA and TCAA, as well as, $CHCl_3$ after chlorination of uracil. $CHCl_3FP$ and DCANFP were unresponsive to chlorine dose (8:1 and 15:1 hypochlorite:compound ratios were tested).

Some DBPs are intermediate products in the formation of other DBPs. Choral hydrate is viewed as an intermediate in the formation of $CHCl_3$ (Meyer *et al.*, 1993). Hydrolysis of DHANs to HAAs has been observed by Leer *et al.* (1986), Oliver (1983), and Peters *et al.* (1990); hydrolysis is more rapid in the presence of free chlorine. Peters *et al.* (1990) indicated that hypochlorite has a role in catalyzing this reaction.

Description of Source Water

The Harwood's Mill Water Treatment Plant provided raw and coagulated water for this analysis. Harwood's Mill has been an active research site for water treatment research since its design and construction in 1986. This section summarizes the facility's current treatment train and previous research by other authors regarding influent water character and DBP formation.

Description of Harwood's Mill Facility

Harwood's Mill Water Treatment Plant is one of two water production facilities operated by the Newport News Water Department. Facility design centers on the use of a Superpulsator®, a patented upflow clarifier produced by Inflico-Degremont (Figure 2.3).

The facility receives water from two sources, the Chickahominy River and the Diasin Creek Reservoir. Both of these facilities are located at substantial distances from the water plant, although both are east of the fall line. Water quality in the Chickahominy and Diasin Creek basins are reflected in the water received at Harwood's Mill, but substantial changes in water quality result from water storage and water transport.

Once water reaches the plant site it is stored in a 500 million gallon, surface water storage reservoir, known as Harwood's Mill Reservoir. The Harwood's Mill Reservoir has a very limited watershed, and surface water runoff to the reservoir has a minimal impact on the

facility's storage capacity. One aspect of reservoir water quality is related to the immediate drainage; the supernatant from the water treatment plant's sludge management component enters the reservoir upstream of the water intake.

The reservoir is 20 feet in depth; drawdown occurs on an as needed basis through gate structures at the northeast end of the impoundment. Gate controls will allow intake to occur at depths of 5 to 10 and 15 to 20 feet. Treatment capacity at the facility is 31 MGD, facility capacity being determined by the Virginia Department of Health based on the most limiting feature of the plant, the filters at 4 gpm/ft^2. This capacity is evenly split between two mirror image treatment trains. Both are operated unless system maintenance requires taking one train off line. Current production is occurring at 24 to 25 MGD, and the plant is in 24 hour operation.

Finished water quality management begins in the reservoir itself. In order to reduce taste and odor, as well as disinfection byproduct issues in the finished water, copper sulfate is applied to the reservoir. Application occurs on an as needed basis based on total colony counts or problems experienced in the water treatment plant. Copper sulfate is applied by boat at 0.5 mg/L; this dosage is calculated based on a ten foot deep photic zone although the photic zone is believed to reach 20 feet. Application of copper sulfate negatively impacts water treatment plant sludge disposal rates, creating an internal check on its usage. Typically copper sulfate is applied twice per month in the summer. Usage in winter months is limited to applications every other month.

Influent raw water quality can be generally described as follows. Turbidity is typically 1.5 to 5 NTU and averages 2 - 2.5 NTU. Color is present at 25 - 50 color units. TOC fluctuates over a diurnal cycle, typically within 2 mg/L, but is relatively stable over the year (range, 4 - 6 mg TOC/L). pH is typically 7.0 to 7.3.

Actual water treatment begins with introduction of water into the plant treatment trains at the pump house. Mechanical screening occurs during the entry of water into the pump chamber. Water samples taken from this chamber clearly reflect the debris collected by these screens. With entry into the water treatment plant several key treatment issues drive plant

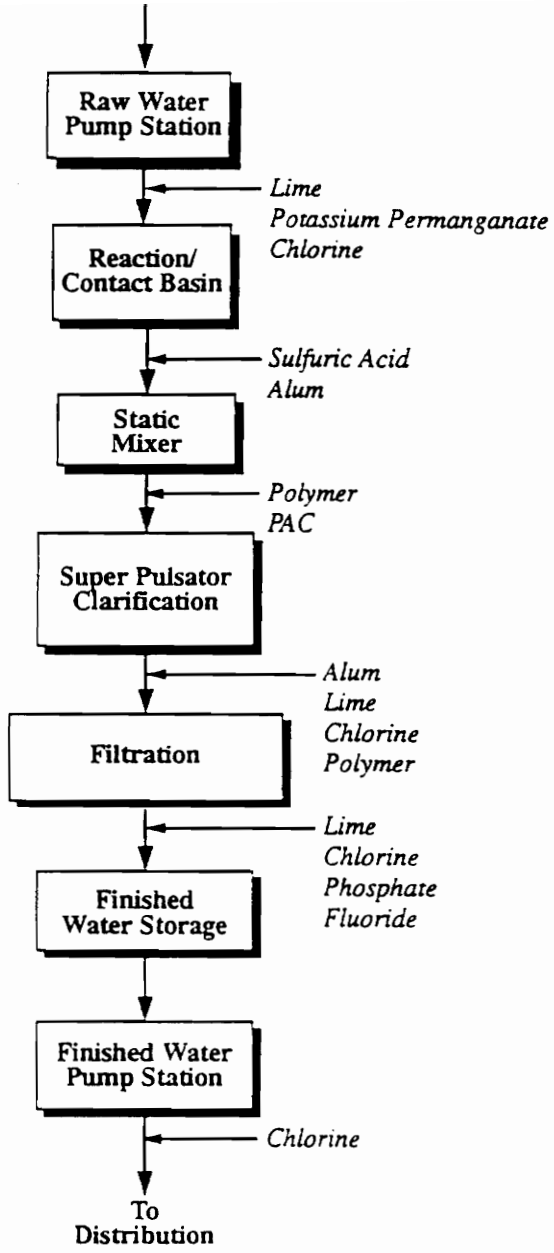

Figure 2.3. Harwood's Mill Water Treatment Plant Flow Diagram

operation: (1) iron and manganese control, (2) improving the character of the coagulation floc, and (3) taste and odor control.

Raw water is pumped to the main facility by two 15 MGD, two 10 MGD, and one 5 MGD pumps. Water moves to the main facility through two 40 inch water lines. Raw water enters the main facility through a weir structure into a contact basin. Potassium permanganate is introduced to the raw water in these contact basins. Permanganate is introduced at 0.3 mg/L dosage to oxidize iron and manganese. Iron concentration ranges from 0.75 to 1.5 mg/L. While there is little change in the total concentration of iron present, the form present changes. Peak periods of management for iron and manganese are associated with the combination of rain events followed by periods of clear warm weather and the accompanying increase in algal activity (i.e., summer months). Complete oxidation is achieved prior to entry into the Superpulsator®. Chlorine addition is also possible at the contact basins but is not used at this time.

The primary coagulant used at the facility is alum. Alum is fed at 30 to 45 mg/L; the average dose over the year is 35 mg/L. Addition of alum takes place at the flash mixer, which is a rotary turbine design. While the plant is also designed for addition of sulfuric acid in the flash mixer, no appreciable benefit was obtained from the pH adjustment so it is not used.

Floc formed does tend to be very fine and settles poorly. To address this operational issue, a cationic polymer (Allied Colloids, LT 22S) is added at the head of the manifold leading into the Superpulsator® basins at 0.3 mg/L. This addition results in a finished water quality of 0.12 NTU. Plant personnel view this polymer addition as critical to the operation of the Superpulsators®. Severe taste and odor episodes require the addition of powdered activated carbon at 4 to 5 mg/L at this point in the treatment train as well. These occasions occur for less than three weeks each year.

The next step in the treatment train is the Superpulsator® basins, per Virginia Department of Health design guidance there are two clarifiers per train just as there were twin contact basins and flash mixers. The Superpulsator® is a patented design but it is essentially an upflow clarifier, where the pulsation of the water flow into each 8 MGD basin maintains a

sludge blanket. Inclined plastic sheets are employed to insure adequate sludge blanket formation and retention (loading 2.5 gpm/ft^2). Each basin is rectangular in plan view having dimensions of 40 x 78 x 20 feet. Clarified water leaves the basin through a horizontal channel system at a depth of 3 feet.

Upon exit from the clarifier, water travels via central channels to paired multimedia filters. Immediately after coagulation pH is 6.0 to 6.2. Just prior to introduction to the filters the clarified water receives a 5 mg/L dose of chlorine. The eight filters employed at Harwood's Mill are each rated at 3.9 MGD. The filters are of conventional design, having a nominal flow rate of 48 gallons per minute per square foot of surface area. Backwashing occurs on approximately a 72 hour cycle.

Treatment continues post-filter with introduction of hydroflorosilicic acid at 1 mg/L for fluoridation. Hydroflorosilicic acid has a pH of less than 1. Zinc orthophosphate is also added at this stage. The zinc orthophosphate is a critical component of the water system's program to comply with the lead and copper rule. Orthophosphate is added at 1.5 mg/L. Lime is also added at this point to control finished water pH, for which plant personnel target 7.0. Water storage in two 3.25 MG finished water holding tanks provide a 4 hour holding time (at half full) to insure adequate disinfection, no post filter chlorination takes place.

Water Quality and Treatability, Owen *et al.*, 1993

Owen *et al.* (1993) viewed Harwood's Mill water as a low turbidity water and selected it for analysis specifically because of this attribute. Average raw water molecular weight, as determined by ultrafiltration ranged over the following data points: 3,000 (April), 3,000 (July) and 4,050 (January). Analysis of NOM took place both with respect to size fraction and chemical characteristic. Formation potential conditions were 96 hour, 20°C, 7.0 pH, and Cl_2:DOC 3:1; SDS conditions were 24 hour, 20°C, 7.0 pH, and Cl_2:DOC 1:1. $Na_2S_2O_3$ was used for quenching; chlorine residuals were typically in the 2-5 mg/L range. Tables 2.7 and 2.8 summarize the data collected with respect to Harwood's Mill source water character.

Table 2.7 . Raw Water Characteristics

	pH	Alk mg/L	Br^- mg/L	DOC mg/L	UV 1/cm	THMFP ug/L	SDSTHM ug/L
Average	**7.5**	**40**	**0.026**	**4.93**	**0.111**	**119.0**	**72**
April	7.7	36	0.025	4.10	0.106	92.9	55.9
July	7.2	47	0.034	5.10	0.119	144	102
January	7.7	38	0.018	5.60	0.107	120	58.3
CV (%)	5	15	31	16	7	22	36

	HAA ug/L	HAN ug/L	Humic %	Turbid ntu	Org.N mg/L	BDOC (%DOC) mg/L	AOC ug/L
Average	**133**	**8.0**	**48.8**	**0.85**	**0.38**		
April	130	3.7	54.0	--	0.36	0.90 (18.4)	198
July	136	7.5	47.0	--	0.40	0.60 (10.2)	74
January	--	12.9	45.5	0.85	--	0.28 (4.9)	183
CV (%)		3	58	9	0	7	

Source: after Owen *et al.*, 1993.
Notes: Average is across seasons. CV is coefficient of variation.

Owen *et al.* employed bench-scale coagulation tests and evaluated subsequent DBP relatedness to AMW, NOM chemical character, and treatment effects. The coagulation test applied was: (1) rapid mix (1 minute at 100 rpm), (2) slow mix (30 minutes at 40 rpm), (3) quiescent settling (1 hour), (4) filtration (0.22 um filter). Coagulant dosage was based on pre-experiment optimization; baseline bench scale tests were dosed at ≈40 mg alum/L.

Little seasonal variation was observed in DOC or associated THMFP. Comparison with other data by the researchers suggests that the reservoir has a stabilizing influence on DOC character. Sinsabaugh *et al.* (1986) had previously observed that coagulation of Harwood's Mill Reservoir water appeared to remove NOM from all observed AMW fractions but was preferentially removed from higher AMW NOM fractions (i.e, >10,000 AMW). Randtke *et al.* (1994) found raw water TOC at Harwood's Mill Reservoir to differ little from settled water DOC, 3.7 and 3.1 respectively.

Table 2.8. Post-Bench Scale Coagulation Character

	pH	Alk. mg/L	Br^- mg/L	DOC mg/L	UV 1/cm	THMFP ug/L	SDSTHM ug/L
April	7.47	--	--	2.87	0.055	69	38
July	7.1	--	--	4.00	0.056	80	25
January	7.25	--	--	4.05	0.062	96	53
CV							

	HAA ug/L	HAN ug/L	Humic %	Turbid ntu	Org.N mg/L
April	99	3.7	43.0	--	--
July	50	4.3	53.0	--	--
January	--	13.0	52.0	--	--
CV					

Source: after Owen *et al.*, 1993.
Notes: Average is across seasons.
CV is coefficient of variation.

Owens *et al.* did not find total HAA and HAN levels to be correlated with THM levels. Brominated THM formation at Harwood's Mill was less than 40 ug/L; brominated THMs represented less than 20 percent of bulk water THMs, and less than 35 and 40 percent respectively for non-humic and <1,000 AMW components (weight basis). HAAs were dominated by chlorine species, TCAA and DCAA, although some monochloroacetic acid (MCAA) and MBAA were created.

NOM Characterization, Bokka and Schafran, 1994

Bokka and Schafran (1994), investigating NOM and its role in enhanced coagulation, evaluated four raw waters from eastern Virginia in the vicinity of Harwood's Mill Reservoir. These authors found that in general DOC was distributed among three major categories: hydrophobic acid fraction (40 percent), hydrophilic acid (23 percent) and hydrophobic

base/neutral (18 percent). These authors observed that the hydrophobic fraction of NOM was most susceptible to coagulation.

Coagulation and DBP Formation Potential, Smith *et al.*, 1994

Smith *et al.* (1994) investigated the effect of enhanced coagulation on chlorination DBPs. Harwood's Mill was one of eight water facilities providing raw water to this study effort.

Table 2.9. Removal of DBP Formation Potential from Raw Water by Coagulation Observed During Bench Scale Coagulation Study of Harwood's Mill Reservoir Water

		Formation Potential (ug/L)		
Coagulation Condition	pH	TTHM	THAN	THK
Baseline Alum	7.8	50%	43%	42%
Enhanced Alum	5.9	58%	52%	32%

Source. Smith *et al.*, 1994.
Note. 7 day, pH 7.0, 25°C, 3 mg/L Cl_2 residual.

THMFP response to coagulation varied. $CHClBr_2$, $CHBr_3$, and CH all occurred at levels below detection using EPA method 551. HAN species TCAN, DCAN, BCAN, and DBAN were observed before and after coagulation. DCAN, BCAN, and DBAN decreased 34, 12, and 54 percent respectively with coagulation. TCAN increased markedly (300 percent) but was present in <0.1 ug/L levels. HKs, DCP and TCP, were also analyzed; DCPFP decreased approximately 50 percent with coagulation, but TCP decreased much less, 10 percent.

Chapter 3. Methods and Experimental Design

Chapter 3 summarizes the experimental methods that were employed in this research. The experimental design is also outlined describing the series of experiments conducted to address the research objectives outlined in Chapter 1.

Sample Preparation

Water samples were collected in 20 liter Nalgene® containers from the Harwood's Mill Water Treatment Plant. Sample bottles were maintained headspace free and cooled on ice during transport to VPI&SU laboratory facilities (6 hours). Samples were immediately refrigerated at 4°C.

Sample water was then filtered using a Gelman Science, Groundwater Sampling Capsule, 0.45 um (part# 12175) and a Cole-Parmer, Master Flex peristaltic pump. The 0.45 um filter was preceded in series by a Millipore Type SS, 3.0 um filter. Initial filter integrity and effluent quality was determined by filtering MilliQ® water and subsequent DOC analysis. Once filtered, the sample water was stored in Nalgene® containers at 4°C until subjected to additional steps in the experimental protocol.

Chlorine Residual

Determination of available chlorine residual required by the experiment protocols was achieved with amperometric titration, Standard Method 4500-Cl D (modified after Gallagher *et al.*, 1994). Amperometric titration was the selected method because of its broad working range (0.1 - 10 mg Cl_2/L) and simplicity of operation (Gordon *et al.*, 1988). Cooper (1982, 1983) demonstrated that amperometric titration yields reproducible results both with respect to a given sample and among multiple analysts. There is general agreement that amperometric titration is more accurate and subject to fewer oxidant, temperature and turbidity interferences than other methods (Wilde, 1991 after APHA *et al.*, 1980). There are potential interferences from $ClNH_2$ and Cl_3N (White, 1972; Gordon

et al., 1988). The method as practiced is sensitive to Cl_2 + $HOCl/OCl^-$ (Gordon *et al.*, 1988; Aieta, 1984).

A Fisher Scientific computer-aided titrimeter (Part No. 52335 Rev. A) was employed in these analyses. Titration was with 0.00564 N phenylarsine oxide. Titrant addition was to a sample diluted with 100 mL of chlorine demand free water. Potassium iodide was then added (1 gram/100 mL) to the diluted sample, which was also buffered to a pH between 6.5 and 7.0 using a phosphate buffer. Actual sample size varied as a function of anticipated chlorine concentration and demand for sample volume by other protocols. Free chlorine levels in the test volume should be below 2.0 mg/L, but did vary in practice between 0.1 and 6 mg/L. The amperometric titration is computer controlled with the endpoint being determined when titrant addition no longer results in change in electron potential at the platinum electrode.

Addition of potassium iodide is a modification of the Standard Method protocol recommended by Gallagher *et al.* (1994). The resulting values are not "combined chlorine" as the necessary pH range (3.5 - 4.5) is not attained. This method was compared to other available methods to determine free chlorine by Gallagher *et al.* (1994) and that comparison was favorable.

Trihalomethane Formation Potential (THMFP)

Introduction of chlorine to artificial and natural waters to observe the amount of disinfection byproducts generated is the central concept underlying this research. Trihalomethane Formation Potential, Standard Method 5710 B, is the accepted methodology employed to observe formation potential in a uniform and comparable way (Standard Methods, 1989).

Typical THMFPs are prepared within the following parameters: (1) neutral pH, (2) overabundance of free chlorine, (3) a standard time period of seven days (168 hours), (4) temperature of 25° C and (5) dark conditions. These conditions are meant to represent finished water conditions leaving a potable water production facility. Standard Method

5710B involves three steps: (1) chlorine demand determination, (2) sample chlorination and stabilization and (3) sample quenching and chlorine determination.

Chlorine demand determination is actually a short (4 hour) TFP test where the chlorine dose is 5 mg/L in the sample container. Actual TFP dosing employs a chlorine concentration based on this abbreviated test period and calculation of an appropriate dose using equations 3.1 and 3.2.

$$CD = D_0 - R \qquad \text{(Eq. 3.1)}$$

$$D_F = \frac{(CD \times 5)}{D_0} + 1 \qquad \text{(Eq. 3.2)}$$

Note: CD= chlorine demand, D_o= 4-hour test chlorine dose, R = 4-hour test free chlorine residual, and D_F = TFP chlorine dose (Equation 2 assumes 250 mL sample volume).

With sample chlorination, pH adjustment to 7.0 using sodium hydroxide or hydrochloric acid is undertaken as needed. The sample is buffered with phosphate buffer to maintain pH. The sample is sealed headspace free and held for seven days at 25°C in the dark. At the end of seven days the sample is partitioned: (1) 40 mL is quenched and acidified for THM analysis, (2) 35 mL is quenched for HAN extraction and analysis, and (3) the remaining volume is tested for chlorine residual. If the chlorine residual is less than 1 mg/L the THMFP test is not valid. Actual levels of DBPs formed during the incubation period are measured using EPA methods 502.1 and 551.

The Standard Method described above provides the fundamental components of the formation potential protocol followed in this analysis for DBPFP. This analysis varied from the basic method in the following ways: (1) the chlorine level was an experimental parameter that varied within the artificial water experiment matrices, (2) the chlorine dosage for natural water experiments was based on a Cl_2 dose:DOC (mg:mg) ratio of 3:1, (3) available storage facilities resulted in an incubation temperature of 20° C, (4) formation periods shorter than seven days were employed (<1, 24, 48, 96 and 168 hours),

and (5) standardized experiment volumes were adjusted downward to take maximum advantage of available sample volumes (eg. 68, 125, and 250 mL).

Non-Purgable Dissolved Organic Carbon (NPDOC)

Determination of dissolved organic carbon employed the persulfate-ultraviolet oxidation method, Standard Method 5310C. The United States Environmental Protection Agency refers to this technique as non-purgable dissolved organic carbon. An automated laboratory total organic analyzer, model DC-80, produced by the Dohrmann Division of Xertex Corporation facilitated this analysis. Standard Method 5310C uses ultraviolet light to promote chemical oxidation of organic carbon to carbon dioxide; the resulting carbon dioxide level is measured via a linearized, non-dispersive infrared detector.

The procedure involves addition of persulfate (less than 0.25 mL of 85 percent solution) to approximately 5 mL of sample acidifying it to pH 2. This volume is then sparged with oxygen for five minutes to remove CO_2. One milliliter of this volume is injected into the TOC Analyzer after proper settings for anticipated DOC range and baseline adjustments are made. The resulting output is in mg/L based on an external standard. Employing a one mL sample and the 0.1 - 20 mg/L response range the Dohrmann TOC analyzer will produce repeatable results within +/- 0.04 mg/L or +/- two percent (Dohrmann, 1985). Results obtained during this research indicated values can be routinely repeated ±10 percent within the range employed (0.1-6.0 mg DOC/L).

Bromide

Isocratic ion chromatography using a Dionex System 2010i with Dionex conductivity meter CDM-3 provided a means to measure bromide ion concentrations. The Dionex suppressor system (ASRS-I 4 mm, self regenerating suppressor) reflects the general concepts described in Standard Method 4110 B. Co-elution of chloride and bromide ion peaks occurred in MilliQ® water necessitating the use of a mixed standard matrix containing 1.2 mg Cl/L and 1.0 mg NO_3-N/L. Co-elution did not occur in the sample

matrix. Pfaff and Brockhoff (1990) report minor shifts in the bromide ion peak retention time (<0.1 min) as a function of concentration (2.0 - 20 mg/L), when using a similarly configured system employing chemical suppression. Peak shifting was not problematic in this analysis. Monitoring of bromide ion levels was limited to the initiation of each experimental run as formation of hypobromous acid and hypobromite ion occurred with chlorination.

System specific enhancements were employed to achieve improved levels of detection particularly the use of a 200 uL sample loop. The instrument was operated under the following conditions: (1) eluant flow was 2.00 mL/min, (2) system pressure was 1,190 psi, (3) conductivity meter output range was 1 - 3 microseimens, and (4) Dionex AG4A and AG9A, 4 mm chromatography columns (AS9A columns were operated at 1 mL/min.). An external standard curve was maintained to quantitate the chromatographic response. All samples including standards were introduced to the ion chromatograph through a disposable 0.45 Gelman Ion Chromatograph Aerodisc filter.

Trihalomethanes

EPA Method 501.1, Analysis of Trihalomethanes in Finished Waters By Purge and Trap Method, was employed to determine THM levels. The method is appropriate for determination of microgram (0.5 - 1,500 ug/L) quantities of $CHCl_3$, $CHCl_2Br$, $CHClBr_2$, and $CHBr_3$. Instrumentation utilized in these analyses include: (1) Tekmar 3000 Purge and Trap Concentrator, (2) Tremetrics 9001 Gas Chromatograph, (3) Tracor 1000 Hall Detector, and (4) Hewlett Packard 3396 Series II Integrator.

Forty milliliter samples from the TFP method were drawn and quenched using ammonium chloride. Quenched samples were stored at 4°C until analysis, at which time two 5 ml samples were introduced to the purge and trap concentrator. Extracted samples are stable for limited periods of time (1-5 days) when stored at 4°C, acidified to pH 4, and maintained headspace free. Sample storage did exceed five days due to sample volume and equipment availability. Sample integrity is rapidly lost once in contact with air.

Sample introduced to the purge apparatus was subjected to an eight minute purge at 30°C and 5 psi. During the purge period the 30.5 x 0.32 cm Tenax trap (part # 12-0083-303) receiving eluant was maintained at 40°C. After the purge step was complete the trap apparatus preheated to 175°C for 5 minutes. Desorbtion from the trap was then accomplished at 180°C; the desorb period was 4 minutes. With desorb the integrated gas chromatograph cycle was automatically initiated; desorbed sample was injected into the gas chromatograph for one minute. After injection the trap apparatus was baked at 225°C for 6 minutes.

The Tremetrics 9001 gas chromatograph contained a Supelco 2-3086 column (2.4 m, 2.0 mm i.d., 1% SP, 1000 60/80 Carbopack B). Chromatography conditions were somewhat modified from Method 501.1 to achieve adequate analyte separation. Helium was employed as the carrier gas through the column; flow was 60 psi at 65°C. The temperature program began at 65°C holding for 3 minutes, then increasing at 15°C/minute to 220°C, and holding 220_{o}C for two minutes prior to returning to 65°C for the next injection. No pressure program was employed. The Hall Detector receiving the column effluent was maintained at 450°C. A Hewlett Packard 3396 Series II integrator captured the Hall Detector signal output; four output parameters were modified: attenuation (2), area reject (0), threshold (0), and peak width (0.1). Peak area was integrated. Figure A-1.1 illustrates a sample chromatogram.

Table 3.1 summarizes retention times and detection limits, comparing observed gas chromatograph response to documented EPA method characteristics.

Table 3.1. Method 501.1 Retention Times and Detection Limits

Analyte	Retention Time (min)		Detection Limit (ug/L)	
	EPA	Observed	EPA	Observed
$CHCl_3$	10.7	9.5	na	1.68
$CHCl_2Br$	13.7	11.5	na	0.04
$CHClBr_2$	16.5	13.4	na	0.11
$CHBr_3$.	19.2	15.4	na	1.77
TTHM			0.5	

Source: EPA Method 501.1 (1979)
40 CFR 141.30

Note: Time expressed in minutes, detection limit expressed in ug/L.
Limit of Detection based on 3 x standard deviation at lowest observed standard concentration.
(na) Not available, values not specified by EPA.

Analyte concentrations are developed from an external standard curve derived from a weight based standard diluted in water.

Haloacetonitriles, Haloketones, and Chloropicrin

EPA Method 551, Determination of Chlorination Disinfection Byproducts and Chlorinated Solvents in Drinking Water by Liquid-liquid Extraction and Gas Chromatography with Electron Capture Detector, was employed to detect and quantitate HANS, HKs, and CP. Observed analytes included: BCAN, DBAN, DCAN, TCAN, TCP, DCP, and CP (Table 3.2). This method also detects the THMs of interest in this research, but Method 501 utilizing the purge and trap is the preferred method. Chloral hydrate analysis was not attempted as quenching with ammonium chloride results in substantial reductions in recovery of this analyte (EPA Method 551, 1990).

Table 3.2. Method 551 Retention Times and Detection Limits

Analyte	Retention Time (min) EPA	Retention Time (min) Observed	Detection Limit (ug/L) EPA	Detection Limit (ug/L) Observed
DCAN	8.72	14.1	0.019	0.03
TCAN	7.59	11.5	0.092	0.03
DCP	10.73	16.9	0.009	0.02
CP	15.80	24.1	0.012	0.03
BCAN	16.77	26.7	0.011	0.05
TCP	21.36	30.9	0.012	0.03
DBAN	24.03	34.1	0.034	0.15

Source: EPA Method 551, 1990.
Note: Time expressed in minutes, detection limit expressed in ug/L.
Limit of Detection based on 3 x standard deviation at lowest observed standard concentration.

A Hewlett Packard 5890 gas chromatograph containing a 30 m, 0.25 mm i.d., DB-1 (1 um film thickness) column produced by J&W Scientific was employed. Chromatography conditions were somewhat modified from EPA Method 551 to achieve adequate analyte separation. Helium was the carrier gas through the column; flow was 23 cm/sec at 33°C. The temperature program began at 33°C holding for 15 minutes, then increasing at 1°C/minute to 40°C, holding at 40°C for three minutes, increasing at 6°C/minute to 120°C for one minute, then ramping to 150°C and holding for 5 minutes prior to returning to 33°C for the next injection.

Optimizing ECD output required splitless operation, 30 mL/minute nitrogen make-up gas flow, and venting of the injection port 0.7 minutes after injection. Venting was not necessary due to pressure pulse, which is negligible in splitless injection, but to minimize continued sample bleed onto the column from the injector (Grob, 1994; Owens, 1994). A Hewlett Packard 7673 autosampler assured consistent sample injection. Autosampler injection was via a shorter than desirable needle, placing the point of evaporation above the bottom of the injection liner (Grob, 1994). To adjust for sample introduction inefficiency a 2 uL sample was injected. Two microliters provided an adequate response and was within the recommended injection volume range of 1-5 mL for splitless injection

(Grob, 1994). Injection insert packing was not used. The injection needle was flushed repeatedly between samples with methyl-tert-butyl-ether (MTBE) and MilliQ® water. A Hewlett Packard 3396 Series II integrator captured ECD signal output; three output parameters were modified: attenuation (1), threshold (500), and peak width (0.01). Peak area was integrated. Figure A-1.2. illustrates a sample chromatogram. These integrator parameters resulted in some loss of valid peak data at low HAN concentrations.

Preparation of 35 ml quenched sample involved the addition of 8 g of sodium chloride and manually shaking the extraction vial (Sci/Spec 40 mL, 27 x 95 mm amber glass EPA vial, teflon septa) for 20 seconds. Then adding 2 mL of MTBE and again manually shaking, now for 2 minutes. Fisher HPLC grade MTBE was distilled prior to use in the extraction procedure. The resulting MTBE-HAN solution forms a surface layer in the extraction vial after approximately 2 minutes, which is removed with a disposable, glass, Pasteur pipette to an amber glass, target vial sealed with a screw cap and silicon-teflon septa [HP part numbers 5182-0716 (vial) and 5182-0730 (septa)]. Target vials were subsequently refrigerated at 4°C until placed in the autosampler. Storage periods for some samples did exceed the seven day maximum storage period suggested in Method 551. Sample exposure to ambient room temperature prior to injection varied from several minutes to 11 hours.

The resulting chromatogram was interpreted using comparisons with: EPA Method 551 example data, single compound and mixed standards, and chromatograms prepared by other researchers (Smith *et al.*, 1994). Certified mixed standards prepared by Supelco were employed throughout the HAN analysis (Supelco Part # 4-8046).

Xie and Reckhow (1994) observed formation of halogenated solvent artifacts in analytical solvents (including MTBE) exposed to free chlorine, chloramines and free bromine. Identified MTBE artifacts include 1-bromo-2-methyl-2-propanol and bromoacetone. Artifacts like these complicate identification of new DBPs, but are not known to interfere with GC analysis of HANs, HKs, or chloropicrin. Quenching of the

sample prior to the extraction process prevented any competitive effects that would impair this analysis.

DOC Equalization

Equalizing DOC of fractionated and unfractionated waters was intrinsic to the experimental design. When DOC concentrations were higher than required the sample was diluted with MilliQ® water. Waters with DOC levels below the desired concentration were freeze concentrated (Aiken, 1985). Sample water (post-ultrafiltration) was placed in acid washed-triple rinsed glass containers and partially frozen in a Whirlpool no-frost freezer. During the freezing process the sample was stirred periodically to maintain access to the liquid fraction. After 9 to 12 hours the remaining liquid volume was decanted, and the ice fraction allowed to melt. During the thawing process, water was periodically decanted to individual fractions. After DOC analysis of the resulting fractions, appropriate volumes were blended from the different fractions to achieve the target DOC. Table 3.3 summarizes DOC concentration manipulation within the experimental matrix.

Ultrafiltration

Aiken (1988, p. 15) states that, "there is not one universally accepted isolation procedure or operation definition for humic substances"; Thurman (1985) noted that ultrafiltration is an imperfect technique that fails to separate substances based on chemical characteristics. There is general agreement that ultrafiltration is less destructive than alternative separation techniques like gel filtration, and ultrafiltration is an accepted separation technique employed by limnologists and engineers for sorting the dissolved fraction of NOM by MWCO between 500 and 100,000 daltons. Proper function of the ultrafiltration process is sensitive to a number of factors including: storage and processing temperatures, time-to-analysis, and proper operation of the filtration apparatus (Aiken, 1985).

Table 3.3. Summary of DOC Manipulation Required by Experimental Matrix

Matrix/Conditions		DOC (mg/L) Raw <1K	Raw <10K	Raw <30K	Raw <0.45um	Clarified <1K	Clarified <10K	Clarified <30K	Clarified <0.45um
3.0	Initial (TOC)	0.6	4.0	4.9	5.4	0.8	3.1	3.3	4.7
	Final (TOC)	1.4	2.4	2.0	2.3	1.5	2.1	2.1	1.8
	Nominal Chang	0.8	(1.6)	(2.9)	(3.1)	0.7	(1.0)	(1.2)	(2.9)
	Percent Change	133%	-40%	-59%	-57%	87%	-32%	-36%	-62%
4.0	Equalibrated								
	Initial (TOC)					2.8	3.0	3.0	3.0
	Final (TOC)					2.0	2.0	2.0	2.0
	Nominal Change					(0.8)	(1.0)	(1.0)	(1.0)
	Percent Change					-29%	-33%	-33%	-34%
	Not-Equalibrated								
	Initial (TOC)					2.8	3.0	3.0	3.0
	Final (TOC)					2.8	3.0	3.0	3.0
	Nominal Change					0.0	0.0	0.0	0.0
	Percent Change					0%	0%	0%	0%
5.1	Initial (TOC)					1.0	3.1	2.7	3.3
	Final (TOC)					1.9	2.1	2.1	2.1
	Nominal Change					0.9	(1.0)	(0.6)	(1.2)
	Percent Change					90%	-33%	-24%	-38%
5.2	Initial (TOC)					1.4			
	Final (TOC)					1.9			
	Nominal Change					0.5			
	Percent Change					36%			
6.0	Initial (TOC)				2.9				
	Final (TOC)				0.5				
	Nominal Change				(2.4)				
	Percent Change				-83%				
	Initial				2.9				
	Final				1.4				
	Nominal Change				(1.5)				
	Percent Change				-52%				
	Initial				2.9				
	Final				2.9				
	Nominal Change				0.0				
	Percent Change				0%				

An ultrafiltration effect important to analysis of raw waters is the separation of NOM from clays (Aiken, 1992). The clay complex is known to bind to hydrous oxides during coagulation processes. Aiken suggests that this fraction be removed employing a 0.1 um filter prior to ultrafiltration. In this way the complexed NOM content can be excluded, and not artificially elevate estimates of DOC below each MWCO.

The level of biological activity in the water tested is also of importance in preparing for ultrafiltration. Immediate filtration of sample waters is emphasized by Aiken (1992) to remove active biota. He notes that addition of silver nitrate ($AgNO_3$) in excess of 10 ug/L to the unfiltered sample will also increase sample life.

Research directed toward biologically active rapid sand filtration-ozonation systems has shown that biodegradation of DOC results in lower total chlorinated-THMs and a relative increase in total brominated THM formation (Symons *et al.*, 1994). During ultrafiltration filter pressure is maintained with nitrogen, rather than compressed air to minimize introduction of oxygen for biological activity.

Maintaining sample pH is important to proper size separation of fulvic and humic molecules that make up the majority of the observed DOC. These compounds change structurally in response to pH. Coiling and uncoiling of the molecular structure can result in an apparent three fold change in molecular size. Humic molecular size is largest at a pH of 7.9 (Christman and Gjessing, 1983). Humic acids in a coiled state are also less reactive, though this effect is moderated by the presence of Ca^{2+} in solution (Murphy *et al.*, 1994). Murphy *et al.* (1994) postulate that reduced reactivity in the coiled state is due to fewer available points of attachment. Changes in molecular configuration or chemical interaction were proposed by Shaw *et al.* (1994) observing higher than anticipated retention failure, to the extent that >100,000 dalton UV-absorbing molecules appeared in 25,000 and 50,000 MWCO permeates.

In practice segregation failure is expected at both high and low molecular sizes (Saar and Weber, 1982). Amy *et al.* (1992) suggests that ultrafiltration filter rejection properties underestimate the lowest MWCO, because charge conditions result in the smaller effective

sieve sizes than predicted. Aiken (1992) offers the opposing view, indicating that ultrafiltration filters do not provide a 100 percent effective positive barrier. To define "true" NOM concentrations associated with each MWCO bin Logan and Jiang (1990) recommend developing a permeation coefficient for each water and membrane used. The coefficient is based on a standard curve of DOC in the filter permeate over the course of a filter run. This process attempts to correct for changes in filter rejection rate due to surface charge effects. Owen *et al.* (1993) recognized Logan and Jiang's research but pointed out that the use of a standard protocol providing an operational definition of AMW was an equally effective tool.

A number of artifacts of ultrafiltration are recognized in the literature. Amy *et al.* (1987, 1992) suggested that aggregation effects at the membrane do not significantly impair ultrafiltration filter performance when humic substances are present at less than 80 mg/L, if the feed solution is vigorously mixed. Experienced researchers (Aiken, 1992; Amy *et al.*, 1987) council use of dilute DOC concentrations, optimization of pH and maintenance of ion balance when ultrafiltering.

In this analysis fractionation of humic materials by apparent molecular weight involved ultrafiltration of stabilized (0.45 um filter, 4°C) water using Amicon 8200 stirred cell membrane filteration apparati with YM Diaflo filters (Amicon) having nominal molecular weight cutoffs of 1,000, 10,000, and 30,000 daltons. Ultrafiltration does not rely exclusively on absolute filter pore size; concentration polarization at the filter surface is an important exclusion mechanism (Amicon,1987). Maintaining the design AMW requires retention of membrane integrity and maintaining a cross current perpendicular to the pressure vector directed toward the membrane. Actual filter performance was measured through nominal clean water flow rates at 55 psi N_2. Ultrafiltration permeate DOC values were not adjusted using permeation coefficients.

Experimental Design

The following section outlines the matrices of experimental conditions employed in this research.

Determining Experimental Conditions

Experimental conditions were selected for simplicity of protocol and to be representative of treatment plant conditions. Bromide is usually present in natural waters (analytical limit, 0.005 mg/L); unamended Harwood's Mill Reservoir water contains 0.03 mg Br^-/L, which is approximately the 40th percentile nationally. Summers *et al* (1993) employed Br^- concentrations of 0.03 mg/L in a DOC dilution analysis of THMs and MWCO. As was noted in Chapter 2, nationally the median surface source water contains 0.04 mg Br^-/L. Ninety-five percent of surface source waters contain less than 0.2 mg Br^-/L. Experimental conditions range from 0.03-0.5 mg Br^-/L.

DOC conditions were limited to those available from nearby source waters, Harwood's Mill Reservoir proved to be an appropriate source due to its typical DOC of 4.7 mg/L, which is between the 50th and 75th percentile DOC concentration among surface water sources nationally. Actual sampling event conditions are summarized in Table 3.4. Utilizing a single water source did not allow consideration of inter-basin variation in NOM character.

Table 3.4. Sampling Event Conditions

	August 18, 1994		November 22, 1994
Parameter	Raw	Clarified	Clarified
Alkalinity (mg/L as $CaCO_3$)	34	17	13
Color	20	0	0
NH_3-N (mg/L)	<0.02	nd	nd
pH	7.1	6.4	6.1
THMFP (ug/L)	356[1]	145	196
TOC (mg/L)	6.3	3.0	4.0
Turbidity (NTU)	2.7	0.1	0.1

Source: Harwood's Mill WTP Records, Values reflect average daily values.
Notes: (nd) indicates no data collected; (1) data collected on 8/16/94

Chlorination at Cl_2-to-DOC ratio of 3:1 (mg/mg) is consistent with research by Owen *et al.* (1993) at Harwood's Mill Reservoir, and facilitated maintaining a constant Br:Cl ratio across trials, without experiencing chlorine expiration within 168 hours. This chlorine dose is higher than chlorine residuals currently utilized by the water industry. Harrington *et al.* (1992) suggested that the chlorine dose to DOC ratio observed in U.S. water treatment plants is typically 1:1 to 2:1 based on a review of databases containing operational data from water utilities in the United States. Typical chlorine doses in the current regulatory environment range from 1.0-2.2 mg/L depending on water source (59 *Federal Register* 38690). AWWA Disinfection Survey in 1991 of 283 utilities found the mean chlorine residual of water entering the distribution system ranged from 0.07-5.0 mg/L (median 1.1 mg/L) (59 *Federal Register* 38690). Chlorine residuals observed in this research after 168 hour contact period were typically within this range.

Summary of Experimental Matrices

The following dilute solutions were chlorinated and monitored for THM, HAN, HK and chloropicrin formation potential at set time points. Each of the matrices described below were developed independently. Table 3.5 summarizes matrix conditions.

Table 3.5. Summary of Experimental Matrices

Matrix	Characteristics	Br^-	Ratio of Cl_2:DOC	DOC	MWCO <1	MWCO <10	MWCO <30	MWCO <4,500 K	Time Points
1	Pure compounds	Varied	Varied	Constant					5
2	Pure compounds	Varied	Varied	Constant					5
3	Raw	Equalized	Constant	Constant	X	X	X	X	5
4	Coagulated	Equalized	Constant	Varied	X	X	X	X	5
	Coag.-DOC equalized	Equalized	Constant	Constant	X	X	X	X	5
5.1	Coagulated	Varied	Constant	Constant	X	X	X	X	4
5.2	Coagulated	Equalized	Constant	Constant	X				5
6	Raw	Varied	Constant	Varied				X	5

Matrix 1

Using MilliQ® water three solutions containing bromide ion at concentrations of 0, 0.05, and 0.2 mg/L were prepared. $CHCl_3$ and DCAN were introduced into each of the solutions at 100 and 2.5 ug/L, respectively. Each solution was subjected to a 0, 2, and 4 mg Cl_2/L dose of chlorine, resulting in initial Br^-:Cl ratios of 0.011, 0.022, 0.044 and 0.089. Chlorination reactions in each of these solutions were subsequently quenched at 0, 24, 48, 96, and 168 hour time points, residual chlorine levels observed and samples prepared for analysis using EPA methods 501 and 551. Experimental controls included a sample blank series (no Br^-), and MilliQ® blank series with 0.05 and 0.2 mg Br^-/L. Control series received chlorine doses of 0, 2, and 4 mg Cl_2/L.

Matrix 2

Using MilliQ® water three solutions containing bromide ion at concentrations of 0, 0.05, and 0.2 mg/L were prepared. $CHCl_3$ and DCAN were introduced into each of the solutions at 220 and 66 ug/L, respectively. Each solution was subjected to a 0, 2, and 4 mg Cl_2/L dose of chlorine, resulting in initial Br^-:Cl ratios of 0.011, 0.022, 0.044, and 0.089. Chlorination reactions in each of these solutions were subsequently quenched at 0, 24, 48, 96, and 168 hour time points, residual chlorine levels observed and samples analyzed using EPA methods 501 and 551. Controls in matrix 2 paralleled those described in matrix 1. In addition a positive control using aspartic acid addition was added to the matrix.

Matrix 3

Raw and coagulated waters collected from the Harwood's Mill Water Treatment Plant and stabilized, were ultrafiltered through 1000, 10,000, and 30,000 MWCO filters. The resulting solutions and a 0.45 um (4,500,000 MWCO) permeate were then diluted or freeze concentrated as required until all eight solutions contained approximately 2.0 mg DOC/L. Each solution was then amended with Br^- such that the Br^- concentration was

0.07 mg/L. These solutions were then subjected to a 6 mg Cl_2/L (initial Br^-:Cl ratio (mM:mM), 0.0013). Chlorination reactions in each of these solutions were subsequently quenched at 0, 24, 48, 96, and 168 hour time points, residual chlorine levels observed and samples analyzed using EPA methods 501 and 551. Two control series were prepared with respect to Br^-, both were MilliQ® water blanks. One received 0.07 mg Br^-/L; both were chlorinated at 6 mg Cl_2/L.

Matrix 4

Coagulated water collected from the Harwood's Mill Water Treatment Plant and stabilized, was ultrafiltered through 1,000, 10,000, and 30,000 MW filters. One-half of each of the resulting solutions and a 0.45 um (4,500,000 MWCO) permeate were diluted or freeze concentrated as required to reach an approximate DOC concentration of 2.0 mg/L. The second-half of the filtrates were not modified to an equal DOC, but observed DOCs at the time of chlorination were relatively uniform, 2.8 - 3.0 mg DOC/L. Each of the resulting eight solutions were then amended with Br^- such that the Br^- concentration was 0.07 mg/L. The solutions were then subjected to Cl_2 at a 3:1 Cl_2:DOC weight:weight ratio; resulting doses were 6-9 mg Cl_2/L, initial Br^-:Cl ratios (mM:mM), 0.009 and 0.013, respectively. Chlorination reactions in each of these solutions were subsequently quenched at 0, 24, 48, 96, and 168 hour time points, residual chlorine levels observed and samples analyzed using EPA methods 501 and 551. Controls were prepared with respect to Br^-, both 0 and 0.07 mg Br^-/L blanks were chlorinated at 6 mg Cl_2/L.

Matrix 5.1

Coagulated water collected from the Harwood's Mill Water Treatment Plant and stabilized, was ultrafiltered through 1,000, 10,000, and 30,000 MWCO filters. The resulting solutions and a 0.45 um permeate (4,500,000 MWCO) were then diluted or freeze concentrated as required until each solution contained 2.0 mg DOC/L. Each solution was then amended with Br^- such that the Br^- concentration was 0.07, 0.2 or 0.5

mg/L. These solutions were then subjected to a 6 mg Cl_2/L dose (initial Br^-:Cl ratio (mM:mM), 0.01, 0.03, and 0.074). Chlorination reactions in each of these solutions were subsequently quenched at 0, 48, 96, and 168 hour time points, residual chlorine levels observed and samples analyzed using EPA methods 501 and 551. As with matrix 4, the control series were prepared with respect to Br^- at 0, 0.07, 0.2 and 0.5 mg Br^-/L; each was dosed at 6 mg Cl_2/L.

Matrix 5.2

In a second series constructed in parallel with matrix 5.1, coagulated water collected from the Harwood's Mill Water Treatment Plant and stabilized, was ultrafiltered through 1,000 MWCO filter. The resulting solution was then freeze concentrated to 1.4 mg DOC/L. The solution was separated into two experimental trials each prepared separately. Each solution was amended with Br^- such that the Br^- concentration was 0.07 mg/L. The solutions were then subjected to chlorine doses of 0 and 6 mg Cl_2/L dose (initial Br^-:Cl ratio (mM:mM), 0.01). Chlorination reactions were subsequently quenched at 0, 24, 48, 96, and 168 hour time points, residual chlorine levels observed and samples analyzed using EPA methods 501 and 551. In addition to the side-by-side trial of 0 and 6 mg Cl_2/L doses on <1,000 MWCO permeate containing 0.07 mg Br^-/L, a parallel series of treatment was applied to MilliQ® water.

Matrix 6

Raw water collected from the Harwood Mills water treatment plant and filtered through a 0.45 um filter (4,500,000 MWCO). The resulting permeate was then diluted to achieve three DOC concentrations: 0.4, 1.5, and 3.0 mg DOC/L. Each solution was then divided in half and amended with Br^- such that Br^- concentrations were 0.2 and 0.5 mg/L. These solution were then subjected to chlorine doses at a 3:1 Cl_2/DOC weight:weight ratio. The resulting doses were 1.5, 4.5, and 9.0 mg Cl_2/L, corresponding to initial Br^-:Cl ratios (mM:mM) 0.039, 0.049, 0.118, and 0.296. Chlorination reactions were subsequently

quenched at 0, 24, 48, 96, and 168 hour time points, residual chlorine levels observed and samples analyzed using EPA methods 501 and 551. The controls for matrix 6 consisted of two series of MilliQ® blanks, dosed with 0.2 and 0.5 mg Br^-/L and 9 mg Cl_2/L.

Chapter 4. Results and Discussion

This chapter will quantitatively present the results of the research undertaken. Results will be presented on an experiment specific basis, as well as, discussion of the data with respect to the research objectives outlined in chapter 1. Several terms used in this description are unique to this text: (1) non-THM, refers to HANs, HKs and CP observed; (2) THK refers to TCP and DCP observed; (3) THAN represents the sum of observed DCAN, TCAN, DBAN, and BCAN concentrations; (4) TDBP refers to the sum of all observed DBP species (eg., THMs, HANs, HKs, and CP); and (5) 0.45 um filter was assumed to approximate a 4,500,000 AMW cutoff..

Preliminary Findings

To reliably measure microgram per liter and micromolar quantities of DBPs, the method detection limits (MDL) associated with EPA methods 501.1 and 551 were evaluated. MDLs represent the analyte concentration below which values obtained from an analytical procedure may not be reliable or appropriate for reporting. MDLs reflect both variation in analytical instrument response and preparatory procedure effects on quantitation. EPA employs a specific method to determine the MDL associated with a test procedure: (1) determining the method response to a sample believed to be near the MDL seven or more times, (2) analyzing an equal number of experimental blanks, and (3) calculating the MDL as follows in equation 4.1.

$$\text{MDL} = \begin{matrix}\text{Average Blank} \\ \text{Response}\end{matrix} + 3 \times \begin{matrix}\text{Standard Deviation} \\ \text{of Response Area}\end{matrix} \times \begin{matrix}\text{Test} \\ \text{Concentration}\end{matrix} \qquad \text{(Eq. 4.1)}$$

Source: EPA, 1990

MDLs estimated at the lowest observed standard concentration are summarized in Table 4.1.

Table 4.1. EPA Method 501.1 and 551 MDLs

Analyte	Concentration Tested	MDL (ug/L)	Analyze	Concentration Tested	MDL (ug/L)
$CHCl_3$	1.00	1.68	DCP	0.10	0.02
$CHCl_2Br$	0.25	0.04	CP	0.10	0.03
$CHClBr_2$	0.25	0.11	BCAN	0.10	0.05
$CHBr_3$	0.50	1.77	TCP	0.10	0.03
TCAN	0.10	0.03	DBAN	0.10	0.15
DCAN	0.10	0.03			

Note: MDL, method detection limit.

Tables 4.2 and 4.3 summarize the level of response observed below the MDLs for Method 501.1 and 551. $CHCl_3$, $CHBr_3$, and DBAN were the only target compounds not identifiable at < 0.15 ug/L and most HAN and HK species could be detected at levels below 0.05 ug/L. Tables 4.2 and 4.3 also illustrate the impact that these MDL values have on subsequent data collected within the matrices of controlled conditions described in Chapter 3; TCAN was not included in Table 4.3 as it only occurred at a quantifiable level once in all seven matrices.

Table 4.2. Application of Method Detection Limit Values to THM Data Generated by Method 501.1

	Number of Recorded Values				MDL Based Exclusions			
Matrix	$CHCl_3$	$CHCl_2Br$	$CHClBr_2$	$CHBr_3$	$CHCl_3$	$CHCl_2Br$	$CHClBr_2$	$CHBr_3$
1	43	45	23	45	0	0	0	57%
2	47	28	32	28	0	0	0	100%
3	45	43	42	11	7%	0	0	100%
4	50	38	33	1	0	3%	0	100%
5.1	53	61	62	57	2%	2%	0	40%
5.2	24	23	23	7	17%	17%	22%	100%
6	40	40	40	40	18%	0	0	18%

Table 4.3. Application of Method Detection Limit Values to THM Data Generated by Method 551

	Number of Recorded Values						MDL Based Exclusions					
Matrix	DCAN	DCP	CP	BCAN	TCP	DBAN	DCAN	DCP	CP	BCAN	TCP	DBAN
1	44	4	11	15	7	17	0	25%	0	13%	0	59%
2	49	1	3	1	5	0	0	0	0	0	0	0
3	43	2	26	35	39	24	2%	0	0	3%	0	58%
4	47	3	8	36	41	14	0	50%	23%	3%	0	43%
5.1	43	0	7	42	36	51	5%	0	0	0	3%	10%
5.2	10	2	2	9	8	9	0	0	0	0	0	0
6	75	5	3	33	19	40	1%	0	0	0	0	3%

With the exception of $CHBr_3$, Method 501.1 detection provided consistent response above MDL. In matrix 5.2, 2-22 percent of the THM data ($CHCl_3$, $CHCl_2Br$, and $CHClBr_2$) were below the MDL. However, in seven matrices, 58-100 percent of all recorded values for $CHBr_3$ were below the MDL. While DCP and CP concentrations reported were frequently below the MDL, quantitation of DBAN was consistently below the MDL (3-59 percent of DBAN values). While values below the MDL are more likely than those above it to be in error, non-zero values below the MDL were used in statistical analysis of experimental results as best estimates of actual concentrations.

EPA MDL Method Response to Variation in Procedure

The EPA MDL method assumes linearity of response and homogeneity of variance: (1) across the range of possible test concentrations and (2) in the region extrapolated from the MDL calculation. EPA Method 551 was employed to test MDL consistency over five test concentrations (0.1-1.0 ug/L) and between two sample counts (n=7, n=34). The EPA Method 551 MDL reflects variation in instrumental response from the gas chromatograph using an ECD detector and variation associated with the method's extraction procedure. Figure 4.1 is a sample chromatogram. The results of the test series are summarized in

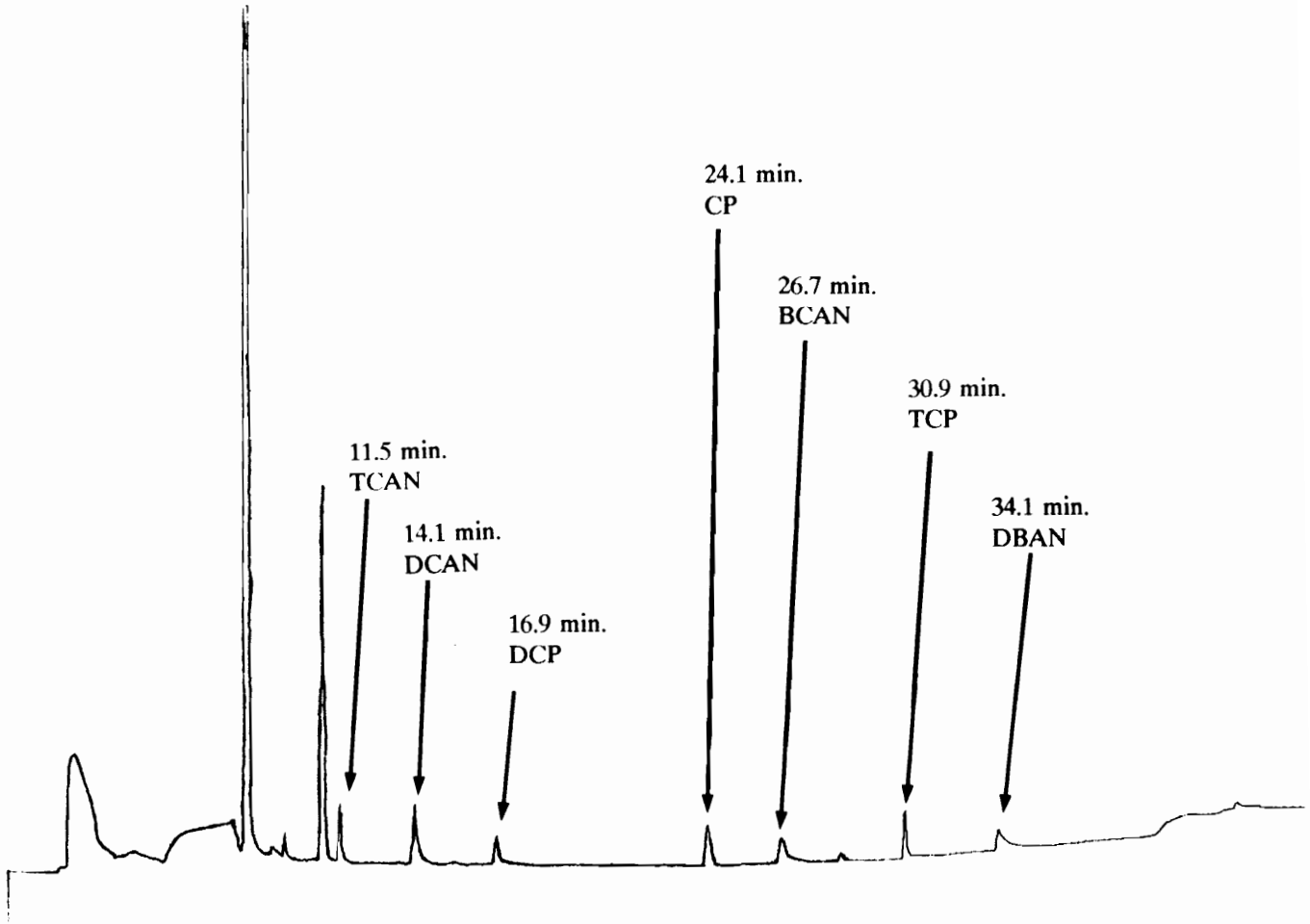

Figure 4.1. Chromatogram of Haloacetonitrile and Haloketone Standard, 0.25 ug/L, Column: 30 m, 0.25 mm i.d., DB-1, helium carrier gas at 23 cm/sec, nitrogen make-up gas at 30 mL/min.; Temperature Program: 15 min at 33°C, 33-40°C at 1°/min., 3 min. at 40°C, 40-120°C at 6°C/min., 1 min. at 120°C.; Injection: splitless, vent at 0.7 min., 2 uL injection volume.

Table 4.4 for each of HAN and HK analytes (TCAN, DCAN, DCP, CP, BCAN, TCP, and DBAN).

Table 4.4. MDL Calculated at Different Low Level Concentrations Using the EPA Method

		MDL (ug/L)						
Concentration	n	TCAN	DCAN	DCP	CP	BCAN	TCP	DBAN
0.10	7	0.031	0.030	0.024	0.032	0.045	0.028	0.147
0.25	7	0.059	0.068	0.079	0.069	0.096	0.111	0.127
0.25	34	0.203	0.203	0.203	0.204	0.226	0.204	0.235
0.50	7	0.094	0.108	0.086	0.085	0.157	0.081	0.232
1.00	7	0.161	0.232	0.163	0.178	0.256	0.171	0.241

Resulting MDLs increased five to six fold for a 10 fold increase in test concentration. While not as responsive to increasing sample number (n), increasing sample number from 7 to 34 at a test concentration of 0.25 ug/L resulted in a two to four fold increase in MDL. MDLs resulting from the n=34 test were higher than n=7 values at 0.25 ug/L and within 20 percent of the MDLs predicted at a test concentration of 1.0 ug/L concentration. Variation increased with the number of preparatory extractions required for the test series.

Analytical variation occurs both among different samples and between measurements of the same sample. Table 4.5 summarizes the percentage of the observed standard deviation at the 0.25 ug/L analyte concentration attributable to intra-sample variation in which one sample was measured seven times. Intra-sample variations of 73 and 84 percent of independent sample variation were measured in BCAN and DBAN response, while TCAN and DCAN, had lower intra-sample variations (<17 percent of variation attributable to intra-sample variation). DCP, TCP, and CP intra-sample variation represented 35, 29, and 37 percent of observed independent sample variation respectively.

Table 4.5. Variation in Method 551 Detection Due to Non-Sample Sources

Compound	Standard Deviation (Response reported in area units)	Inter-Sample Variation Attributable to Intra-Sample Variation
TCAN	91	16.3%
DCAN	135	16.9%
DCP	187	35.0%
CP	232	37.4%
BCAN	476	72.7%
TCP	209	29.2%
DBAN	546	84.1%

Note: Seven replicate samples taken from same vial at 0.25 ug/L. Compared against standard deviation from analysis of seven individual vials at 0.25 ug/L. Values with respect to integrator response area.

Intra-sample variation decreased with increasing bromide content. With the exception of TCP, intra-sample variation increased with retention time.

EPA Method vs Inverse Regression.

An alternative MDL procedure to EPA's Method was discussed by Sharaf *et al.* (1986). This method is called inverse regression; it was also applied to the same dataset to determine detection limits. The inverse regression method employs the confidence interval associated with response over a range of test concentrations to predict the MDL. This method was assumed to provide a conservative estimate of the MDL. The analysis responds to increasing variation in response through growth of the confidence interval (i.e., as the experimental protocol approaches the MDL). Figures A-2.1 through A-2.7 illustrate such a plot for each of the analytes. Inverse regression analysis resulted in MDL values typically 2.5 to 5 times higher than previously predicted using the EPA MDL method (Table 4.6). However, with respect to DBAN, where the standard deviation was high relative compared to the mean response at the lowest measured test concentration (49 percent at 0.1 ug/L), inverse regression was less conservative than the

EPA calculation. The EPA MDL was 1.36 times greater than the MDL predicted by inverse regression.

Table 4.6. Description of Sharaf Method MDL Analysis

Compound	MDL (ug/L) Sharaf	MDL (ug/L) EPA	EPA MDL/ Sharaf MDL[1]
TCAN	0.08	0.03	0.38
DCAN	0.10	0.03	0.30
DCP	0.09	0.02	0.22
CP	0.10	0.03	0.30
BCAN	0.11	0.04	0.36
TCP	0.12	0.03	0.25
DBAN	0.11	0.15	1.36

Note: (1) Calculation based on EPA MDL at 0.10 ug/L test concentration..

Matrix 1

Matrix 1 tested for degradation or conversion of $CHCl_3$ and/or DCAN to other THM, HK, or HAN species with time (<1, 24, 48, 96, and 168 hours). Matrix 1 contained three solutions made with MilliQ® water where: Br^- concentrations were 0, 0.05, and 0.2 mg/L; $CHCl_3$ and DCAN were 100 and 2.5 ug/L, respectively; and chlorine doses were 0, 2, and 4 mg Cl_2/L creating initial Br^-:Cl ratios of 0.011, 0.022, 0.044 and 0.089.

Total observed DBP concentrations were typically less than initial conditions. Average TDBP was 0.86 uM/L and ranged from 0.6 uM/L to 1.1 uM/L. Variation in total DBP concentration varied little over the five observed time points. Relatively constant $CHCl_3$ concentrations were similar under each chlorine dose condition including the no chlorine condition. DCAN did decline with time under all conditions including the no chlorine series. Figure 4.2 illustrates $CHCl_3$ and DCAN concentration in the procedure blank.

Formation potentials observed in the experimental controls, reflected Br^- reactivity when chlorine was absent. Neither mass balances or occurrence patterns under substrate limited conditions, indicate utilization of DCAN in absence of chlorine by Br^- to DBPs

quantified at detectable levels. DCANFP's decline with time occurs in later matrices employing natural waters and is recognized in the literature.

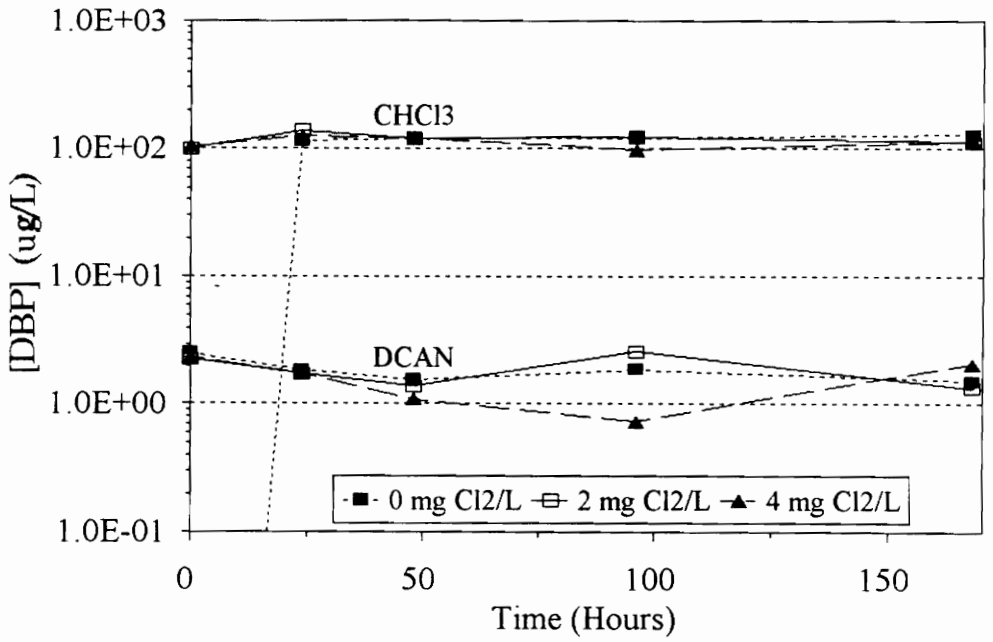

Figure 4.2. $CHCl_3$ and DCAN Concentration Over Time in Matrix 1 (MilliQ®, 100 ug $CHCl_3$/L, 2.5 ug DCAN/L, 0 mg Br^-/L)

$CHCl_3$, $CHCl_2Br$, $CHClBr_2$, $CHBr_3$, and DCAN were consistently observed under all the initial Br^-:Cl ratio (mM:mM) conditions. $CHCl_3$ concentration in $CHCl_3$ concentration did not change with time or Br^- concentration; Figure 4.3 illustrates observed $CHCl_3FP$ response. DCAN decay occurred with time under all Br^- concentrations (Figure 4.4).

Present in quantities 1-10 percent of the initial $CHCl_3$ concentration, concentrations of $CHCl_2Br$ generally exceeded $CHClBr_2$ concentration by a factor of two or more. Both $CHCl_2BrFP$ and $CHClBr_2FP$ increased with reaction time; this pattern is illustrated in Figures 4.5 and 4.6. $CHCl_2Br$ and $CHClBr_2$ also demonstrated response to the initial Br^-:Cl ratio. Formation at any given time point for both species peak at

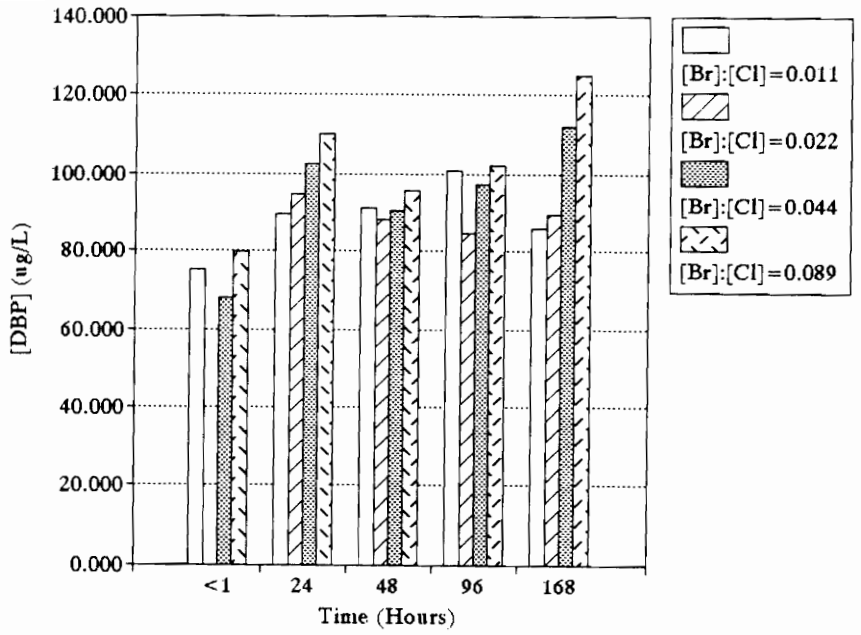

Figure 4.3. $CHCl_3$ Concentration Observed in Matrix 1 Over Time (MilliQ®, 100 ug $CHCl_3$/L, 2.5 ug DCAN/L)

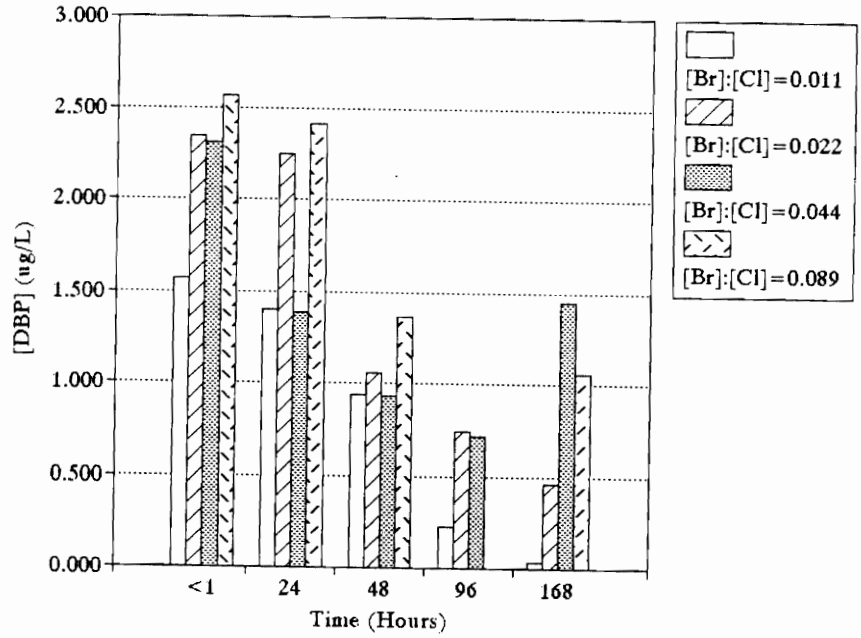

Figure 4.4. DCAN Concentration Observed in Matrix 1 Over Time (MilliQ®, 100 ug $CHCl_3$/L, 2.5 ug DCAN/L)

maximum Br^-:Cl ratio conditions rather than under maximum chlorine dose conditions. $CHBr_3$ was most often detected below the MDL, but reported values also demonstrated increasing formation with increasing Br^-:Cl ratio.

Most HANs and HKs occurred at concentrations at or below quantitation; accepted responses varied little with respect to time. BCAN and TCP formation were observed under specific conditions, bromide addition and no bromide series respectively.

While greater than their respective MDLs, DCP, BCAN, and DBAN were present at low levels. Both BCAN and DBAN appeared to respond positively to increasing Br:Cl ratio; CP, DCP, and TCP did not demonstrate a clear pattern of response. Table 4.7 is a summary of formation potentials after a 96 hour reaction period. The 96 hour time point is indicative of the trends observed illustrating limited HK and HAN response, THM speciation shifts, and DCAN decline with chlorine dose.

Table 4.7. THMFP at 96 Hour Time Point as Function of Initial Br^-:Cl Ratio (0.5 mg Br^-/L, 0, 2, and 4 mg Cl_2/L)

		Br^-:Cl	Concentration (ug/L)							
Br^-	Cl	Ratio	$CHCl_3$	$CHCl_2Br$	$CHClBr_2$	$CHBr_3$	DCAN	DCP	BCAN	DBAN*
0.05	0	0	105.9	1.9	--	1.2	1.66	--	--	--
0.05	2	0.02	84.7	2.2	1.3	3.0	0.74	0.08	0.02	0.12
0.05	4	0.01	100.7	5.7	2.3	2.5	0.23	0.19	0.14	0.12
0.20	0	0	97.7	1.7	--	1.0	1.43	--	--	--
0.20	2	0.09	102.2	7.4	2.5	2.6	--	--	--	--
0.20	4	0.05	97.3	5.0	1.6	3.2	0.72	0.01*	0.27	0.13

Note. (*) Concentration below MDL.

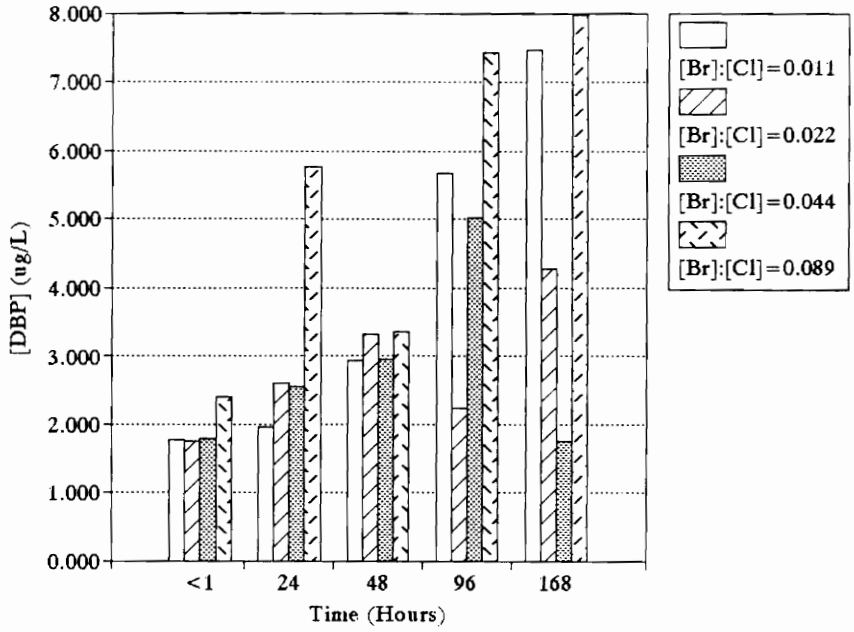

Figure 4.5. $CHCl_2BrFP$ Observed in Matrix 1 Over Time (MilliQ®, 100 ug $CHCl_3$/L, 2.5 ug DCAN/L)

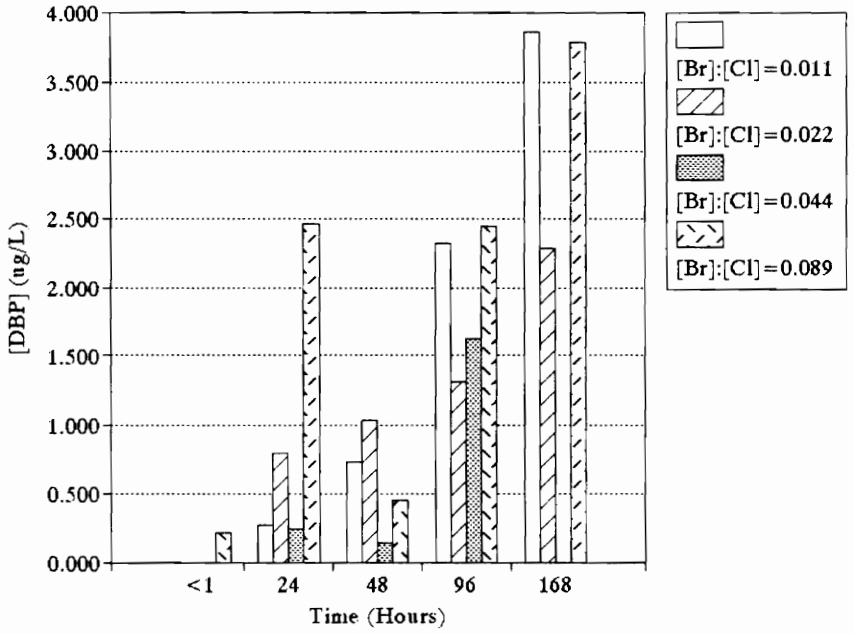

Figure 4.6. $CHClBr_2FP$ Observed in Matrix 1 Over Time (MilliQ®, 100 ug $CHCl_3$/L, 2.5 ug DCAN/L)

Matrix 2

Matrix 2 was constructed to verify matrix 1. Like matrix 1 three solutions containing Br^- at concentrations of 0, 0.05, and 0.2 mg/L were prepared using MilliQ® water. $CHCl_3$ and DCAN were again introduced into each of the solutions, but in larger concentrations, 220 and 66 ug/L, respectively. Each solution was subjected to 0, 2, and 4 mg Cl_2/L, resulting in initial Br^-:Cl ratios of 0.011, 0.022, 0.044, and 0.089.

$CHCl_3$ again remained constant over the five reaction time periods. DCAN concentration declined with time, but response was much more variable than in matrix 1. The remaining THMs when observed were unresponsive to experimental conditions. HAN and HKs, other than DCAN, seldom occurred at levels that could be quantitated, and did not occur in a discernable trend. Matrix 2 also included a positive control, addition of aspartic acid, which is a known DCAN substrate. This control did not present any response to the chlorine concentrations tested. Chlorine residual levels indicated chlorine dose exhaustion within 48 hours; quantifiable HAN formation was not witnessed. Matrix 2 did not contribute any additional data toward understanding $CHCl_3$ or DCAN's role in formation of other THMs, HANs, HKs, or CP.

Matrix 3

To investigate the effect of coagulation on AMW distribution and subsequent distribution of DBP formation, formation potential tests (6 mg Cl_2/L, 20°C, pH 7) were conducted on raw and coagulated waters filtered through 0.45 um filter and permeates from 1,000, 10,000, and 30,000 MWCO ultrafilters. To reduce ultrafilter induced effects DOC and Br^- concentration in each solution were modified to 2.0 mg/L and 0.07 mg/L, respectively. The resulting formation potentials in this scenario were more reflective of the DOC fraction reactivity under equalivent conditions. DOC levels in each fraction varied substantially prior to equalization (Table 4.8). When compared to "real world data" DOC equalization emphasizes the importance of the <1,000 MWCO fraction and under estimates the total mass of DBPs contributed by the larger AMW fractions.

Table 4.8. Initial DOC Concentration by MWCO Fraction, Matrix Three

	MWCO			
	<1,000	<10,000	<30,000	<4,500K
Raw Water DOC (mg/L)	0.6	4.0	4.9	5.4
Percent Change to obtain 2.0 mg DOC/L	133%	-50%	-59%	-57%
Clarified Water (mg/L)	0.8	3.1	3.3	4.7
Percent Change to obtain 2.0 mg DOC/L	87%	-32%	-36%	62%

Matrix controls demonstrated responses above the MDL in 22 of 121 condition-time point combinations. In some instances $CHClBr_2$, DCAN, CP, BCAN, DBAN formation potentials under control conditions exceeded 10 percent of 168 hour 4,500 K MWCO fraction formation potential response. These excursions suggest that the <0.1 mg/L DOC observed in MilliQ® water is reactive with Br^- and may have contributed to experimental findings when dilution volume was large.

General

TDBP formation increased with time across all MWCO fractions in both raw and coagulated waters. Figures 4.7, 4.8, and 4.9 illustrate DBP formation with time in the <1,000, <30,000, and <4,500 K MWCO fractions. This increase was due to THM formation, HANs typically remained constant or decreased with time.

THMs

$CHCl_3$ was the dominant DBP formed in all fractions across all time points. $CHCl_2BrFP$ occurred at approximately 20 percent of $CHCl_3$ levels regardless of time point, MWCO fraction, or coagulation. $CHClBr_2FP$ ranged from 12 to 26 percent of

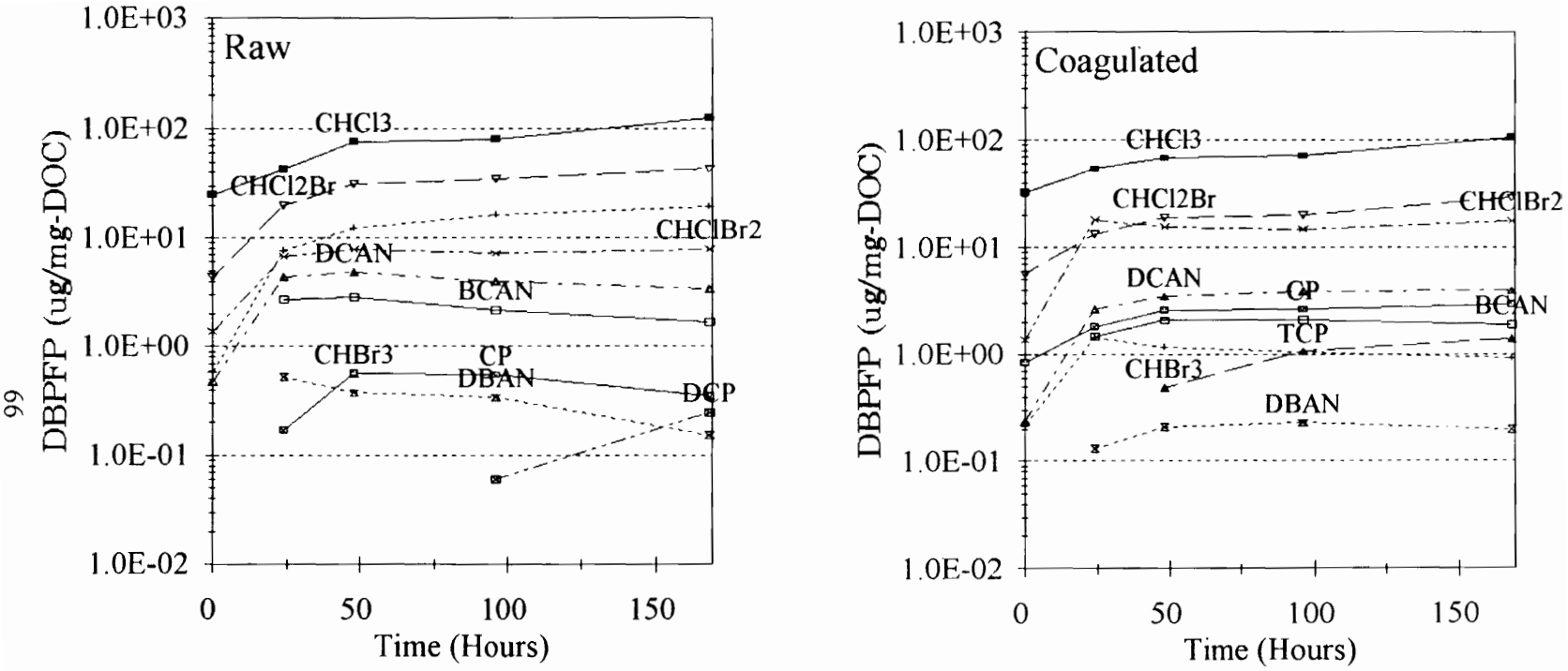

Figure 4.7. Comparison of DBP Formation from Raw and Coagulated Waters, <1,000 MWCO, 2 mg DOC/L, 0.07 mg Br^-/L, 3:1 Cl_2:DOC Ratio

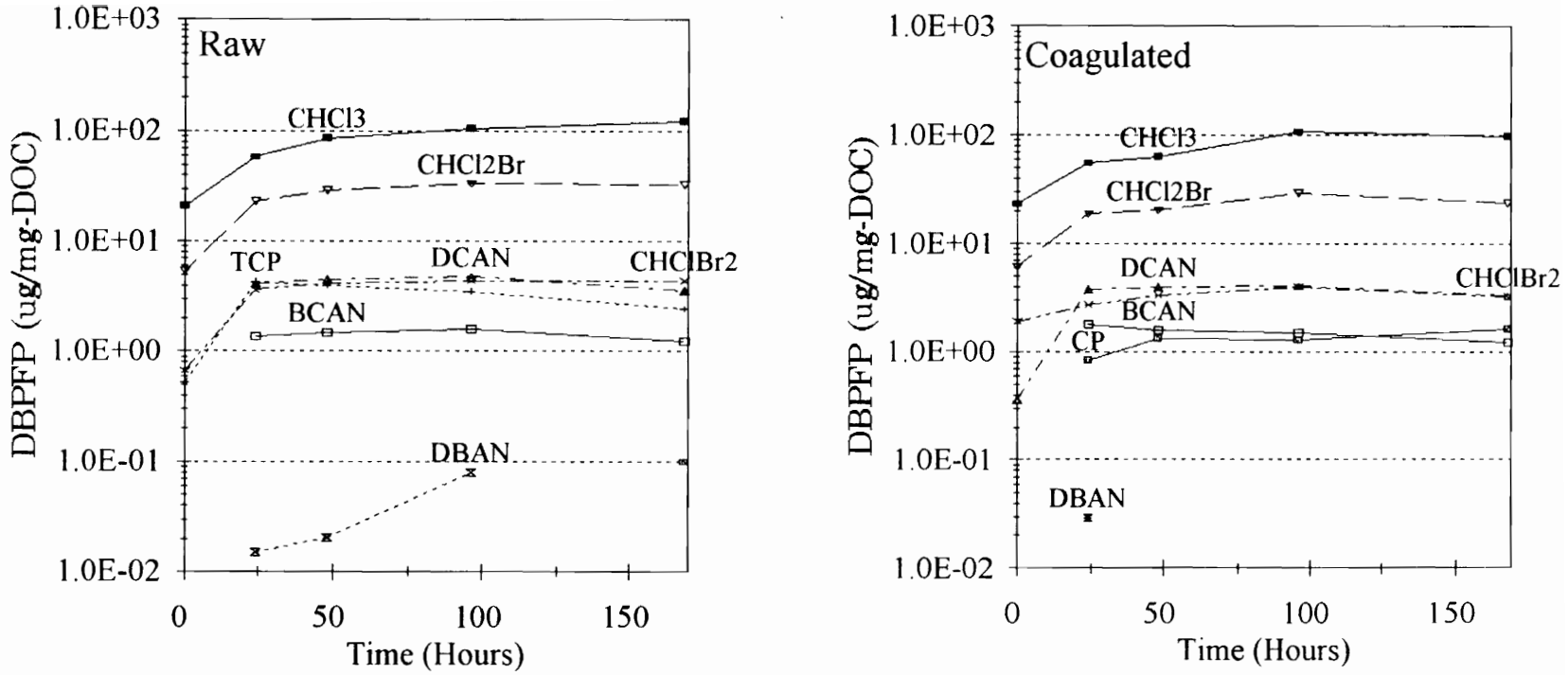

Figure 4.8. Comparison of DBP Formation from Raw and Coagulated Waters, <30,000 MWCO, 2 mg DOC/L, 0.07 mg Br^-/L, 3:1 Cl_2:DOC Ratio

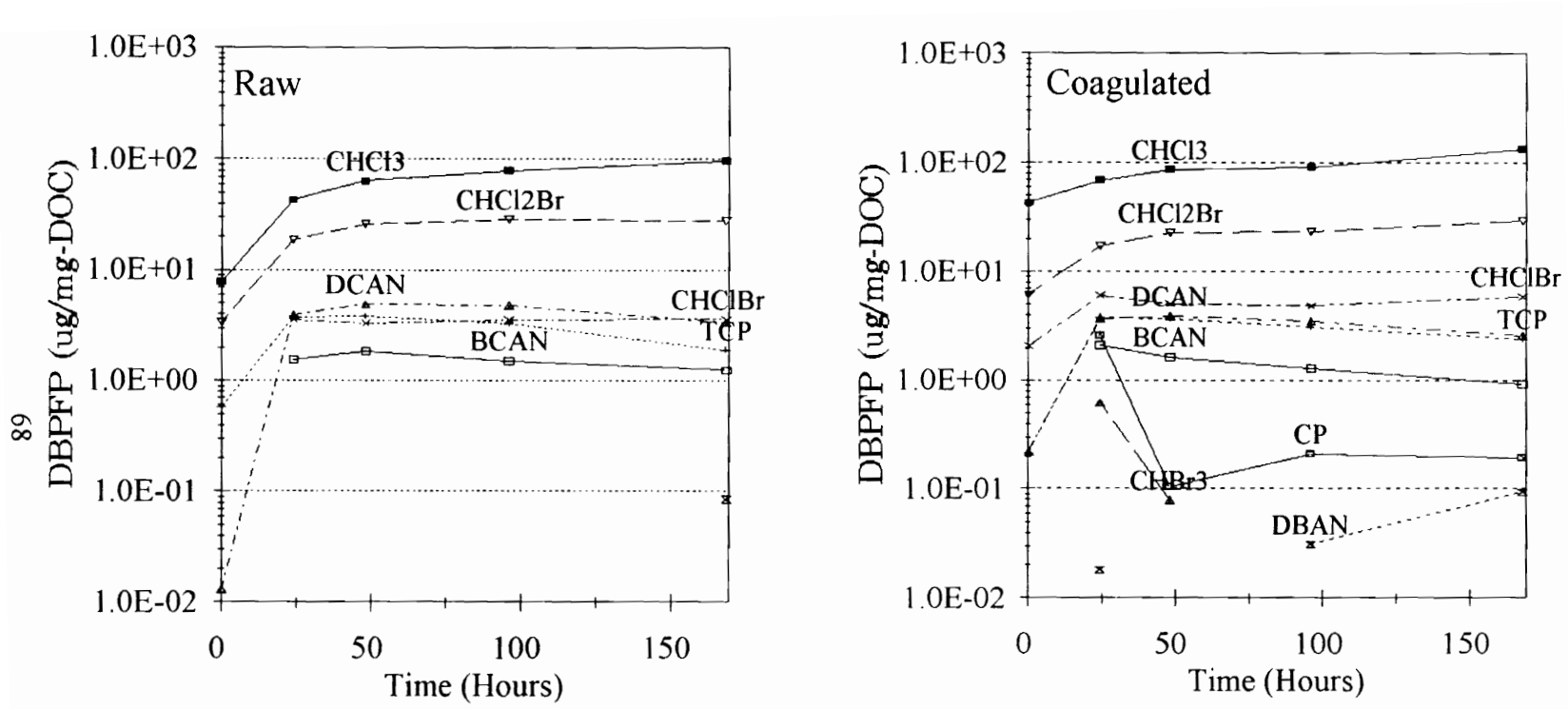

Figure 4.9. Comparison of DBP Formation from Raw and Coagulated Waters, <4,500,000 MWCO, 2 mg DOC/L, 0.07 mg Br^-/L, 3:1 Cl_2:DOC Ratio

$CHCl_3$ formation, increasing with time, and decreasing with increasing AMW. $CHBr_3$ formation was consistently below the MDL obscuring any coagulation related effects, but $CHBr_3$ was only observed consistently in the <1,000 MWCO fraction and like $CHClBr_2FP$ increased with reaction time.

HANs

Non-THM formation potentials occurred in the following order from largest to smallest concentration: DCAN, TCP, BCAN, and CP. THAN concentration ranged from 0 to 8.27 ug/L, usually reached maximum values by 48 hours, then decreased with increasing reaction time. DCAN was the HAN species present in greatest concentration, representing 60-80 percent of THAN concentration.

Formation of DCAN was independent of MWCO and did not respond to either time or coagulation. DCANFP (0.22-4.87 ug/L) did not exceed 10 percent of $CHCl_3$ (7.75-144.19 ug/L) for equivalent conditions. BCAN formation decreased with time and seldom exceeded 2.0 ug/L, however, both the raw and coagulated <1,000 AMW fraction values, were larger than the typical response (1.45-2.87 ug/L).

While a minor product, DBAN, also demonstrated a similar pattern of response to DCAN and BCAN. DBANFP was higher in 1,000 MWCO fraction for both raw and coagulated waters, but appeared to decrease after coagulation, even in the 1,000 MWCO fraction.

HKs and CP

Peak HKs and CP formation also occurred after 48-96 hours. CP formation occurred throughout at 0.5 ug/L and greater, but was more consistently observed in coagulated water, where observations were distributed across all fractions. TCP formation was reduced by coagulation in the <1,000 MWCO fraction.

Coagulation's Effect on Specific Formation Potential

In a comparison of DOC normalized formation potentials from raw and coagulated waters using the Wilcoxon Matched Pairs Ranked Sign test statistic, divergence of the mean response was indicated but not significant at α=0.1. Divergence between raw and coagulated formation potential was observed for $CHCl_3$, $CHBr_3$, TCP, and DBAN (Table 4.9). $CHClBr_2$ and BCAN data yielded probability values associated with more similar means.

Table 4.9. Coagulation Effect, Matched Pair Wilcoxon Ranked Sum Test Analysis of Matrix 3 Data

DBP	Probability
$CHCl_3$	0.136
$CHCl_2Br$	0.534
$CHClBr_2$	0.859
$CHBr_3$	0.317
DCAN	0.683
BCAN	0.959
TCP	0.173
DBAN	0.173

Note: Probability assumed to have normal approximation; 2-sided probability employed. α=0.10

Absent significant statistical difference it appears that (1) the precursor material for or (2) DBP stability of $CHCl_3$, TCP, and DBAN are more affected by coagulation than the other DBP species enumerated.

Investigating Br^-:DOC Ratio Effect

Owen *et al.* (1993) emphasized that Br:DOC ratios are effected by ultrafiltration, as Br^- is equally represented in the sample water and permeate while some DOC is retained by the MWCO filter. The authors suggested that the ultrafilter process may be analogous to coagulation removing larger AMW NOM, but they acknowledged that equalization of

the Br^-:DOC ratio prior to formation potential tests would provide a more effective inter-fraction comparison of per unit weight reactivity.

While Figures 4.7-4.9 and Wilcoxon Signed Rank Test illustrate minor DBP mass removal with coagulation, relative change in DBP formation potential is also visible in a fraction-by-fraction comparison, particularly when observed as normalized DBP formation potential. Treated sample TTHMs are 92 percent of observed formation potential from coagulated water in <10,000 AMW. Expanding the comparison to TDBPs, the <10,000 AMW resulted in 1.13 times the TDBPFP as the >10,000 bins.

Table 4.10 compares 96 hour DOC normalized DBPFP by MWCO. Coagulation appeared to have MWCO specific results. On a DOC normalized basis removal of <1,000 AMW fraction appeared to reduce $CHCl_3$, $CHCl_2Br$, DCP, TCP, and DBAN formation. DBAN removal continued through the 10,000 and 30,000 MWCO, but only DCAN decreased in the 30,000 MWCO (9 and 6 percent of DCAN reduction in 30,000 and 4,500K MWCO fraction). Formation potential on a DOC normalized basis rose for $CHCl_3$, $CHCl_2Br$, $CHClBr_2$, BCAN, and TCP in the <4,500 K fraction as a function of treatment.

Matrix 4

Matrix 4 investigated the effect equalizing DOC across MWCO fraction has on subsequent formation potential testing. Identification of a change in DOC normalized response would indicate that Br^-:DOC ratio is a factor affecting the rate of DBP formation.

Coagulated water was filtered through 1,000, 10,000, and 30,000 MWCO filters, equalized to 2.0 mg DOC/L, and analyzed for formation potential in parallel with a similarly fractionated but unequalized series of waters. Br^-:DOC ratios were ≈0.035 and ≈0.023 mg:mg for the equalized and unequalized series, respectively; Br^- concentration was 0.07 mg/L while chlorine was dosed at a 3:1 Cl_2/DOC ratio (mg:mg). Chlorination reactions in each of these solutions were subsequently quenched after 0, 24, 48, 96, and

Table 4.10. Raw and Coagulated DOC Normalized DBPFP by MWCO Fraction (96 hour)

	Raw (ug DBP/mg DOC)				Coagulated (ug DBP/mg DOC)				Change with Coagulation (ug DBP/mg-DOC)			
DBP	<1K	<10K	<30K	<4500K	<1K	<10K	<30K	<4500K	<1K	<10K	<30K	<4500K
CHCl3	56.92	47.32	45.14	34.18	47.49	46.04	50.18	50.45	17%	3%	-11%	-48%
CHCl2Br	24.4	13.05	14.43	12.36	13.43	12.6	13.72	12.79	45%	3%	5%	-3%
CHClBr2	5.12	3.63	1.89	1.55	9.88	2.19	1.86	2.65	-93%	40%	2%	-71%
CHBr3	0	0.24	0	0	0.7	0	0	0	---	100%	---	---
TCAN	0	0	0	0	0	0	0	0	---	---	---	---
DCAN	2.8	1.88	2.06	2.06	2.55	2.14	1.88	1.93	9%	-14%	9%	6%
DCP	0.04	0	0	0	0	0	0	0	100%	---	---	---
CP	0.39	0.59	0	0	1.74	0.56	0.61	0.12	-346%	5%	---	---
BCAN	1.55	0.67	0.69	0.66	1.39	0.86	0.71	0.71	10%	-28%	-3%	-8%
TCP	11.57	1.28	1.5	1.41	0.69	1.67	1.57	1.7	94%	-30%	-5%	-21%
DBAN	0.24	0.02	0.03	0	0.15	0	0	0.02	38%	100%	100%	---

Source: Matrix 3

168 hour time points. Both $CHCl_3$ and DCAN consistently appeared at low levels in the experimental controls. Response decreased with increasing Br^- and reaction time. This response was attributed to background levels of DOC in MilliQ® water; observed DOC levels in MilliQ® were ≈0.1 mg/L.

General Summary of Response and Comparison to Matrix Three

Equalized conditions were very similar to coagulated water conditions applied in matrix 3 (Table 4.11 summarizes DOC conditions), as such matrix 4 represents a partial, independent replicate of matrix 3.

Table 4.11. DOC Concentrations in Matrix 4 by MWCO Fraction

	DOC (mg/L)			
Series	<1K MWCO	<10K MWCO	<30K MWCO	<4,500K MWCO
Equalized	2	2	2	2
Unequalized	2.8	3	3	3

THMs

$CHCl_3$ and $CHClBr_2$ formation under equalized DOC conditions were in ranges similar to those observed in matrix 3, 9.5-75.2 ug/L and 4.2-39.6 ug/L, respectively. Change in $CHCl_3$ as a function of time was also consistent with the previous matrix. $CHCl_3$ and $CHCl_2Br$ formation ranged from 30 to 40 percent of $CHCl_3FP$ for similar conditions where DOC was not equalized. $CHClBr_2FP$ represented 1-17 percent of unequalized DOC series $CHCl_3$ formation. Again, slightly higher $CHClBr_2$:$CHCl_3$ ratio existed in equalized DOC series (96 hour, 4,500 K MWCO, 11 percent and 32 percent respectively). $CHCl_2BrFP$ and $CHClBr_2FP$ appeared consistently in both equalized and unequalized MWCO fraction and were present at similar concentrations across the DOC equalized, MWCO fractions. $CHBr_3$ was not present at quantifiable concentrations in matrix 4.

HANs and HKs

DCAN and BCAN were observed at higher levels in lower MWCO fractions. DCANFP in matrix 4 equalized series was lower but generally comparable to matrix 3 responses (e.g., within 20 percent error bar). With equalization, 168 hour DCANFP was 40 percent higher in 10,000 MWCO than in 4,500 K MWCO fraction, while BCAN increased 48 percent. AMW distribution of formation potentials were similar in unequalized series; DCAN and TCP formation potential in 4,500 K fraction were 43 and 47 percent less than 1,000 MWCO levels, respectively. Peak DCAN formation occurred sooner in low AMW fractions than higher AMW fractions. This retarding of DCAN formation rate occurred in both series implying greater DCAN substrate reactivity in lower MWCO fraction.

TCP peak values were consistently obtained at 24 to 48 hours under both equalized and unequalized conditions. TCP values ranged from 1.73 to 3.96 ug/L when DOC was equalized and were 2.5-4.9 ug/L when DOC was 3.0 mg/L (e.g., 48 hour reaction time). BCANFP occurred at a similar scale (0.01 - 3.43 ug/L) to that observed in matrix 3. Like DCAN, BCAN formation was focused in the lower MWCO fractions. TCAN was not observed in either DOC equalized or unequalized series.

Effect of DOC Equalization On DOC Normalized Formation Potential

Comparison of DOC normalized 168 hour DBP formation potentials suggests that significant change in normalized response occurred in the 10,000 MWCO DBPFP with equalization (Table 4.12). Figures 4.10 and 4.11 illustrate $CHCl_3FP$ over time and a reversal of fraction contribution after equalization (no equalization: 30,000 MWCO > 4,500 K MWCO > 10,000 AMW; equalized: 30,000 MWCO > 10,000 AMW > 4,500 K MWCO). Change in normalized formation potential reflects either concentration dependant reactivity or introduction of experimental artifacts. Potential experimental artifacts due to ultrafiltration and equalization techniques include: physical shearing of molecules, biological degradation, and DOC aggregation.

Table 4.12. Matrix 4, 168 Hour DOC Normalized Specific Formation Potentials by MWCO

	Formation Potential (ug/L)					
	Equalized (2 mg DOC/L)			Unequalized (≈3 mg DOC/L)		
DBP	10,000 MWCO	30,000 MWCO	4,500 K MWCO	10,000 MWCO	30,000 MWCO	4,500 K MWCO
$CHCl_3$	33.24	46.81	43.88	43.31	48.47	37.35
$CHCl_2Br$	12.67	20.69	19.04	26.88	24.89	25.90
$CHClBr_2$	7.76	2.56	1.51	3.77	3.68	4.66
DCAN	0.31	0.40	0.45	0.94	0.97	0.57
BCAN	0.06	0.25	0.27	0.69	0.67	0.37
TCP	0.41	0.55	0.60	1.83	0.76	0.49

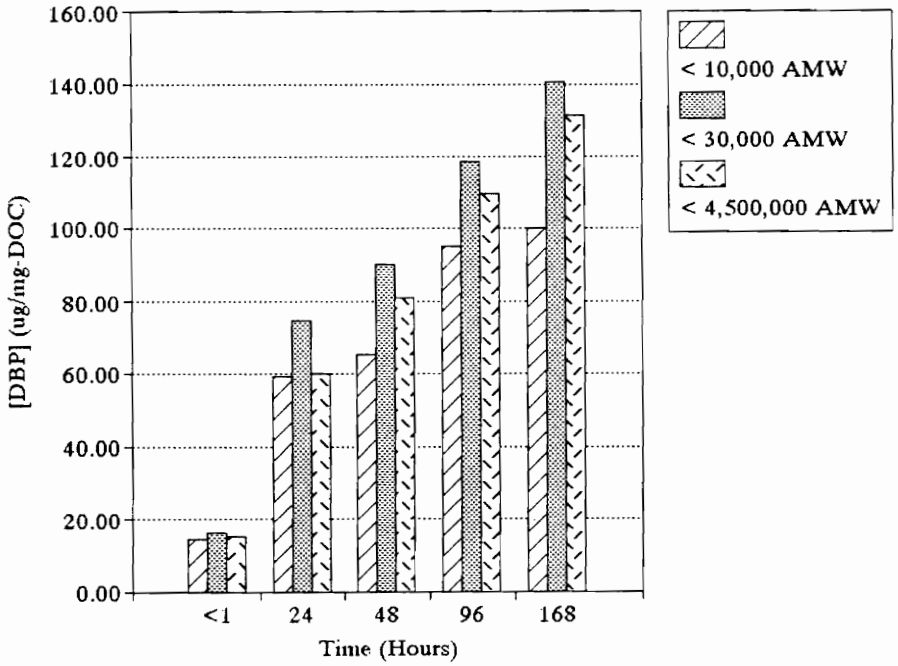

Figure 4.10. $CHCl_3$ Formation in Unequalized Coagulated Water by MWCO Fraction, 96 Hour, 3 mg DOC/L, 6 mg Cl_2/L, 0.07 mg Br^-/L

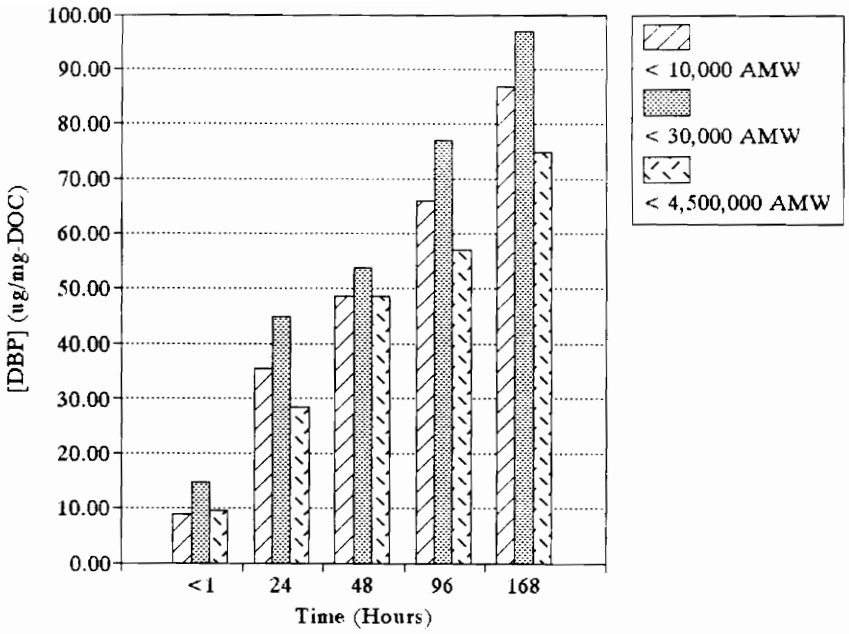

Figure 4.11. Equalized Coagulated Water $CHCl_3FP$ by MWCO Fraction, 96 Hour, 2 mg DOC/L, 6 mg Cl_2/L, 0.07 mg Br^-/L

Species specific change, as well as cumulative effects, were evaluated using a comparison (Wicoxon Ranked Sign Test) of DOC equalized and unequalized series formation potentials. The Wilcoxon Ranked Sign Test probability values presented in Table 4.13 illustrate that for individually observed DOC normalized specific DBPFPs and summations of DOC normalized DBPFP the equalization process altered the formation potential per unit weight of DOC. Probability values indicating significantly different populations are noted.

Matrix 4 results suggest that (1) physical effects of equalization or (2) response to variation in DOC make physical equalization have a significant effect on DBP formation. Matrix 6 investigates DOC concentration effects further.

Table 4.13. Effect of Equalization on DBPFP Associated with Each MWCO Fraction, Paired Wilcoxon Ranked Sum Probability

	MWCO		
DBP	10,000	30,000	4,500 K
$CHCl_3$	0.345	0.500	0.043 [1]
$CHCl_2Br$	0.080 [1]	0.080 [1]	0.138
$CHClBr_2$	0.715	0.715	0.068 [1]
DCAN	0.225	0.080 [1]	0.225
BCAN	0.043 [1]	0.068 [1]	0.068 [1]
TCP	0.345	0.138	0.500
TDBP	0.080 [1]	0.043 [1]	0.893
TTHM	0.080 [1]	0.893	0.893
THAN	0.138	0.080 [1]	0.080 [1]

Note: Probability assumed to have normal approximation; 2-sided probability employed.
(1) Indicates significantly different populations at α=0.1.

Effect of Experimental Parameters on DOC Normalized Specific Formation Potential

The Wilcoxon Ranked Sign Test evaluated matrix 4 data for change due to equalization. Another nonparametric statistic, the Spearman Coefficient, provided a measure of other experimental parameter effects (Table 4.14). This analysis investigated the impact of time, fraction, Br^-:DOC, and Br^-:Cl on formation potential trends across all matrix data.

The Spearman coefficients obtained from this analysis indicated formation potential correlated poorly with all test parameters. While correlations were weak, degree of correlation occurred in the following order, time > initial Br^-:Cl (mM:mM) > Br^-:DOC (mg:mg) > MWCO. Time was the only factor producing significant correlation coefficients (i.e., >|0.6|). Correlations to time were strongest and positive for the THMs, $CHCl_3$ and $CHClBr_2$. DCAN was significantly (Spearman coefficient = -0.735) and negatively correlated with time. Correlation for aggregated parameters TDBP, TTHM, and THAN weakened with divergent signs and correlation coefficients of the individual DBP species. In part, the absence of stronger correlations with these parameters is believed to reflect the impact of equalization on DBP formation.

Table 4.14. Correlation Between DOC Normalized Molar Response to Matrix 4 Experimental Factors, Spearman Correlation Coefficient.

	Spearman Correlation Coefficient			
DBP	Time (hours)	Fraction (MWCO)	[Br]:[DOC] (mg:mg)	[Br]:[Cl] (mM:mM)
$CHCl_3$	0.722 [1]	0.283	-0.165	0.144
$CHCl_2Br$	0.577	0.567	0.312	0.577
$CHClBr_2$	0.722 [1]	-0.283	-0.349	-0.577
DCAN	-0.733 [1]	-0.094	0.184	0.289
BCAN	-0.289	0.000	0.385	0.577
TCP	0.144	0.378	0.165	0.577
DBAN	0.144	-0.094	-0.459	-0.289
TDBP	0.577	0.472	0.110	0.433
TTHM	0.722 [1]	0.283	-0.165	0.144
THAN	-0.433	-0.094	0.184	0.289
THK	0.000	0.000	-0.128	0.289

Note: (1) Spearman coefficient indicates correlation between independent parameter and dependant variable (significant when coefficient is greater than |0.6|).

Matrix 5.1

The ratio of Br^-:Cl in water is known to affect speciation of THMs and HAAs. This matrix explicitly investigated Br^-:Cl ratio effects on ultrafilter fractions of coagulated water, where DOC concentration and Cl_2 dose were held constant and Br^- concentration varied. Coagulated water was filtered through 1,000, 10,000, and 30,000 MWCO filters. The resulting solutions and a 0.45 um permeate (4,500,000 MWCO) were then equalized to 2.0 mg DOC/L and amended to Br^- concentrations of 0.07, 0.2 and 0.5 mg/L. These solutions were then subjected to a 6 mg Cl_2/L dose (initial Br^-:Cl ratio (mM:mM), 0.01, 0.03, and 0.07).

EPA Method 551 analytes did not demonstrate a consistent response pattern in the control series; there was sporadic occurrence of brominated HAN species. Six of the 112 Method 551 blank condition-time point combinations presented formation potentials greater than the MDL. With higher Br^- concentrations $CHBr_3$, $CHClBr_2$, and $CHCl_2Br$ did form consistently in the control series and in clear relation to Br^-concentration and

time. Under control conditions species formation was consistently less than 10 percent of the 168 hour 4,500 K MWCO fraction formation potential. This response was attributed to background DOC in MilliQ® (≈0.1 mg DOC/L).

THMs

Previous authors and matrices in this research demonstrated THMFP increase with reaction time; this trend was also observed in this matrix (Figure 4.12). $CHCl_3$ formation increased with time (6.4-96.3 ug/L, 0-168 hour, 4,500 K MWCO, 0.07 mg Br^-/L, 2 mg DOC/L) and with decreasing initial Br^-:Cl ratio in all AMW fractions. DOC normalized $CHCl_3$FP varied little with MWCO fraction; moreover, responsiveness to the ratio varied little with increasing AMW. Like $CHCl_3$FP, $CHCl_2Br$ and $CHClBr_2$ formation increased with time (42.8 and 9.2 ug/L respectively, 168 hour, 4,500 K MWCO, 0.07 mg Br^-/L, 2 mg DOC/L). $CHCl_2Br$ and $CHClBr_2$ formation increased with increasing initial Br^-:Cl ratio in all AMW fractions. Among the ratios tested, $CHCl_2Br$ formation appeared to peak at initial Br^-:Cl ratio of 0.075 (83.2 ug/L, 168 hour, 0.5 mg Br^-/L, 2 mg DOC/L). $CHBr_3$FP was absent lacking Br^- addition; $CHBr_3$ concentration increases with increasing initial Br^-:Cl. $CHBr_3$ response to initial Br^-:Cl ratio was most rapid in larger AMW fractions, but reached a greater final concentrations in <1,000 AMW fraction (47.6 ug/L in 1,000 MWCO; 24.7 ug/L in 4,500 K MWCO; 0.5 mg Br^-/L, 2 mg DOC/L).

HANs

THAN decreased over time (Figure 4.13) with DCAN formation decreasing with time after peaking at 48 hour time point (12.27 ug/L, 4,500 K MWCO, 48 hour, 0.07 mg Br^-/L, 2 mg DOC/L). DCAN concentration also decreased with increasing initial Br^-:Cl ratio in all AMW fractions. DBAN formation was stable with respect to time (4.2 ug/L, 48 hours; 3.95 ug/L, 168 hours; 4,500 K MWCO, 0.5 mg Br^-/L, 2 mg DOC/L) while BCAN reached peak values after 48-96 hours (2.05 ug/L, 48 hours, 4,500 K MWCO, 0.07 mg

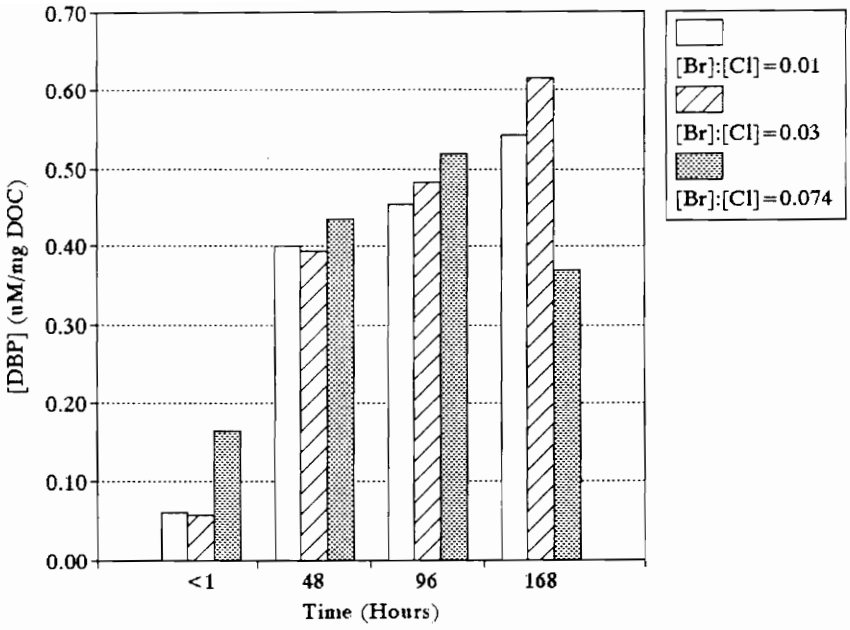

Figure 4. 12. THM DOC Normalized Formation Potential Identified in <30,000 MWCO Fraction as a Function of Br^-:Cl Ratio

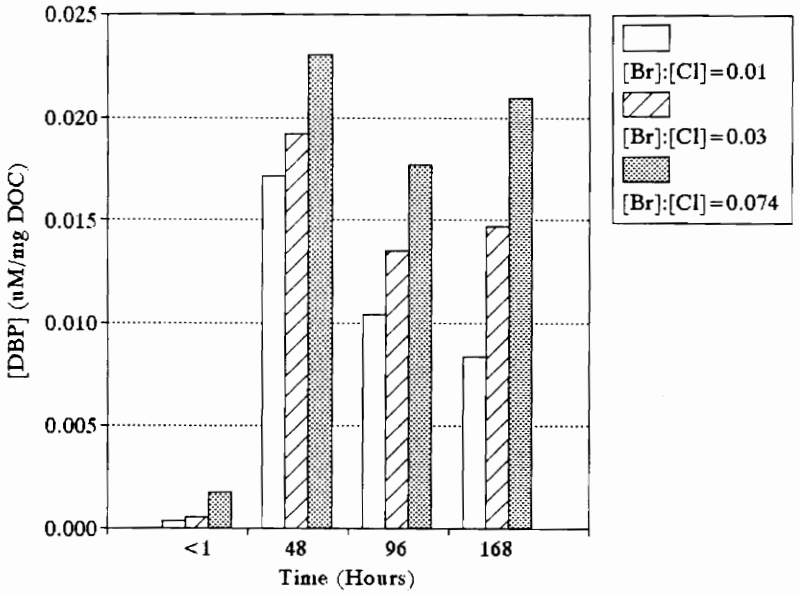

Figure 4. 13. THAN DOC Normalized Specific Formation Potential Identified in <30,000 MWCO Fraction as a Function of Br^-:Cl Ratio

Br^-/L, 2 mg DOC/L) and subsequently declined. Both maximum observed BCAN and DBAN formation increased with increasing initial Br^-:Cl ratio in all AMW fractions. Shifting of peak BCAN formation was not discerned. With BCAN and DBAN response to initial Br^-:Cl ratio, BCAN showed greater change with movement between lower ratio values, while DBAN demonstrated a uniform response over the range of ratios tested. Formation of BCAN and DBAN was greatest in 1,000 MWCO fraction (3,3 ug/L and 6.0 ug/L respectively, 168 hour, 1,000 MWCO, 0.5 mg Br^-/L, 1.9 mg DOC/L).

HKs and CP

TCP was the only quantified HK species in this matrix (0.03-5.04 ug/L). TCP formation decreased with increasing initial Br^-:Cl ratio; this effect was strongest in 1,000 MWCO fraction (5.04 ug/L and 0.06 ug/L, 0.07 and 0.5 mg Br^-/L respectively) . When the ratio reached 0.074, TCP formation approached zero. Maximum TCP formation occurred at 48 hour time point and declined with time (2.99 ug/L, 4,500 K MWCO, 48 hour, 0.07 mg Br^-/L, 2 mg DOC/L); the 1,000 MWCO fraction was an exception to this pattern, maintaining a constant TCP concentration (Figure 4.14). In previous matrices TCP had increased in the 1,000 MWCO fraction with time while larger MWCO fraction declined. CP concentrations were observed in the 1,000 MWCO fraction; response ranged from 0.18 ug/L at 48 hours to 3.2 ug/L at 168 hours (1,000 MWCO, 0.07 Br^-/L, 2 mg DOC/L).

Effect of Initial Br^-:Cl Ratio on DOC Normalized Specific Formation Potential

DOC normalized 168 hour TDBP formation potential varied with initial Br^-:Cl dose and MWCO fraction (Table 4.15). TTHM was consistently 94 to 97 percent of TDBP formation, with increasing initial [Br]:[Cl] ratio more DBP formation occurred on a weight basis but the fraction attributable to TTHMs remained consistent across 1, 10, and 4,500 K fractions and initial [Br]:[Cl]. Individual THMFPs, $CHBr_3$ and $CHClBr_2$, responded positively to increasing Br^- concentration while $CHCl_3$FP was negatively

correlated with Br^-:Cl. TTHM formation was greatest in the <1,000 MWCO fraction (1.49 uM/L, 168 hour, 0.5 mg Br^-/L, 2.0 mg DOC/L).

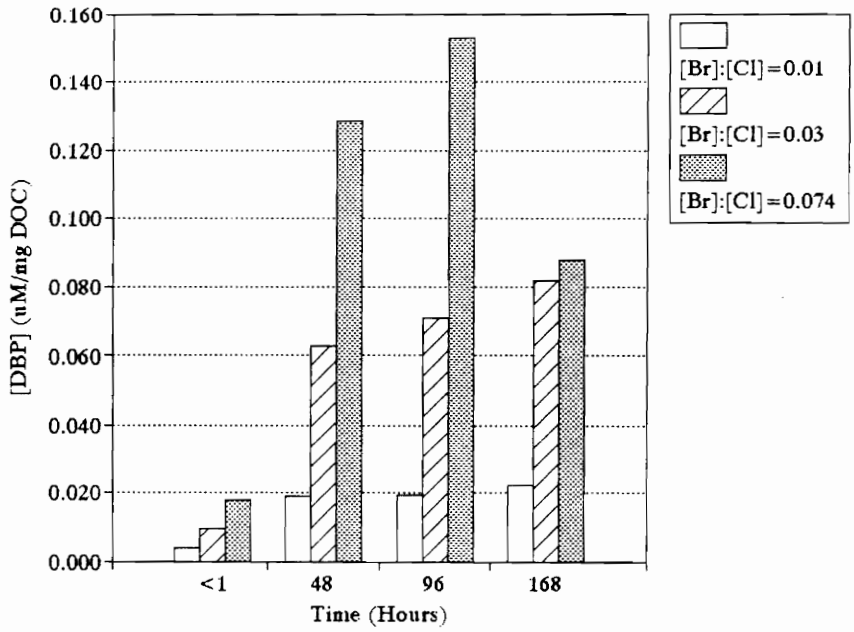

Figure 4. 14. TCP DOC Normalized Specific Formation Potential Identified in <30,000 MWCO Fraction as a Function of Br^-:Cl Ratio

Table 4.15. DOC Normalized 168 Hour Formation Potential by MWCO Fraction

	Specific Formation Potential (ug DBP/-mg DOC)											
	Br:Cl=0.013				Br:Cl=0.04				Br:Cl=0.09			
DBP	1K	10K	30K	4,500K	1K	10K	30K	4,500K	1K	10K	30K	4,500K
$CHCl_3$	59.14	44.65	47.60	46.76	21.11	29.15	35.75	32.22	14.55	15.95	16.63	14.05
$CHCl_2Br$	25.94	19.96	19.92	20.75	54.75	34.73	36.74	35.39	46.14	32.86	19.38	40.38
$CHClBr_2$	6.55	5.07	4.58	4.47	36.99	16.23	17.03	17.35	51.73	34.25	18.28	38.00
$CHBr_3$	0.19	0.17	0.09	0.05	10.72	2.17	2.29	2.34	24.79	13.22	5.91	14.61
DCAN	0.62	0.84	0.47	0.51	0.35	0.77	0.38	0.42	0.38	0.41	0.27	0.25
BCAN	0.68	0.76	0.46	0.49	1.37	1.32	0.90	0.95	1.71	1.23	1.14	0.95
TCP	2.56	0.72	0.64	0.62	0.14	0.57	0.41	0.42	0	0.04	0.06	0.01
DBAN	0.36	0.46	0.22	0.22	2.31	1.48	1.09	1.18	3.14	2.32	2.21	1.92
TTHM	91.82	69.85	72.20	72.04	123.57	82.28	91.81	87.31	137.20	96.28	60.20	107.04
THAN	4.36	2.88	1.79	1.83	4.18	4.13	2.77	2.97	5.23	3.99	3.68	3.13
TDBP	96.19	72.73	73.98	73.87	127.75	86.41	94.58	90.28	142.43	100.27	63.88	110.17

DOC normalized DCAN and TCP declined with increasing Br^-:Cl in all MWCO fractions. Peak DCAN formation potential values were observed consistently in 10,000 MWCO fraction, declining 50 percent with six fold increase in Br^-:Cl. TCP declined much more but response was less consistent in each MWCO fraction. BCAN and DBAN DOC normalized formation potentials increased with Br^-:Cl and were consistently higher in 1,000 and 10,000 MWCO fractions. DOC normalized BCAN and DBAN formation potentials increased 151 and 772 percent respectively over range observed (e.g., 1,000 MWCO).

Spearman Correlation Coefficient Analysis

The Spearman Correlation Coefficient, a nonparametric correlation statistic, was employed to determine if a statistically significant relationship existed between DOC normalized DBP formation potential and experimental design parameters, particularly the Br^-:Cl ratio. DOC normalized molar formation potential (uM/mg) response was tested against time, MWCO, initial Br^-:DOC ratio (mg:mg) and initial Br^-:Cl (uM:uM) ratio. The resulting coefficients suggest a consistent relationship between both THM and HAN species and initial Br^-:Cl ratio (Table 4.16).

Particular DBPs showed positive or negative correlations (>|0.60|) depending on incorporation of Br^-. $CHCl_3$, DCAN, and TCP were negatively correlated with initial Br^-:Cl dose, while $CHCl_2Br$, $CHClBr_2$, $CHBr_3$, BCAN, and DBAN were positively correlated. Br^- in the range tested (0.07-0.2 mg/L) was sufficiently active in DBAN formation to impart a positive and significant correlation coefficient to DBAN. As TCP was the only consistently quantitated HK in this matrix the THK correlation coefficient was negative.

Table 4.16. Correlation Between DOC Normalized DBPFP and Initial Br^-:Cl Ratio by MWCO Fraction, Spearman Correlation Coefficients,

	Probability			
	MWCO			
DBP	<1,000	<10,000	<30,000	<4,500 K
$CHCl_3$	-0.624 [1]	-0.686 [1]	-0.686 [1]	-0.748 [1]
$CHCl_2Br$	0.089	0.321	0.089	0.045
$CHClBr_2$	0.383	0.722 [1]	0.508	0.722 [1]
$CHBr_3$	0.811 [1]	0.935 [1]	0.811 [1]	0.935 [1]
DCAN	-0.641 [1]	-0.659 [1]	-0.613 [1]	-0.631 [1]
BCAN	0.196	0.196	0.353	0.321
TCP	-0.761 [1]	-0.720 [1]	-0.671 [1]	-0.671 [1]
DBAN	0.686 [1]	0.766 [1]	0.766 [1]	0.722 [1]
TDBP	-0.089	0.080	-0.365	-0.027
TTHM	-0.890 [1]	0.080	-0.365	-0.134
THAN	0.196	0.321	0.445	0.383

Note: (1) Indicates Spearman coefficient indicates correlation between independent parameter and dependant variable (>|0.6|).

Responses to the initial Br^-:Cl in the 10,000, 30,000, and 4,500 K MWCO fractions were somewhat more similar perhaps reflecting the minor role of larger AMW fraction after coagulation. Increasing response with increasing MWCO only occurred with respect to $CHBr_3$, while other species responded at a stable or declining rate with increasing MWCO: DCAN, BCAN, DBAN, $CHClBr_2$, $CHCl_2Br$, and $CHCl_3$.

With increasing initial Br^-:Cl ratio there was a consistent increase in percentage of TDBP represented by HANs on a DOC normalized basis reflecting BCAN and DBAN formation potential increases exceeding declines in DCAN (Figure 4.15). DBAN demonstrated positive association with increasing initial Br^-:Cl ratio, reaching a peak abundance at test conditions in the 30,000 MWCO fraction. Response across fractions increased 6 fold over the range of ratios tested.

Individual THM species shifts occurring in a balanced fashion across MWCO fractions resulted in a smaller effect on DOC normalized TDBP than the HAN shift with Br^-:Cl ratio increase. Table 4.17 summarizes DBP composition shifts with Br^-:Cl ratio at the

168 hour time point. Figures 4.16 illustrates the effect of Br^-:Cl ratio on normalized specific DBPFPs over time in 1,000 MWCO fraction.

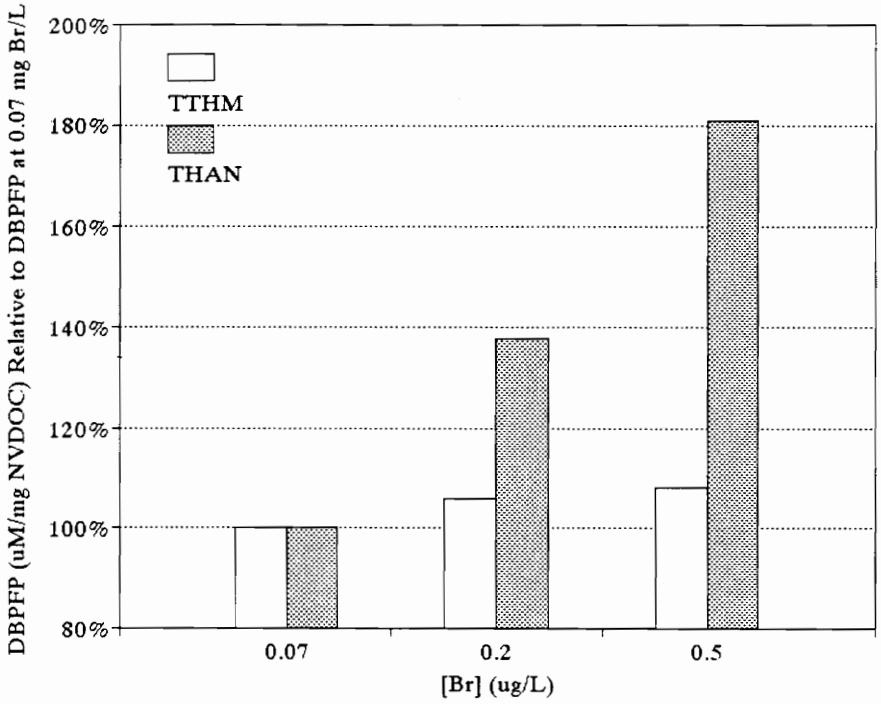

Figure 4.15. Relative Change in DOC Normalized TTHM and THAN Formation Potential with Respect to Br^- Concentration in 10,000 MWCO Fraction at 96 Hours

Table 4.17. Individual DBP Formation Potentials as Percentage of TDBP Formation at 168 Hour Time Point (Averaged Across Fractions)

	Percent of TDBPFP (DBPFP/TDBPFP)		
	Br^-:Cl Ratio (uM:uM)		
DBP	0.013	0.04	0.09
$CHCl_3$	62.6±1.2	30.9±8.4	16.2±6.0
$CHCl_2Br$	27.4±0.5	40.3±1.6	33.0±2.3
$CHClBr_2$	6.5±0.4	21.2±4.5	33.4±2.9
$CHBr_3$	0.2±0.1	4.0±2.5	13.3±2.9
DCAN	0.8±0.2	0.5±0.2	0.3±0.1
BCAN	0.8±0.2	1.2±0.2	1.3±0.3
TCP	1.3±0.08	0.4±0.2	---
DBAN	0.4±0.1	1.5±0.3	1.5±0.6

TCP formation potential responded negatively to Br^-:Cl ratio. TCP decreased from 1.3%±0.8 to below quantitation over the range of initial Br^-:Cl ratios tested. Normalized response in 10,000, 30,000, and 4,500 K MWCO fractions were very similar while 1,000 MWCO fraction demonstrated a smaller response to increasing ratio value from 0.01 to 0.03 (mM:mM). From the very limited CP response it appears to be associated with the 1,000 MWCO fraction and to form at lower initial Br^-:Cl ratios.

Wilcoxon Signed Rank Test

The Paired Wilcoxon Signed Rank Test was used to further investigate the relationship between MWCO and DOC normalized DBP formation. This analysis found that high-chlorine content DBPs (e.g., $CHCl_3$ and TCP) did not significantly change with MWCO fractions (α=0.1) (Table 4.18). Brominated species formation in 1,000 MWCO fraction was significantly different from formation potential associated with larger MWCO fractions reflecting differences in reactivity with Br^- between larger and smaller MWCO fractions.

Matrix 5.2

Matrix 5.2 like matrix 4 provides an independent, partial replicate of matrix 3; matrix 5.2 is a replicate with respect to formation potential in DOC equalized, 1,000 MWCO fraction. This matrix also contains two independent series under identical conditions, testing procedure repeatability.

Coagulated water collected from the Harwood's Mill Water Treatment Plant, was filtered through a 1,000 MWCO filter. The permeate was then concentrated to 1.4 mg DOC/L, and divided among two experimental trials, each of which was prepared separately. Independently, the two solutions were amended with Br^- such that the Br^- concentration was 0.07 mg/L, then subjected to chlorine doses of 0 and 6 mg Cl_2/L (initial Br^-:Cl ratio (mM:mM), 0.01). The control series did not result in any DBPFPs greater than the MDL (0.07 mg Br^- /L, 1.4 mg DOC/L).

Figure 4.16. Formation Potential Response to Initial Br:Cl in 10,000 MWCO Fraction, 0.07 and 0.2 mg Br^-/L

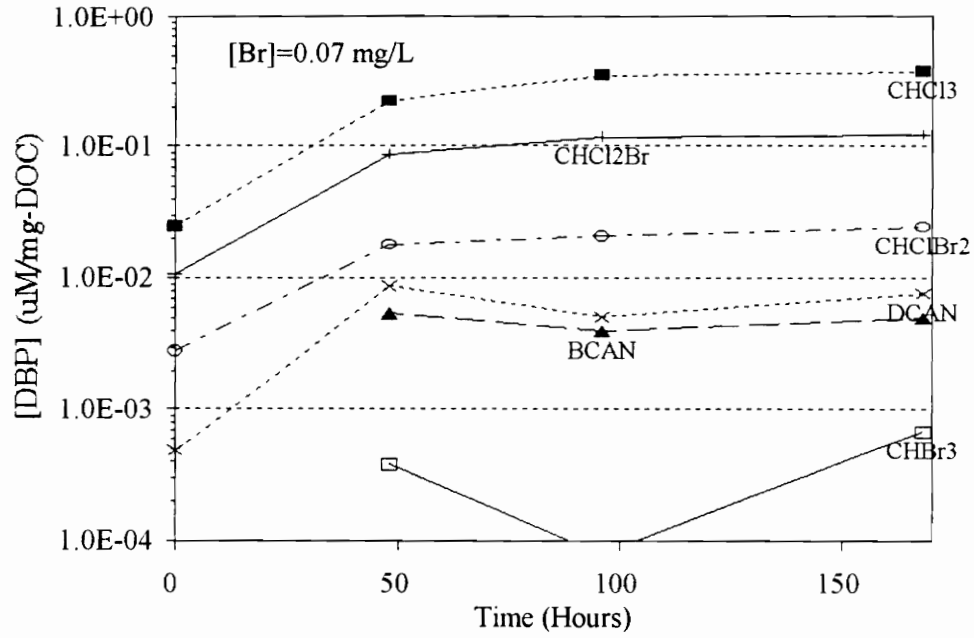

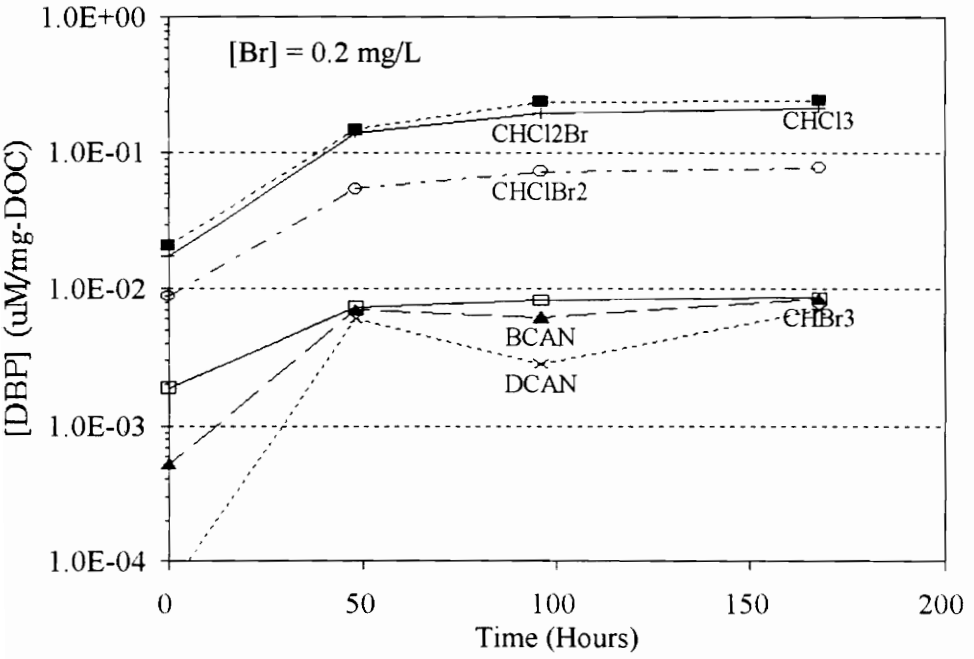

Table 4.18. DOC Normalized DBP Formation Relatedness to MWCO Fraction as Reflected by Wilcoxon Signed Rank Statistic (Varied Initial Br^-:Cl dose, 168 Hour)

		Probability		
		MWCO		
MWCO	DBP	10,000	30,000	4,500 K
1,000	$CHCl_3FP$	0.239	0.937	0.754
	$CHCl_2BrFP$	0.006 (1)	0.010 (1)	0.005 (1)
	$CHClBr_2FP$	0.005 (1)	0.003 (1)	0.003 (1)
	$CHBr_3FP$	0.008 (1)	0.003 (1)	0.017 (1)
	DCANFP	0.477	0.050 (1)	0.213
	BCANFP	0.021 (1)	0.013 (1)	0.008 (1)
	TCPFP	0.575	0.646	0.445
	TDBPFP	0.002 (1)	0.005 (1)	0.019 (1)
	TTHMFP	0.002 (1)	0.008 (1)	0.015 (1)
	THANFP	0.117	0.060 (1)	0.308
10,000	$CHCl_3FP$		0.012 (1)	0.530
	$CHCl_2BrFP$		0.695	0.583
	$CHClBr_2FP$		0.638	0.875
	$CHBr_3FP$		0.062	0.878
	DCANFP		0.477	0.182
	BCANFP		0.424	0.155
	TCPFP		0.646	0.508
	TDBPFP		0.239	0.433
	TTHMFP		0.239	0.308
	THANFP		0.272	0.209
30,000	$CHCl_3FP$			0.209
	$CHCl_2BrFP$			0.695
	$CHClBr_2FP$			0.638
	$CHBr_3FP$			0.646
	DCANFP			0.959
	BCANFP			0.508
	TCPFP			0.314
	TDBPFP			0.583
	TTHMFP			0.583
	THANFP			0.695

Note: Probability assumed to have normal approximation; 2-sided probability employed.
(1) Indicates significant at $\alpha = 0.10$.

Comparison with Matrix 3

This matrix provided a measure of quality control both through intra-test comparison of repeatability, and by comparison with values observed in matrix 3. $CHCl_3$ formation was smaller than observed in matrix 3, but the scale of the response was similar (3.97-147.97 ug/L). As previously, $CHCl_3$ formation increased with increasing time (35.1-147.9 ug/L, 168 hour, 0.07 mg Br^-/L). $CHCl_2Br$ formation rate increased with time within a scale similar to matrix 3, though the maximum value reached was twice the maximum value in matrix 3 (89.7 ug/L, 168 hour, 0.07 mg Br^-/L). The $CHClBr_2$ formation trend mirrored matrix 3 in scale and rate, but at a slightly lower concentration (15.68 ug/L, 168 hour, 0.07 mg Br^-/L). As in matrix 3, $CHBr_3$ was only observed at baseline levels, and typically below the MDL.

Independent 1,000 MWCO-Br^-:Cl Condition Trials

Matrix 5.2 illustrated the reproducibility of the results obtained from any one treatment scenario. While most of the data described in this research reflects independent trials of a given condition, Matrix 5.2 is a side-by-side comparison of two independent trials. The results from both trials were very similar. Table 4.19 summarizes the average 168 hour DOC normalized formation potential for each DBP observed and each analyte's percentage representation of the mean observation. Only DCP and CP diverge from the average DOC normalized response by more than 10 percent. Figures A-8.1 through A-8.10 illustrate individual DBP response over time with error bars illustrating variation occurring over time.

Matrix 6

Matrix 6 evaluates formation potential as a function of DOC in 0.45 um filter permeate while the Cl_2:DOC ratio was held constant. Raw water was collected from the Harwood's Mill water treatment plant and filtered through a 0.45 um filter (4,500,000

Table 4.19. DBP Formation Potentials (168 Hour), A Side-by-Side Trial

		Formation Potential (ug DBP/mg DOC)			
		Sample 1		Sample 2	
DBP	Mean	DBPFP	% of Mean	DBPFP	% of Mean
$CHCl_3$	0.847	0.885	105%	0.809	95%
$CHCl_2Br$	0.381	0.391	103%	0.370	97%
$CHClBr_2$	0.050	0.538	107%	0.047	93%
DCAN	0.008	0.008	104%	0.007	96%
DCP	0.003	0.004	119%	0.003	81%
CP	0.001	0.001	81%	0.001	119%
BCAN	0.005	0.005	110%	0.004	90%
TCP	0.072	0.075	104%	0.069	96%
DBAN	0.003	0.003	104%	0.003	96%
TDBP	1.371	1.427	104%	1.314	96%
TTHM	1.279	1.33	104%	1.227	96%
THAN	0.015	0.016	106%	0.014	94%
THK	0.073	0.076	103%	0.071	97%

MWCO). The resulting permeate was then diluted to achieve three DOC concentrations: 0.4, 1.5, and 3.0 mg DOC/L. Each solution was divided in half and amended with Br^- such that Br^- concentrations were 0.2 and 0.5 mg/L. These solution were then subjected to chlorine doses at a 3:1 Cl_2/DOC (mg:mg) ratio. The resulting doses were 1.5, 4.5, and 9.0 mg Cl_2/L, corresponding to initial Br^-:Cl dose ratios (mM:mM) 0.04, 0.05, 0.12, and 0.3.

General

TTHM and THANs increased five and 2.75 times, respectively, with increasing DOC (0.5-2.9 mg DOC/L; 168 hour). TCP appeared at higher DOC but was not detected at lower concentrations. Increasing Br^- concentration resulted in greater TDBP and more brominated species formation. Proportional comparisons of the Br^- concentration effect was greater at lower DOC concentrations. Increasing brominated species formation was proportionally greater for HANs than THMs, except $CHBr_3$. As previously demonstrated THM response was positively correlated with time and with DOC concentration; DOC

concentration appeared to more strongly affect the maximum formation reached than reaction rate.

As in previous matrices the MilliQ® control series demonstrated a response consistent with a low level DOC concentration in the MilliQ® water. Method 501.1, 168 hour formation potential tests in the control series consistently produced less than 8 percent of actual treatment series formation potentials. DBAN demonstrated a similar occurrence level in Method 551 controls.

Comparison to Matrix 3

$CHCl_3$ and BCAN concentrations were comparable with matrix 3. DCAN concentrations were lower than those observed in matrix 3 (approximately one third lower) and DBAN concentrations were higher than previously observed. Timing of peak TCP formation varied, but not in a consistent manner; in matrix 3 TCPFP had decreased over time (maximum observed value 2.58-4.34 ug/L). Dissipation subsequent to peaking at 24-96 hours was observed in DCANFP, BCANFP, and DBANFP; early peak formation tended to reflect increased Br^- and DOC concentrations. Maximum HANFP for brominated species increased with increasing bromide dose and DOC concentration; DBAN formation occurred at levels three times matrix 3 peak values. DCP and CP concentrations were seldom at quantifiable levels.

Effect of Br^-:DOC Ratio

Matrix 6 compared the effect of six Br^-:DOC ratio conditions under known chlorine dose:DOC ratio conditions but varying Br^-:Cl conditions. Spearman correlation coefficients presented in Table 4.20 with respect to significant experimental parameters confirm that THM formation is closely correlated with DOC concentration within the range tested. The data are not adequate to suggest any significant relationship with respect to HANs or HKs. In contrast to matrix 5.1 results, among the THMs correlation between formation potential and DOC concentration decreased with increasing bromide

concentration. Initial Br^-:Cl dose was observed with a negative correlation to $CHCl_3$ and $CHCl_2Br$ formation potential, while the initial Br:DOC ratio was covariant with the initial Br^-:Cl ratio.

Table 4.20. Spearman Correlation Coefficient Analysis of DBPFP with Respect to Experimental Parameters.

DBP	[Br^-]	[DOC]	[Cl]	[Br]:[DOC]
$CHCl_3$	-0.196	0.851 [1]	0.835 [1]	0.824 [1]
$CHCl_2Br$	-0.058	0.836 [1]	0.821 [1]	-0.714 [1]
$CHClBr_2$	0.258	0.603 [1]	0.599	-0.393
$CHBr_3$	0.782 [1]	-0.265	-0.222	0.583
THAN	0.743 [1]	0.326	0.429	-0.006
TTHM	0.112	0.730 [1]	0.730 [1]	-0.578
TDBP	0.173	0.726 [1]	0.755 [1]	-0.567

Note: (1) Indicates correlation >|0.6|.

Once transformed to a DOC normalized formation potential, Spearman Correlation Coefficient analysis found relatedness to time to be more apparent (Table 4.21).

Table 4.21. DOC Normalized DBPFP with Respect to Experimental Parameters.

DBP	Time	Br^-:DOC
$CHCl_3$	0.528	-0.558
$CHCl_2Br$	0.735 [1]	-0.461
$CHClBr_2$	0.765 [1]	-0.138
$CHBr_3$	0.305	-0.917 [1]
DCAN	0.054	0.414
BCAN	0.164	0.315
TCP	-0.000	0.577
DBAN	0.068	0.269
TTHM	0.920 [1]	0.055
THAN	0.128	0.463
TDBP	0.858 [1]	0.177

Note: Indicates correlation >|0.6|.

Analyzed graphically the observed formation potentials reflect time, Br^-:Cl, and Br^-:DOC effects (Figure 4.17). TDBP formation increased with time; change with respect to time was the largest change observed. The covariance of Br^-:Cl and Br^-:DOC ratio obscure identifying a definitive trend from Matrix 6 alone. However, a comparison of responses observed in matrix 5.1 and 6 illustrate Br^-:DOC ratio effect on DBP response. BCAN formation potential is a particularly good example, where Br^-:DOC ratio is correlated with maximum DBP formation (Figure 4.18 and 4.19).

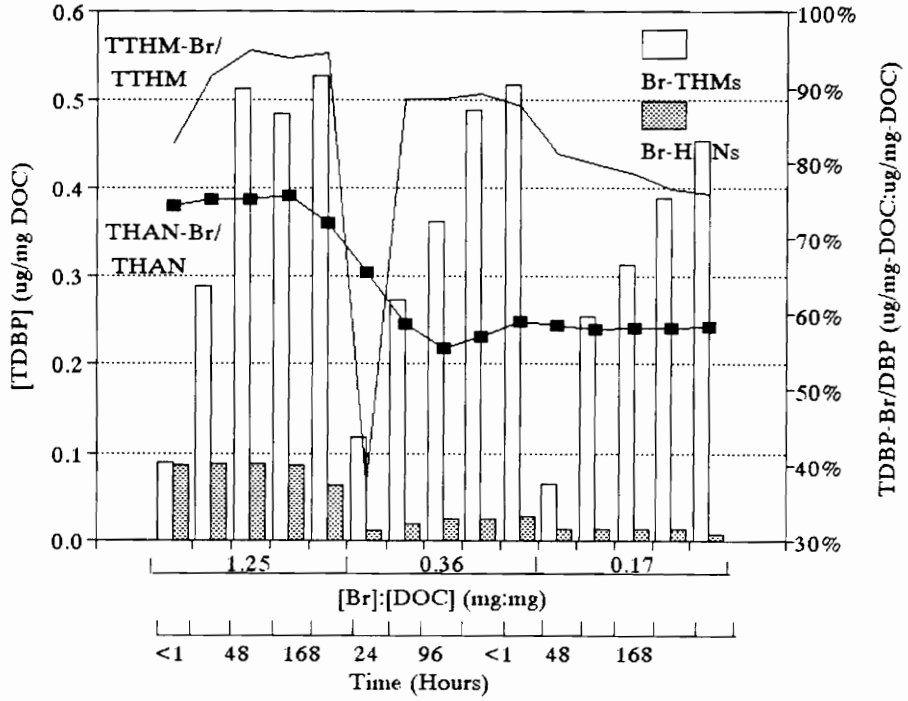

Figure 4.17. TTHM and THAN Response to Br^-:DOC ratio (0.4, 1.5, 3 mg DOC/L; 0.07 mg Br^-/L, 0, 24, 48, 96, and 168 time points).

Relationship to Research Objectives

The following is a comparison of the results obtained in this research with previous research directly related to this study's research objectives. Particular comparisons are drawn with research by other authors particularly those: (1) using the same source water, (2) investigating Br^-:Cl ratio effects, (3) investigating Br^-:DOC trends and (4) investigating DBP formation mechanisms.

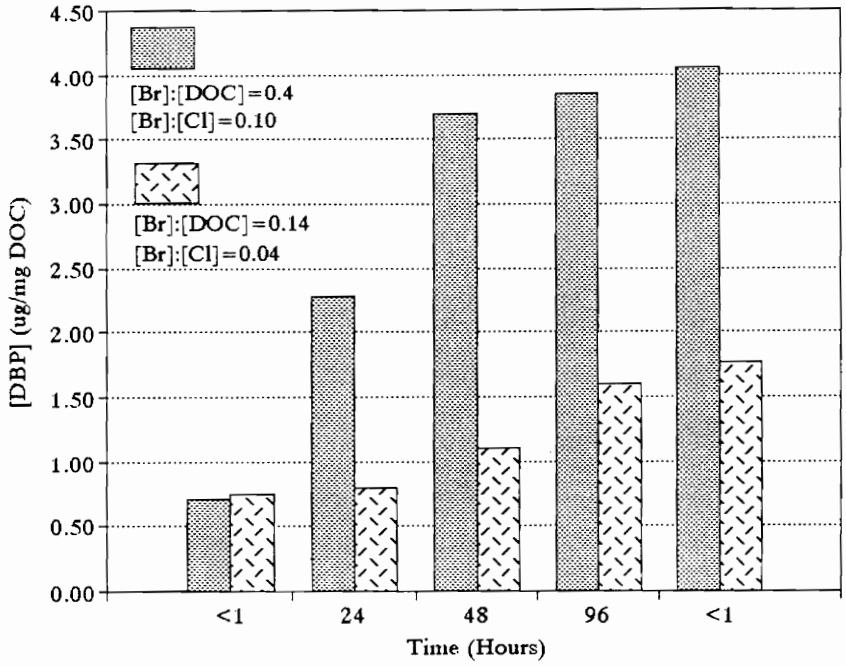

Figure 4.18. BCAN Specific Formation Potential with Respect to Time (4,500 K MWCO, 2 mg DOC/L; 0.07 mg Br^-/L).

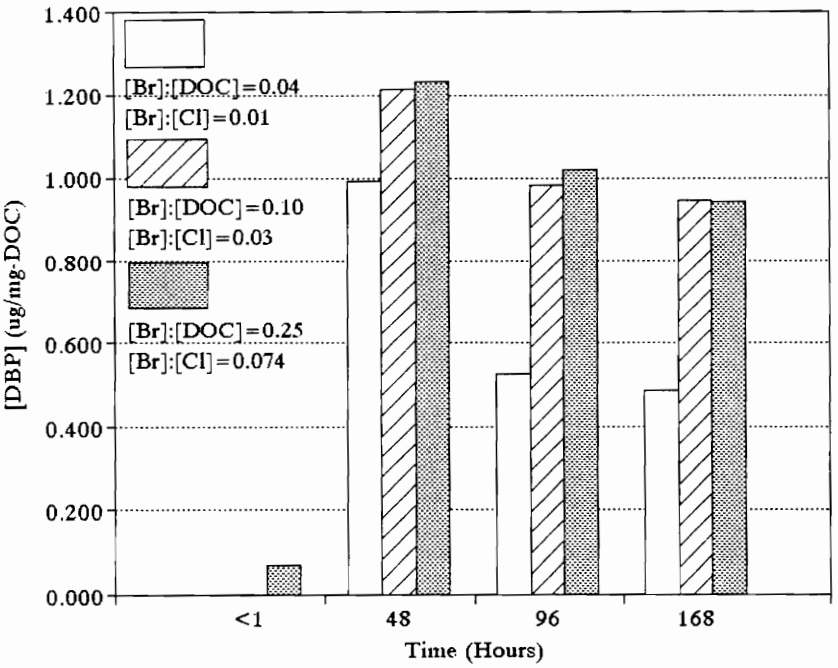

Figure 4.19. BCAN Specific Formation Potential with Respect to Time (4,500 K MWCO, 0.4, 1.5, 3 mg DOC/L; 0.07 mg Br^-/L).

Harwood's Mill Reservoir Water

In benchscale coagulation studies, Owen *et al.* (1993) and Smith *et al.* (1994) observed THMFP decline in coagulated water compared with raw water. Smith *et al.* noted HANFP decline from ≈7 ug/L in raw water to 4-5 ug.L with coagulation, while Owen *et al.* indicated that HANFPs increased upon coagulation of raw water. Smith *et al.* also observed HK formation decline with coagulation. While this research found TCAN and DCP difficult to quantitate, Smith *et al.* were unable to consistently quantify $CHClBr_2$ and $CHBr_3$.

Both Owen *et al.* and Smith *et al.* conducted trials at coagulant doses similar to actual plant operating conditions and each achieved 30 and 52 percent TOC removal, respectively. This analysis employing clarified water obtained from the Harwood's Mill Water Treatment Plant; observed TOC removal during this analysis was 49 percent; DOC removal was 40 percent.

Owen *et al.* found 63 percent of the raw water TOC in less than 10,000 AMW fraction and 24 percent less than 1,000 AMW fraction. Smith *et al.* found 87 percent of TOC in less than 10,000 AMW and 28 percent less than 1,000 AMW. This research found the distribution of DOC in these fractions to be 88 and 10 percent, respectively.

THAN and individual HAN levels observed in coagulated water tests by this research were also similar to those observed by Smith *et al.* and Owen *et al.*. In 4 day SDS tests (clearwell water, pH 7.25, TOC 3.18) Smith *et al.* reported: $CHCl_3$SDS, 159.5 ug/L; $CHCl_2$BrSDS, 19.7 ug/L; DCANSDS, 0.72 ug/L, BCANSDS, 0.48 ug/L; TCPSDS, 2.85 ug/L; and DCPSDS, 0.68 ug/L. Owen *et al.*'s observations of formation potential with respect to AMW included a marked decrease in DCAN with coagulation in 5,000, 10,000 MWCO and 30,000 MWCO fractions; a trend this research supports for 10,000 MWCO. Owen *et al.* noted a leveling of DCAN formation across MWCO fractions with coagulation, while this research observed HAN to be independent of MWCO (equalized,

2 mg/L). This research found HANFP to be focused in 1000-10,000 AMW fraction, and little change in any fraction with coagulation.

Br⁻:Cl Ratio

Symons *et al.* (1993) thoroughly investigated the Br⁻:Cl relationship with respect to TTHM and THM speciation. Symon's work concluded that increasing the Br⁻:Cl ratio increases the Br-THM and TTHM formation. This research observed similar behavior for THMs in raw, coagulated and fractionated waters. By investigating HAN response with respect to Br⁻:Cl ratio this research identified a similar response in HANs. THANFP increased with increasing Br⁻:Cl ratio. The increase in Br-THANFP occurred to a greater extent on a relative basis than Br-THMFP, indicating that Br⁻ interacts with more reactive sites in NOM than chlorine to produce HANs.

Br⁻:DOC Ratio

Higher Br⁻:DOC ratios are achieved at lower Br⁻ concentrations when DOC is small. As DOC concentration declines and Br⁻ concentration is unaffected by filtration, Br⁻:DOC ratios increase with decreasing MWCO. Summers *et al.* evaluated Br⁻:DOC effects on THM species formation in SDS tests (16 mg Cl_2/L, 23°C, 3 days), observing higher percentage brominated-THM formation with increasing Br⁻:DOC ratio.

Formation of brominated DBP species was observed by Owen *et al.* (1993) to increase with decreasing AMW as would be predicted from change in Br⁻:DOC ratio. Owen *et al.* attributed increased brominated species to Br⁻:DOC ratio and NOM chemical character. In this research where Br⁻:DOC ratio was held constant across all AMW fractions, brominated species were more distributed across fractions. Difference in response between the two analyses supports Owen *et al.*'s contention that Br⁻:DOC ratios created during ultrafiltration favor brominated DBP formation in smaller AMW fractions.

Matrix 4 and 6 explored the impact of varying the Br⁻:DOC ratio. The resulting observation provide a comparison with DOC dilution experiments conducted by Summers

et al. (1993) investigating Br^-:DOC ratio effects on brominated THM formation, and broaden Owen *et al.*'s investigation of membrane process effects on HANs. The effect on HANs occurs on a similar scale (<10 percent) to that observed in THMs within the observed range of DOC and Br^- conditions (0.4-2.9 mg DOC/L, 0.07 mg Br^-/L). Also, while Summers *et al.* demonstrated Br^-:DOC effect with a single point in time, this research demonstrated that Br^-:DOC effects are increasingly unmasked from Br^-:Cl effects with increased reaction time, appearing most distinctly after 48 hours.

Construction of matrix 4 maintained Cl_2 dose:DOC constant for comparison purposes, however in this construct Br^-:Cl ratio in the DOC equalized series was 1.4 times Br^-:Cl ratio in the unequalized DOC series. As a result the matrix results complied with guidance for formation potential testing proposed by Symons *et al.* (1993) but did not provide as clear an insight into Br^-:DOC relationship as Summers *et al.* (1993) using fixed Cl_2 dose THMSDS analysis. It is comparable to a parallel analysis by Summers in that same paper using a 2:1 Cl_2:DOC ratio.

Comparison of 96 and 168 hour time points between equalized and unequalized conditions (Br^-:DOC ratios 0.35 and 0.023 mg:mg) illustrate consistently higher brominated species concentrations relative to TTHM and THAN with equalized condition (higher Br^-:DOC ratio). The 52 percent increase in Br^-:DOC resulted in a 6 percent increase in Br-THM/THM and 7 percent increase in Br-HAN/THAN.

Br^-:DOC ratio effects were explicitly observed in matrix 6. Monitoring HANs a similar shift was observed between DCAN, BCAN, and DBAN to the shift in Br^--THM/TTHM observed by Summers *et al.*. TCAN was also monitored but did not occur above limit of detection. While Summers *et al.* premised Br^-:DOC ratio research on the reactivity of Br^-, their investigation evaluated change in response with respect to a single point in time. In this research the effect could be observed to occur across all time points monitored, the effect reflected most in maximum formation potential achieved.

Substrates and DBP Formation

Commonalities exist with previous research both with respect to (1) MWCO fraction specific response and (2) previously identified formation mechanisms. DBP formation involves very reactive species (Br^+ and Cl^+) and a number of complex and inadequately characterized organic precursors. The chemical reactions occurring among these molecules will be many and diverse, but two simple processes which could be occurring are halogen substitution and DCAN hydrolysis.

Halogen Substitution

The observed Br^-:Cl ratio effect in the absence of $CHCl_3$ concentration change would suggest a halide exchange phenomena may be occurring. An equilibrium driven process known as the Finkelstein reaction (March, 1977) is a known nucleophilic alkyl halide reaction process. The Finkelstein reaction is a nucleophilic substitution reaction, a type of reaction considered collision frequency dependant; therefore concentration and temperature dependant (Solomons, 1988). Reaction rate is dependant on halide reactivity and the stability of the leaving compound (Solomons, 1988). Research investigating taste-and-odor issues associated with chlorine dioxide disinfection observed a similar substitution reaction occurring to chlorodecane added to treated drinking water (Dietrich and Hoehn, 1991). In that research chlorine residual levels less than 1.5 mg/L and high bromide concentrations (<2 mg/L) contributed to the formation of bromooctane from 1-clorooctane.

The hypothesis that halogen substitution accounts for increasing bromination as a percentage of HAN species with time agrees with Cooper *et al.*'s (1985) suggestion that chlorine is a more effective oxidant than bromine and bromine is a better substitution agent. It is also in keeping with decline of DCAN observed by Smith *et al.* and by Reckhow *et al.* (1992). Accepting this hypothesis would extend the accepted theory with regard to THM speciation to HAN speciation with the additional observation that the proportional effect on THAN is greater than the effect on TTHM.

Hydrolysis of DCAN

An alternative mechanism explaining the decline of DCAN with time is hydrolysis. de Leer *et al.* (1986) observed hydrolysis of DCAN to hydroxamoyl chlorides which subsequently form amide intermediates that are subject to breakpoint chlorination reactions. Hydrolysis of DCAN in this manner, might result in DCAN acting as an intermediate in the formation of another DBP. Matrix 1 does not contain sufficient data to infer a relationship with one of the measured DBPs.

Molecular Weight Cutoff Fraction

The specific reactivity of the lower MWCO fractions and greater degree of NOM coagulation in >10,000 AMW fraction was documented in greatest detail by Owen *et al.*(1993) and observed by others.

1,000 MWCO Nitrogen Sources

Findings by previous researchers that DCANFP declined with coagulation complies with Reckhow *et al.*'s (1992) identification of the humic acid extract hydrophobic-fulvic fraction's richness in DCAN precursors. However, both Owen *et al.* (1993) and this research found that the Harwood's Mill Reservoir 1,000 MWCO fraction was a source of HAN formation that was not amenable to coagulation. This finding is in keeping with another of Reckhow *et al.*'s findings, that the hydrophilic base fraction produced more DCAN on a weight basis than the hydrophobic acid fraction. The hydrophilic base fraction was less abundant and contributed less to total formation potential in Reckhow *et al.*'s analysis.

Identification of high HANFP in 1,000 MWCO fraction is in keeping with Thurman's (1985) observation that 15-20 percent of nitrogen in humic fraction is contributed by amino acids. Amino acids would be found in 1,000 MWCO permeate, while many larger nitrogen containing protein structures would be retained by larger MWCO filters.

Oliver and Visser (1980) pointed out that microbial extract was an excellent source of 1,000 MWCO precursor material. Harwood's Mill Reservoir is a reservoir water source, which can act as both a biological reactor to support microbial growth and act as a settling basin for sediment and associated organic matter. A combination of Oliver and Visser's and the findings relative to the 1,000 MWCO fraction would indicate that investigation of aquatic microbial products produced in the reservoir would be a useful extension of this research.

Coagulation and Formation Potential

Coagulation is viewed as a major tool in water treatment to control DBP formation. An important aspect of coagulation is preferential removal of DBP precursors. Evaluating change in specific formation potential with coagulation provided an opportunity to evaluate this effect with respect to 0.45 um filtered Harwood's Mill Reservoir water. Comparison of DBPFP from Harwood's Mill Reservoir did not demonstrate a strong DBP formation potential reduction.

Like Smith *et al.* (1994) this research found THK to be recalcitrant to coagulation. TCP was consistently produced under the conditions tested, including the range of Br^-:Cl ratios tested.

Chapter 5. Summary and Conclusions

In July 1994, the U.S. Environmental Protection Agency (EPA) proposed revising maximum contaminant levels (MCL) and expanding the number of DBPs subject to regulation. In 1996 the Information Collection Rule will require many water treatment facilities to monitor for previously unregulated disinfection byproducts (DBPs) including haloacetonitriles (HANs) and haloketones (HKs). Proper monitoring of non-trihalomethanes (THMs), like HANs and haloketones (HKs), would be assisted by increased understanding of DBP formation rates and speciation. Moreover, DBP management currently focuses on total organic carbon (TOC) removal (e.g., enhanced coagulation and nanofiltration). The research undertaken here investigated the DBPs associated with chlorination of coagulated waters, specifically the relationship between non-THM DBP formation and (1) Br^-:Cl ratio and (2) natural organic matter (NOM) nominal size fraction. HAN, HK, and THM formation potentials were determined for raw and coagulated waters under conditions of variable NOM apparent molecular weight (AMW) distribution and constant bromide, dissolved organic carbon (DOC), and chlorine dose.

Observed Formation Potential

THMs occurred at concentrations similar to those reported in the literature (Owen *et al.*, 1993) (TTHM, 104-263 ug/L; $CHCl_3$, 36-114 ug/L; $CHCl_2Br$, 36-105 ug/L; $CHClBr_2$, 25-99 ug/L; $CHBr_3$, 8-48 ug/L). Under typical formation potential conditions (0.07 mg Br^-/L, 2.3 mg DOC/L, and chlorine dose of 6 mg/L) DCAN was the most consistently observed HAN, peaking at 48-96 hours and occurring in a range from 2.6-4.0 ug/L. BCAN also occurred and decreased with reaction time (2.1-0.9 ug/L). TCAN and DCP occurred consistently at concentrations below < 0.03 ug/L. TCP formation declined from 3.8 to < 2.0 ug/L over the same range of reaction times. DBAN formation was present at a low level, frequently < 0.15 ug/L. CPFP extended over a range extending from 0.2

to 2.54 ug/L, declining with reaction time. Figures 5.1 and 5.2 illustrate HAN, TCP, and CP formation with time in raw and coagulated waters.

Br^-:Cl Ratio Effect

At Br^-:Cl ≥0.03 mM:mM brominated HAN and HK species occur at concentrations comparable to $CHBr_3$ (Figure 4.9). With increasing initial Br^-:Cl dose ratio there was a consistent increase in percentage of TDBP represented by HANs on a DOC normalized weight basis. Individual THM species resulted in an average increase in TTHMFP of 23 percent over the Br^-:Cl range tested (0.01 - 0.07 mM:mM) while THAN increased 122 percent on average over the same range (Figure 4.18). This pattern recurred in a consistent manner across MWCO fractions and reaction periods ≥48 hours (Figure 4.17), suggesting that bromide not only competed with chlorine for available precursor reaction sites, it is also reacted with sites unavailable to the chlorine.

Molecular Weight Cutoff and Non-THM Formation

Specific HAN formation potential were greatest in the <1,000 MWCO fractions, but THAN was relatively insensitive to MWCO. DCAN was the dominant HAN formed under all conditions, consistently representing 75 percent of DOC normalized THAN formation in coagulated water. DBAN demonstrated strong positive association with increasing initial Br^-:Cl ratio; the greatest DBAN formation occurring in the <30,000 MWCO fraction. TCP formation potential was strongly and negatively correlated to the initial Br^-:Cl ratio but insensitive to MWCO. CP response also appears to be associated with the <1,000 MWCO fraction and to form at lower initial Br^-:Cl ratios.

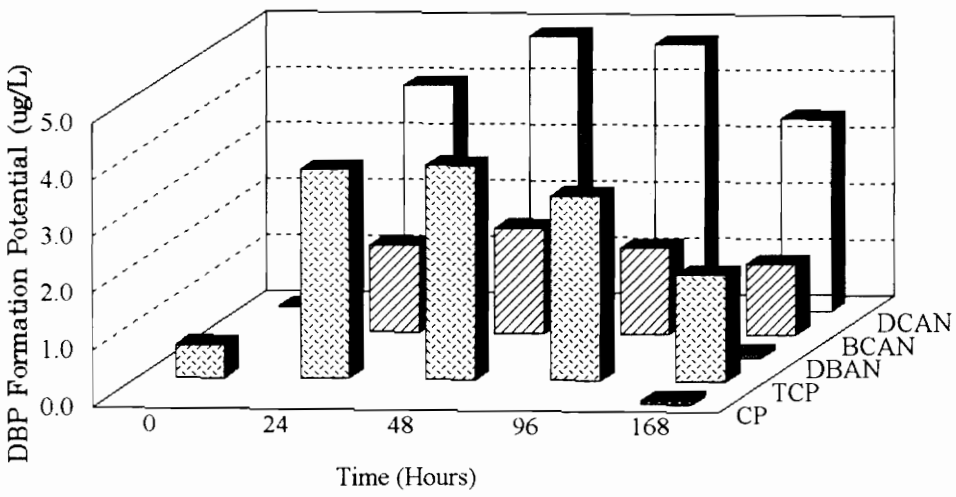

Figure 5.1 Raw Water HAN Species Formation with Time (2 mg DOC/L, 0.07 mg Br^-/L, 6 mg Cl_2/L)

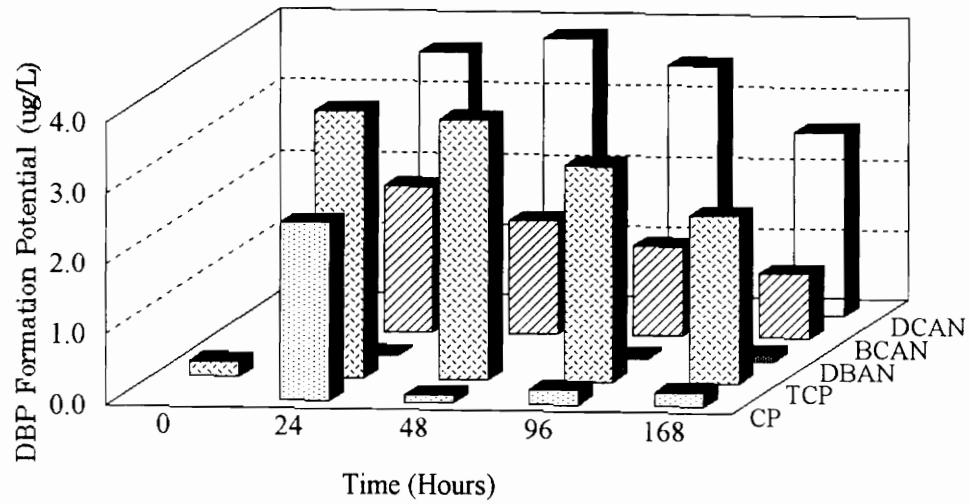

Figure 5.2 Coagulated Water HAN Species Formation with Time (2 mg DOC/L, 0.07 mg Br^-/L, 6 mg Cl_2/L)

Formation Potential for Coagulated vs. Raw Water

For this water, coagulation did not appear to affect specific formation potentials (Figures 5.3 and 5.4) or actual DBP formation potential. Nonparametric statistical analysis found that HANs, $CHCl_2Br$ and $CHClBr_2$ did not demonstrate significant change with coagulation. Coagulation resulted in changes in $CHCl_3$, $CHBr_3$, and TCP distribution, but not at a significant level (Wilcoxon Signed Rank Test, probability: 0.136, 0.317, and 0.173, respectively; α=0.1).

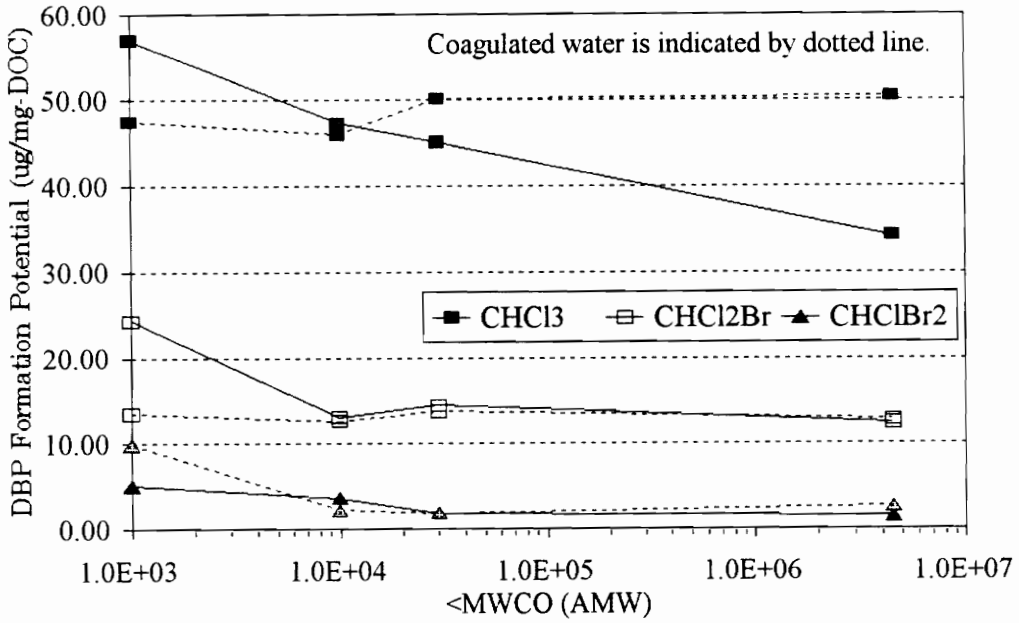

Figure 5.3. DOC Normalized THM Species Specific Formation Potentials, Change with Coagulation (2 mg DOC/L, 0.07 Br^-/L, 6 mg Cl_2/L, 96 Hours)

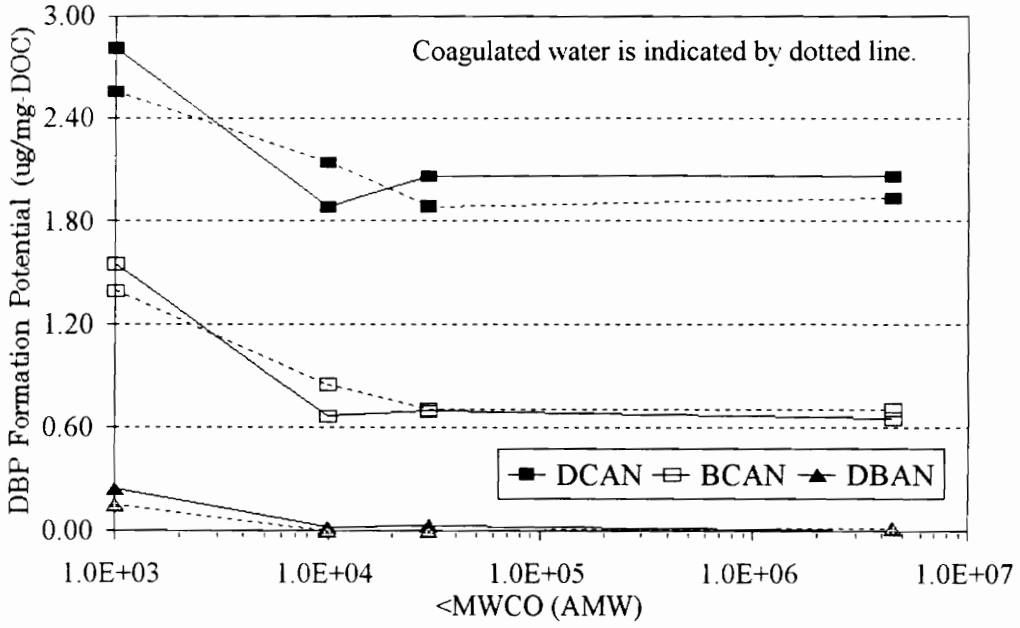

Figure 5.4. DOC Normalized HAN Species Specific Formation Potentials, Change with Coagulation (2 mg DOC/L, 0.07 Br^-/L, 6 mg Cl_2/L, 96 Hours)

Conclusions

The following observations were drawn from this research effort; each conclusion is directly related to the research objectives outlined in Chapter 1.

Reaction Time

1. HAN and HK species formation were optimally observed at 24-48 hours under Br^- and DOC conditions studied rather than longer periods of time typically reported for THM species.

2. CP was an infrequently occurring DBP, typically associated with 1,000 MWCO fraction and was observed at lower Br^- concentrations (i.e., 0.07 mg Br^-/L) and reaching peak formation potential with reaction times of more than 24 hours.

Br^-:DOC Ratio

1. Br-HAN/THAN formation was responsive to Br^-:DOC ratio, increasing with increasing Br^-:DOC ratio to an extent and in a similar manner to the THM response previously described by Stevens *et al.* (1994).

MWCO Fraction

1. HAN formation appears to not only be a product of reaction with proteinaceous material (>30,000 AMW), but also reaction with smaller, more reactive amino acids and other simple amines (<1,000 AMW).

2. Specific formation potential changes resulting from coagulation were not apparent in dissolved NOM fractions.

Br^-:Cl Ratio

1. Change in HAN and HK species is apparent with respect to changes in Br^-:Cl ratio; increasing quantities of brominated species form with increasing ratio value.

2. Increases in brominated species with Br^-:Cl represented a more significant effect on THANFP than on TTHMFP, resulting in concentrations of HANs comparable to brominated THM species.

Testing $CHCl_3$ and DCAN as DBP Formation Substrates

1. DCAN and $CHCl_3$ may be substrates for chlorine or bromine reactions under DOC limited conditions, but the resulting products are not THMs, HANs, or HKs

2. Decline in DCAN via hydrolysis may result in DBPs not enumerated or DBPs at lower concentrations than detected.

Method Detection Limit Analysis

1. EPA method detection limit determination method is different from MDLs predicted using the inverse regression method. EPA's method was more responsive to higher variation in method response but yields very low MDL values in most cases tested.

2. The MDL calculated by the EPA method varies with the initial concentration chosen for testing.

Chapter 6. Future Research Opportunities

This research expanded on work by previous researchers investigating DBP formation. There are several lines of research that follow from this effort.

Nanofiltration

Effective prevention of DBP formation through pilot and full-scale nanofiltration is a current research topic. Laine (1993), Jacangelo (1995), Allgeier (1995) and others have investigated nanofilter exclusion of NOM and the resulting effects on THM, HAA, and THAN formation. Their research has demonstrated that Br^-:DOC effects due to the filtration process are evident in THM and HAA formation of nanofiltration permeates. The research conducted here demonstrates a similar effect could be anticipated for HANs and HKs. It also indicates that HAN precursors exist in 1,000 MWCO fraction, raising the possibility that brominated HANs may represent a more significant fraction of DBP formation in nanofiltration permeates than the observed, ultrafilter permeates. Owen *et al.*'s <500 MWCO HAN data is in keeping with this hypothesis, where this fraction represented 61 percent of total THAN formation, and greater than 100 percent when ozonated).

While experimental design at the pilot-scale filtration apparatus scale would be preferable, adaption of tangential flow bench-scale membrane test (TFBSMT) method developed by Allgeier and Summers (1995), provides a more economical method to pursue this line of research. Potential avenues of research include targeted NOM controls, coagulation studies, and chemical characterizations. If the small AMW fraction is viewed as critical to DBP management, NOM control may involve reservoir management to minimize introduction of algal metabolites into the water treatment process. Characterization and comparison of metabolites in the <1,000 AMW fraction extracted by TFBSMT, concentrated with continuous liquid-liquid extraction (Rashash, 1994), and

identified using GC-MS could be used to determine if known algal metabolites are significant contributors to <1,000 AMW fraction DBP formation.

The TFBSMT could also be modified to create a portable nanofiltration apparatus that would be used to generate large volume (e.g., 10 liter) nanofilter permeate samples for chemical analysis of 200 and 500 MWCO fractions. This research, Owen *et al.* and plant operations at Harwood's Mill WTP indicate that management of the <1,000 AMW fraction is important to DBP control. Using the TFBSMT as a sampling device could allow a "real-world" analysis of change in this fraction's mass, chemical character, and physical behavior with movement through the facility's treatment train.

Stable Isotope Analysis

HANs are distinct from most other currently monitored DBPs as they contain nitrogen. This unique characteristic can be exploited to explore both the source of HANs and investigate NOM behavior in the coagulation process. Radiolabeling is a frequently used technique to track the movement of particular elements and their associated structures through complex chemical pathways; experimental constructs ultimately rely on differences in observed energy emission as detected via a scintillation counter to determine reservoirs and paths of the targeted element. Unfortunately a radioactive nitrogen isotope with an appropriate half-life does not exist.

A less robust but viable alternative analysis for simple model compounds is stable isotope analysis. A viable stable isotope for nitrogen, ${}_7N^{15}$, could be employed. Stable isotope analysis employs knowledge of natural isotope abundance rather than energy emission to trace elements through reaction series. Isotope ${}_7N^{14}$ is the most abundant naturally occurring N isotope, 99.64 percent of N; isotope ${}_7N^{15}$, is typically 0.4 percent of natural N. By amending the ${}_7N^{15}$ content of an experimental substrate, such as a model protein or amino acid (accomplished using metabolic production of the desired substrate), and using a finely tuned mass spectrometer to monitor the ratio of ${}_7N^{15}$ to ${}_7N^{14}$ in

experimental products a researcher could analyze the fate of nitrogen from different classes of hypothesized, nitrogenous, precursor material.

Distribution System Data

Collecting HAN, HK and THM formation potential data at <1, 24, 48, 96, and 168 hour time points illustrated that while THMs increased with increasing contact time other species did not. Most notably the HANs were constant or decreased with reaction time. This is consistent with data collected by previous researchers indicating that reaction time will like pH and temperature conditions effect specific DBP and TDBP concentration delivered to water system customers. Trends in formation potential over time will affect sampling strategies for formation potentials collected under the ICR. Analysis of properly constructed distribution system data sets would provide interesting and useful insights into which DBPs, particularly non-THM DBPs are delivered to water system customers. Such an effort could be undertaken in conjunction with utilities preparing for the ICR at very little cost.

Appendix 1. Sample Chromatograms

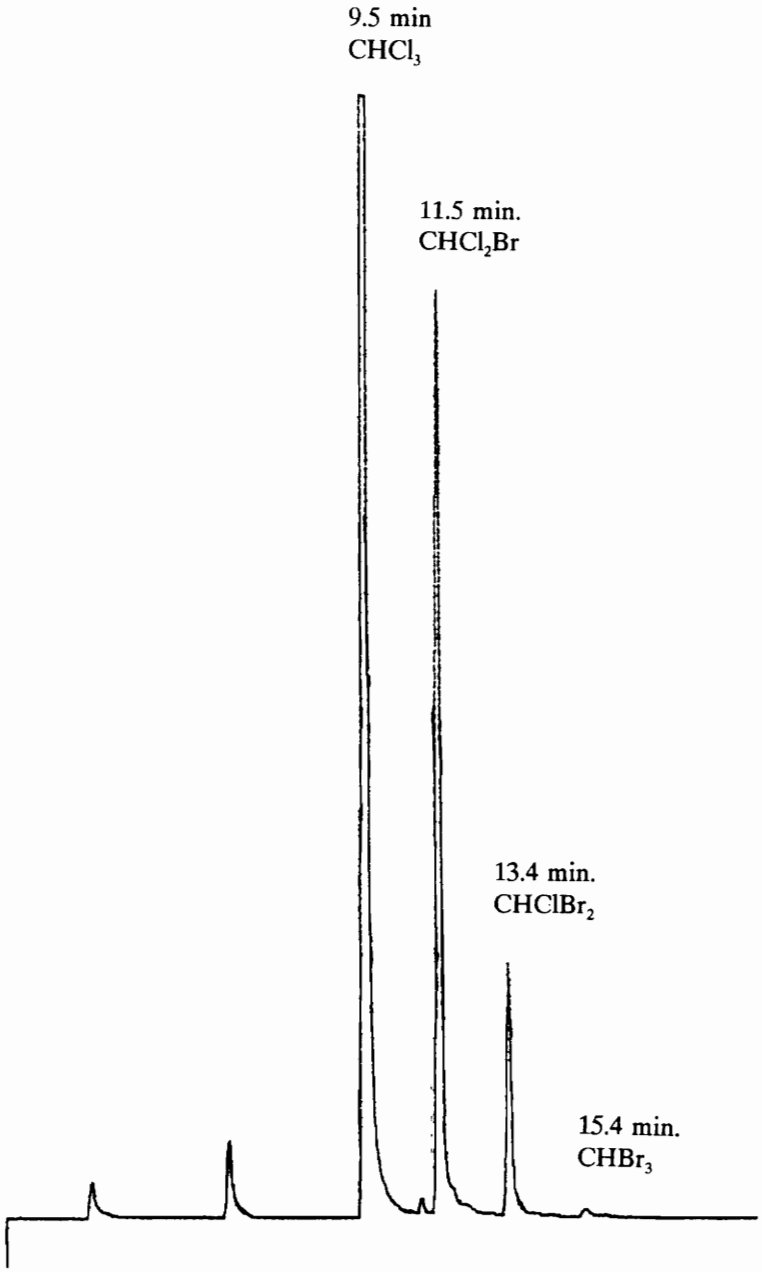

Figure A-1.1. Sample Chromatogram from EPA Method 501.1. Column: 2.4 m, 2.0 mm i.d., 1% SP, 1000 60/80 Carbopack B; Purge and trap sequence: 8 min. purge at 30°C, desorb 4 min. at 180°C. Chromatography conditions: Helium carrier gas at 60 psi at 65°C; Temperature program: 3 min. at 65°C, ramping 15°C/minute to 220°C, 2 min at 220°C; Detector: Hall detector

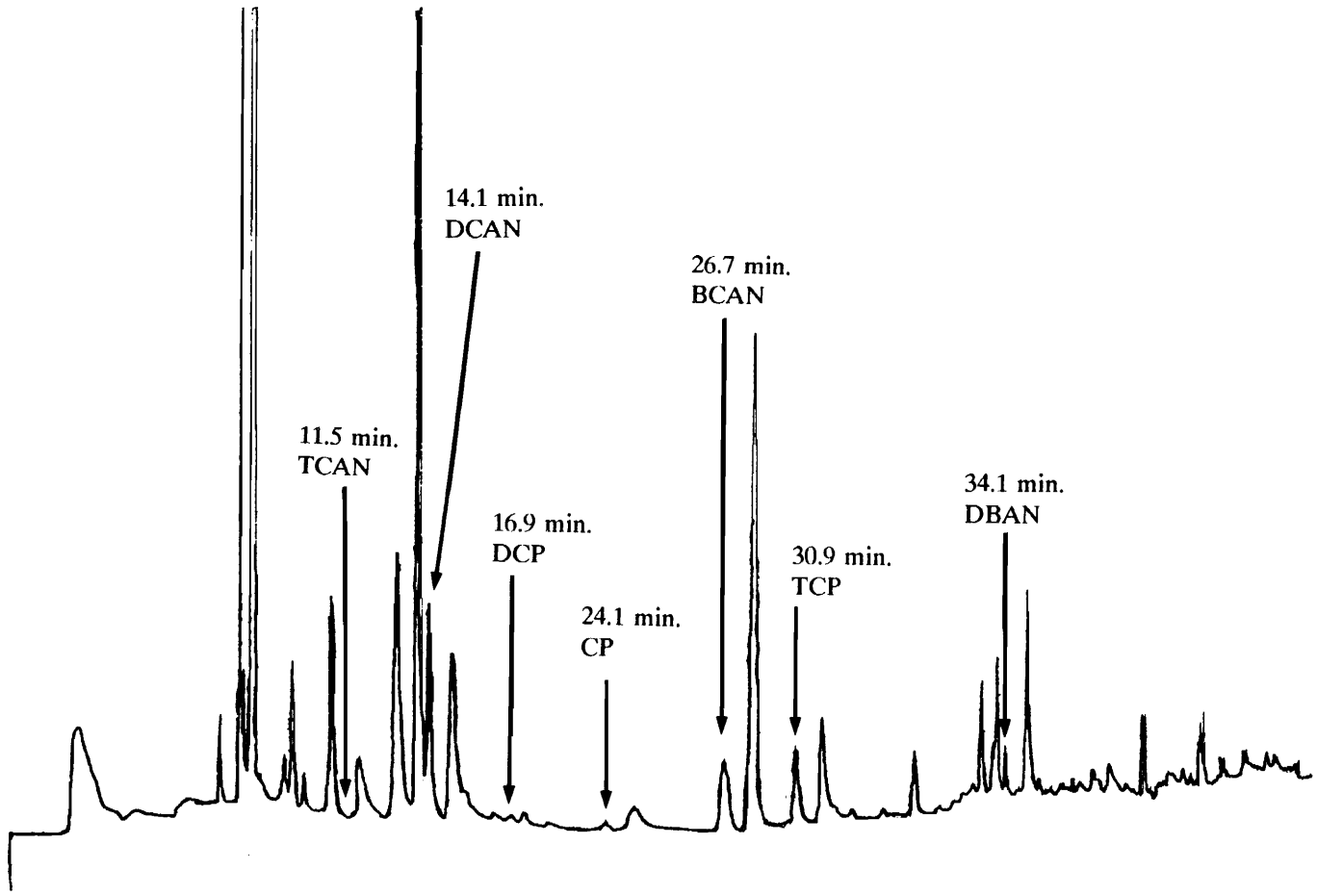

Figure A.1.2. Sample Chromatogram from EPA Method 551. Column: 30 m, 0.25 mm i.d., DB-1, helium carrier gas at 23 cm/sec, nitrogen make-up gas at 30 mL/min.; Temperature Program: 15 min at 33°C, 33-40°C at 1°/min., 3 min. at 40°C, 40-120°C at 6°C/min., 1 min. at 120°C.; Injection: splitless, vent at 0.7 min., 2 uL injection volume.

Appendix 2. Inverse Regression Plots for Method Detection Limit Determination

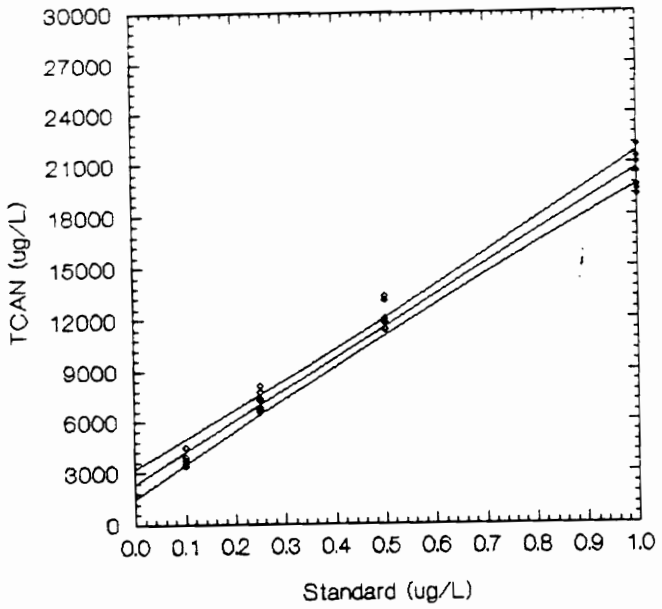

Figure A-2.1. TCAN, Schraf 95% Confidence Interval Plot, EPA Method 551, n=7, (Test Concentrations 0.1, 0.25, 0.5, and 1.0 ug/L in mixed standard)

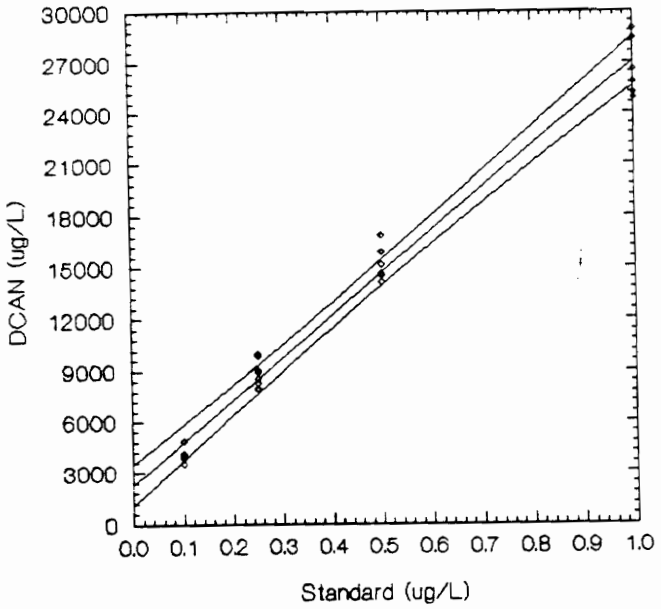

Figure A-2.2. DCAN, Schraf 95% Confidence Interval Plot, EPA Method 551, n=7, (Test Concentrations 0.1, 0.25, 0.5, and 1.0 ug/L in mixed standard)

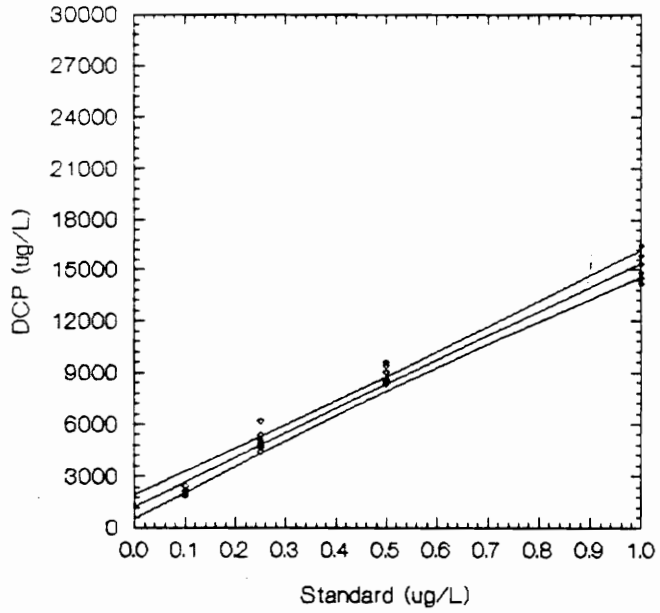

Figure A-2.3. DCP, Schraf 95% Confidence Interval Plot, EPA Method 551 (Test Concentrations 0.1, 0.25, 0.5, and 1.0 ug/L in mixed standard)

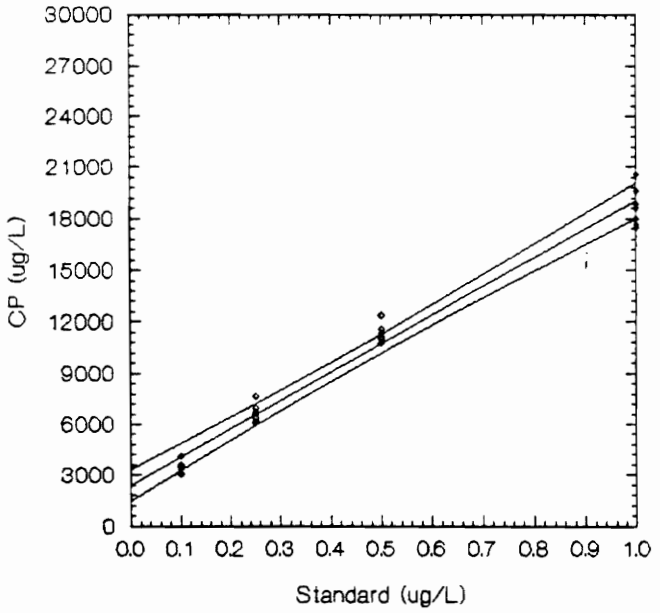

Figure A-2.4. CP, Schraf 95% Confidence Interval Plot, EPA Method 551 (Test Concentrations 0.1, 0.25, 0.5, and 1.0 ug/L in mixed standard)

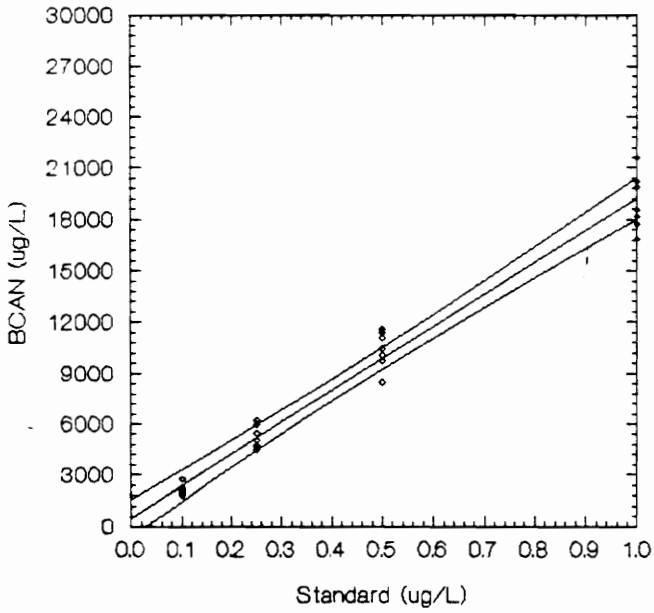

Figure A-2.5. BCAN, Schraf 95% Confidence Interval Plot, EPA Method 551 (Test Concentrations 0.1, 0.25, 0.5, and 1.0 ug/L in mixed standard)

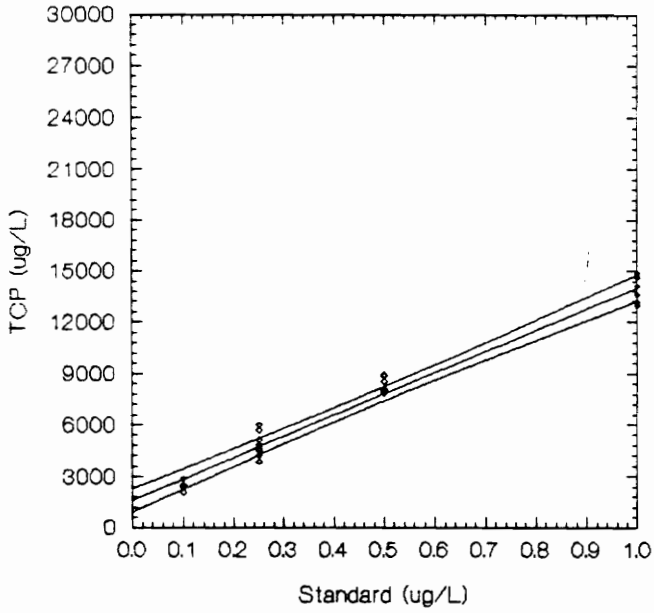

Figure A-2.6. TCP, Schraf 95% Confidence Interval Plot, EPA Method 551 (Test Concentrations 0.1, 0.25, 0.5, and 1.0 ug/L in mixed standard)

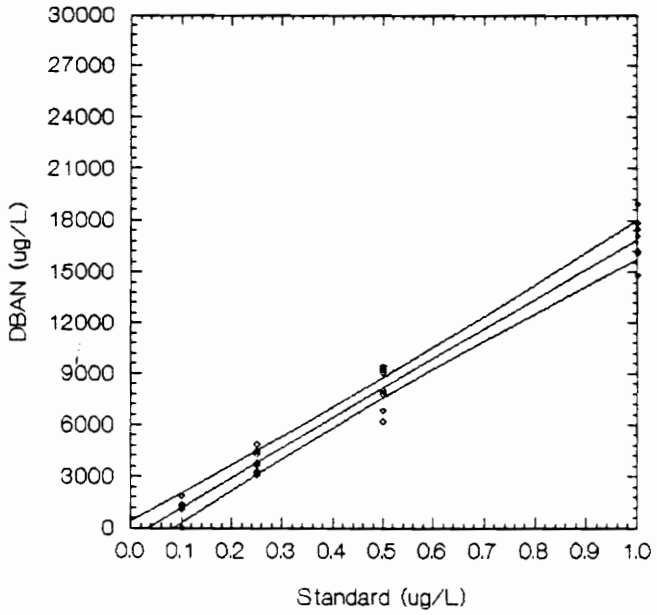

Figure A-2.7. DBAN, Schraf 95% Confidence Interval Plot, EPA Method 551 (Test Concentrations 0.1, 0.25, 0.5, and 1.0 ug/L in mixed standard)

Appendix 3. Matrix 1, Graphs of DOC Normalized DBP Concentration with Time

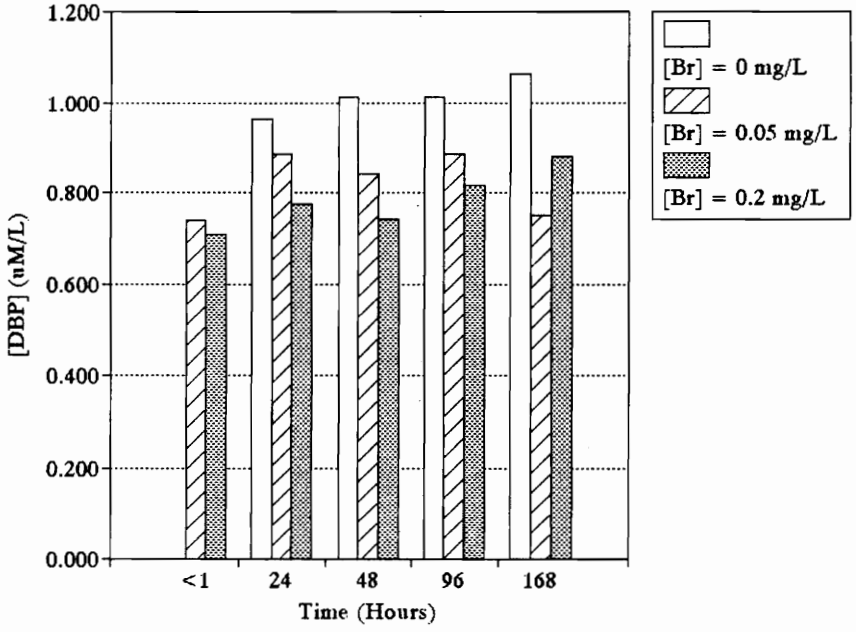

Figure A-3.1. CHCl3 Concentration in MilliQ Water, 0.6 mg DOC/L, 0 mg Cl2/L, 100 ug CHCl3/L, 2.5 ug DCAN/L

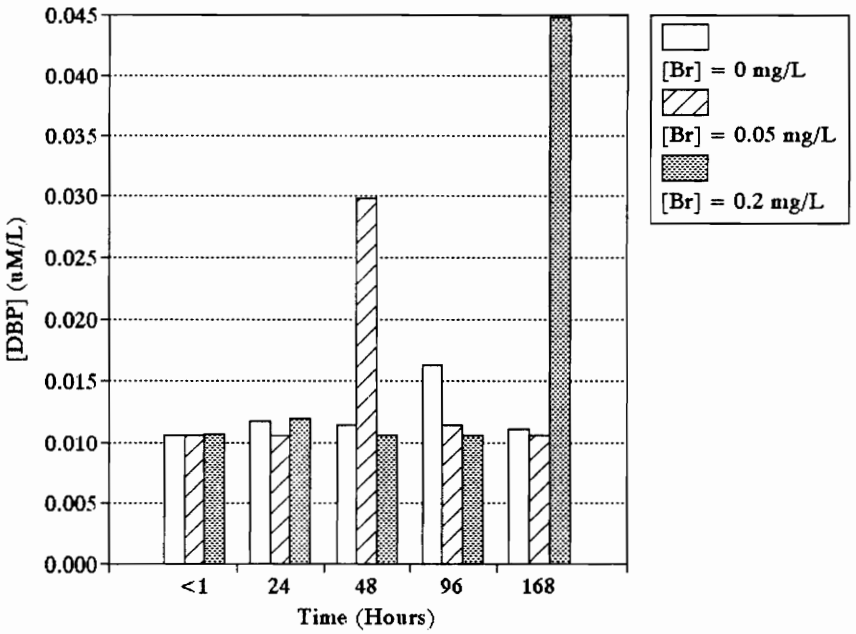

Figure A-3.2. CHCl2Br Formation Potential in MilliQ Water, 0.6 mg DOC/L, 0 mg Cl2/L, 100 ug CHCl3/L, 2.5 ug DCAN/L

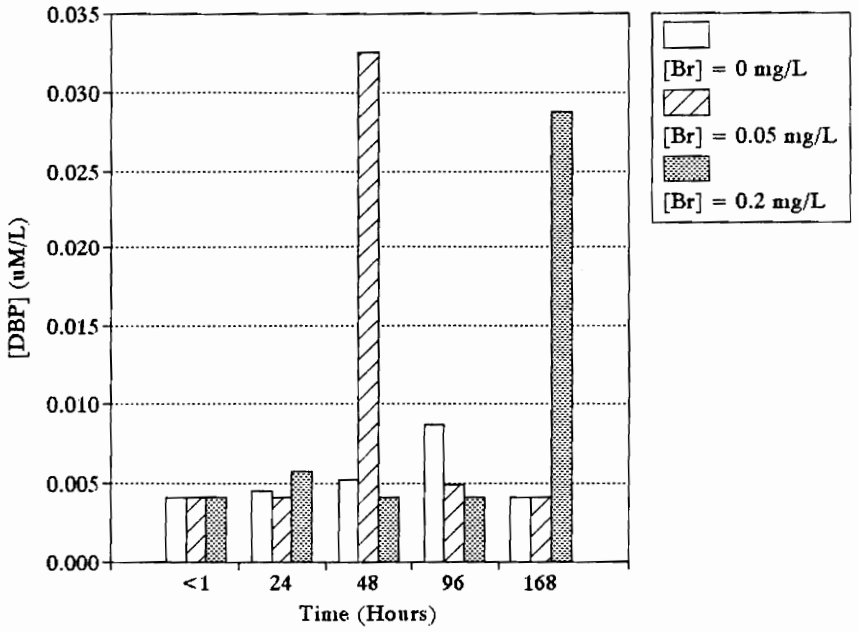

Figure A-3.3. CHBr3 Formation Potential in MilliQ Water, 0.6 mg DOC/L
0 mg Cl2/L, 100 ug CHCl3/L, 5 ug DCAN/L

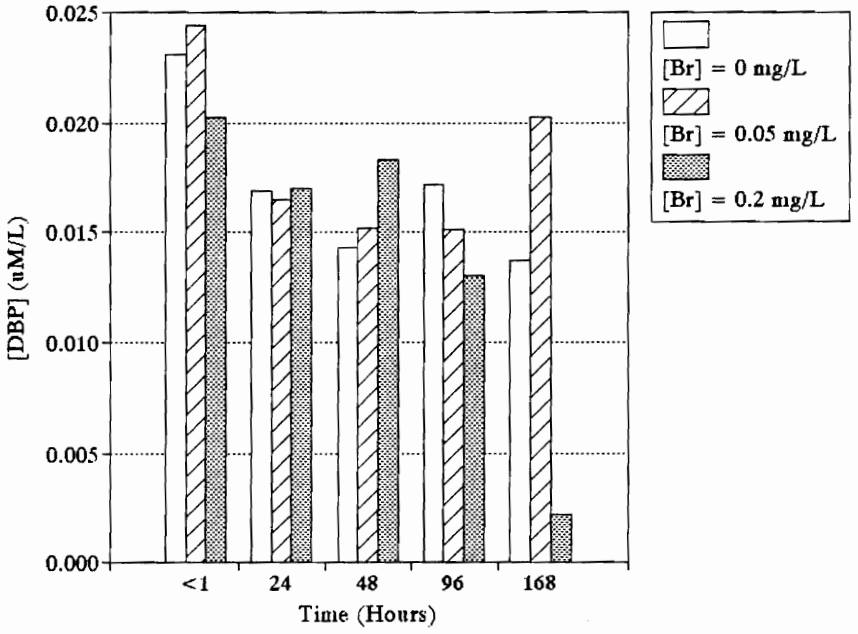

Figure A-3.4. DCAN Concentration in MilliQ Water, 0.6 mg DOC/L
0 mg Cl2/L, 100 ug CHCl3/L, 5 ug DCAN/L

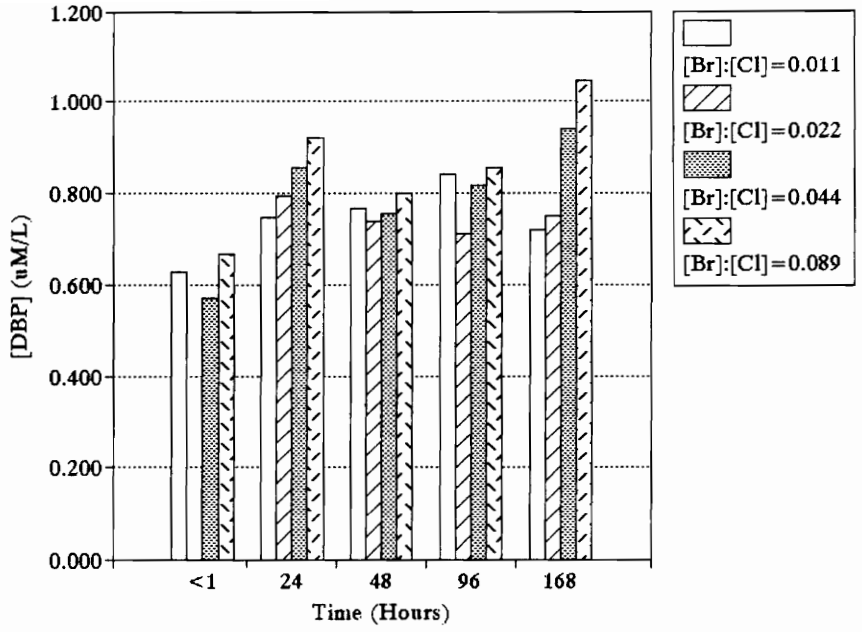

Figure A-3.5. CHCl3 Concentration in MilliQ Water, 0.6 mg DOC/L, 100 ug CHCl3/L, 5 ug DCAN/L, [Br]:[Cl] ratio (mM:mM)

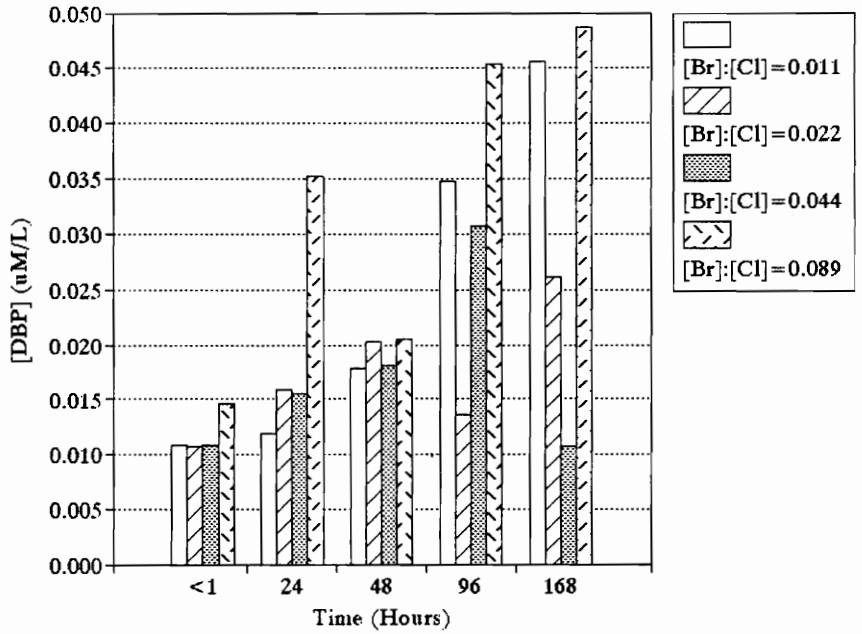

Figure A-3.6. CHCl2Br Formation Potential in MilliQ Water, 0.6 mg DOC/L, 100 ug CHCl3/L, 5 ug DCAN/L, [Br]:[Cl] ratio (mM:mM)

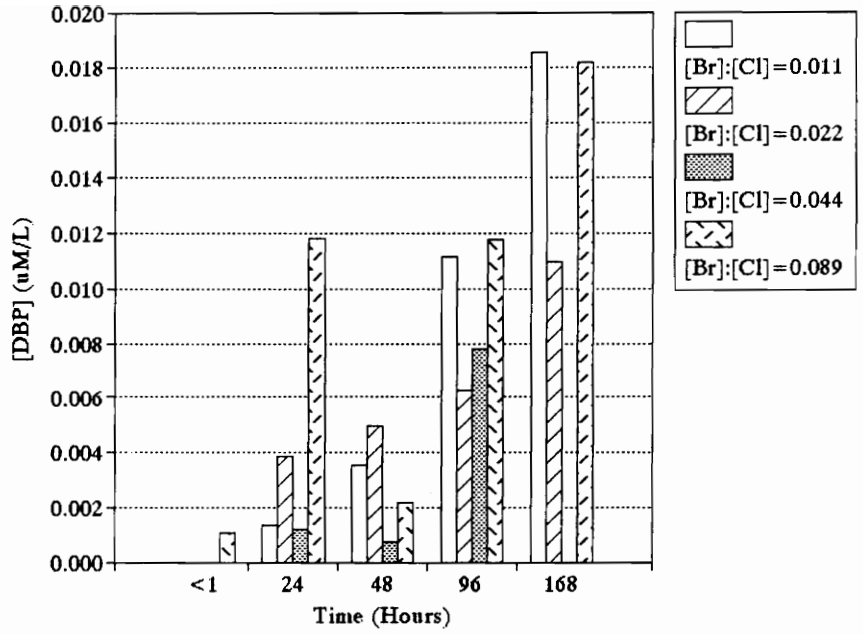

Figure A-3.7. CHClBr2 Formation Potential in MilliQ Water, 0.6 mg DOC/L, 100 ug CHCl3/L, 5 ug DCAN/L, [Br]:[Cl] (mM:mM)

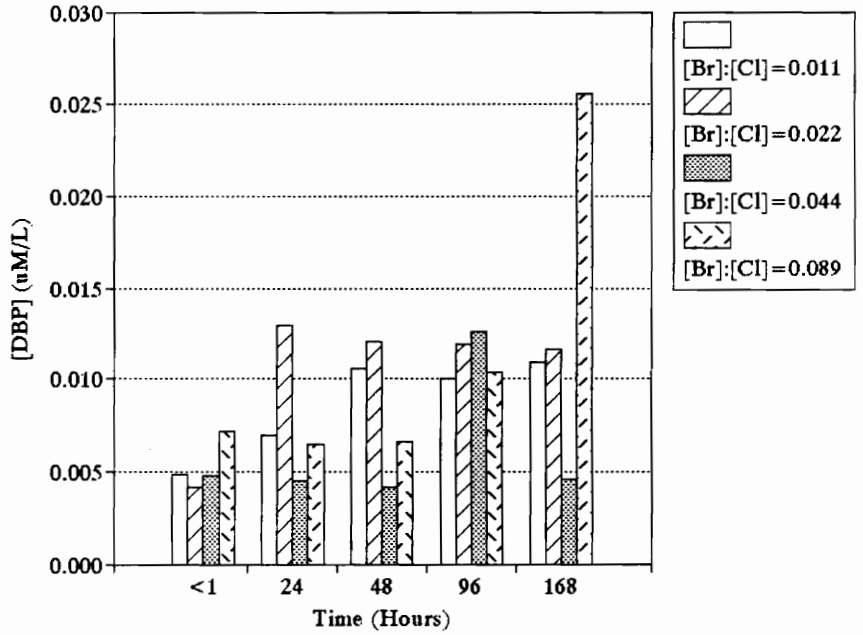

Figure A-3.8. CHBr3 Formation Potential in MilliQ Water, 0.6 mg DOC/L, 100 ug CHCl3/L, 5 ug DCAN/L, [Br]:[Cl] (mM:mM)

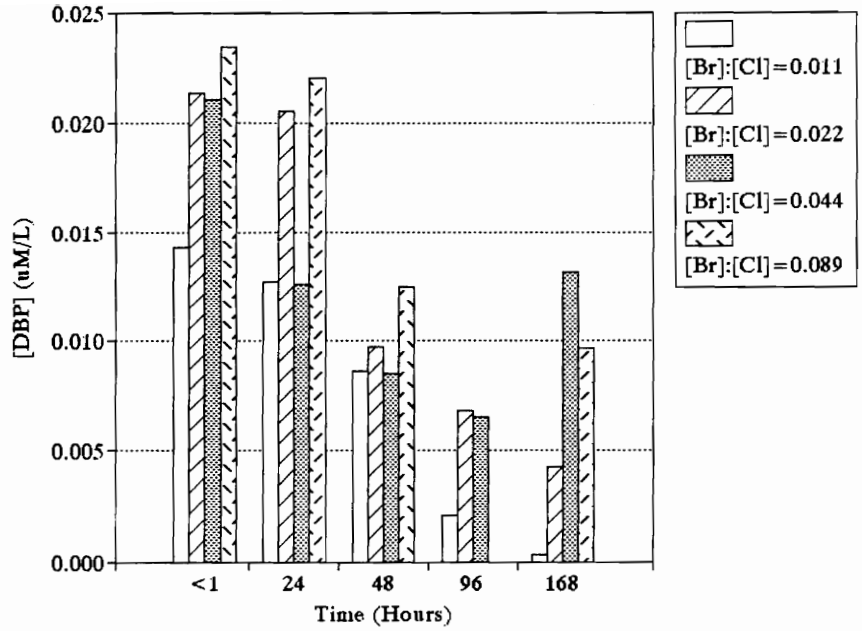

Figure A-3.9. DCAN Concentration in MilliQ Water, 0.6 mg DOC/L, 100 ug CHCl3/L, 5 ug DCAN/L, [Br]:[Cl] (mM:mM)

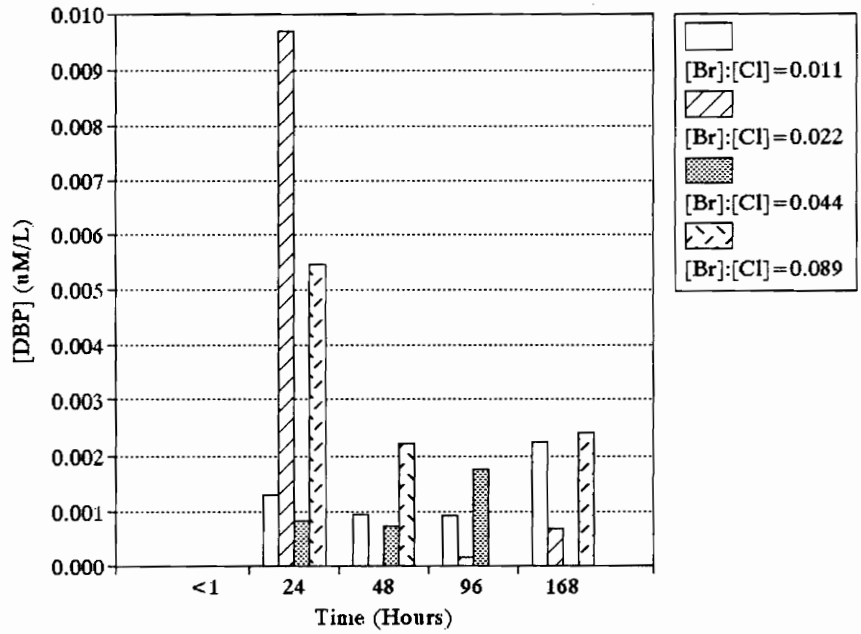

Figure A-3.10. BCAN Formation Potential in MilliQ Water, 0.6 mg DOC/L, 100 ug CHCl3/L, 5 ug DCAN/L, [Br]:[Cl] (mM:mM)

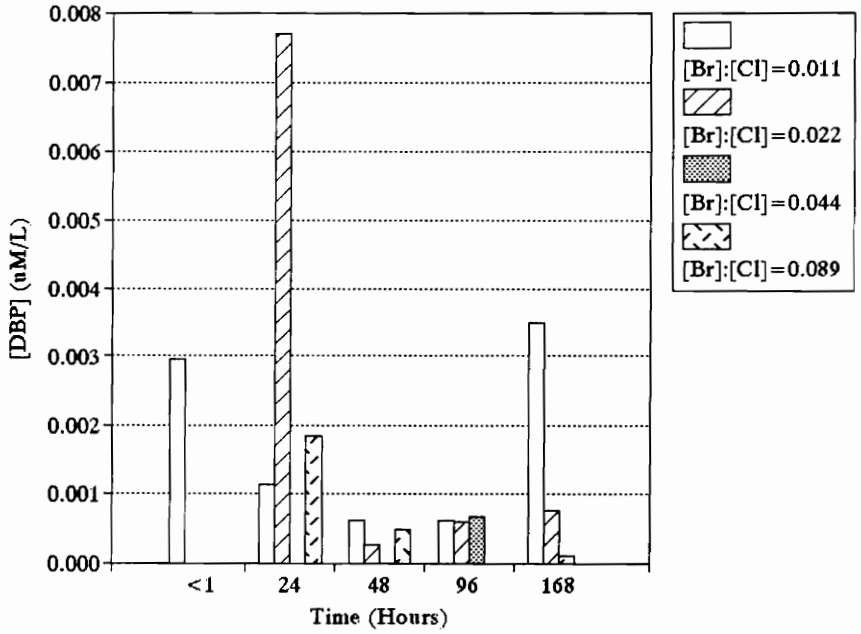

Figure A-3.11. DBAN Formation Potential in MilliQ Water, 0.06 mg DOC/L, 100 ug CHCl3/L, 5 ug DCAN/L, [Br]:[Cl] (mM:mM)

Appendix 4. Matrix 2, Graphs of DOC Normalized DBP Concentration with Time

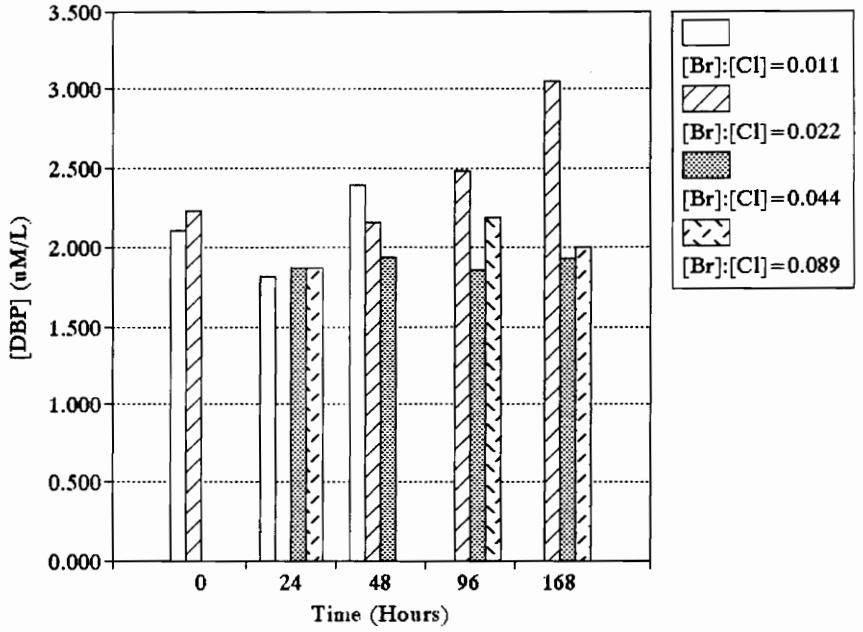

Figure A-4.1. CHCl3 Concentration in MilliQ Water, 250 ug CHCl3/L, 60 ug DCAN/L, [Br]:[Cl] ratio (mM:mM)

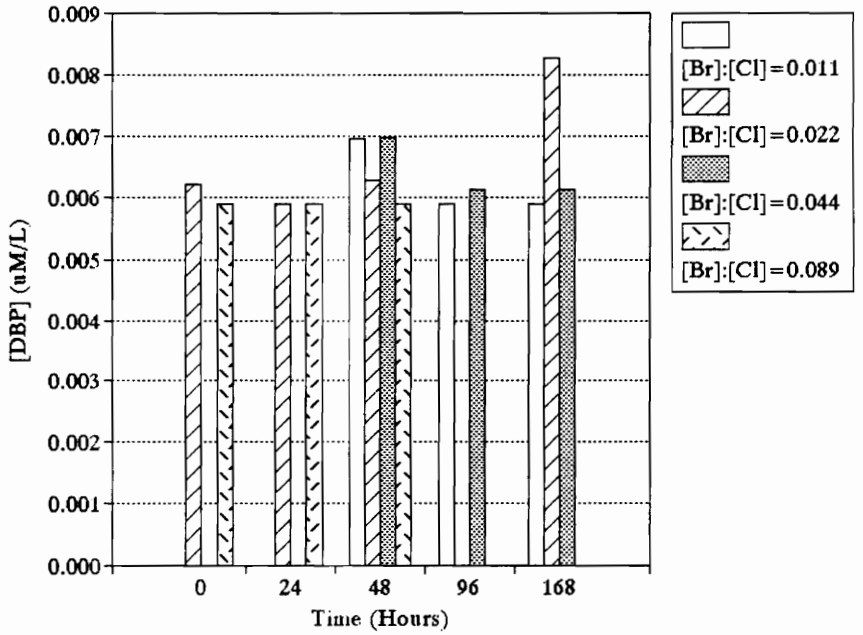

Figure A-4.2. CHCl2Br Formation Potential in MilliQ Water, 250 ug CHCl3/L, 60 ug DCAN/L, [Br]:[Cl] ratio (mM:mM)

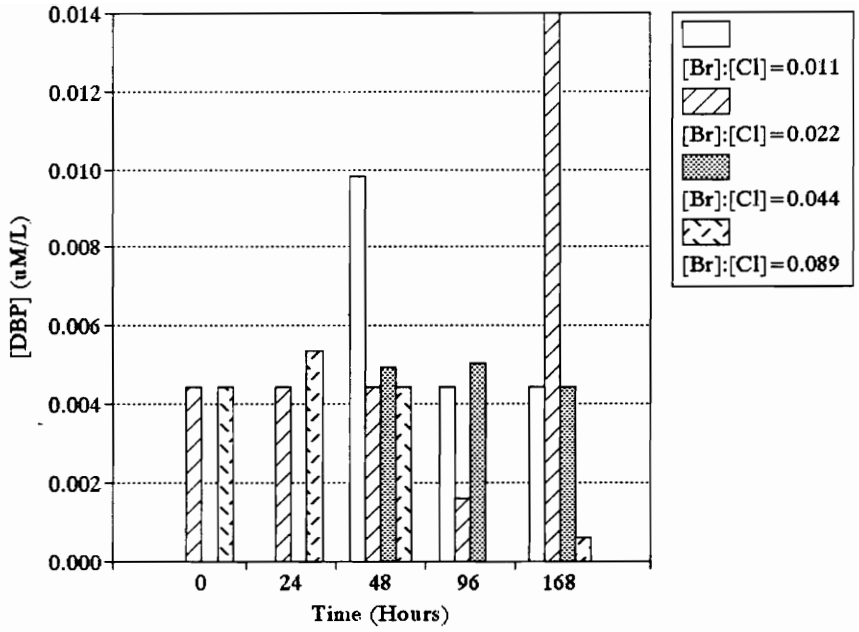

Figure A-4.3. CHClBr2 Formation Potential in MilliQ Water, 250 ug CHCl3/L, 60 ug DCAN/L, [Br]:[Cl] ratio (mM:mM)

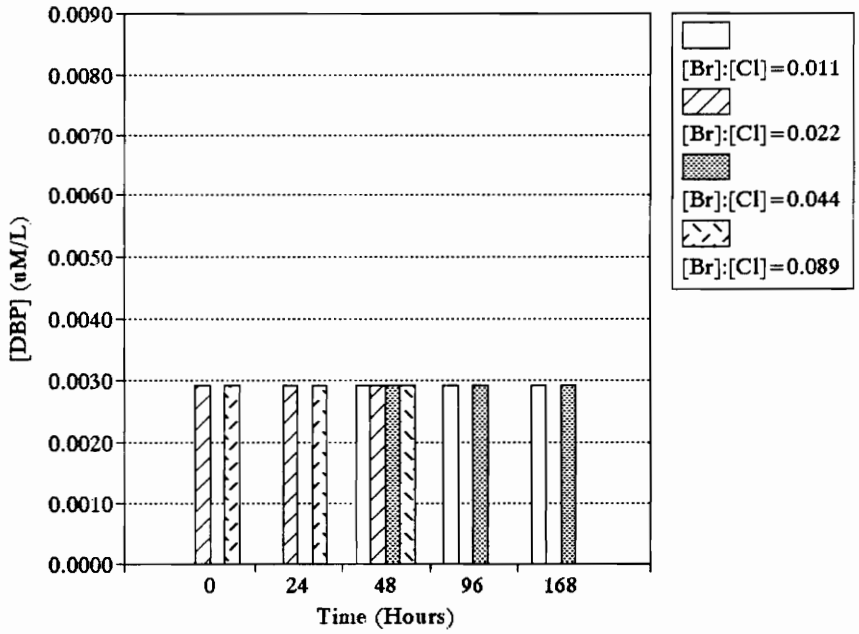

Figure A-4.4. CHBr3 Formation Potential in MilliQ Water, 250 ug CHCl3/L, 60 ug DCAN/L, [Br]:[Cl] ratio (mM:mM)

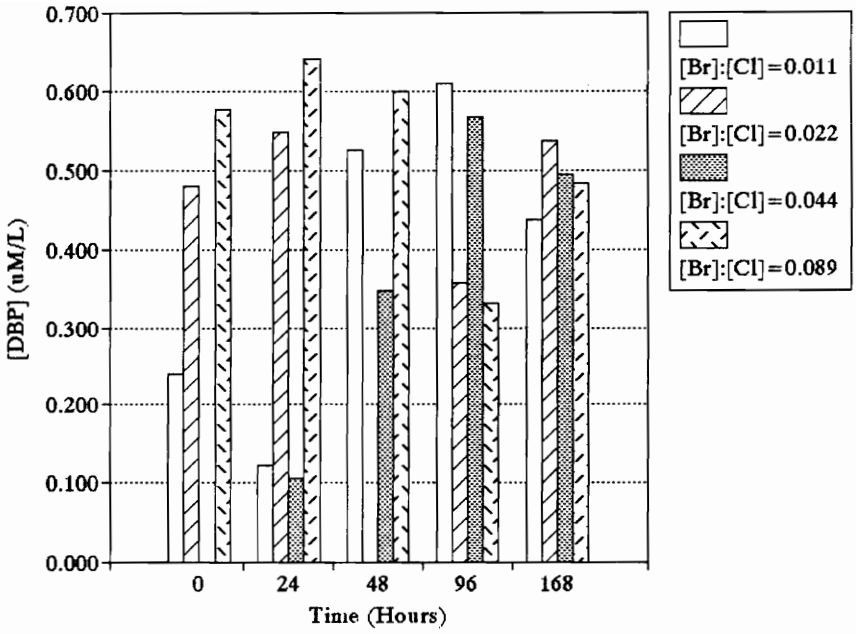

Figure A-4.5. DCAN Concentration in MilliQ Water, 250 ug CHCl3/L, 60 ug DCAN/L, [Br]:[Cl] ratio (mM:mM)

Appendix 5. Matrix 3, Graphs of DOC Normalized DBP Concentration with Time

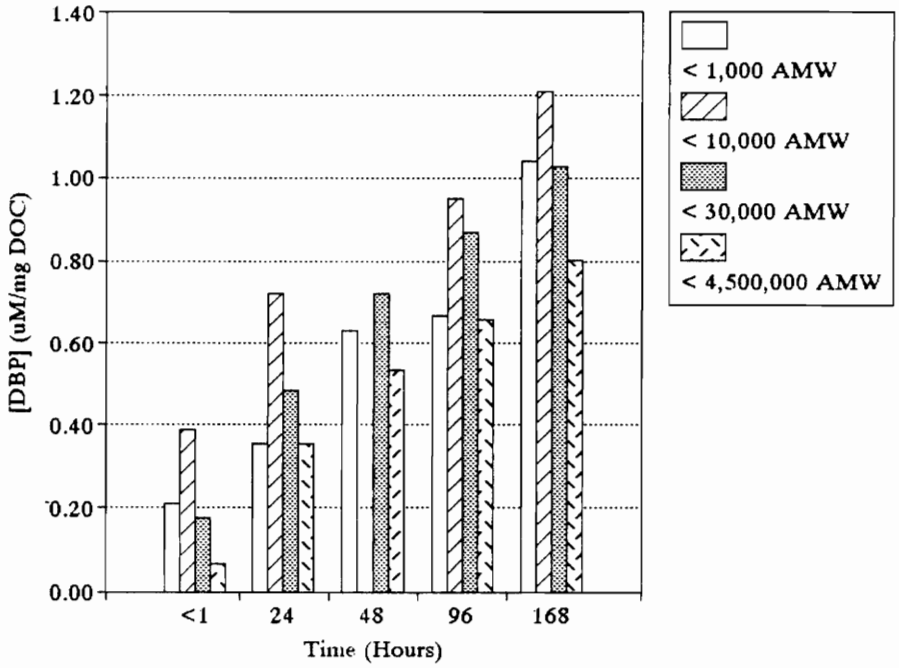

Figure A-5.1. CHCl3 Formation Potential in Raw Water, 2 mg DOC/L, 6 mg Cl2/L, 0.07 mg Br/L

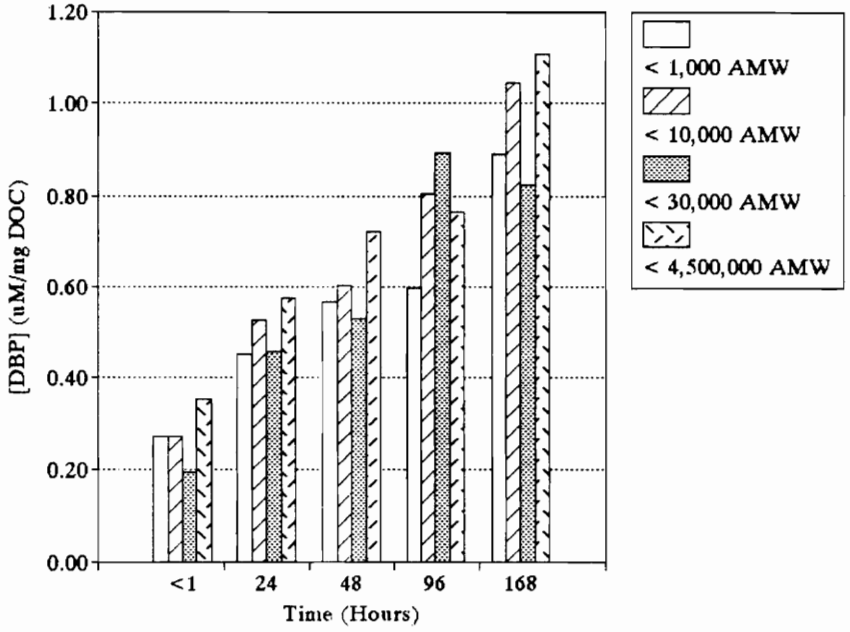

Figure A-5.2: CHCl3 Formation Potential in Coagulated Water 2 mg DOC/L, 6 mg Cl2/L, 0.07 mg Br/L

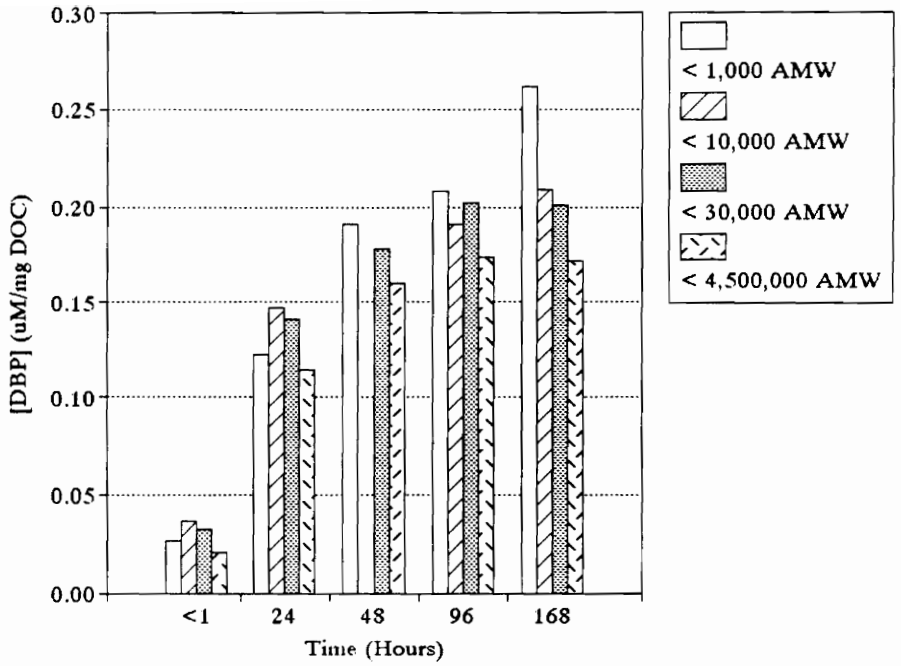

Figure A-5.3. CHCl2Br Formation Potential in Raw Water, 2 mg DOC/L, 6 mg Cl2/L, 0.07 mg Br/L

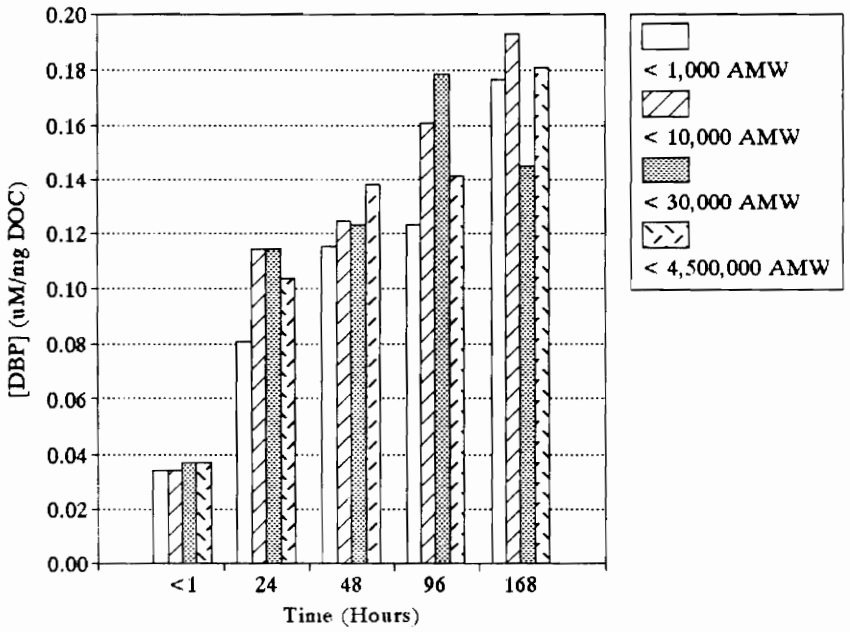

Figure A-5.4. CHCl2Br Formation Potential in Coagulated Water 2 mg DOC/L, 6 mg Cl2/L, 0.07 mg Br/L

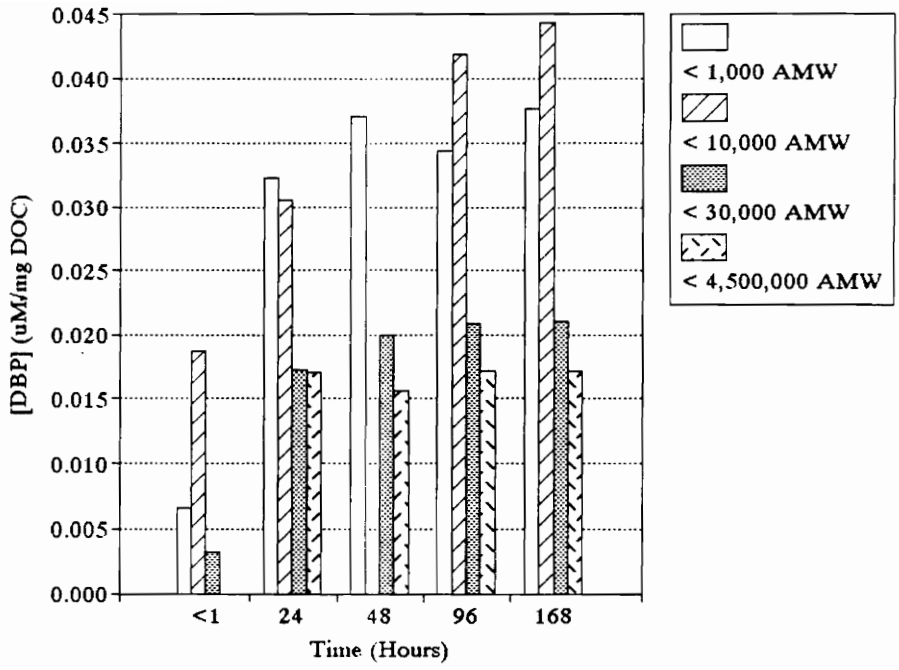

Figure A-5.5. CHClBr2 Formation Potential in Raw Water, 2 mg DOC/L, 6 mg Cl2/L, 0.07 mg Br/L

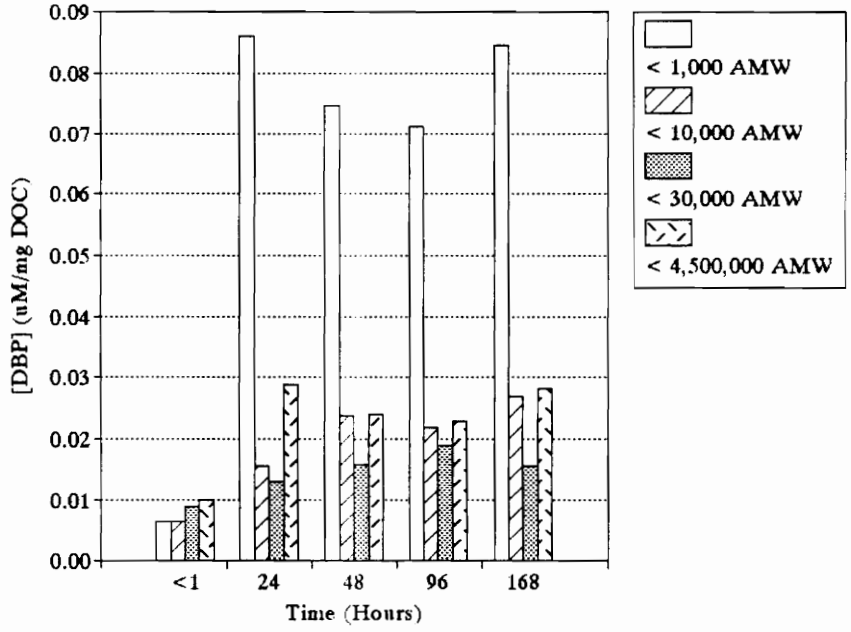

Figure A-5.6. CHClBr2 Formation Potential in Coagulated Water 2 mg DOC/L, 6 mg Cl2/L, 0.07 mg Br/L

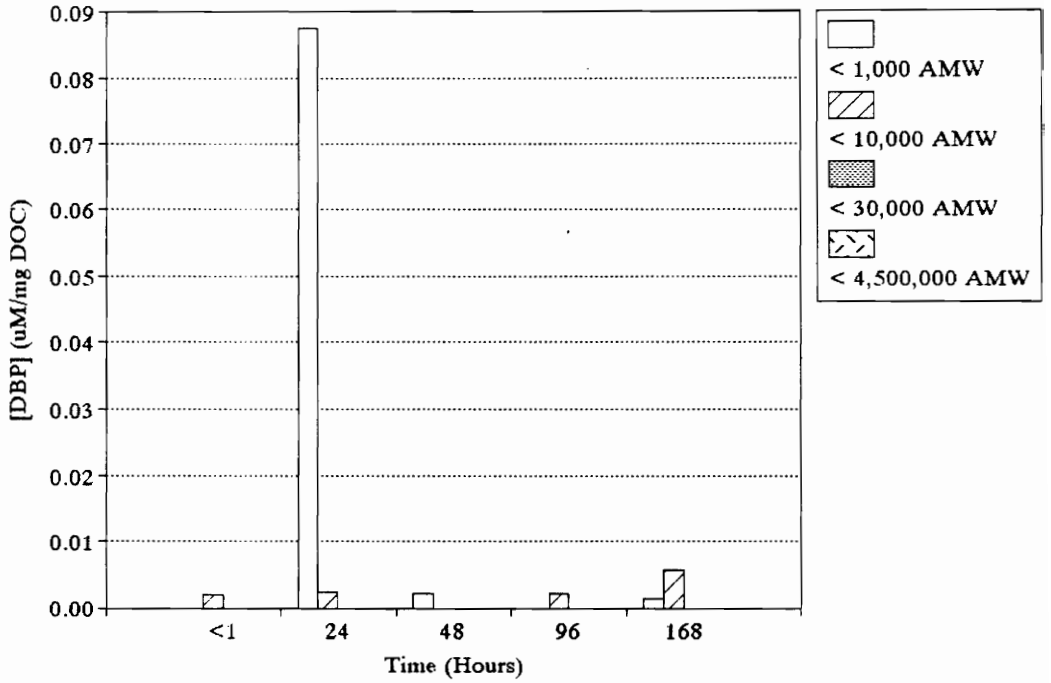

Figure A-5.7. CHBr3 Formation Potential in Raw Water, 2 mg DOC/L, 6 mg Cl2/L, 0.07 mg Br/L

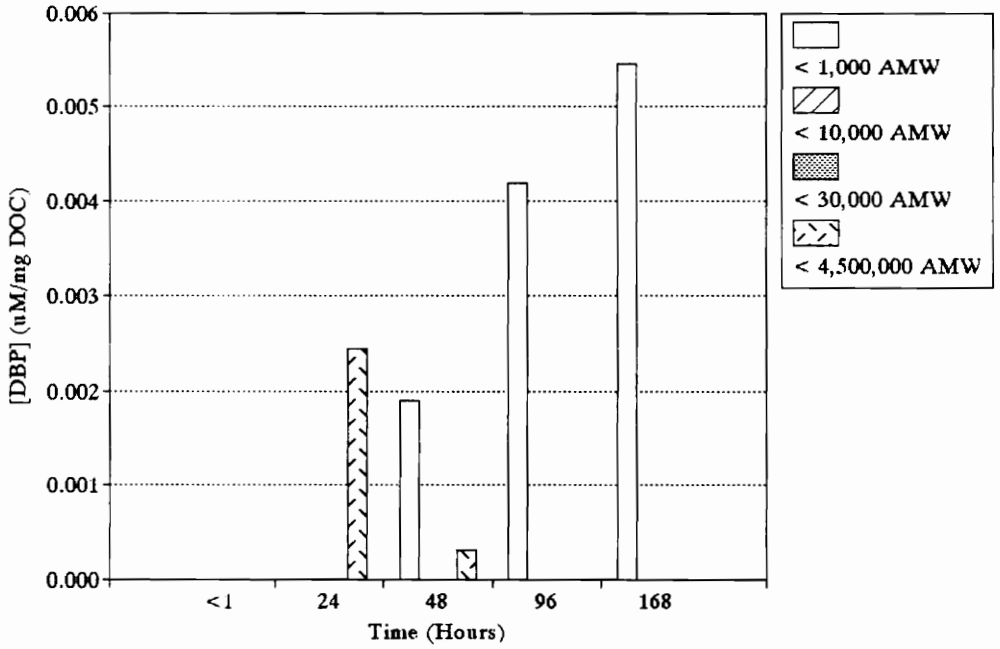

Figure A-5.8. CHBr3 Formation Potential in Coagulated Water 2 mg DOC/L, 6 mg Cl2/L, 0.07 mg Br/L

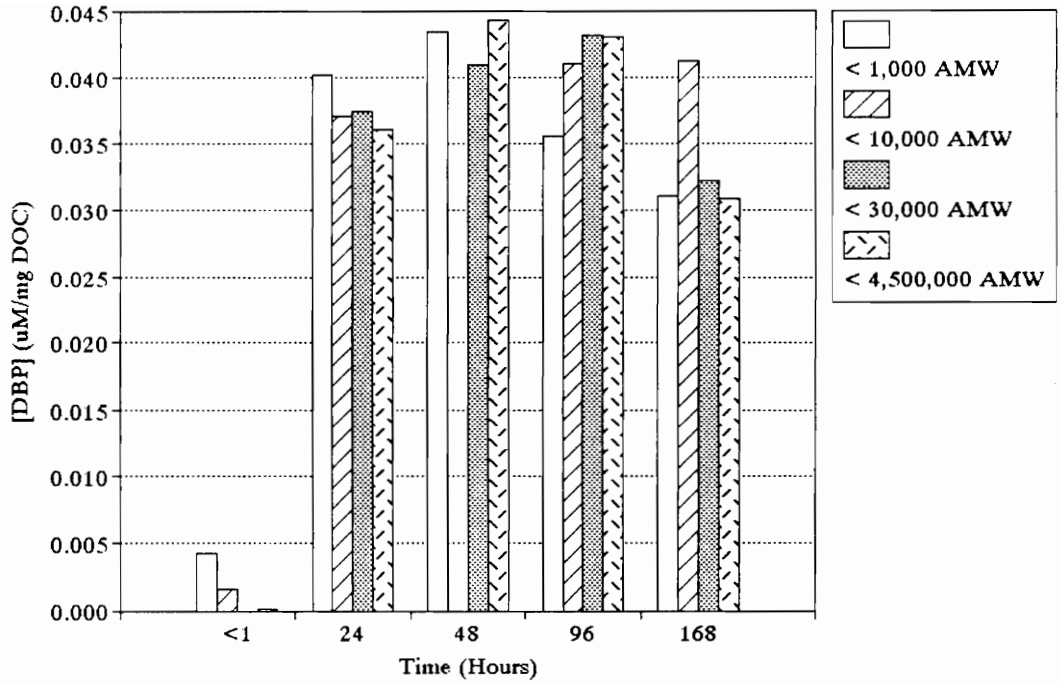

Figure A-5.9. DCAN Formation Potential in Raw Water, 2 mg DOC/L 6 mg Cl2/L, 0.07 mg Br/L

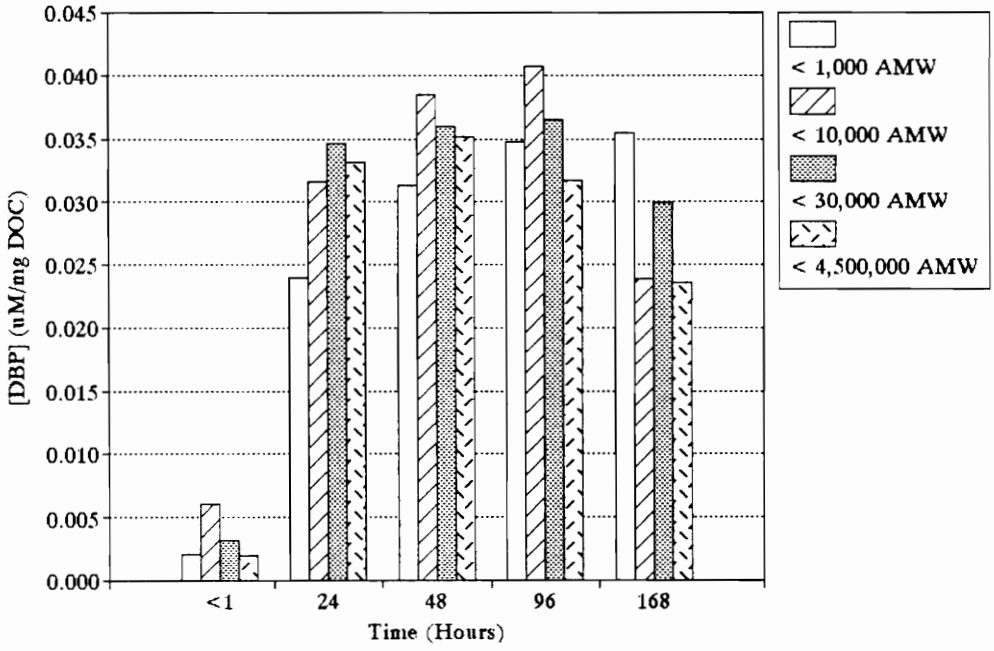

Figure A-5.10. DCAN Formation Potential in Coagulated Water, 2 mg DOC/L, 6 mg Cl2/L, 0.07 mg Br/L

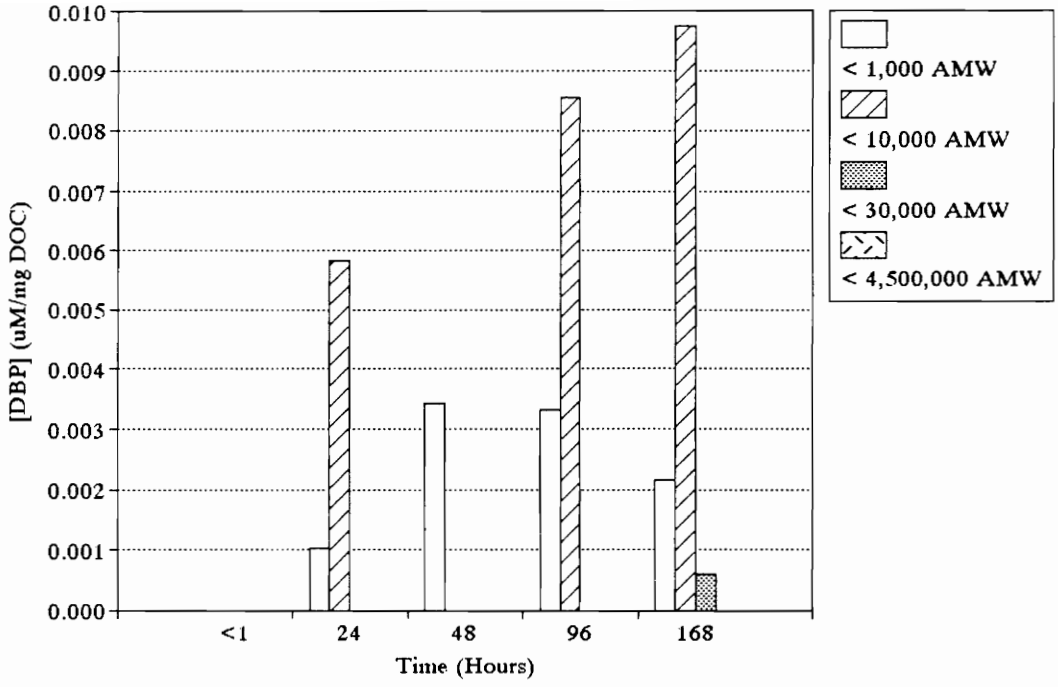

Figure A-5.11. CP Formation Potential in Raw Water, 2 mg DOC/L, 6 mg Cl2/L, 0.07 mg Br/L

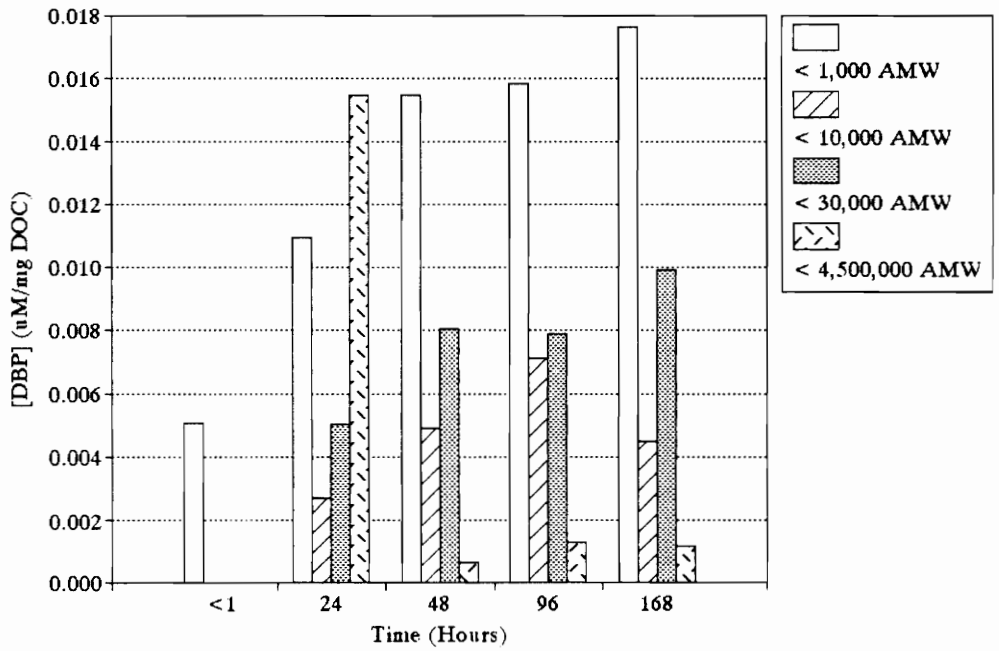

Figure A-5.12. CP Formation Potential in Coagulated Water, 2 mg DOC/L, 6 mg Cl2/L, 0.07 mg Br/L

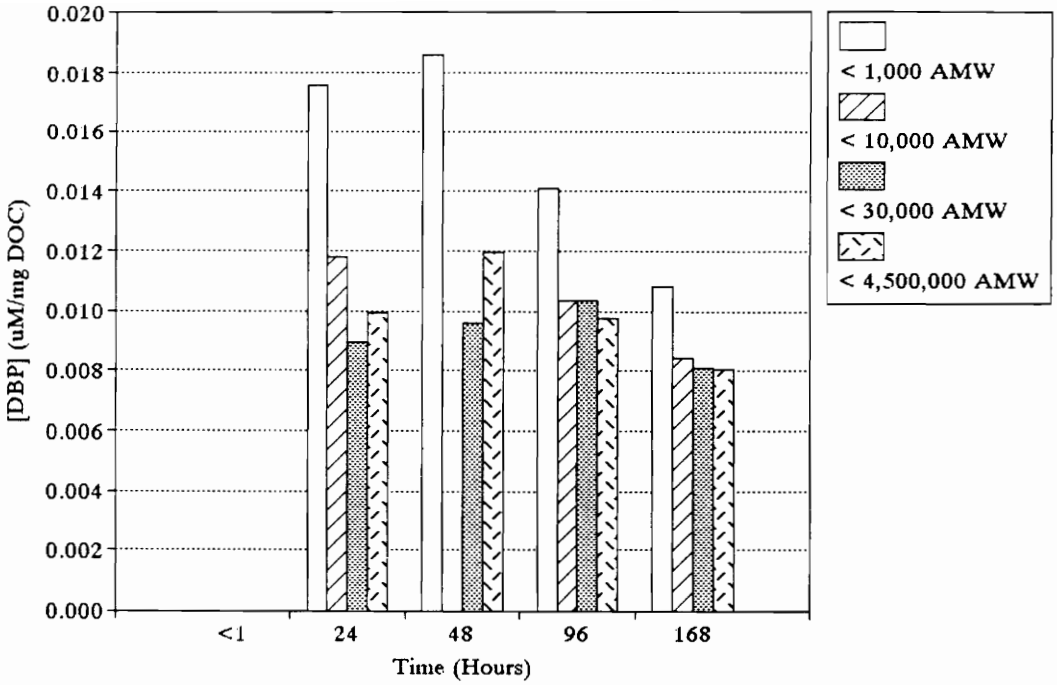

Figure A-5.13. BCAN Formation Potential in Raw Water, 2 mg DOC/L, 6 mg Cl2/L, 0.07 mg Br/L

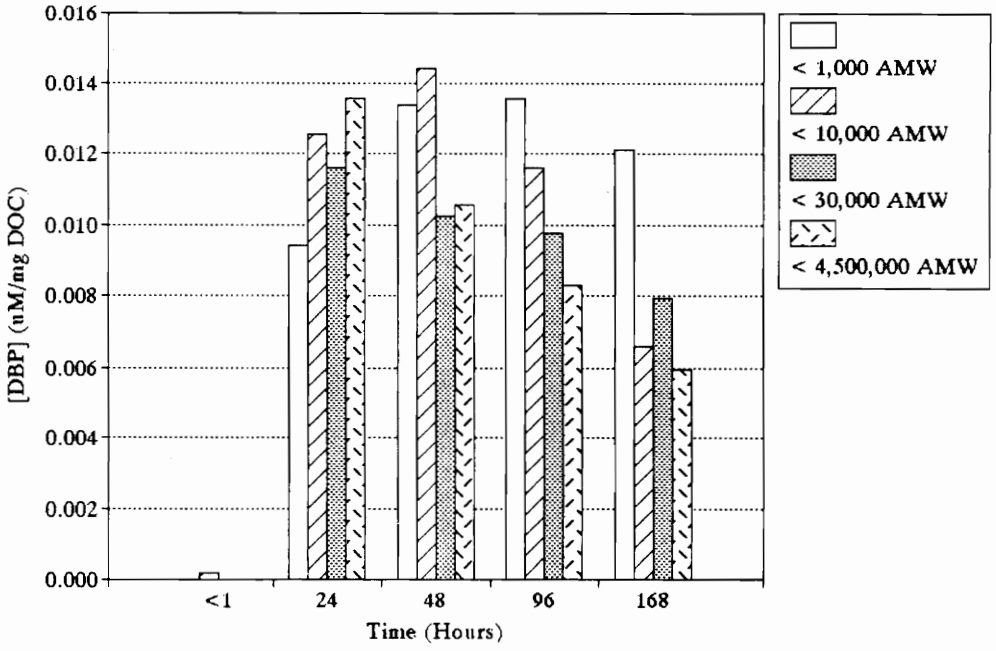

Figure A-5.14. BCAN Formation Potential in Coagulated Water 2 mg DOC/L, 6 mg Cl2/L, 0.07 mg Br/L

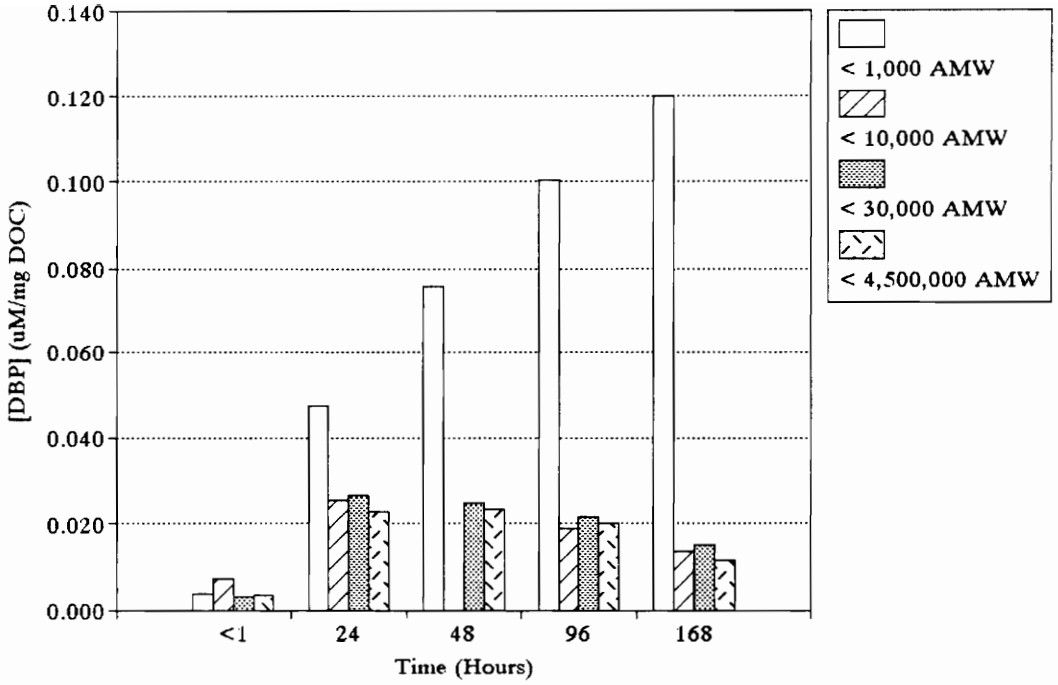

Figure A-5.15. TCP Formation Potential in Raw Water, 2 mg DOC/L, 6 mg Cl2/L, 0.07 mg Br/L

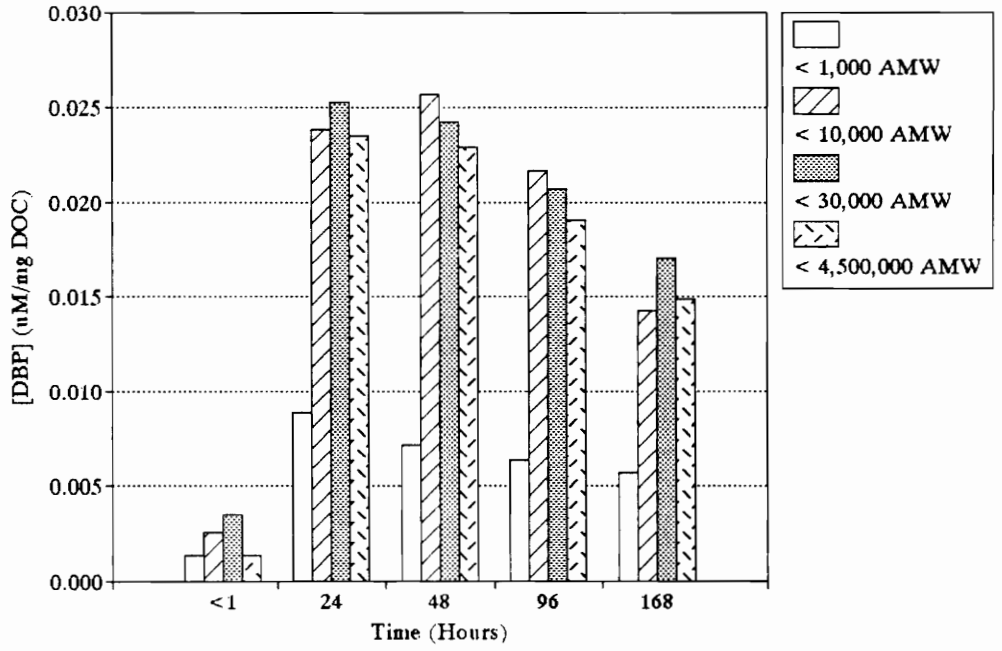

Figure A-5.16. TCP Formation Potential in Coagulated Water 2 mg DOC/L, 6 mg Cl2/L, 0.07 mg Br/L

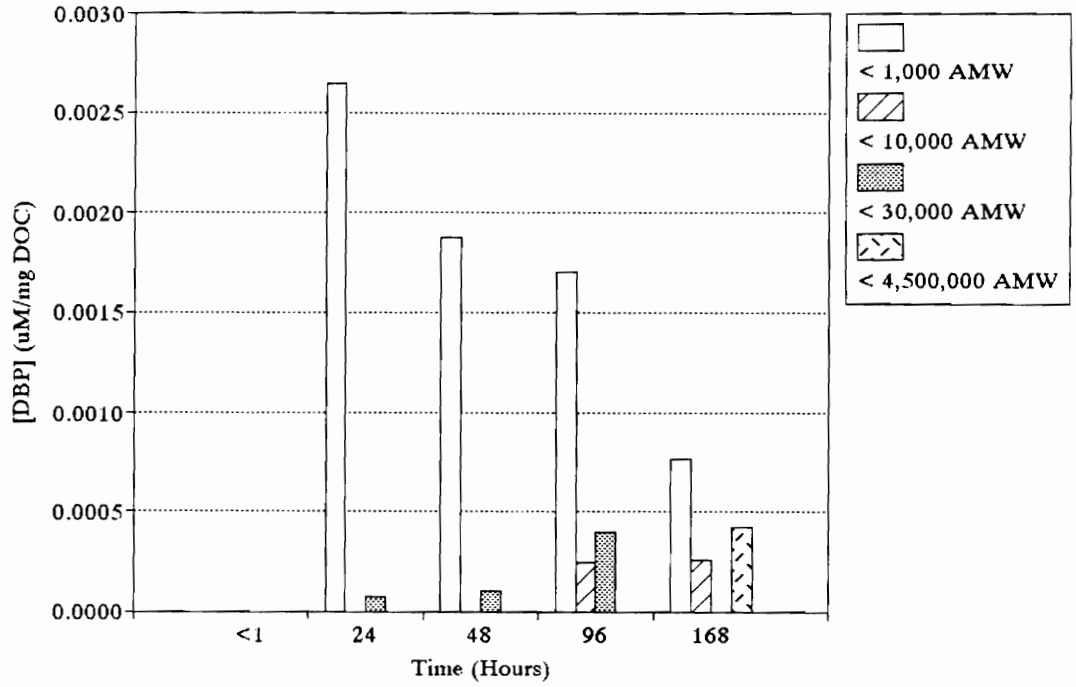

Figure A-5.17. DBAN Formation Potential in Raw Water, 2 mg DOC/L, 6 mg Cl2/L, 0.07 mg Br/L

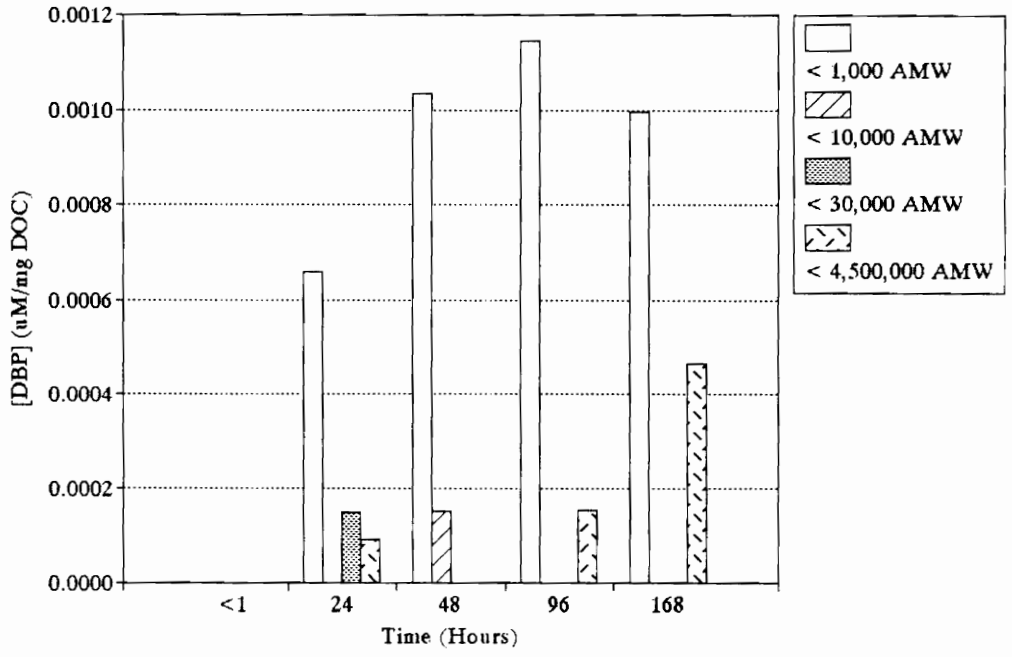

Figure A-5.18. DBAN Formation Potential in Coagulated Water 2 mg DOC/L, 6 mg Cl2/L, 0.07 mg Br/L

Appendix 6. Matrix 4, Graphs of DOC Normalized DBP Concentration with Time

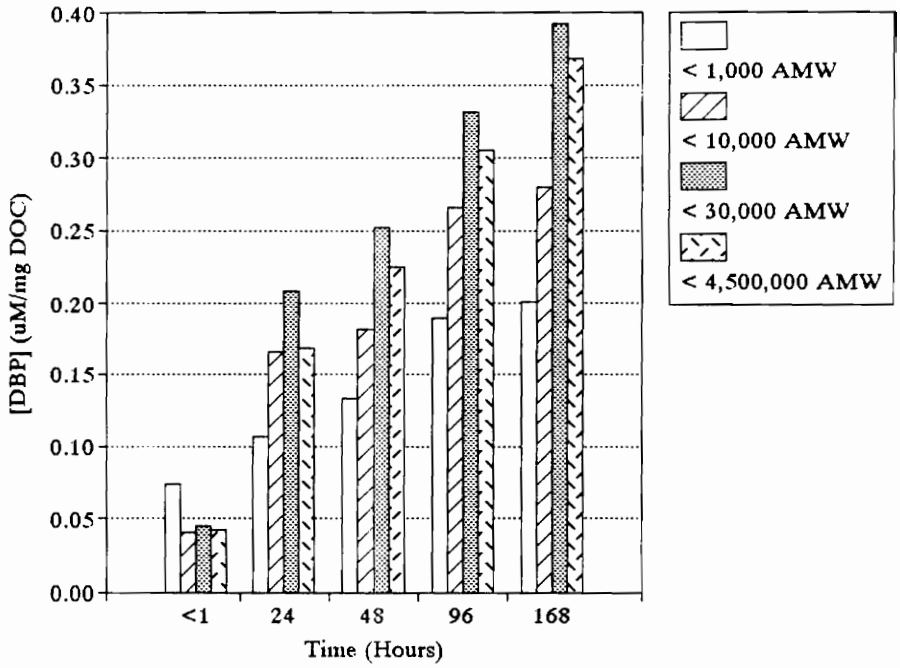

Figure A-6.1. CHCl3 Formation Potential in Coagulated Water, DOC varies, Cl2 Dose= 3 x mg DOC/L, 0.07 mg Br/L

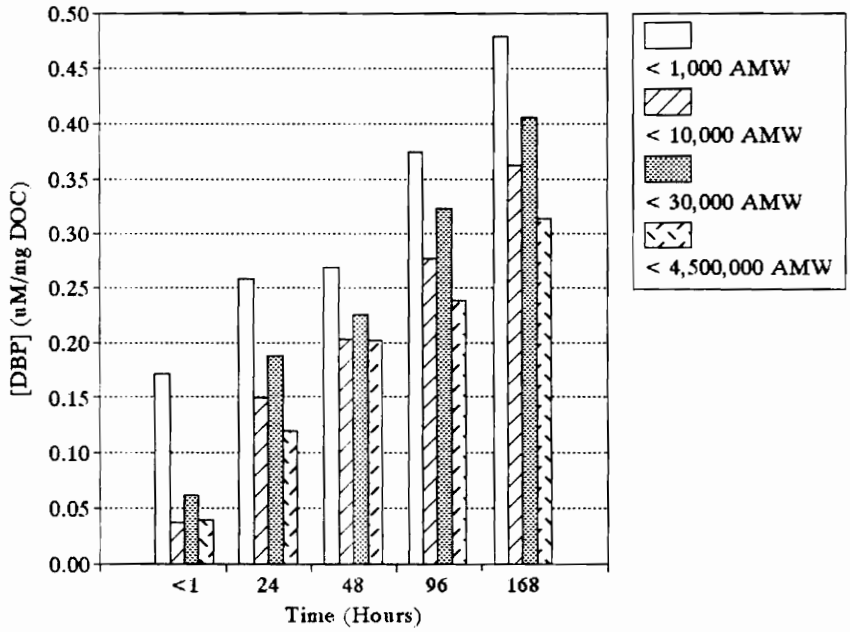

Figure A-6.2. CHCl3 Formation Potential in Coagulated Water, 2 mg DOC/L, 6 mg Cl2/L, 0.07 mg Br/L

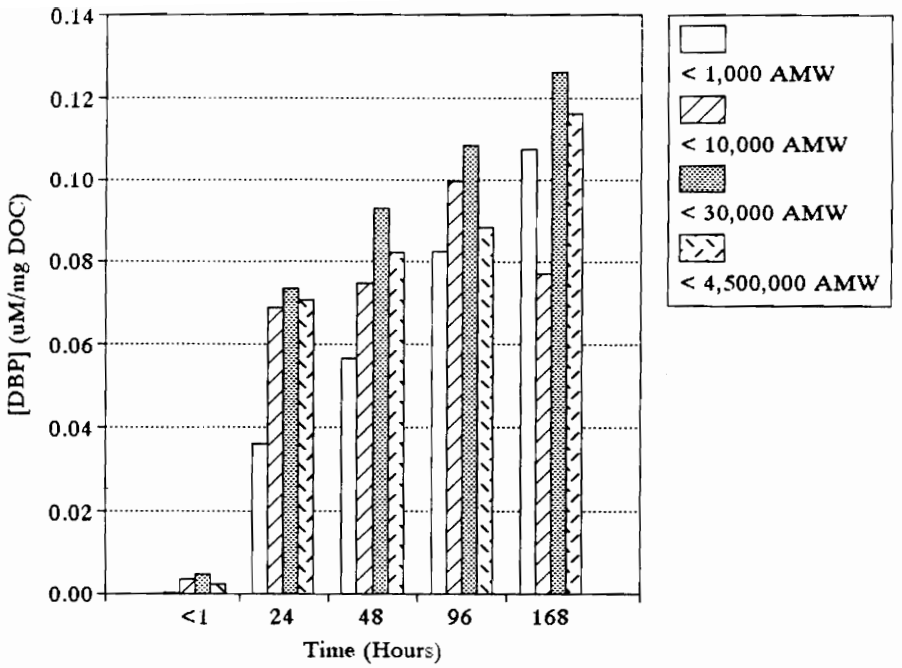

Figure A-6.3. CHCl2Br Formation Potential in Coagulated Water, [DOC] varies, Cl2 Dose = 3 x mg DOC/L), 0.07 mg Br/L

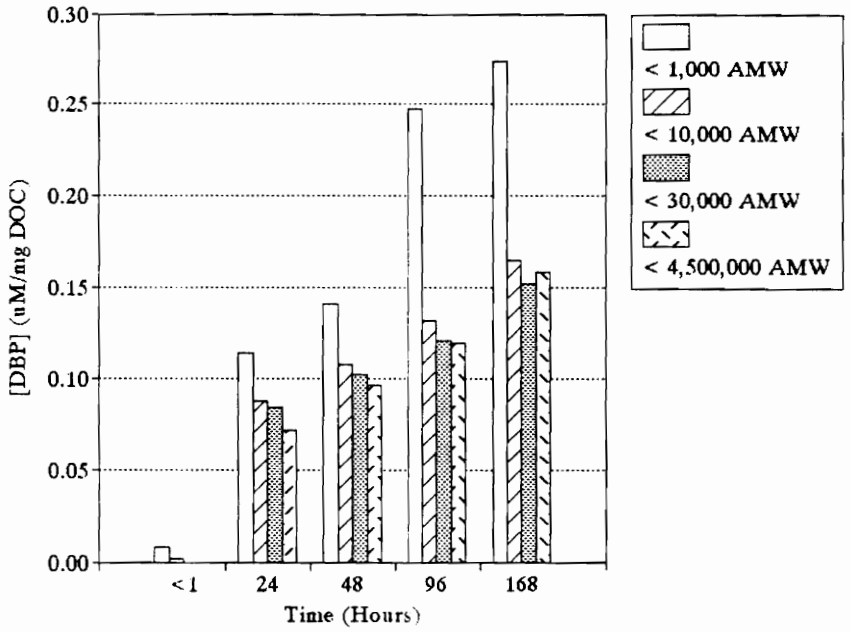

Figure A-6.4. CHCl2Br Formation Potential in Coagulated Water, 2 mg DOC/L, 6 mg Cl2/L, 0.07 mg Br/L

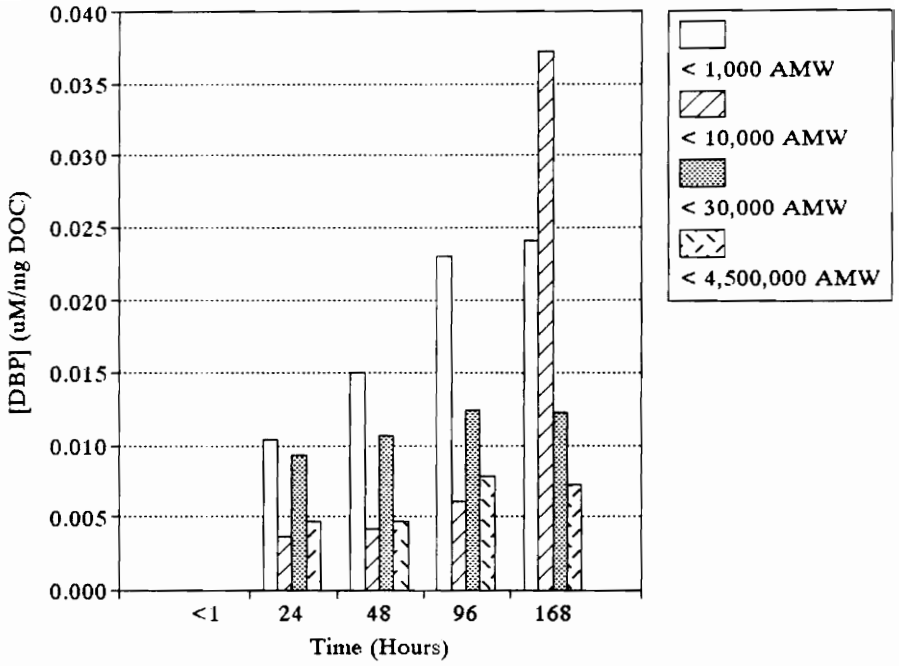

Figure A-6.5. CHClBr2 Formation Potential in Coagulated Water, [DOC] varies, Cl2 Dose= 3 x mg DOC/L, 0.07 mg Br/L

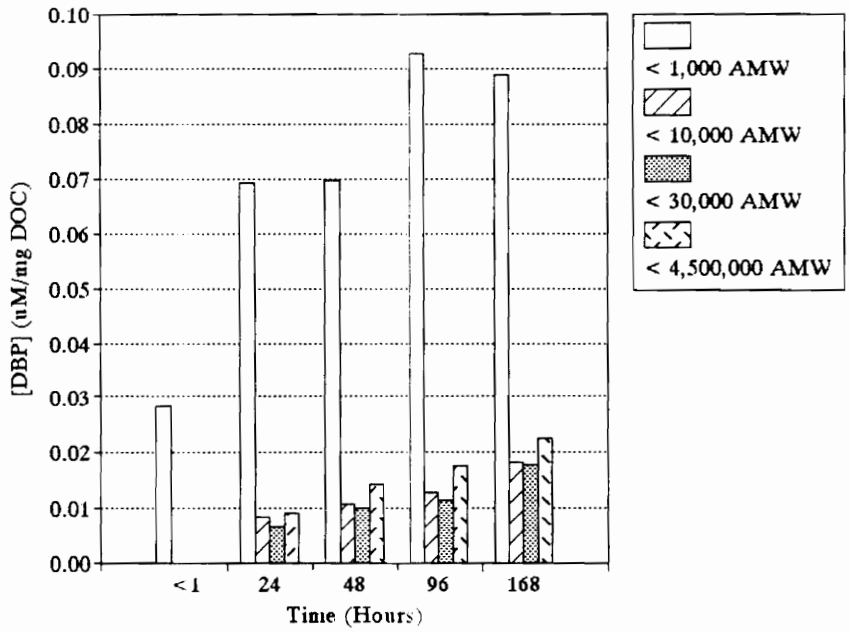

Figure A-6.6. CHClBr2 Formation Potential in Coagulated Water, 2 mg DOC/L, 6 mg Cl2/L, 0.07 mg Br/L

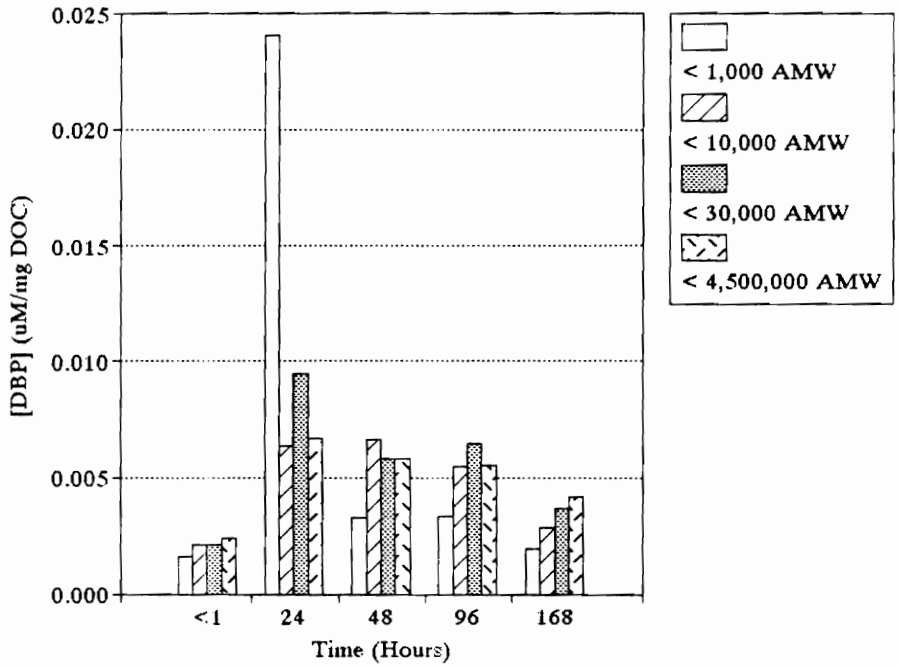

Figure A-6.7. DCAN Formation Potential in Coagulated Water, [DOC] varies, Cl2 Dose= 3 x mg DOC/L, 0.07 mg Br/L

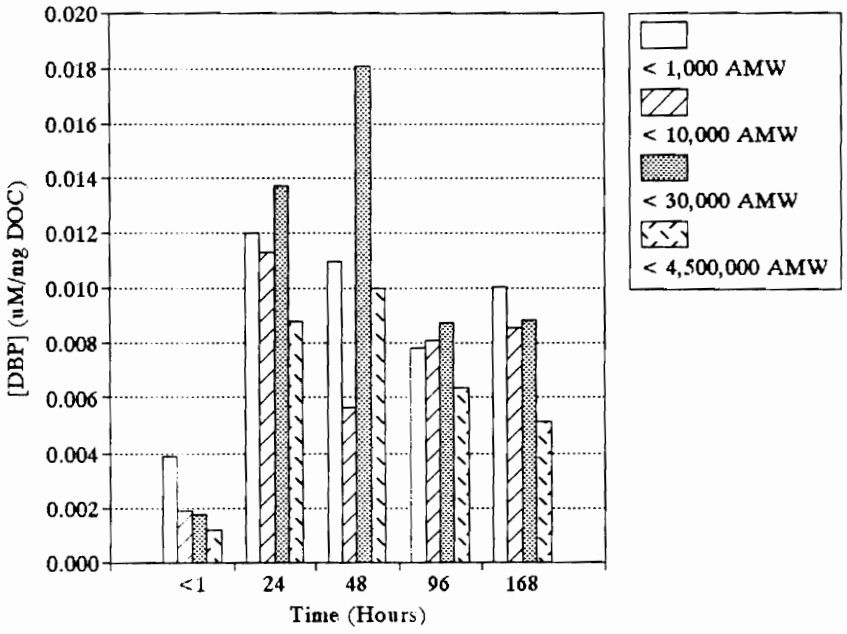

Figure A-6.8. DCAN Formation Potential in Coagulated Water, 2 mg DOC/L, 6 mg Cl2/L, 0.07 mg Br/L

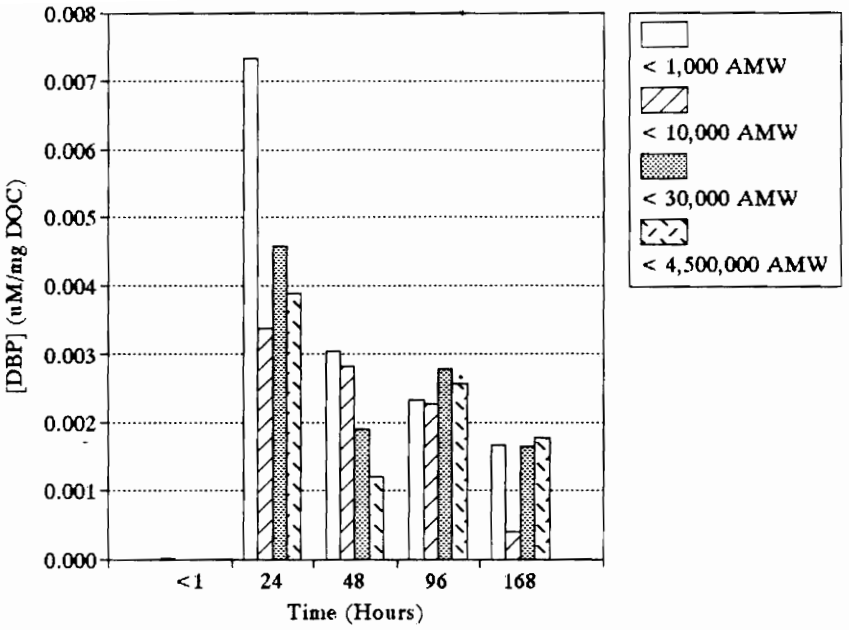

Figure A-6.9. BCAN Formation Potential in Coagulated Water, [DOC] varies, Cl2 Dose= 3 x mg DOC/L, 0.07 mg Br/L

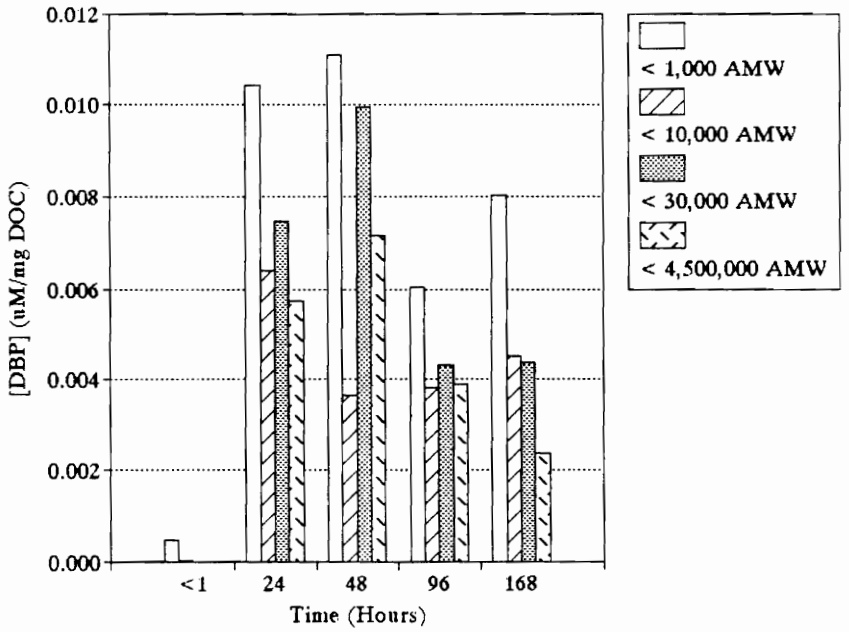

Figure A-6.10. BCAN Formation Potential in Coagulated Water, 2 mg DOC/L, 6 mg Cl2/L, 0.07 mg Br/L

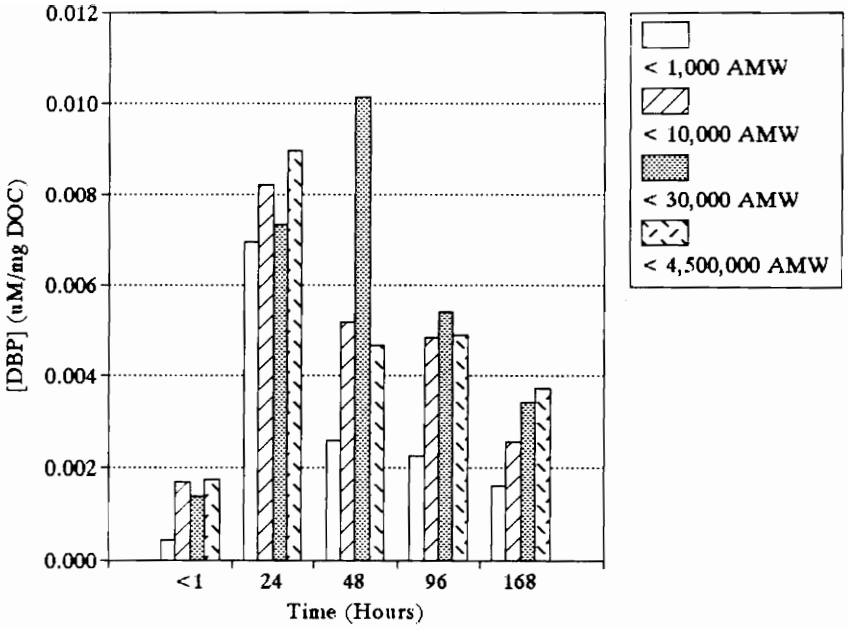

Figure A-6.11. TCP Formation Potential in Coagulated Water, [DOC] varies, Cl2 Dose= 3x mg DOC/L, 0.07 mg Br/L

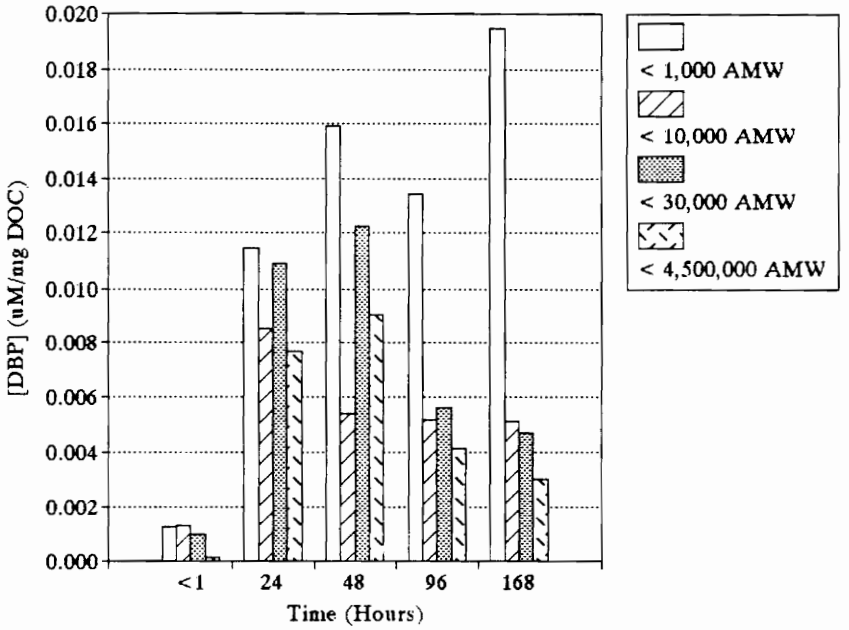

Figure A-6.12. TCP Formation Potential in Coagulated Water, 2 mg DOC/L, 6 mg Cl2/L, 0.07 mg Br/L

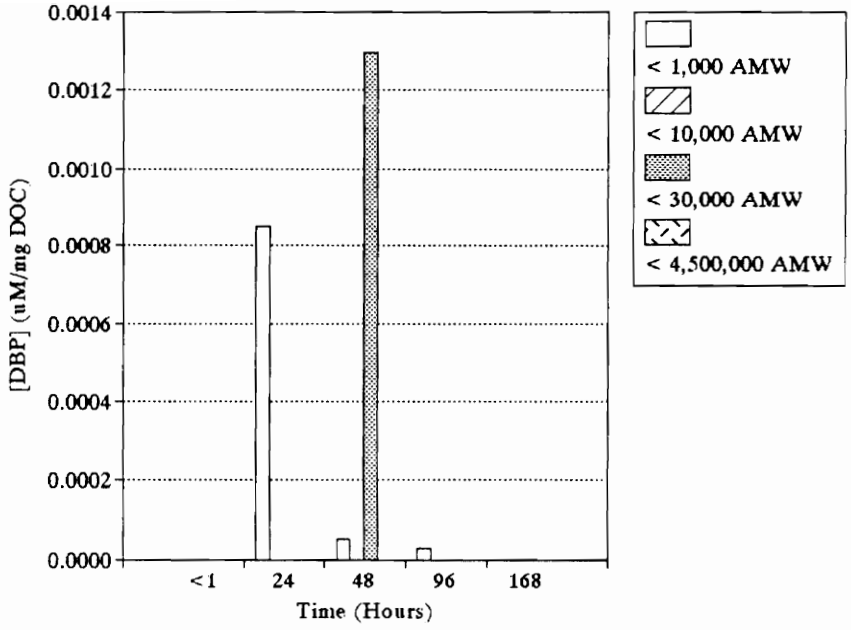

Figure A-6.13. DBAN Formation Potential in Coagulated Water, [DOC] varies, Cl2 Dose= 3 x mg DOC/L, 0.07 mg Br/L

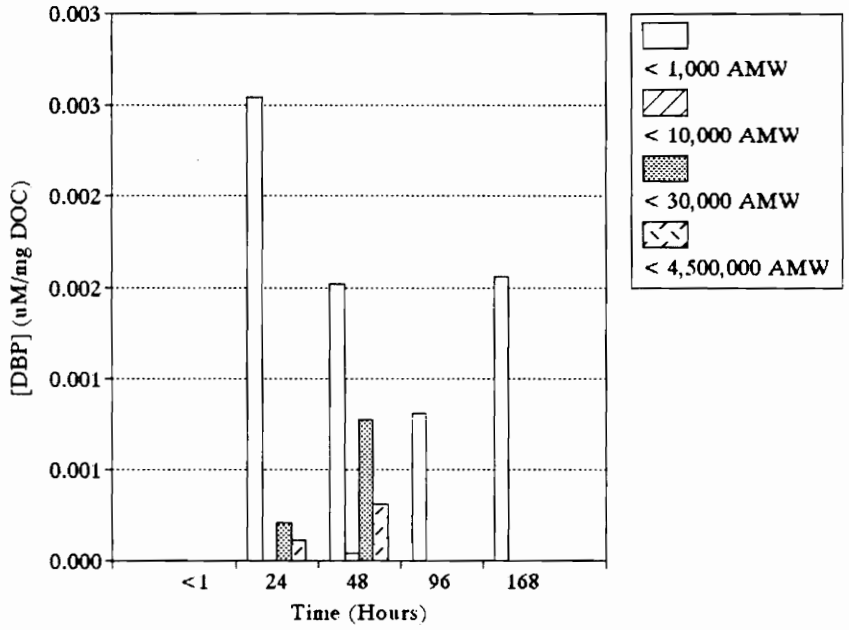

Figure A-6.14. DBAN Formation Potential in Coagulated Water, 2 mg DOC/L, 6 mg Cl2/L, 0.07 mg Br/L

Appendix 7. Matrix 5.1, Graphs of DOC Normalized DBP Concentration with Time

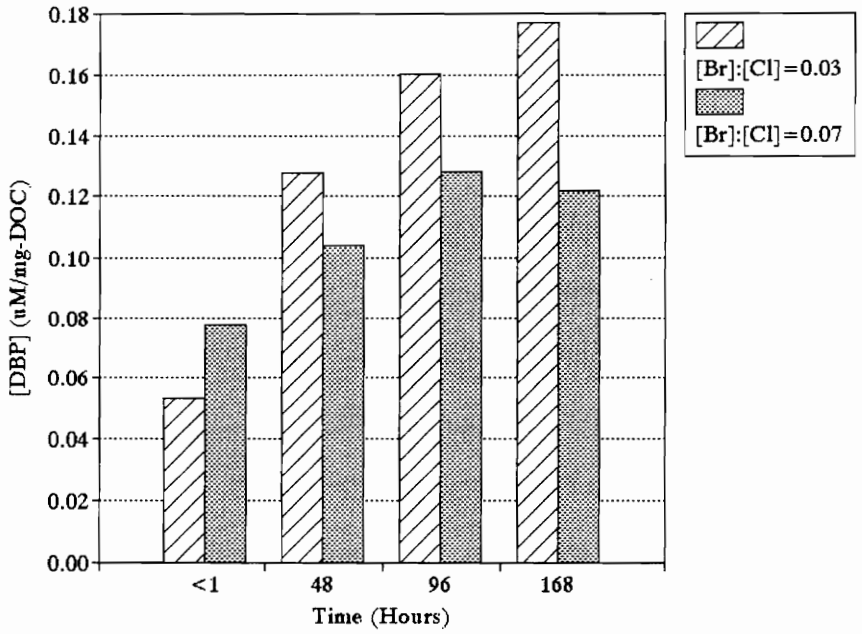

Figure A-7.1. CHCl3 Formation Potential, AMW<1K, [Br]:[Cl] (mM:mM), 2 mg DOC/L

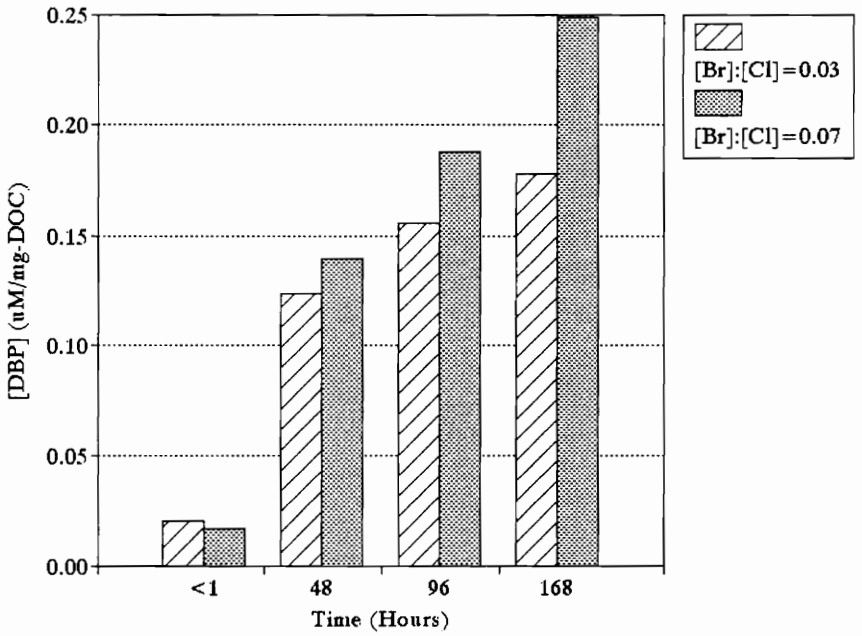

Figure A-7.2. CHCl2Br Formation Potential, AMW<1K, [Cl]:[Brl] (mM:mM), 2 mg DOC/L

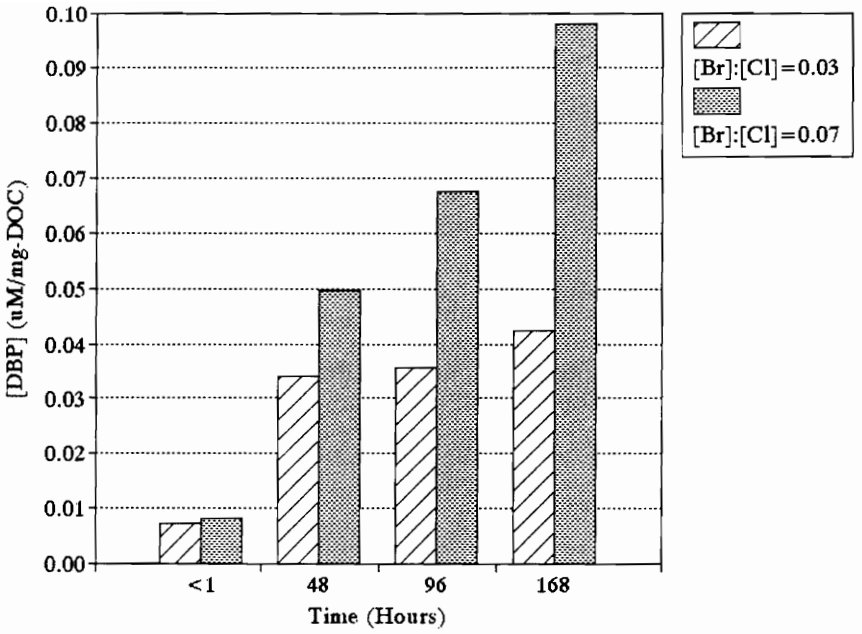

Figure A-7.3. CHClBr2 Formation Potential, AMW<1K, [Br]:[Cl] (mM:mM), 2 mg DOC/L

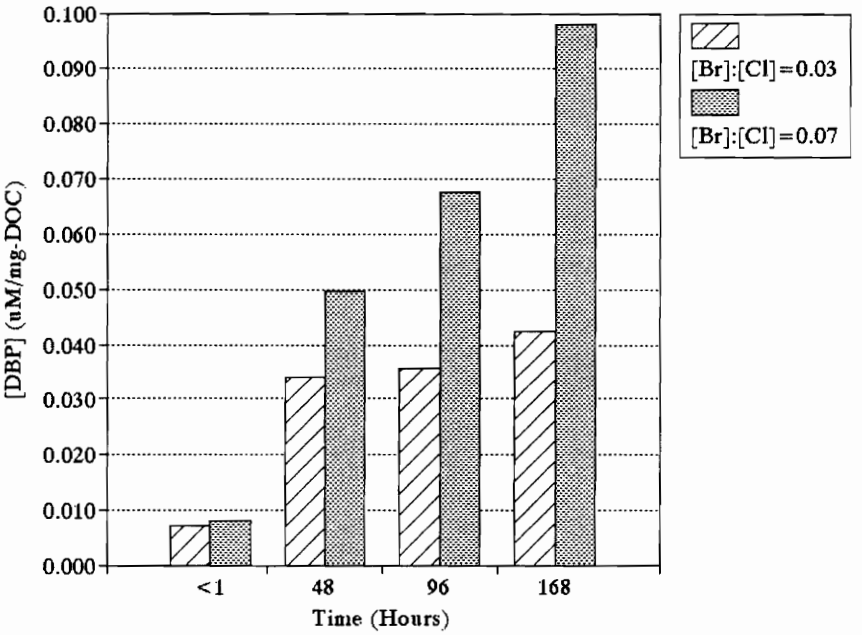

Figure A-7.4. CHBr3 Formation Potential, AMW<1K, [Br]:[Cl] (mM:mM), 2 mg DOC/L

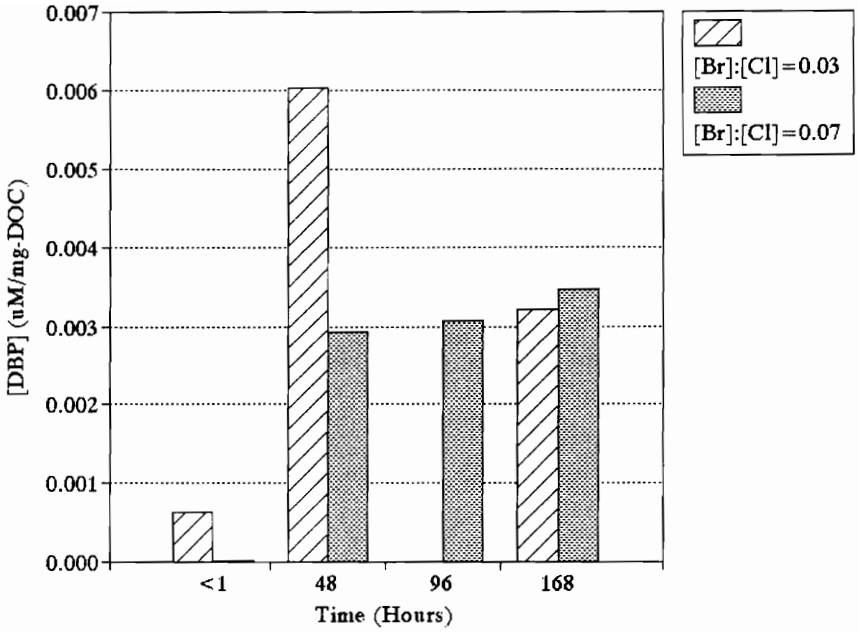

Figure A-7.5. DCAN Formation Potential, AMW<1K, [Br]:[Cl] (mM:mM), 2 mg DOC/L

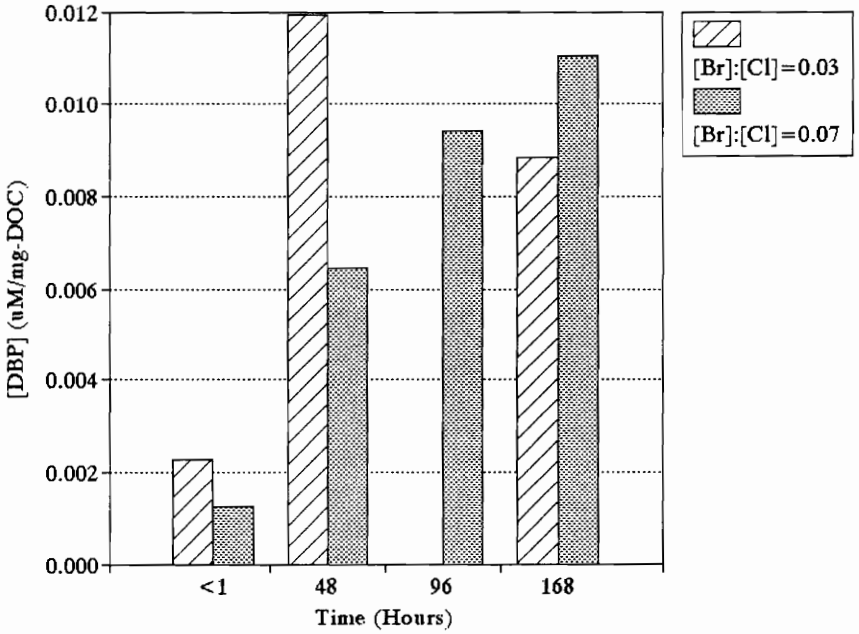

Figure A-7.6. BCAN Formation Potential, AMW<1K, [Br]:[Cl] (mM:mM), 2 mg DOC/L

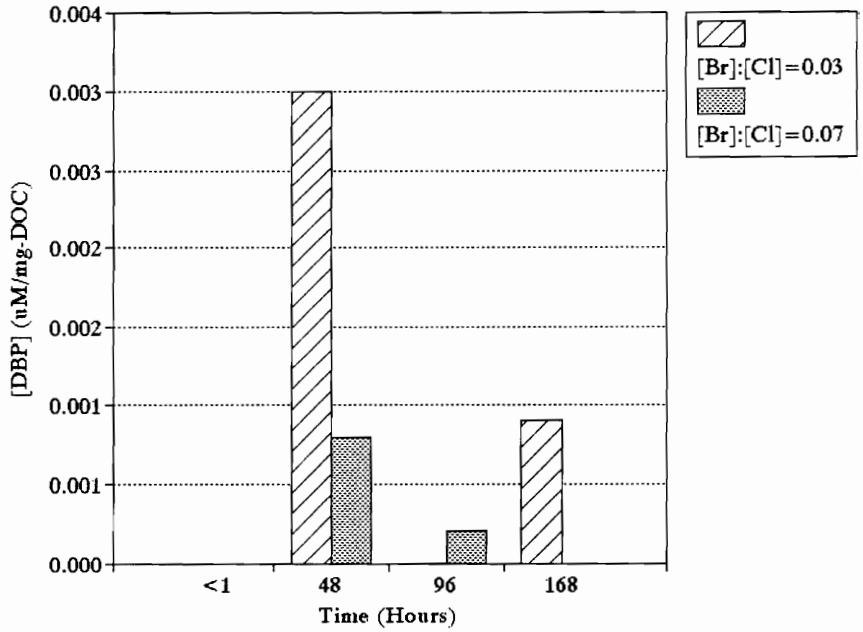

Figure A-7.7. TCP Formation Potential, AMW<1K, [Br]:[Cl] (mM:mM), 2 mg DOC/L

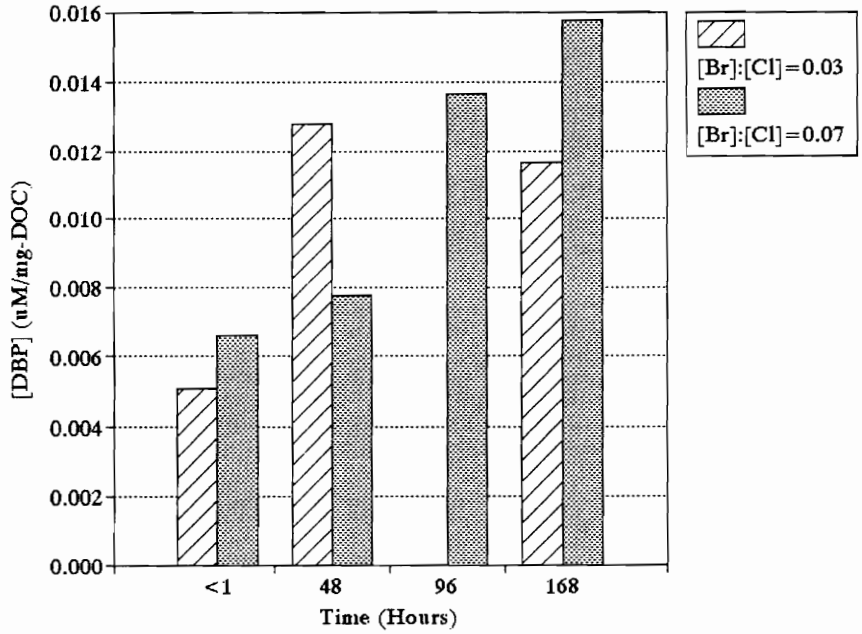

Figure A-7.8. DBAN Formation Potential, AMW<1K, [Br]:[Cl] (mM:mM), 2 mg DOC/L

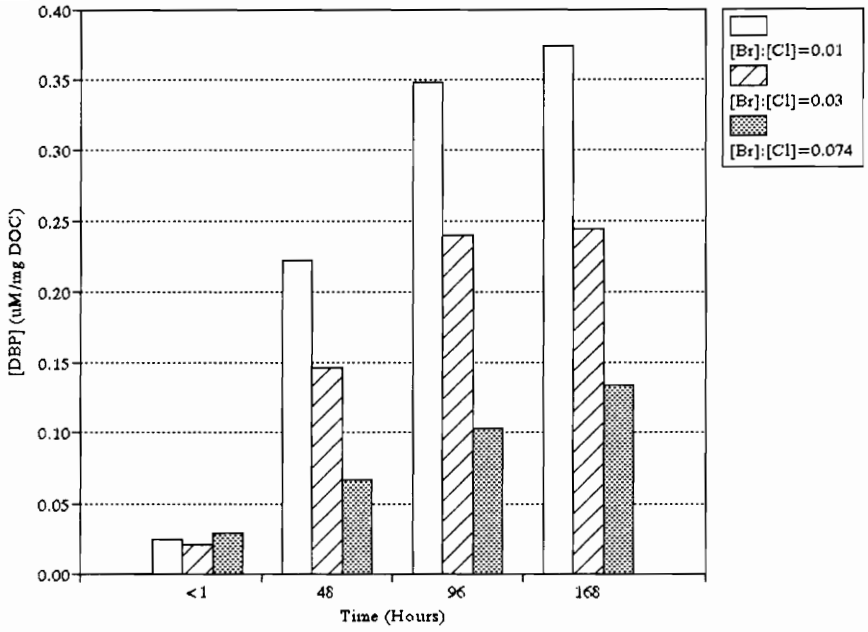

Figure A-7.9. CHCl3 Formation Potential, AMW<10K, [Br]:[Cl] (mM:mM), 2 mg DOC/L

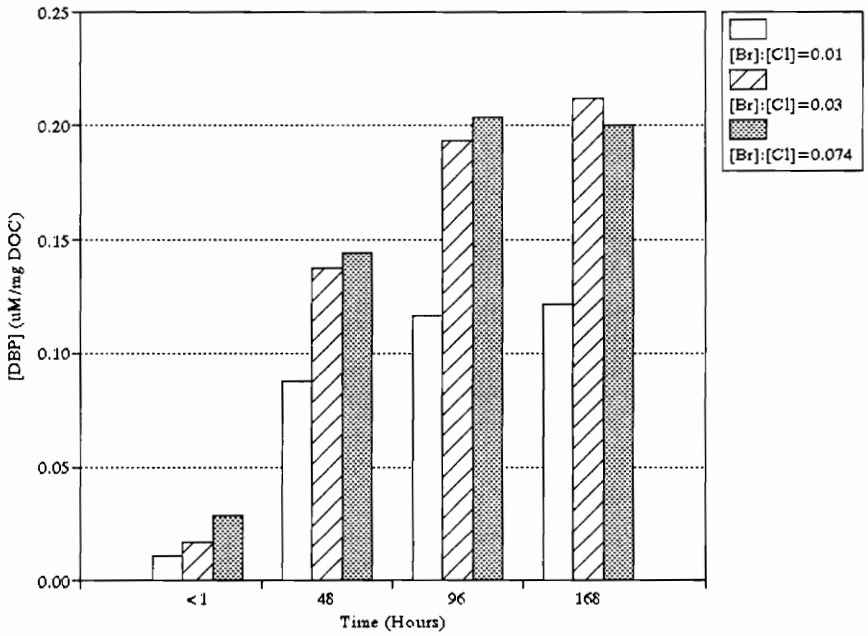

Figure A-7.10. CHCl2Br Formation Potential, AMW<10K, [Br]:[Cl] (mM:mM), 2 mg DOC/L

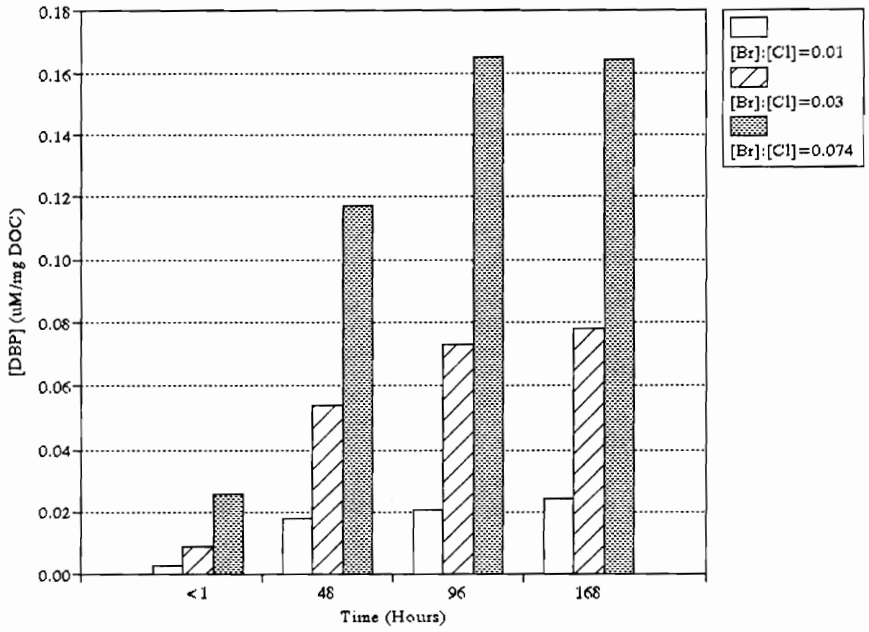

Figure A-7.11. CHClBr2 Formation Potential, AMW<10K, [Br]:[Cl] (mM:mM), 2 mg DOC/L

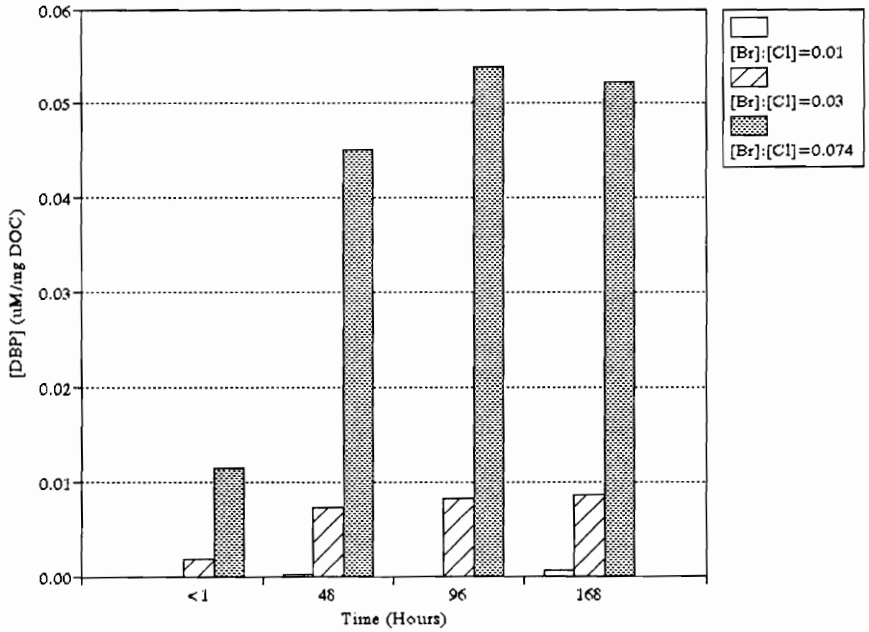

Figure A-7.12. CHBr3 Formation Potential, AMW<10K, [Br]:[Cl] (mM:mM), 2 mg DOC/L

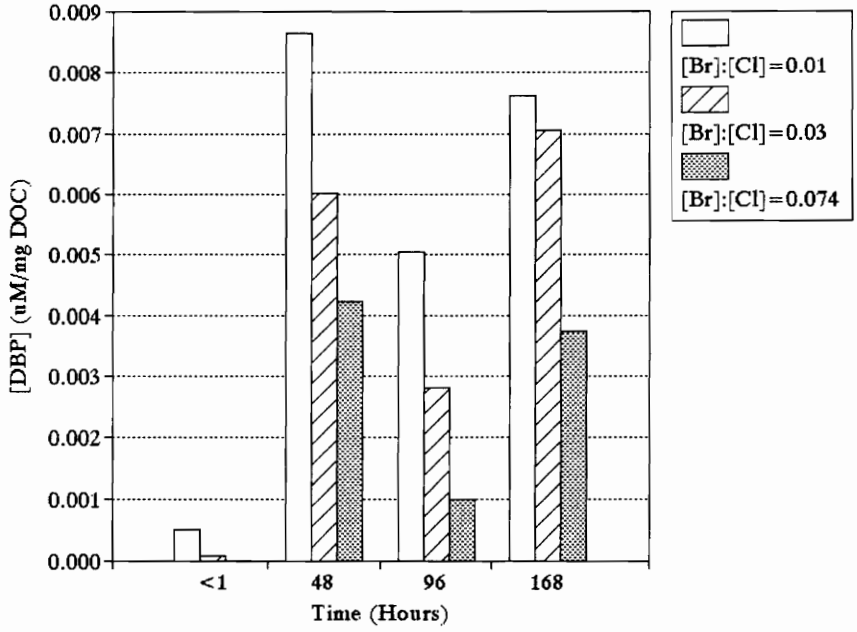

Figure A-7.13. DCAN Formation Potential, AMW<10K, [Br]:[Cl] (mM:mM), 2 mg DOC/L

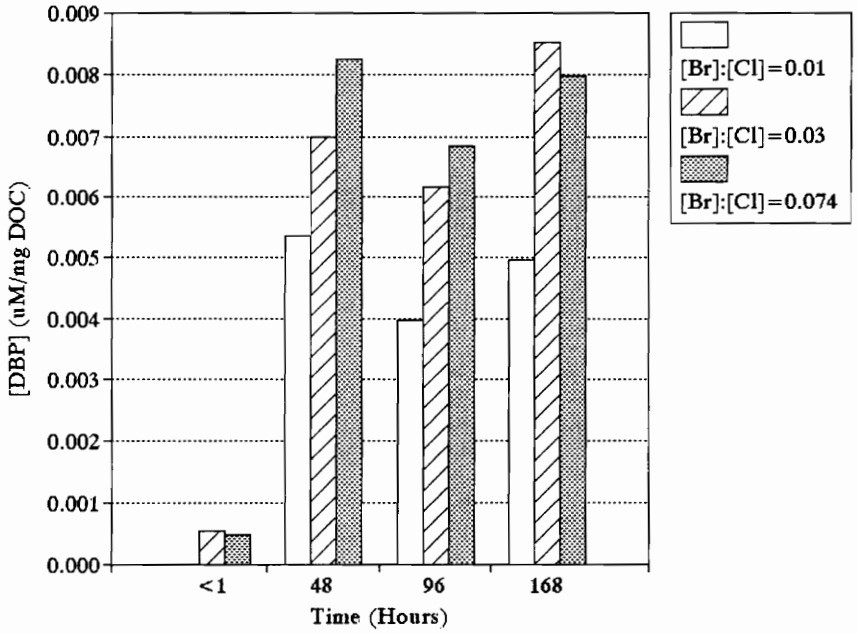

Figure A-7.14. BCAN Formation Potential, AMW<10K, [Br]:[Cl] (mM:mM), 2 mg DOC/L

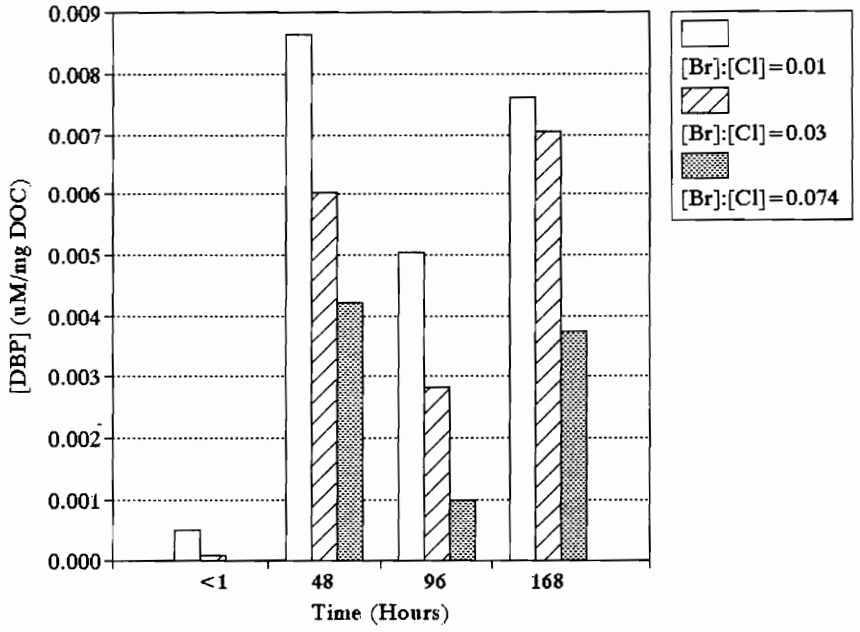

Figure A-7.15. TCP Formation Potential, AMW<10K, [Br]:[Cl] (mM:mM), 2 mg DOC/L

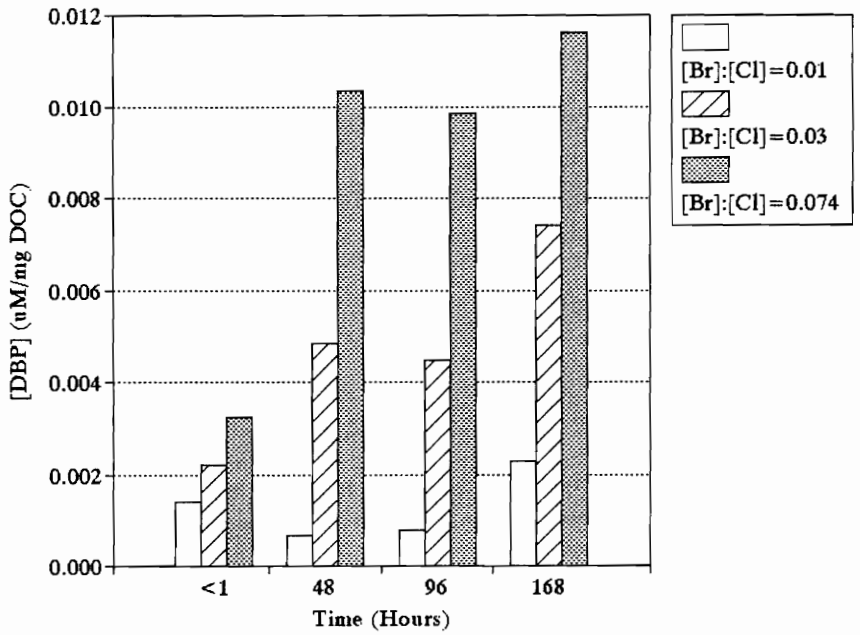

Figure A-7.16. DBAN Formation Potential, AMW<10K, [Br]:[Cl] (mM:mM), 2 mg DOC/L

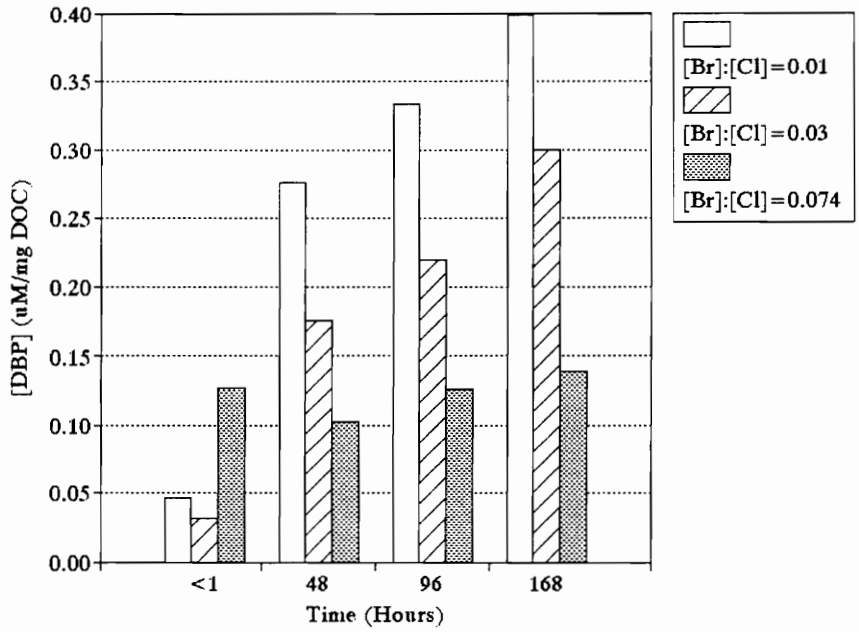

Figure A-7.17. CHCl3 Formation Potential, AMW<30K, [Br]:[Cl] (mM:mM), 2 mg DOC/L

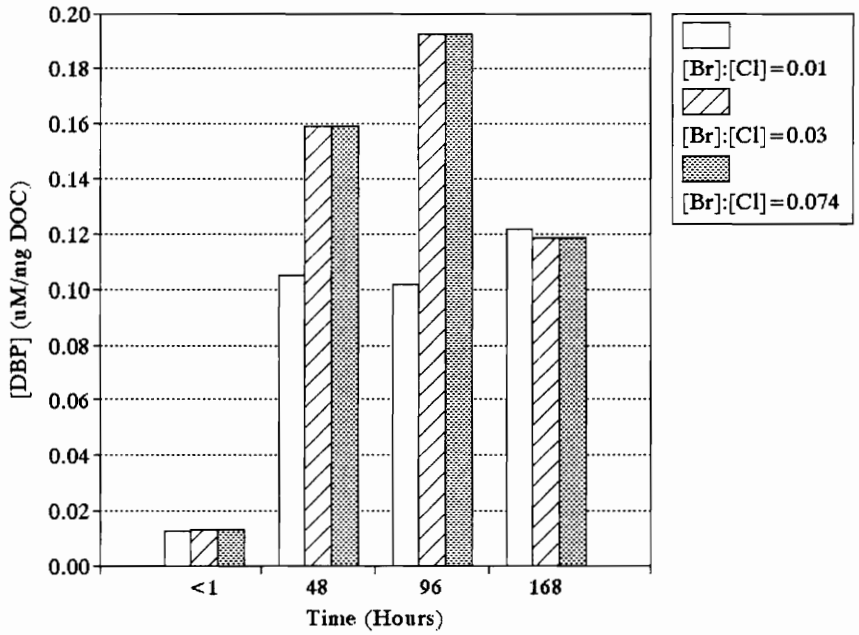

Figure A-7.18. CHCl2Br Formation Potential, AMW<30K, [Br]:[Cl] (mM:mM), 2 mg DOC/L

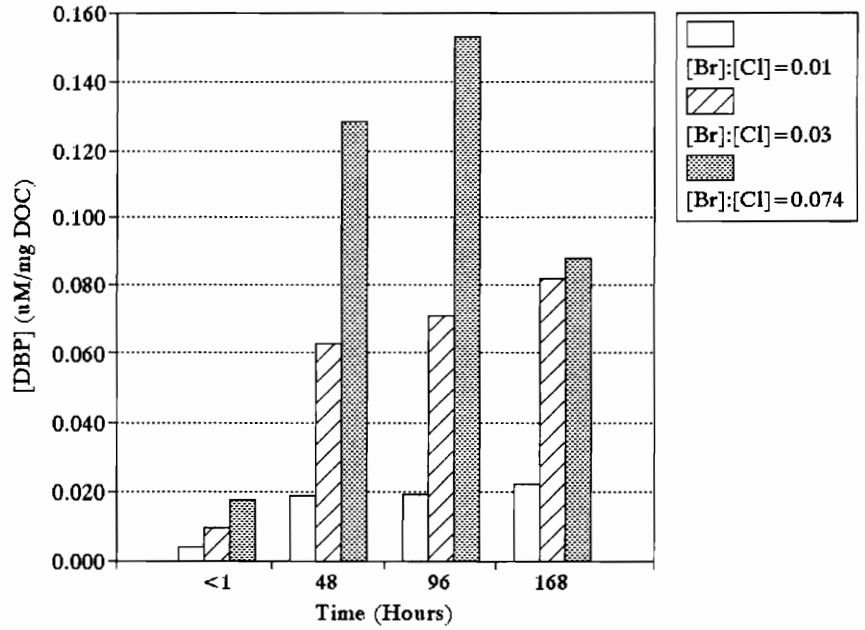

Figure A-7.19. CHClBr2 Formation Potential, AMW<30K, [Br]:[Cl] (mM:mM), 2 mg DOC/L

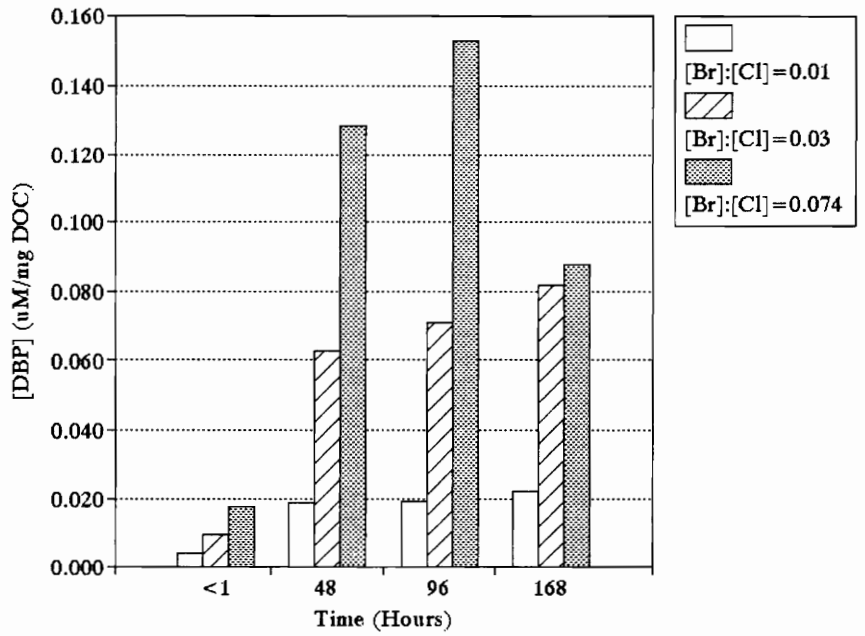

Figure A-7.20. CHBr3 Formation Potential, AMW<30K, [Br]:[Cl] (mM:mM), 2 mg DOC/L

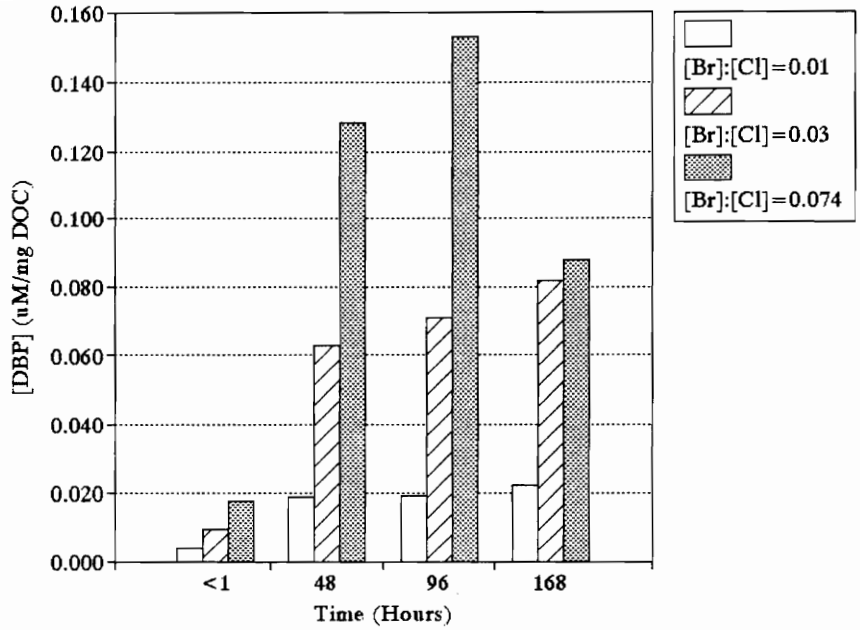

Figure A-7.21. DCAN Formation Potential, AMW<30K, [Br]:[Cl] (mM:mM), 2 mg DOC/L

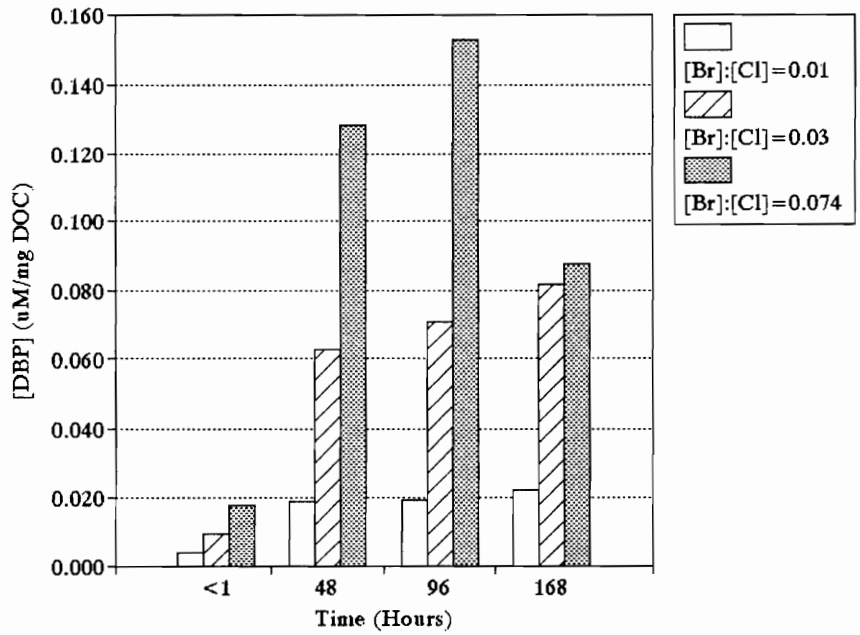

Figure A-7.22. BCAN Formation Potential, AMW<30K, [Br]:[Cl] (mM:mM), 2 mg DOC/L

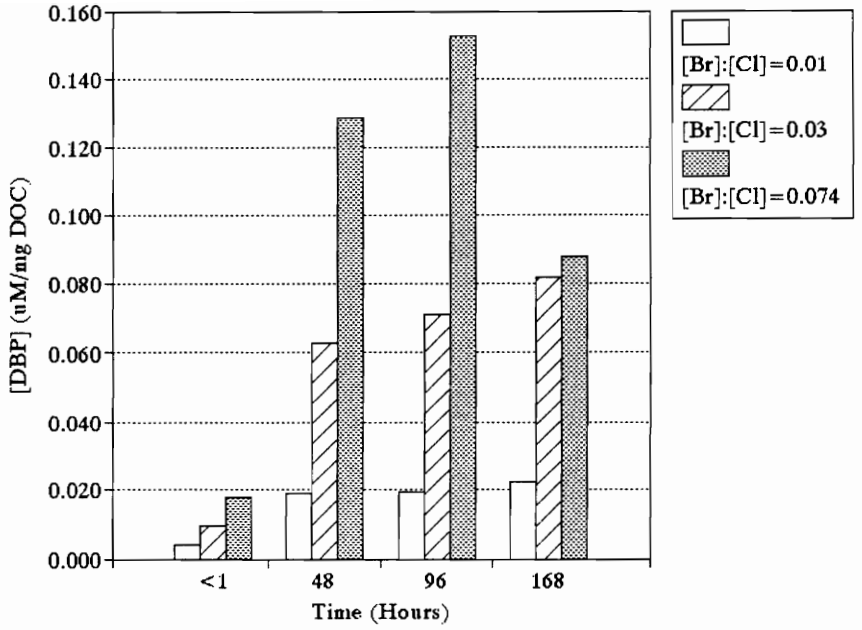

Figure A-7.23. TCP Formation Potential, AMW<30K, [Br]:[Cl] (mM:mM), 2 mg DOC/L

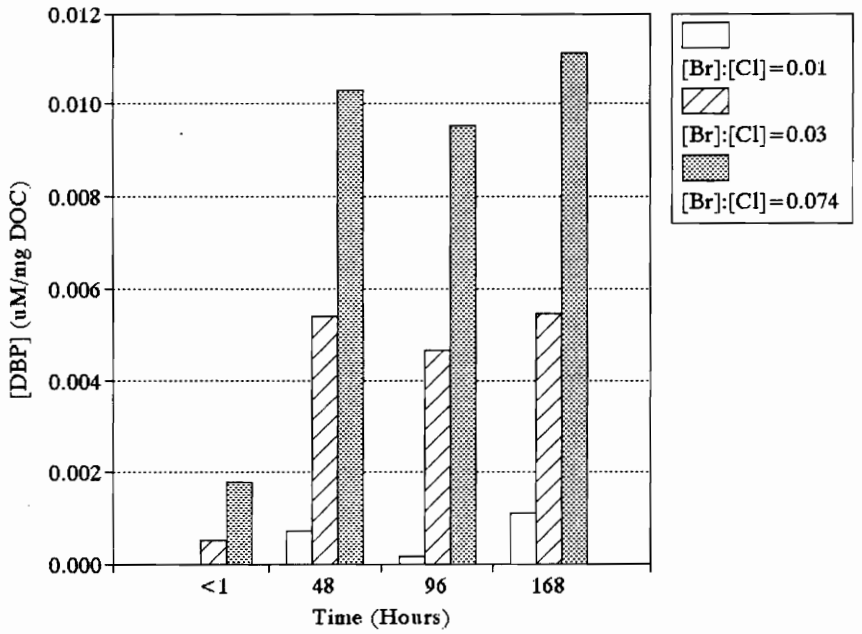

Figure A-7.24. DBAN Formation Potential, AMW<30K, [Br]:[Cl] (mM:mM), 2 mg DOC/L

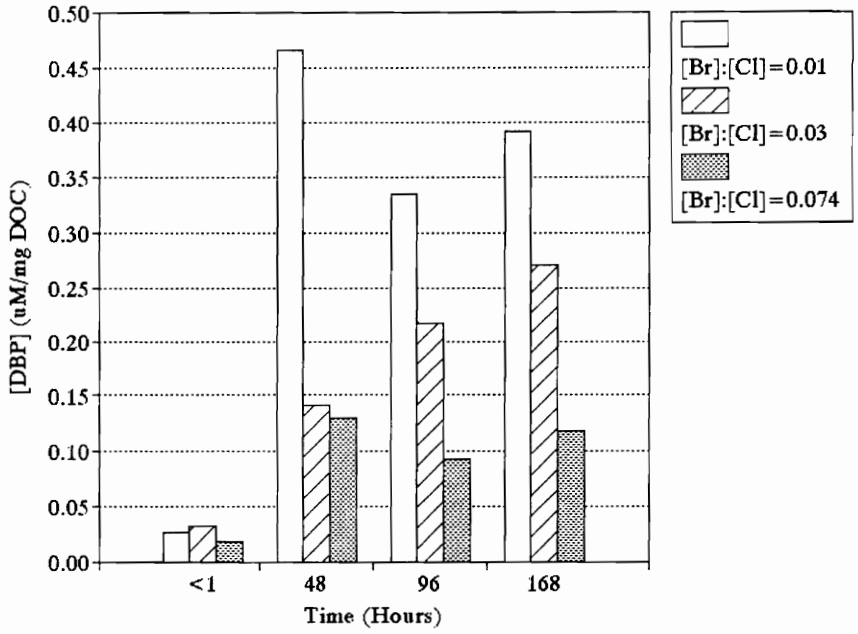

Figure A-7.25. CHCl3 Formation Potential, AMW<4500K, [Br]:[Cl] (mM:mM) 2 mg DOC/L

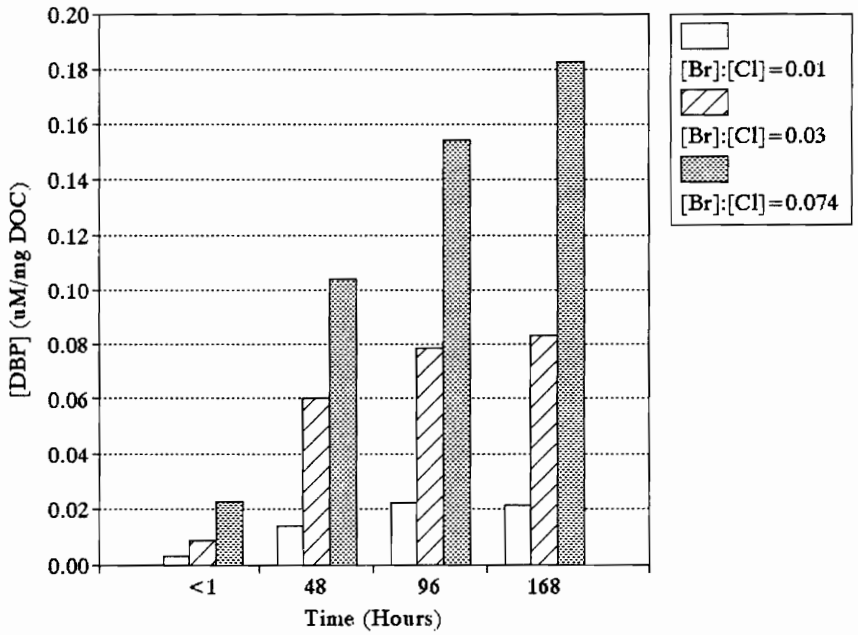

Figure A-7.26. CHCl2Br Formation Potential, AMW<4500K, [Br]:[Cl] (mM:mM) 2 mg DOC/L

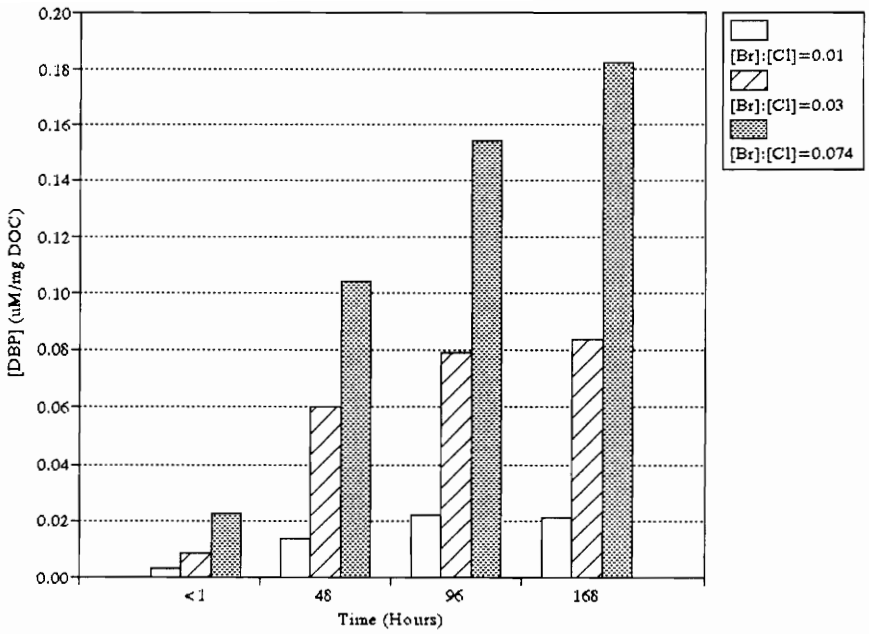

Figure A-7.27. CHClBr2 Formation Potential, AMW<4500K, [Br]:[Cl] (mM:mM) 2 mg DOC/L

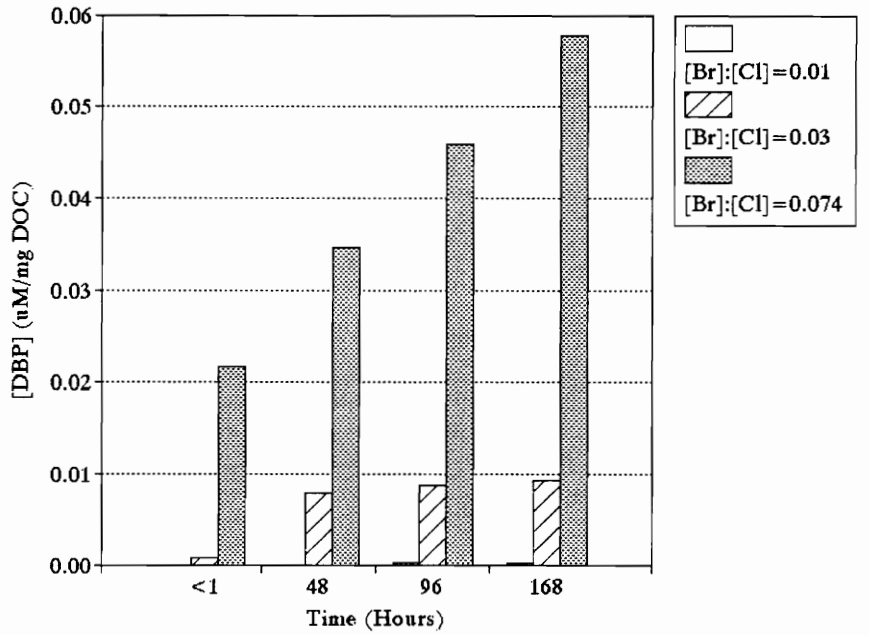

Figure A-7.28. CHBr3 Formation Potential, AMW<4500K, [Br]:[Cl] (mM:mM) 2 mg DOC/L

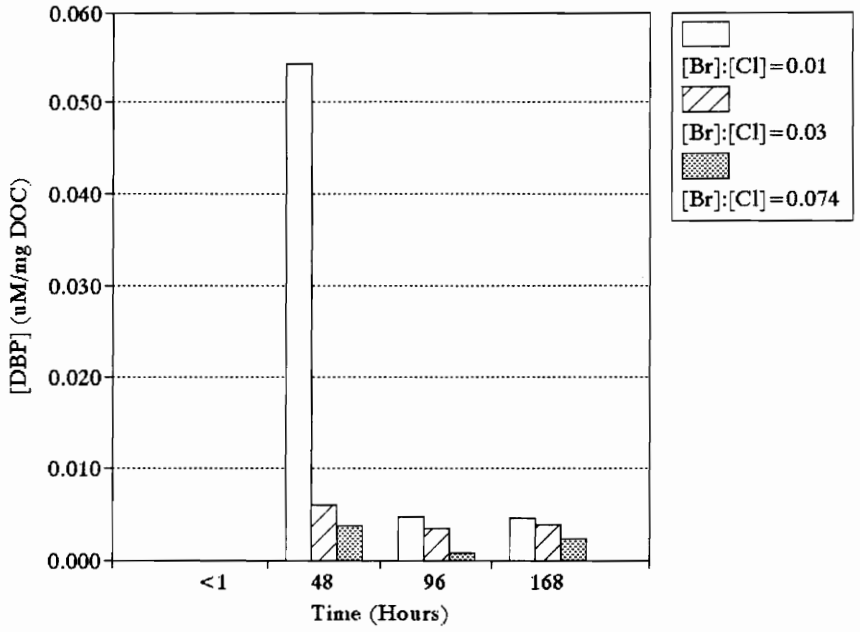

Figure A-7.29. DCAN Formation Potential, AMW<4,500K, [Br]:[Cl] (mM:mM), 2 mg DOC/L

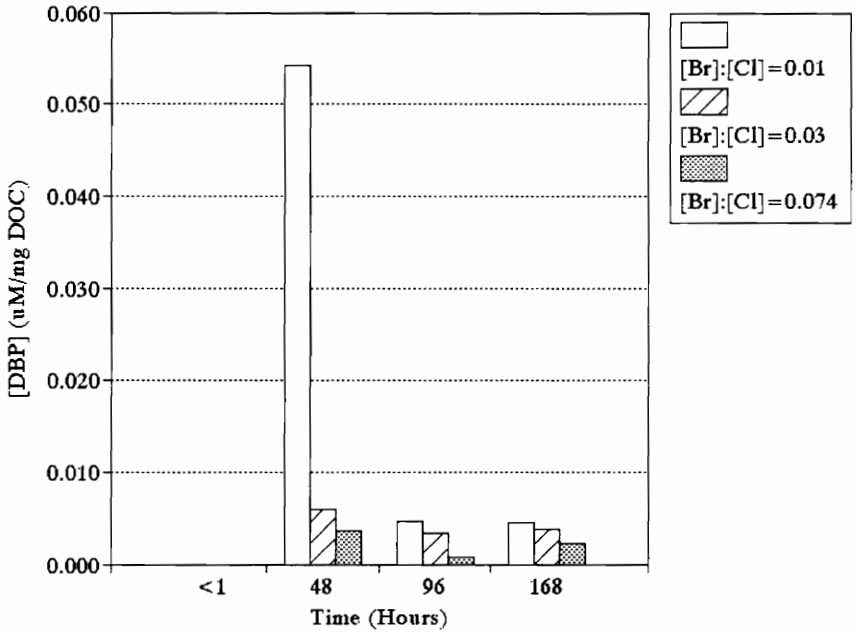

Figure A-7.30. BCAN Formation Potential, AMW<4,500K, [Br]:[Cl] (mM:mM), 2 mg DOC/L

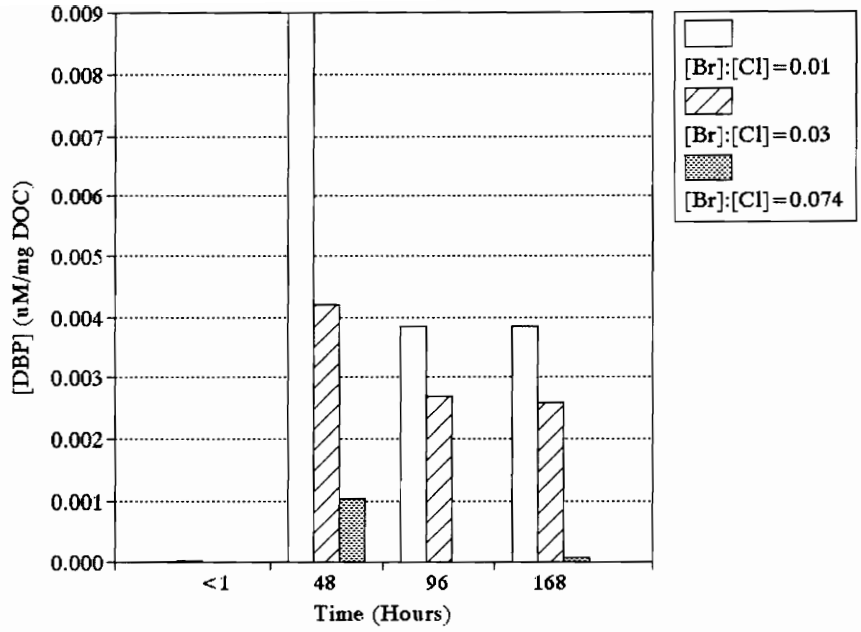

Figure A-7.31. TCP Formation Potential, AMW<4,500K, [Br]:[Cl] (mM:mM), 2 mg DOC/L

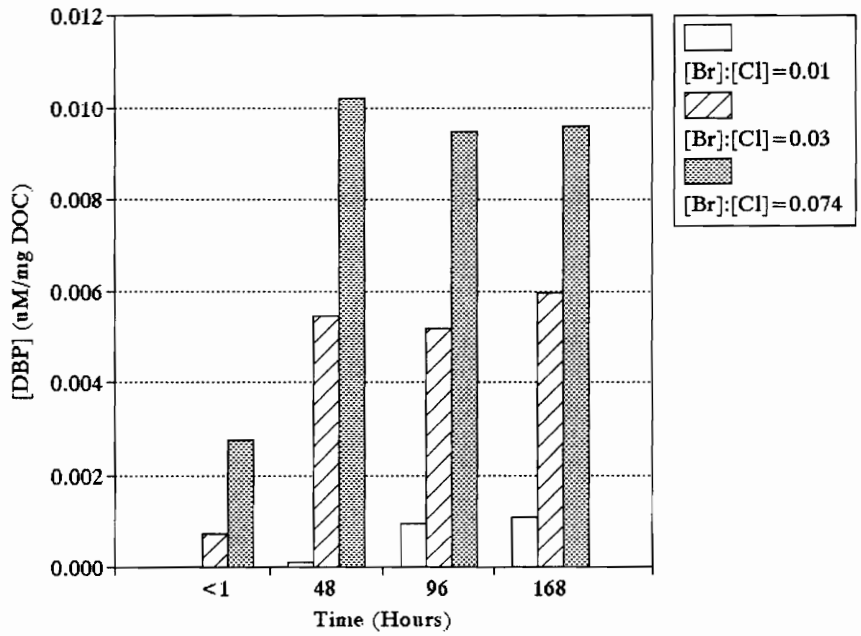

Figure A-7.32. DBAN Formation Potential, AMW<4,500K, [Br]:[Cl] (mM:mM), 2 mg DOC/L

Appendix 8. Matrix 5.2, Graphs of DOC Normalized DBP Concentration with Time

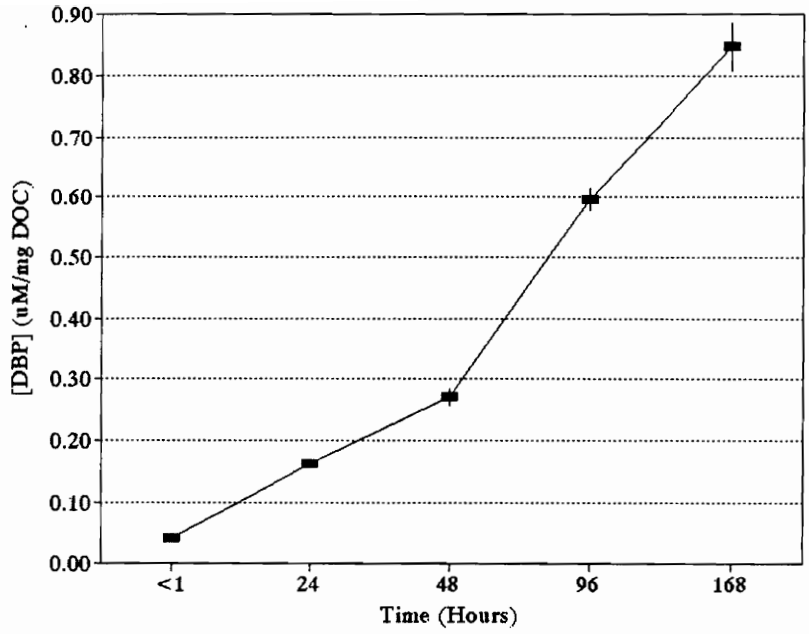

Figure A-8.1. CHCl3 Formation Potential, AMW<1K, 1.4 mg DOC/L
4.5 mg Cl2/L, 0.07 mg Br/L

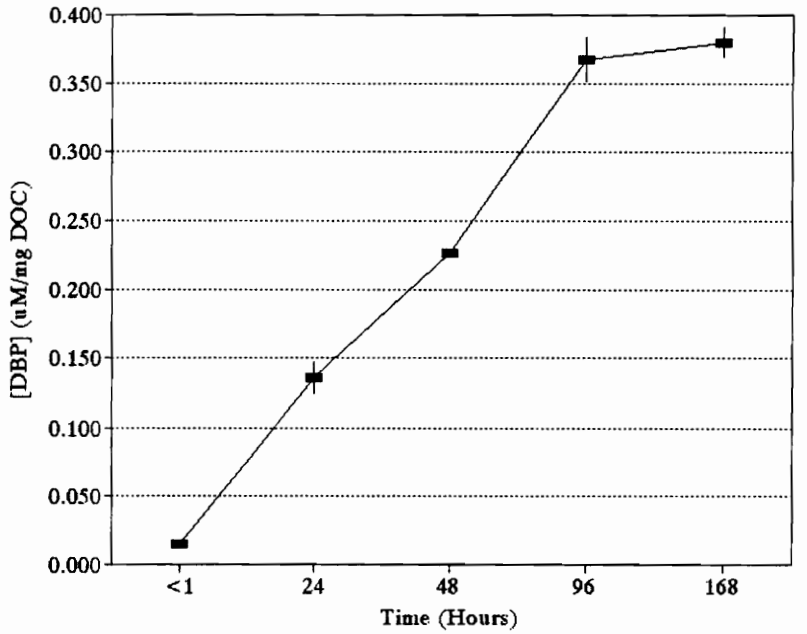

Figure A-8.2. CHCl2Br Formation Potential, AMW<1K, 1.4 mg DOC/L
4.5 mg Cl2/L, 0.07 mg Br/L

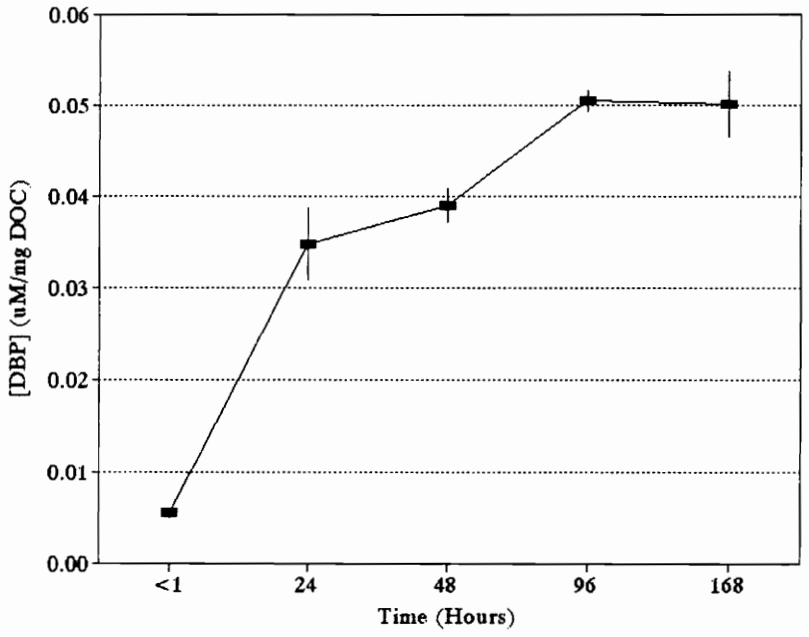

Figure A-8.3. CHCl2Br Formation Potential, AMW<1K, 1.4 mg DOC/L, 4.5 mg Cl2/L, 0.07 mg Br/L

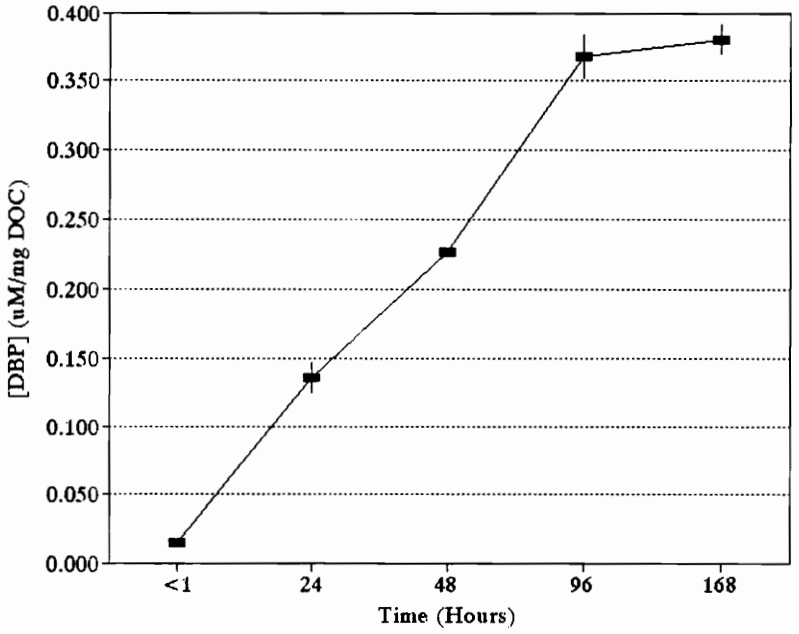

Figure A-8.4. CHBr3 Formation Potential, AMW<1K, 1.4 mg DOC/L, 4.5 mg Cl2/L, 0.07 mg Br/L

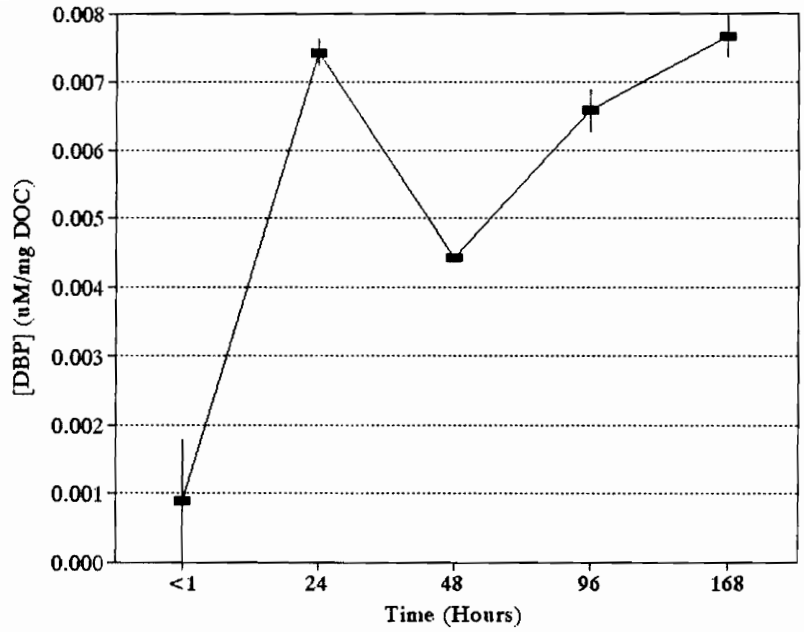

Figure A-8.5. DCAN Formation Potential, AMW<1K, 1.4 mg DOC/L, 4.5 mg Cl2/L, 0.07 mg Br/L

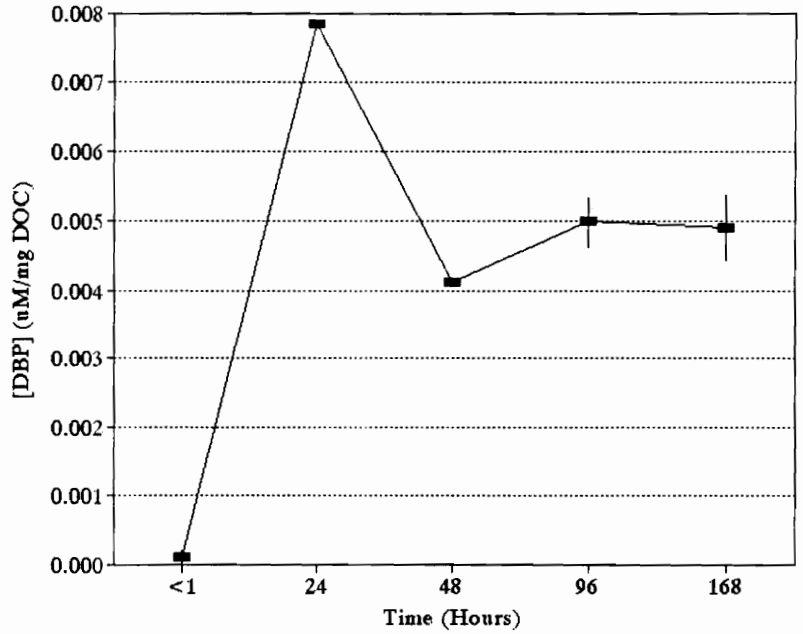

Figure A-8.6. BCAN Formation Potential, AMW<1K, 1.4 mg DOC/L, 4.5 mg Cl2/L, 0.07 mg Br/L

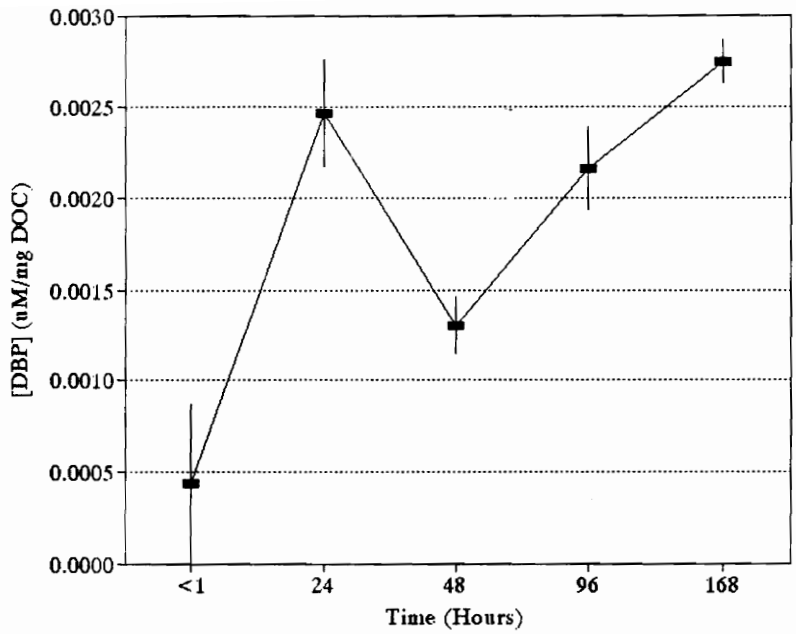

Figure A-8.7. DBAN Formation Potential, AMW<1K, 1.4 mgDOC/L, 4.5 mg Cl2/L, 0.07 mg Br/L

Appendix 9. Matrix 6, Graphs of DOC Normalized DBP Concentration with Time

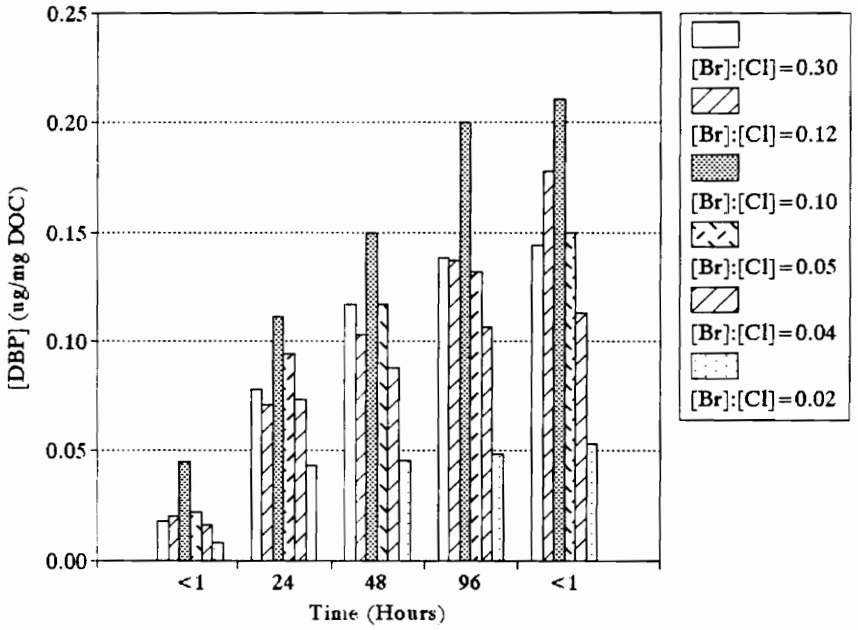

Figure A-9.1. CHCl3 Formation Potential in Coagulated Water,
[DOC] varies, Cl2 Dose= 3 x mg DOC/L, AMW < 4,500 K
[Br]:[Cl] (mM:mM)

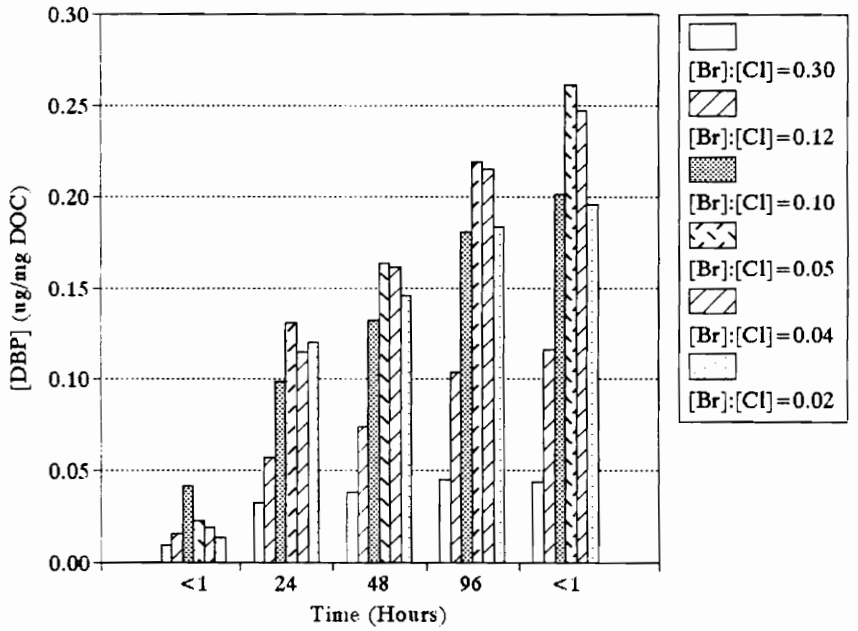

Figure A-9.2. CHCl2Br Formation Potential in Coagulated Water,
[DOC] varies, Cl2 Dose= 3 x mg DOC/L, AMW < 4,500 K
[Br]:[Cl] (mM:mM)

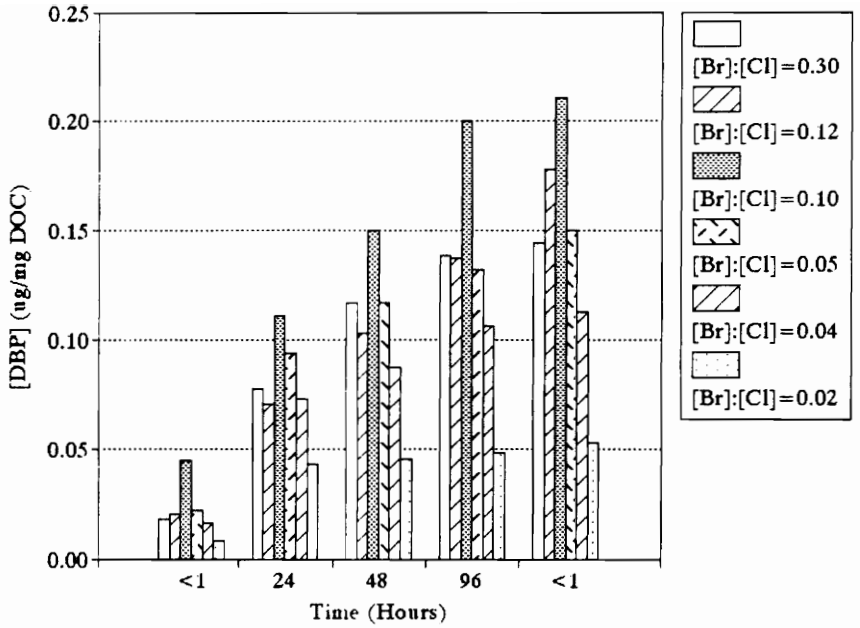

Figure A-9.3. CHClBr2 Formation Potential in Coagulated Water, [DOC] varies, Cl2 Dose= 3 x mg DOC/L, AMW < 4,500 K, [Br]:[Cl] (mM:mM)

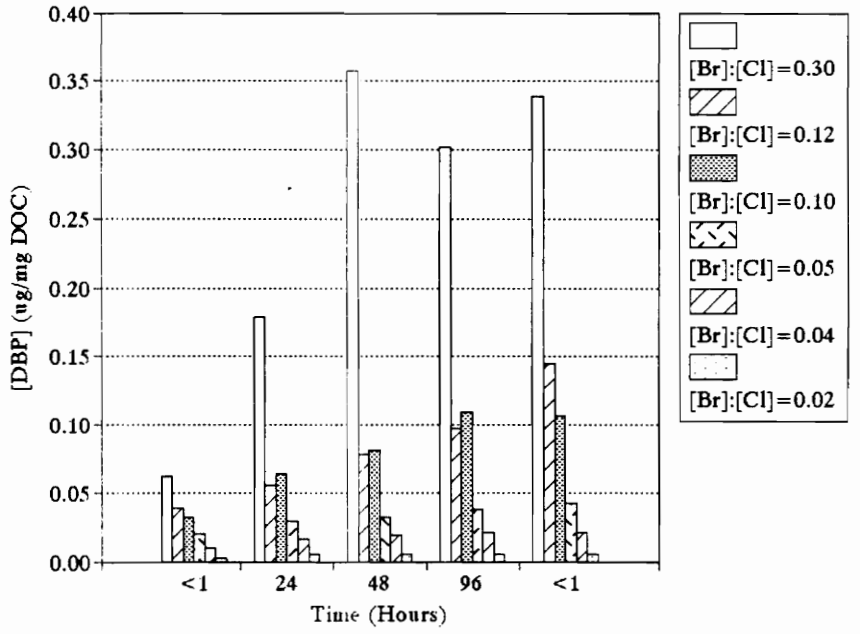

Figure A-9.4. CHBr3 Formation Potential in Coagulated Water, [DOC] varies, Cl2 Dose= 3 x mg DOC/L, AMW < 4,500 K, [Br]:[Cl] (mM:mM)

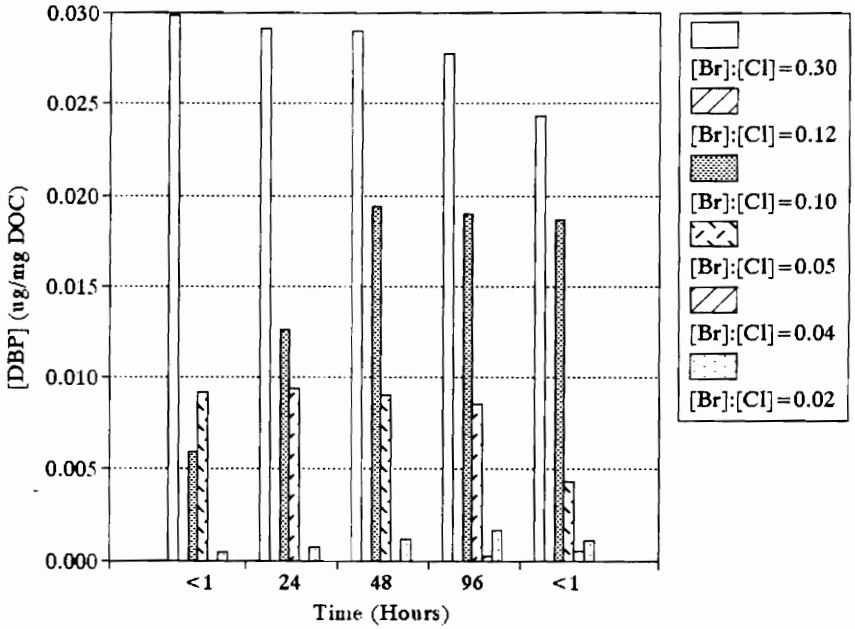

Figure A-9.5. DCAN Formation Potential in Coagulated Water, [DOC] varies, Cl2 Dose= 3 x mg DOC/L, AMW < 4,500 K, [Br]:[Cl] (mM:mM)

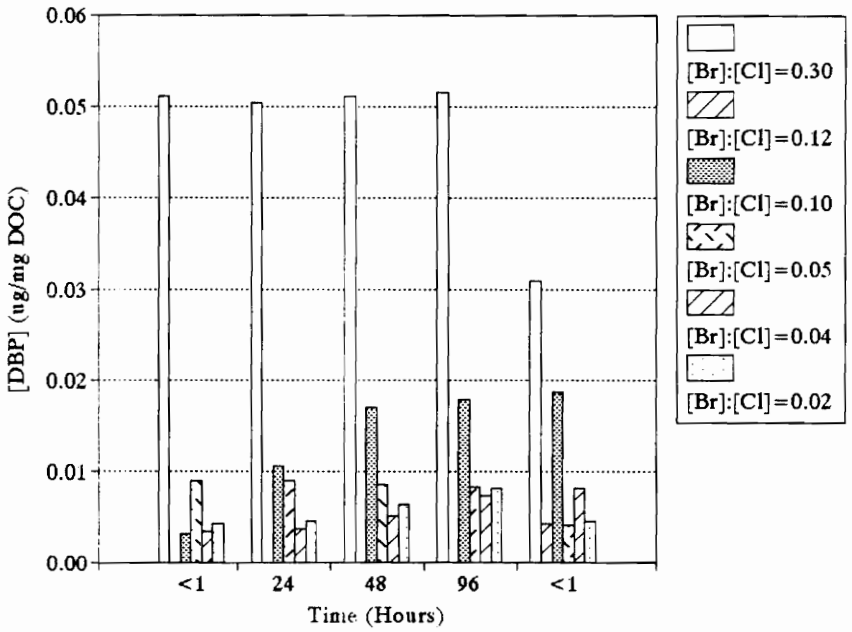

Figure A-9.6. BCAN Formation Potential in Coagulated Water, [DOC] varies, Cl2 Dose= 3 x mg DOC/L, AMW < 4,500 K, [Br]:[Cl] (mM:mM)

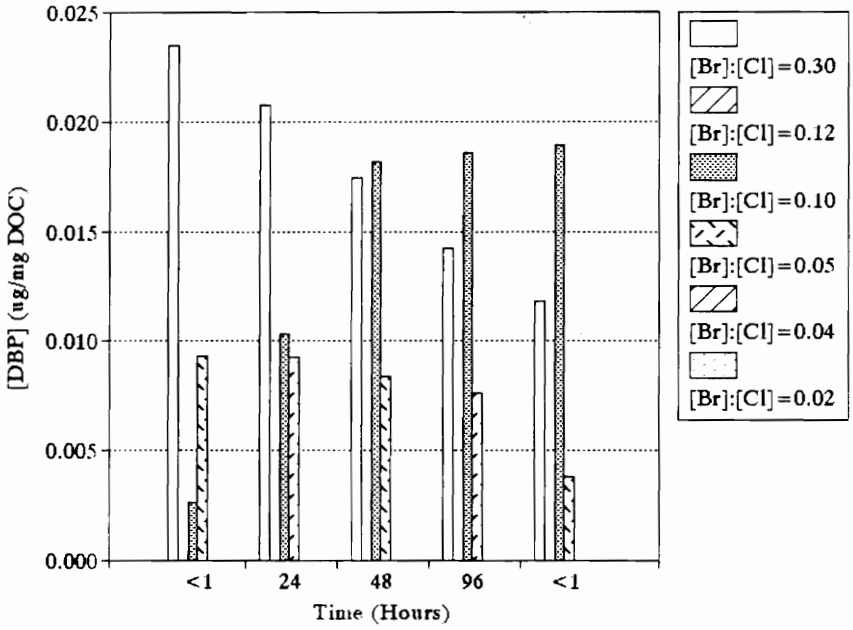

Figure A-9.7. TCP Formation Potential in Coagulated Water, [DOC] varies, Cl2 Dose= 3 x mg DOC/L, AMW < 4,500 K, [Br]:[Cl] (mM:mM)

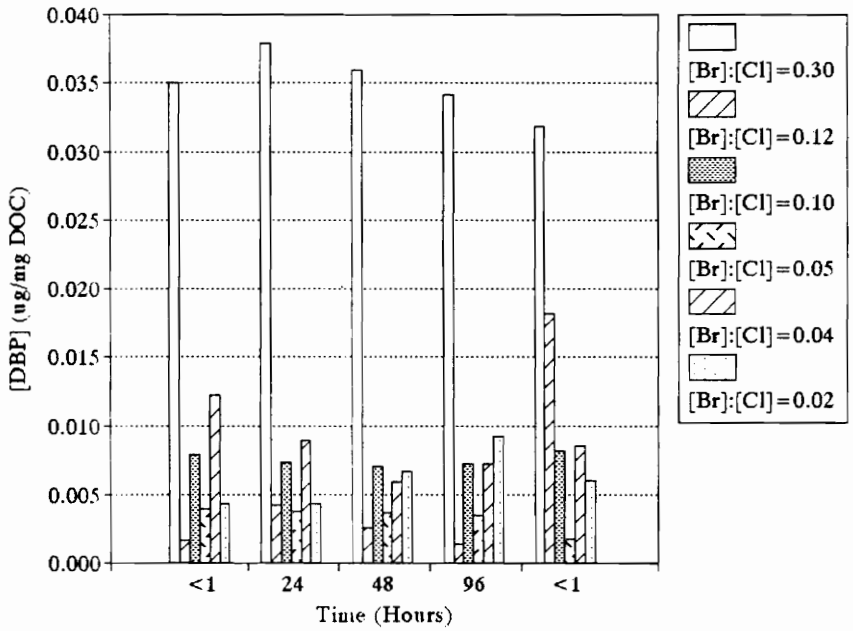

Figure A-9.8. DBAN Formation Potential in Coagulated Water, [DOC] varies, Cl2 Dose= 3 x mg DOC/L, AMW < 4,500 K, [Br]:[Cl] (mM:mM)

Bibliography

Abbt-Braun, Gudrun, Fritz H. Frimmel, Hans-Rolf Schulten. 1989. Structural Investigations of Aquatic Humic Substances by Pyrolysis-Field Ionization Mass Spectrometry and Pyrolysis-Gas Chromatography/Mass Spectrometry. *Water Research*. 23(12):1579-1591.

Adin, A., J. Katzhendler, D. Alkaslassy, and Ch. Rav-Acha. 1991. Trihalomethane Formation in Chlorinated Drinking Water: A Kinetic Model. *Water Research*. 25(7):797-805.

Aieta, E. Marco, Paul V. Roberts, and Margarita Hernandez. 1984. Determination of Chlorine Dioxide, Chlorine, Chlorite, and Chlorate in Water. *Journal American Water Works Association*. 76 (1):64-70.

Aiken, G.R. 1985. Isolation and Concentration Techniques for Aquatic Humic Substances. *Humic Substances in Soil, Sediment and Water: Geochemistry, Isolation, and Characterization*. Edited by G.R. Aiken, D.M. McKnight, R.L. Wershaw, P. MacCarthy. New York, New York. Wiley-Interscience. 363-385.

Aiken, George and Evangelo Cotsaris. 1995. Soil and Hydrology: Their Effect on NOM. *Journal American Water Works Association*. 87 (1):36-45.

Allard, B., H. Boren, C. Petterson, and G. Zhang. 1994. Degradation of Humic Substances by UV Irradiation. *Environment International*. 20(1):97-101.

Allgeier and R. Scott Summers. 1995. Evaluating NF for DBP Control with the RBSMT. *Journal American Water Works Association*. 87 (3):87-99.

Amicon. 1993. *Catalog with Prices: Membrane Filtration Chromatography*. Amicon a GRACE company. Beverly, Massachusetts

Amicon. 1987. *Laboratory Separation Membrane Filtration Chromatography*. Amicon a GRACE company. Danvers, Massachusetts.

Amy, Gary L., Michael R. Collins, C. James Kuo, and Paul H. King. 1987. Comparing Gel Permeation Chromatography and Ultrafiltration for the Molecular Weight Characterization of Aquatic Organic Matter. *Journal American Water Works Association*. 79 (1):43-49.

Amy, Gary L., Raymond A. Sierka, James Bedessem, David Price, and Lo Tan. 1992. Molecular Size Distributions of Dissolved Organic Matter. *Journal American Water Works Association*. 84 (6):67-75.

Backlund, Peter. 1994. Destruction of Natural Mutagen and Trihalomethane Precursors in Water by Ozonation, UV-Irradiation, and Photolytic Oxonation. *Environment International*. 20(1):113-120.

Benschoten, John E. Van, James K. Edzwald. 1990. Chemical Aspects of Coagulation Using Aluminum Salts--II. Coagulation of Fulvic Acid Using Alum and Polyaluminum Chloride. *Water Research*. 24(12):1527-1535.

Berne, F. Dossier, B. Panais, N. Merlot, B. Cauchi, B. Legube. 1994. Total Dissolved Amino Acid Analysis in Natural and Drinking Waters. *Environmental Technology*. 15:901-916.

Blondeau, Roland. 1986. Comparison of Soil Humic and Fulvic Acids of Similar Molecular Weight. *Organic Geochemistry*. 9(1):47-50.

Bokka, Usha Lavanya., Gary C. Schafran. 1994. Enhanced Coagulation for Removal of Dissolved Organic Matter. Presented at *Annual Meeting of the Virginia Section, American Waterworks Association*. Charlottesville, Virginia.

Bousher, A., P. Brimblecombe, D. Midgley. 1989. Kinetics of Reactions in Solutions Containing Monochloramine and Bromide. *Water Research*. 23(8):1049-1058.

Christman, Russell F., Egil T. Gjessing. 1983. *Aquatic and Terrestrial Humic Materials*. Ann Arbor Science Publishers, Inc. *Ann Arbor, Michigan:*

Choudhry, Ghulam Ghaus. 1984. *Humic Substances: Structural, Photophysical, Photochemical and Free Radical Aspects and Interactions with Environmental Chemicals*. Gordon and Breach Science Publishers. New York, New York.

Cooke, G.D., R.E. Carlson. 1989. THM Production and Eutrophication. Chapter 3 in: *Reservoir Management for Water Quality and THM Precursor Control*. American Water Works Association Research Foundation. Denver, Colorado. pp.5-20.

Cooper, William J., Linda M. Meyer, Clara C. Bofill, and Elena Cordal. 1980. Quantitative Effects of Bromine on the Formation and Distribution of Trihalomethanes in Groundwater with a High Organic Content. *Water Chlorination Chemistry, Environmental Impact and Health Effects*. Edited by R.I. Jolley *et al.* 1:285-295.

Cooper, William J., Paul H. Gibbs, Edward M. Ott, and Perin Patel. 1983. Equivalency Testing of Procedures for Measuring Free Available Chlorine: Amperometric Titration, DPD, and FACTS. *Journal American Water Works Association*. 75 (12):625-629.

Cooper, William J., M.F. Mehran, R.A. Slifker, D.A. Smith, J.T. Villate and P.H. Gibbs. 1982. Comparison of Several Instrumental Methods for Determining Chlorine Residuals in Drinking Water. *Journal American Water Works Association*. 74 (10):546-552.

Cooper, William J., Rod G. Zika, Margarete S. Steinhauer. 1985. Bromide-Oxidant Interactions and THM Formation: A Literature Review. *Journal American Water Works Association*. 77 (4):116-121.

Davis, James A., Rolf Gloor. 1981. Adsorption of Dissolved Organics in Lake Water by Aluminum Oxide, Effect on Molecular Weight. *Environmental Science and Technology*. 15(10):1223-1229.

Dietrich, Andrea, M., Robert C. Hoehn. 1991. *Taste-and-Odor Problems Associated with Chlorine Dioxide*. American Water Works Association Research Foundation. Denver, Colorado.

Dore, M., N. Merlet, J. De Laat, and J. Golchon. 1982. Reactivity of Halogens with Aqueous Micropollutants: A Mechanism for the Formation of Trihalomethanes. *Journal American Water Works Association*. 74 (2):103-107.

Edzwald, James K., William C. Becker, Kevin L. Wattier. 1985. Surrogate Parameters of Monitoring Organic Matter and THM Precursors. *Journal American Water Works Association*. 77 (4):122-131.

El-Rehaili, Ardullah M., Walter J. Weber Jr. 1987. Correlation of Humic Substance Trihalomethane Formation Potential and Adsorption Behavior to Molecular Weight Distribution in Raw and Chemically Treated Waters. *Water Research*. 21(5):575-582.

Engerholm, Bruce A., Gary L. Amy. 1983. A Predictive Model for Chloroform Formation from Humic Acid. *Journal American Water Works Association*. 75 (8):418-422.

Environmental Protection Agency. 1994. National Primary Drinking Water Regulations; Disinfectants and Disinfection Byproducts; Proposed Rule. *Federal Register*. 59(145):38668-38829.

Fayad, Nabil M. 1993. Seasonal Variations of THMs in Saudi Arabian Drinking Water. *Journal American Water Works Association.* 85 (1):46-50.

Gallagher, Daniel L., Robert C. Hoehn, and Andrea M. Dietrich. 1994. *Sources, Occurrence, and Control of Chlorine Dioxide By-Product Residuals in Drinking Water.* American Water Works Association. Denver, Colorado.

Glaze, William H., Howard S. Winberg, and Joseph E. Cavanaugh. 1993. Evaluating the Formation of Brominated DBPs During Ozonation. *Journal American Water Works Association.* 85 (1):96-103.

Gillford, John S., Dennis B. George, V. Dean Adams. 1989. Synergistic Effects on Potassium Permanganate and PAC in Direct Filtration Systems for THM Precursor Removal. *Water Research* 23(10):1305-1312.

Gordan, Gilbert, William J. Cooper, Rip G. Rice, and Gilbert E. Pacey. 1988. Methods of Measuring Disinfectant Residuals. *Journal American Water Works Association.* 80 (9):94-108.

Greiner, Anthony D., Alexa Obolensky, and Philip C. Singer. 1992. Technical Note: Comparing Predicted and Observed Concentrations of DBPs. *Journal American Water Works Association.* 84 (9):99-102.

Gribble, Gordon W. 1994. The Natural Production of Chlorinated Compounds. *Environmental Science and Technology. 28(7):310A-319A.*

Grob, Konrad. 1994. Injection Techniques in Capillary GC. *Analytical Chemistry.* 66(20)1009A-1019A.

Harrington, Gregory W., Zaid K. Chowdhury, and Douglas M. Owen. 1992. Developing a Computer Model to Simulate DBP Formation During Water Treatment. *Journal American Water Works Association.* 84 (11):78-87.

Hautman, Daniel P., Michele Bolyard. 1992. Using Ion Chromatography to Analyze Inorganic Disinfection By-products. *Journal American Water Works Association.* 84 (11):88-93.

Hering, J.G., M. Elimelech ed. 1995. Colloidal and Interfacial Phenomena in Aquatic Environments. *Preprints of Papers Presented at the 209th ACS National Meeting.* Anaheim, CA 35 (1).

Hoehn, Robert C., Donald B. Barnes, Barbara C. Thompson, Clifford W. Randall, Thomas J. Grizzard, and Peter T.B. Shaffer. 1980. Algae as Sources of Trihalomethane Precursors. *Journal American Water Works Association*. 72 (6):344-351.

Hoehn, Robert C., Kevin L. Dixon, Jill K. Malone, John T. Novak, and Clifford W. Randall. 1984. Biologically Induced Variations in the Nature and Removability of THM Precursors by Alum Treatment. *Journal American Water Works Association*. 76 (4):134-140.

Hoehn, Robert C., Paul H. Hargette, W.R. Knocke, A.M. Dietrich, Steven J. Randtke, Bruce W. Long. 1994. The Influence of Raw Water Quality on the Formation of Disinfection By-Products During Drinking Water Treatment. Presented at *American Water Works Association Water Quality Technology Conference*. San Francisco, California.

Hutton, Paul H., Francis I. Chung. 1994. Bromine Distribution Factors in THM Formation. *Journal of Water Resources Planning and Management*. ASCE.120(1):1-15.

Ishiwatari, Ryoshi. 1985. Geochemistry of Humic Substances in Lake Sediments. In *Humic Substances in Soil, Sediment, and Water*. Edited by George R. Aiken, Diane M. McKnight, Robert L. Wershaw, and Patrick MacCarthy. New York, New York. John Wiley and Sons.

Jacangelo, Joseph G., Jack DeMarco, Douglas M. Owen, and Stephen J. Randtke. 1995. Selected Processes for Removing NOM: An Overview. *Journal American Water Works Association*. 87 (1):64-77.

Jacangelo, Joseph G., Jean-Michel Laine, Edward W. Cummings, and Samer S. Adham. 1995. UF with Pretreatment for Removing DBP Precursors. *Journal American Water Works Association*. 87 (3):100-112.

Jodellah, Abdullah, Walter J. Weber Jr. 1985. Controlling Trihalomethane Formation Potential by Chemical Treatment and Adsorption. *Journal American Water Works Association*. 78 (10):95-100.

Johnson, J. Donald, James N. Jensen. 1986. THM and TOX Formation: Routes, Rates and Precursors. *Journal American Water Works Association*. 78 (4):156-162.

Joyce, Wendy Saracen, Francis A. DiGiano, and Peter C. Uden. 1984. THM Precursors in the Environment. *Journal American Water Works Association*. 76 (6):102-106.

Kavanaugh, Michael C., Albert R. Trussell, John Cromer, R. Rhodes Trussell. 1980. An Empirical Kinetic Model of Trihalomethane Formation: Applications to Meet the Proposed THM Standard. *Journal American Water Works Association*. 72 (10):578-580.

Knocke, William R., Sara West, Robert C. Hoehn. 1986. Effects of Low Temperature on the Removal of Trihalomethane Precursors by Coagulation. *Journal American Water Works Association*. 78 (4):189-195.

Krasner, Stuart W., Michael J. McGuire, Joseph G. Jacangelo, Nancy L. Patania, Kevin M. Reagan, and E. Marco Aieta. 1989. *Journal American Water Works Association*. 81 (8):41-53.

Laat, J. de., N. Merlet, M. Dore. 1982. Chlorination of Organic Compounds: Chlorine Demand and Reactivity in Relationship to the Trihalomethane Formation Incidence of Ammonia Nitrogen. *Water Research* 16:1437-1450.

Laine, Jean-Michel, Joseph G. Jacangelo, Edward W. Cummings, Keith E. Carns, Joel Mallevialle. 1993. Influence of Bromide on Low-Pressure Membrane Filtration for Controlling DBPs in Surface Waters. *Journal American Water Works Association*. 85 (6):87-99.

MacCraith, B., K.T.V. Grattan, D.Connolly, R. Briggs, W.J.O. Boyle, and M. Avis. 1991. Cross Comparison of Techniques for the Monitoring of Total Organic Carbon (TOC) in Water Sources and Supplies. *Water Science and Technology*. 28(11):457-463.

March, J.. 1977. *Advanced Organic Chemistry: Reactions, Mechanisms and Structures*. McGraw Hill. New York, New York. p393.

Maskarinec, Michael P., Lynne H. Johnson, Susan K. Holladay, Ronnie L. Moody, Charles K. Bayne, and Roger A. Jenkins. 1990. Stability of Volatile Organic Compounds in Environmental Water Samples During Transport and Storage. *Environmental Science and Technology*. 24(11):1665-1670.

Means, Edward, G. III, Stuart W. Krasner. 1993. D-DBP Regulation:P Issues and Ramifications. *Journal American Water Works Association*. 85 (2):68-73.

Metropolitan Water District of Southern California and James M. Montgomery Consulting Engineers, Inc. 1989. *Disinfection By-Products in United States Drinking Waters, Final Report for U.S. Environmental Protection Agency and Association of Metropolitan Water Agencies, Volume 1.*

Meyer, I., T. Francais, B. Lykins, M. Dutang, and P. Hartemann. 1993. Influence of Biofilm on Disinfection By-products in a Distribution Network. *Water Supply*. 11(3/4):355-364.

Minear, Roger, A. 1990. Trihalomethanes: Impact of Bromide Ion Concentration on Yield, Species Distribution, Rate of Formation and Influence of Other Variables. *Water Chlorination Chemistry, Environmental Impact and Health Effects*. Edited by R.I. Jolley *et al.* 3:151-160.

Murphy, Ellyn M., John M. Zachara, Steven C. Smith, Jerry L. Phillips, and Thomas W. Wietsma. 1994. Interaction of Hydrophobic Organic Compounds with Mineral-Bound Humic Substances. *Environmental Science and Technology*. 28:1291-1299.

Najm, Issam N., Nancy L. Patania, Joseph G. Jacangelo, and Stuart W. Krasner. 1994. Evaluating Surrogates for Disinfection By-products. *Journal American Water Works Association*. 86 (6):98-106.

Newport News, Virginia Department of Public Utilities. nd. *Harwood's Mill Water Treatment Plant: Flow into the Future, Flexibility by Design*. Newport News, Virginia: Newport News, Virginia Department of Public Utilities.

Oliver, Barry. 1982. Effect of Temperature, pH, and Bromide Concentration on the Trihalomethane Reaction of Chlorine with Aquatic Humic Material. *Water Chlorination Chemistry, Environmental Impact and Health Effects*. Edited by R.I. Jolley *et al.* 3:141-147.

Oliver, Barry G. and Simon A Visser. 1980. Chloroform Production from the Chlorination of Aquatic Humic Material: The Effect of Molecular Weight, Environment and Season. *Water Research*. 14:1137-1141.

Ott, R. Lyman. 1992. An Introduction to Statistical Methods and Data Analysis, 4th Edition. Duxbury Press. Belmont, California.

Owen, Douglas M.. 1995. Planning for the ICR. *Journal American Water Works Association*. 87 (2):68-75.

Owen, Douglas M., Gary L. Amy, and Zaid K. Chowdhury. 1993. *Characterization of Natural Organic Matter and Its Relationship to Treatability*. American Water Works Association Research Foundation. Denver, Colorado.

Owen, Douglas M., Gary L. Amy, Zaid K. Chowdhury, Rajendra Paode, George McCoy, and Kathy Viscosil. *Journal American Water Works Association*. 87 (1):46-63.

Peterson, Hans G., Joe P. Milos, David R. Spink, Steve E. Hurdey, and Joanne Sketchell. 1993. Trihalomethanes in Finished Drinking Water in Relation to Dissolved Organic Carbon and Treatment Process for Alberta Surface Waters. *Environmental Technology*. 14:877-884.

Peters, Ruud J. B., Corrie Erkelens, Ed W. B. de Leer, Leo de Galan. 1991. The Analysis of Halogenated Acetic Acids in Dutch Drinking Water. *Water Research* 25(4):473-477.

Peters, Ruud J. B., Ed W. B. de Leer, and Leo de Galan. 1990. Dihaloacetonitriles in Dutch Drinking Waters. *Water Research*. 24(6):797-800.

Peschel, G., Th. Wildt. 1988. Humic Substances of Natural and Anthropogeneous Origin. *Water Research*. 22(1):105-108.

Pfaff, John D., Carol A. Brockhoff. 1990. Determining Inorganic Disinfection By-products by Ion Chromatography. *Journal American Water Works Association*. 82 (4):192-195.

Pourmoghaddas, Hossein, Alan A. Stevens, Riley N. Kinman, Ronald C. Dressman, Leown A. Moore, and John C. Ireland. 1993. Effect of Bromide Ion on Formation of HAAs During Chlorination. *Journal American Water Works Association*. 85 (1):82-87.

Randtke, Stephen, F. deNoyelles, Jr., and C.E. Burkhead. 1987. *Trihalomethane Precursors in Kansas Lakes: Sources and Control, Phase II.* Kansas Water Resources Research Institute, University of Kansas. Lawrence, Kansas.

Randtke, Stephen J., Robert C. Hoehn, Bruce W. Long. 1994. A Comprehensive Assessment of DBP Precursor Removal by Enhanced Coagulation and Softening. Presented at *The Universities Forum, American Water Works Association, 1994 Annual Conference*. New York, New York.

Rashash, Diana. M. 1994. Identification and Characterization of Odorous Metabolites Produced by Selected Freshwater Algae. Doctoral Dissertation. Virginia Tech, Blacksburg, Virginia.

Rav-Acha, Ch. 1984. The Reactions of Chlorine Dioxide with Aquatic Organic Materials and Their Health Effects. *Water Research*. 18(11):1329-1341.

Reckhow, David A., Purnedu Bose, Boijayanta Bezbarua, Eric Hesse, and Andrew MacNeill. 1992. Transformations of Natural Organic Material During Preozonation. EPA. Cincinnati, OH.

Reckhow, David A., Phillip C. Singer. 1990. Chlorination By-products in Drinking Waters: From Formation Potentials to Finished Water Concentrations. *Journal American Water Works Association*. 82 (4):173-180.

Reckhow, David A., Phillip C. Singer, Ronald L. Malcolm. 1990. Chlorination of Humic Materials: Byproduct Formation and Chemical Interpretations. *Environmental Science and Technology*. 24:1655-1664.

Reckhow, David A., Phillip C. Singer. 1984. The Removal of Organic Halide Precursors by Preozonation and Alum Coagulation. *Journal American Water Works Association*. 76 (4):151-156.

Reynolds, Tom D. 1982. *Unit Operations and Process in Environmental Engineering*. PWS-Kent Publishing Co. Boston, Massachusetts.

Rook, Johannes J.. 1983. Possible Pathways for the Formation of Chlorinated Degradation Products During Chlorination of Humic Acids and Resorcinol. *Water Chlorination Chemistry, Environmental Impact and Health Effects*. Edited by R.I. Jolley *et al.* 3:85-97.

Rook, J.J., A. Graveland, and L.J. Schultink. 1982. Considerations on Organic Matter in Drinking Water Treatment. *Water Research*. 16:113-122.

Saar, Robert A., James H. Weber. 1982. Fulvic Acid: Modifier of Metal-ion Chemistry. *Environmental Science and Technology*. 16(9):510A-516A.

Scheuch, Lise E., James K. Edzwald. 1981. Removing Color and Chloroform Precursors from Low Turbidity Waters by Direct Filtration. *Journal American Water Works Association*. 73 (9):497-502.

Schnitzer, M. 1975. Chemical, Spectroscopic, and Thermal Methods for the Classification and Characterization of Humic Substances. *Humic Substances, Their Structure and Function in the Biosphere*. Edited by D. Povoledo and H.L. Golterman. Wageninden: Centre for Agricultural Publishing and Documentation. 293-301

Schnitzer, M. 1978. Humic Substances: Chemistry and Reactions. in *Soil Organic Matter.* Edited by M. Schnitzer and S.U. Khan. Elsier Scientific Publishing Company. New York, New York

Semmens, M.J., A.B. Staples. 1986. The Nature of Organics Removed During Treatment of Mississippi River Water. *Journal American Water Works Association.* 78 (1):76-81.

Servais, Pierre, Gilles Billen and Marie-Claude Hascoet. 1987. Determination of the Biodegradable Fraction of Dissolved Organic Matter in Waters. *Water Research.* 21(4):445-450.

Siddiqui, Mohamed S., Gary L. Amy. 1993. Factors Affecting DBP Formation During Ozone-Bromide Reactions. 85 (1):63-72.

Sinsabaugh, Robert L. III. 1985. Removal of Dissolved Organic Matter from Surface Waters by Coagulation with Trivalent Iron. Doctoral dissertation. Virginia Polytechnic Institute and State University, Blacksburg, Virginia.

Sinsabaugh, Robert L. III., Robert C. Hoehn, William R. Knocke, arthur E. Linkins III. 1986. Removal of Dissolved Organic Carbon by Coagulation With Iron Sulfate. *Journal American Water Works Association.* 78 (5):74-82.

Smith, Lynessa A., Andrea M. Dietrich, Pamela D. Mann, Paul H. Hargette, William R. Knocke, Robert C. Hoehn. 1994. Effects of Enhanced Coagulation on Halogenated Disinfection Byproduct Formation Potentials. Presented at *The Universities Forum, American Water Works Association, 1994 Annual Conference.* New York, New York.

Solomons, T.W. Graham. 1988. *Organic Chemistry, Fourth Edition.* John Wiley and Sons. New York, New York.

Stevens, Alan A., Leown A. Moore, and Richard J. Miltner. 1989. Formation and Control of Non-Trihalomethane Disinfection By-products. *Journal American Water Works Association.* 81 (8):54-60.

Summers, R. Scott, Mathias A. Benz, Hiba M. Shukairy, and Laura Cummings. 1993. Effect of Separation Processes on the Formation of Brominated THMs. *Journal American Water Works Association.* 85 (1):88-95.

Sutherland, Ian W. 1990. *Biotechnology of Microbial Exopolysaccharides.* Cambridge, England. Cambridge University Press.

Symons, James M., Gerald E. Speitel Jr., Alicia C. Diehl, and Harvey W. Sorensen Jr. 1994. Precursor Control in Waters Containing Bromide. *Journal American Water Works Association*. 86 (6):48-60.

Symons, James M., Stuart W. Krasner, Louis A. Simms, and Michael Sclimenti. 1993. Measurement of THM and Precursor Concentrations Revisited: The Effect of Bromide Ion. *Journal American Water Works Association*. 85 (1):51-62.

Taugbol, Geir, and Hans Martin Seip. 1994. Study of Interaction of DOC with Aluminum and Hydrogen Ion in Soil and Surface Water Using a Simple Equilibrium Model. *Environment International*. 20(3):353-361.

Thurman, Earl M., Ronald L. Malcolm. 1981. Preparative Isolation of Aquatic Humic Substances. *Environmental Science and Technology*. 15(4):463-466.

Thurman, E.M. 1985. *Organic Geochemistry of Natural Waters*. Martinus Nijhoff/Dr W. Junk Publishers. Dordrecht, The Netherlands

Tranvik, Lars J. 1990. Bacterioplankton Growth on Fractions of Dissolved Organic Carbon of Different Molecular Weights from Humic and Clear Waters. *Applied and Environmental Microbiology*. 56(6):1672-1677.

Trehy, Michael L and T.I. Bieber. 1979 Detection, Identification and Quantitative Analysis of Dihaloacetonitriles in Chlorinated Natural Waters. In Advances in the Identification and Analysis of Organic Pollutants in Water. Edited by L.H. Keith, Ann Arbor Science, Ann Arbor. Michigan. 2:941-975.

Trehy, Michael L., Richard A. Yost, and Carl J. Miles. 1986. Chlorination Byproducts of Amino Acids in Natural Waters. *Environmental Science and Technology*. 20:1117-1122.

Uden, Peter C., Joel W. Miller. 1983. Chlorinated Acids and Chloral in Drinking Water. *Journal American Water Works Association*. 75 (10):524-527.

Veenstra, John N., Jerald L. Schnoor. 1980. Seasonal Variations in Trihalomethane Levels in an Iowa River Water Supply. *Journal American Water Works Association*. 72 (10):583-590.

Visser, Simon A. 1983. Comparative Study on the Elementary Composition of Fulvic and Humic Acids of Aquatic Origin and from Soils and Microbial Substrates. *Water Research*. 17(10):1393-1396.

Voit, Donald, Judith G. Voit. 1990. *Biochemistry*. John Wiley and Sons. New York, New York.

Volk, Christian, Christophe Renner, Coralie Robert and Jean Claude Joret. 1994. Comparison of Two Techniques for Measuring Biodegradable Dissolved Organic Carbon in Water. *Environmental Technology*. 15:545-556.

Water Quality Division Disinfection Committee of American Water Works Association. 1992. Survey of Water Utility Disinfection Practices. *Journal American Water Works Association*. 84 (9):121-128.

Weber, Walter J. Jr., Abdullah M. Jodellah. 1985. Removing Humic Substances by Chemical Treatment and Adsorption. *Journal American Water Works Association*. 77 (4):132-137.

White, Geo. Clifford. 1972. *Handbook of Chlorination for Potable Water, Wastewater, Cooling Water, Industrial Processes, and Swimming Pools*. Van Nostrand Reinhold. New York, New York, 182-301.

White, Geo. Clifford. 1992. *Handbook of Chlorination and Alternative Disinfectants, Third Edition*. Van Nostrand Reinhold. New York, New York, 89-390.

Wilde, Edward W. 1991. Comparison of Three Methods for Measuring Residual Chlorine. *Water Research*. 25(10):1303-1305.

Xie, Yuiang, David A. Reckhow. 1994. Formation of Halogenated Artifacts in Brominated, Chloraminated, and Chlorinated Solvents. *Environmental Science and Technology*. 28(7):1357-1360.

Young, Michael S., Peter C. Uden. 1994. Byproducts of the Aqueous Chlorination of Purines and Pyrimidines. *Environmental Science and Technology*. 28(9):1755-1758.

Vita

Steve Via graduated from the University of Virginia in 1985 earning a Bachlor of Arts and Sciences degree, with a major in Environmental Sciences. Upon graduation, Mr. Via joined ICF, Technology assisting the Environmental Protection Agency, Office of Solid Waste develop national regulations under the Resource Conservation and Recovery Act and other statutes. Subsequently, Mr. Via was employed by the Central Virginia and New River Valley Planning District Commissions coordinating local government efforts to comply with state and federal environmental regulations, manage natural resources, and development basic infrastructure facilities. Mr. Via entered the Environmental Sciences and Engineering Program at Virginia Polytechnic Institute and State University in 1991 on a part-time basis while employed as Senior Planner at the New River Valley Planning District Commission. He subsequently completed the program as a full-time student in 1995.